OPTIMAL DESIGN OF SUSTAINABLE CHEMICAL PROCESSES VIA A COMBINED SIMULATION-OPTIMIZATION APPROACH

Robert Brunet Solé

Dipòsit Legal: T. 458-2013

Robert Brunet Solé

OPTIMAL DESIGN OF SUSTAINABLE CHEMICAL PROCESSES VIA A COMBINED SIMULATION-OPTIMIZATION APPROACH

DOCTORAL THESIS

Department of Chemical Engineering

UNIVERSITAT ROVIRA I VIRGILI

Tarragona
2012

Robert Brunet Solé

OPTIMAL DESIGN OF SUSTAINABLE CHEMICAL PROCESSES VIA A COMBINED SIMULATION-OPTIMIZATION APPROACH

DOCTORAL THESIS

Department of Chemical Engineering
Supervised by: Dr. Gonzalo Guillén Gosálbez
Dr. Laureano Jiménez Esteller

UNIVERSITAT ROVIRA I VIRGILI

Tarragona
2012

UNIVERSITAT ROVIRA I VIRGILI
OPTIMAL DESIGN OF SUSTAINABLE CHEMICAL PROCESSES VIA A COMBINED SIMULATION OPTIMIZATION APPROACH
Robert Brunet Solé
Dipòsit Legal: T. 458-2013

Universitat Rovira i Virgili
Departament d'Enginyeria Química
Campus Sescelades,
Avda. Països Catalans, 26
43007 Tarragona
Tel: 977 55 86 75
Fax: 977 55 96 67

Dr. Gonzalo Guillén Gosálbez and Dr. Laureano Jiménez Esteller,

CERTIFY:

That the present study, entitled "Optimal design of sustainable chemical processes via a combined simulation-optimization approach" presented by Robert Brunet Solé for the award of the degree of Doctor, has been carried out under our supervision at the Chemical Engineering Department of the University Rovira i Virgili.

Tarragona, 31st May 2012,

Dr. Gonzalo Guillén Gosálbez Dr. Laureano Jiménez Esteller

UNIVERSITAT ROVIRA I VIRGILI
OPTIMAL DESIGN OF SUSTAINABLE CHEMICAL PROCESSES VIA A COMBINED SIMULATION OPTIMIZATION APPROACH
Robert Brunet Solé
Dipòsit Legal: T. 458-2013

Acknowledgements

First of all, I would like to give my thanks to my supervisors Dr. Gonzalo Guillén Gosálbez and Dr. Laureano Jiménez Esteller, for their advice and support during the PhD. They teach me how to be a good researcher and also they gave me this incredible opportunity to carry out a PhD in the University Rovira i Virgili.

Also I am thankful to Dr. Dieter Boer, Prof. José Caballero and Prof. Ignacio Grossmann for their help and involvement in my project and for clarify specific problems. I would like to extend this thanks to the people that I have meet during the PhD, the people of SUSCAPE.

Moreover I would like to give my thanks for my family, mainly my father for his continuous support in our decisions; he was always there to listen and to give advice. He taught me how to ask questions and express my ideas. He showed me different ways to approach a problem and the need to be persistent to accomplish any goal. He is an example to follow such as an engineer as a father. I also I would like to give the thanks to the rest of my life; my mother and my two brothers, since they are the people whose I love more in this world.

Besides, I would like to thank my university for the education I have been given during these last years. It has been essential to achieve the technical skills that are necessary to become a good scientist.

Finally I want to finish this acknowledgment with a sentence that I try to repeat every day, because now and always is the moment to improve our skills to explore new places and enjoy the life.

Twenty years from now you will be more disappointed by the things you didn't do than by the ones you did. So throw of the bowlines. Sail away from the safe harbor. Catch the trade winds in your sails. Explore. Dream. Discover.

Mark Twain

UNIVERSITAT ROVIRA I VIRGILI
OPTIMAL DESIGN OF SUSTAINABLE CHEMICAL PROCESSES VIA A COMBINED SIMULATION OPTIMIZATION APPROACH
Robert Brunet Solé
Dipòsit Legal: T. 458-2013

Resúm

La societat es cada dia més conscient de la escassetat i els canvis ambientals. Per lo que les empreses químiques tenen la necessitat d'adaptar i desarrollar processos químics més sostenibles. Llavors s'ha creat una clara demanda dins de la comunitat científica en desarrollar eines sistemàtiques per aconseguir reduccions en els costos de producció i en el impacte ambiental en els processos químics.

Aquesta Tesis introdueix un nou mecanisme per el disseny de processos químics més sostenibles. El sistema que es presenta està basat en l'ús combinat de simulació de processos, eines d'optimització multi-objectiu, anàlisis econòmic, anàlisis de cicle de vida i sistemes de suport a la presa de decisions. L'estratègia presentada es utilitzada en la resolució de problemes complexes, per el que serà també necessari desarrollar nous algoritmes i estratègies de descomposició per dividir el problema original, en sub-problemes els quals seran més manejables, per obtindre el disseny òptim del procés.

La Tesis es presentada utilitzant sis articles que han estat publicats en diferents revistes científiques internacionals. La primera part, la qual inclou dos publicacions, està enfocada en el disseny de bioprocessos sostenibles, ja que aquestos processos han guanyat molt interès en el mercat degut al seu alt valor. En el 1r treball, s'ha estudiat la maximització del Valor Actual Net en la producció de l'amino-acid L-Lyisne. El problema es formulat com un problema d'optimització dinàmica entera mixta, el qual es soluciona mitjançant un mètode de descomposició que itera entre els sub-problemes esclau i el mestre. L'optimització dinàmica del problema esclau es resolta mitjançant un algoritme seqüencial que integra el simulador de procés (SuperPro Designer®) amb un solver de problemes de programació no lineal implementat en Matlab®. En el segon article, el problema d'optimització permet una resolució conjunta dels aspectes econòmics i ambientals del procés. En aquest cas s'optimitza el Valor Actual Net conjuntament amb diversos indicadors ambientals. La solución del problema es presentada mitjançant diverses corbes de Pareto, i en elles s'aplica l'anàlisi de components principals per tal de trobar objectius redundants entre els diversos indicadors ambientals.

Degut a que la demanda d'energia a incrementat dràsticament durant els últims anys, l'anàlisi energètic en els processos industrial ha guanyat molt interès. Es per tant, que en aquesta segona part de la Tesis està enfocada en el disseny òptim de cicles termodinàmics. En aquesta secció s'han publicat dos articles. En el primer dels articles d'aquesta segona part es presenta un mètode per el disseny òptim de cicles d'absorció d'ammonia-aigua a condicions de refredament i de refrigeració, tenint en compte l'anàlisi econòmic i ambiental. El problema es plantejat com un problema de programació no-lineal entera amb multiples objectius i es resolt amb una estratègia d'aproximació exterior. En el segon article, s'aplica una estratègia similar al primer però a diversos cicles termodinàmics. En aquest article es demostren les capacitats del mètode amb diversos cicles termodinàmics. Entre ells un cicle Rankine de 10 MW modelat en Aspen Hysys® i un cicle d'absorció d'ammonia-aigua de 90 kW modelat en Aspen Plus®.

La producció de biocombustibles segueix creixent a nivell mundial a una gran velocitat. Per tant, en la tercera part d'aquesta Tesis, hem aplicat tècniques matemàtiques a desenvolupar processos de producció de biocombustibles. Aquesta tercera part inclou novament dos publicacions. En el primer treball s'adreça el problema de reduirl impacte ambiental de les plantes de producció de biodiesel mitjançant la inclusió de panels solar per la generació del vapor utilitzat en la planta. Per dur a terme l'estudi s'utilitza un model de sistemes d'energia solar que inclou emmagatzematge d'energia implementat en GAMS®. Aquest model es combinat amb un model de simulació rigorós Aspen Plus® de la planta de biodiesel. En el problema el sistema d'energia solar té en compte la minimització del cost i del potencial d'escalfament global de la planta. En el segon treball, el problema adreça el disseny multi-objectiu d'una planta de producció de bio etanol combinada amb un sistema de panels solars per la generació de vapor en la planta.

En general, es pot considerar que la Tesis presenta un marc interessant en l'àmbit del disseny òptim de processos sostenibles. Els resultants numèrics mostren com es possible aconseguir millores ambientals i econòmiques utilitzant aquest procés rigorós. Addicionalment, aquest mètode ha estat aplicat a diferents tipus de processos com: bioprocesos, cicles termodinàmics i bio combustibles. Aquest mètode serà molt útil per els prenedors de decisions a fi d'avaluar la topologia i les condicions de funcionament en l'enginyeria de procés.

UNIVERSITAT ROVIRA I VIRGILI
OPTIMAL DESIGN OF SUSTAINABLE CHEMICAL PROCESSES VIA A COMBINED SIMULATION OPTIMIZATION APPROACH
Robert Brunet Solé
Dipòsit Legal: T. 458-2013

Resumen

La sociedad es cada día más consciente de la escasez i los cambios ambientales. Por lo que las empresas químicas tienen la necesidad de adaptarse y desarrollar procesos químicos más sostenibles. Entonces se ha creado una clara demanda dentro de la comunidad científica en desarrollar herramientas sistemáticas para conseguir reducciones en los costos y en el impacto ambiental de los procesos químicos.

Esta Tesis introduce un nuevo mecanismo para el diseño de procesos químicos más sostenibles. El sistema que se presenta esta basado en el uso combinado de simulación de procesos, herramientas de optimización multi objetivo, análisis económico, análisis de ciclo de vida i sistemas de soporte a la toma de decisiones. La estrategia presentada es utilizada en la resolución de problemas complejos, por lo que será también necesario desarrollar nuevos algoritmos y estrategias de descomposición para dividir el problema original, en sub-problemas los cuales serán más manejables, para obtener el diseño óptimo del proceso.

La Tesis es presentada utilizando seis artículos que han estado publicados en diferentes revistas científicas internacionales. La primera parte, la cual incluye dos publicaciones, esta enfocada en el diseño de bioprocessos sostenibles, ya que estos procesos han ganado mucho interés en el mercado debido a su alto valor. En el primer trabajo, se ha estudiado la maximización del Valor Actual Neto en la producción de l'amino-acido L-Lyisne. El problema es formulado como un problema de optimización dinámica entera mixta, el cual es solucionado mediante un método de descomposición que itera entre los sub-problemas esclavo i maestro. La optimización dinámica del problema esclavo es resulta mediante un algoritmo secuencial que integra el simulador de proceso (SuperPro Designer®) con un solver de problemas de programación no lineal implementado en Matlab®. En el segundo artículo, el problema de optimización permite una resolución conjunta de los aspectos económicos y ambientales del proceso. En este caso se optimiza el Valor Actual Neto conjuntamente con diferentes indicadores ambientales. La solución del problema es presentada mediante diferentes curvas de Pareto, y en ellas se aplica el análisis de componentes principales.

Debido a que la demanda de energía a incrementado drásticamente durante los últimos años, el análisis energético en los procesos industriales ha ganado mucho interés. Es por eso que en esta segunda parte de la Tesis nos enfocamos en el diseño óptimo de ciclos termodinámicos. En esta sección se han publicado dos artículos. En el primero de los artículos de esta segunda parte se presenta un método para el diseño óptimo de ciclos de absorción de amonio-agua a condiciones de enfriamiento y de refrigeración, teniendo en cuenta el análisis económico y ambiental. El problema es planteado como un problema de programación no-lineal entera con múltiples objetivos. En el segundo, aplica una estrategia similar al primero pero a diversos cicles termodinámicos. En este se demuestran las capacidades del método con diversos ciclos termodinámicos. Entre ellos un ciclo Rankine de 10 MW modelado en Aspen Hysys® y un cicle de absorción de amonio-agua de 90 kW modelado en Aspen Plus®.

La producción de biocombustibles sigue creciendo a nivel mundial a una gran velocidad. Por tanto, en la tercera parte de la Tesis, hemos aplicado herramientas matemáticas a desarrollar procesos de producción de biocombustibles. Esta tercera parte incluye nuevamente dos publicaciones. En el primer trabajo el problema es el de reducir el impacto ambiental de les plantas de producción de biodiesel mediante la inclusión de paneles solares para la generación de vapor utilizado en planta. Para realizar este estudio se utiliza un modelo de sistemas de energía solar en GAMS®. Este modelo es combinado con un modelo de simulación riguroso Aspen Plus® de la planta de biodiesel. En el problema el sistema de energía solar tiene en cuenta la minimización del coste y del potencial de calentamiento global de la planta. En el segundo trabajo, el problema es el diseño multi-objectivo de una planta de producción de bioetanol combinada con un sistema de paneles solares para la generación de vapor en la planta.

En general, se puede considerar que la Tesis presenta un marco interesante en el ámbito del diseño optimo de procesos sostenibles. Los resultados numéricos muestran cómo es posible conseguir mejoras ambientales y económicas utilizando estos procesos rigurosos. Adicionalmente, este método ha sido aplicado a diferentes tipos de procesos com0: bioprocesos, cicles termodinámicos i biocombustibles. Este método será muy útil para los tomadores de decisiones a fin de evaluar la topología y las condiciones de funcionamiento en la ingeniería de proceso.

Summary

The society is every day more conscious about the scarce of resources, the global economy, and environmental changes. Hence, chemical companies have the necessity to be adapted and develop more sustainable processes. There is a clear demanding to the scientific community to develop systematic tools to achieve reductions in the production costs as well as the associated environmental impact in order to develop decision support tools for the design of chemical plants.

This thesis introduces a novel framework for the optimal design of sustainable chemical processes. Our approach combines process simulation, multi-objective optimization tools (MOO), economic analysis, life cycle assessment (LCA) and decision support systems (DSS). The developed strategy will be used to solve very complex problems. For that it will be necessary to develop new algorithms and decomposition strategies to divide the original problem in more manageable sub-problems, to obtain the optimum design of the process. The capabilities of the methodology will be tested in different processes along the Ph.D Thesis.

This PhD dissertation is presented using six articles that have been published in different international peer reviewed journals. The first part, which includes two publications, is focused in the development of sustainable bioprocesses, as these processes have recently gained wider interest for their potential to produce high-value products. In the first work, we studied the maximization of the Net Present Value (NPV) in the production of the amino acid L-lysine. The design task is mathematically formulated as a MIDO problem, which is solved by a decomposition method that iterates between primal and master sub-problems. The dynamic optimization primal sub-problems are solved via a sequential approach that integrates the process simulator SuperPro Designer® with an external NLP solver implemented in Matlab®, while the task of the master problem is to decide on the value of the integer variables. In the second work, the optimization allows for the simultaneous consideration of economic and environmental concerns. We optimize in this case the economic (NPV) and different environmental indicators. The solution is given by various bi-objective Pareto sets, and then we applied principal component analysis

(PCA) in order to find redundant objective functions between the environmental indicators.

Because the energy demand has drastically increased over the last few years, the energetic analysis of industrial processes has gained wider interest. Hence, we focused in the second part of the thesis in the optimal design of thermodynamic cycles. In this section, we published two papers. In the first article of the second part we present a method for the optimal design of ammonia-water absorption cycles for cooling and refrigeration applications with economic and environmental concerns. The design task is posed as a moMINLP and it is solved with an outer-approximation (OA) strategy. In the second article, we expand our work to different thermodynamic cycles. We demonstrate the capabilities of the approach with a 10 MW Rankine cycle modelled in Aspen Hysys® and a 90 kW ammonia-water absorption cooling cycle implemented in Aspen Plus®.

Biofuels production worldwide is continuing to grow at very rapid pace. Hence, in the third part of the thesis, we applied the techniques developed in different biofuels production processes. This third part includes two publications. In the first work we address the problem of reducing the environmental impact of biodiesel plants through their integration with a solar thermal energy system that generates steam. A mathematical model of the solar energy system that includes energy storage is programmed and coupled with a rigorous simulation model of the biodiesel facility developed in Aspen Plus®. The solar energy system accounts for the simultaneous minimization of cost and global warming potential. In the second work, we address MOO of a corn-based bioethanol plant coupled with solar assisted steam generation system with heat storage. Our approach relies on the combined use of process simulation, rigorous optimization tools and, economic and energetic plant analysis.

Overall, we can consider that this thesis presents an interesting framework for the optimal design of sustainable chemical processes. Numerical results show that it is possible to achieve environmental and cost saving using this rigorous approach. Additionally, this approach has been applied in very different type of processes, such as: bioprocesses, thermodynamic cycles and biofuels. This methodology will be very useful for decision-makers in order to evaluate the topology and operating conditions in process system engineering.

UNIVERSITAT ROVIRA I VIRGILI
OPTIMAL DESIGN OF SUSTAINABLE CHEMICAL PROCESSES VIA A COMBINED SIMULATION OPTIMIZATION APPROACH
Robert Brunet Solé
Dipòsit Legal: T. 458-2013

Table of contents

1. Introduction

1.1. Research scope and objectives

Sustainability has recently gained wider interest in process systems engineering (PSE). As a result, intensive research effort is currently being devoted towards the incorporation of environmental criteria in the decision-making process. This general trend has motivated the development of systematic strategic for quantifying and minimizing the environmental impact of process industries (Grossmann & Guillén-Gosálbez, 2010).

The main approaches to synthesizing standard chemical process flowsheets are based on (1) the use of heuristics (e.g. hierarchical decomposition (Douglas 1988)), (2) the development of physical insights (e.g. pinch analysis (Linnhoff, 1993)), and (3) the optimization of superstructures (Grossmann, Caballero & Yeomans, 1999).

The overwhelming majority of the works in the optimization of superstructures follow the so called simultaneous approach, which relies on formulating algebraic optimization models described in an explicit form. For simplicity purposes, most of these formulations contain short-cut models that avoid the numerical difficulties stemming from highly nonlinear equations. These simplified formulations provide "good" approximations when certain assumptions hold, but can lead to large numerical errors otherwise. Sequential process simulation models are more difficult to optimize due to the presence of nonconvexities of different types, but provide more accurate results. The pivotal idea of the simulation-optimization methods is also used in a variety of chemical engineering applications, including the design of systems such as: heat exchangers and chemical reactions (Diwekar et al. 1992; Reneaume et al. 1995; Kravanja & Grossmann 1996), design of chemical plants (Díaz and Bandoni 1996; Kim et al. 2010) and distillation columns (Caballero et al. 2005). An efficient solution method is presented for tackling these problems based on decomposing them into two sub-levels between which an algorithm iterates until a stopping criterion is satisfied.

This algorithm performs the calculations using both a process simulation and an external optimizer. However this strategies it was never used for minimizing the environmental impact.

At this point there still very few papers that have reported the use of process synthesis techniques with the explicit incorporation of sustaianablity issues. The combined use of optimization tools and environmental impact indicators, has recently attracted an increasing attention in PSE. This approach, was formally introduced by Azapagic and Clift (1999a). This methodology couples life cycle assessment (LCA) principles, used to quantify the environmental performance of a process, with multi-objective optimization (MOO) tools. Examples of this general approach can be found in the works by Azapagic and Clift (1999b) (production of boron compounds), Alexander et al. (2000) (nitric acid plant), Kahn et al.(2001) (production of vinyl chloride monomer), Baratto et al. (2005) (design of auxiliary power units), Carvalho et al. (2006) (design of a methyl tertiary butyl ether plant), Guillen-Gosalbez et al. (2008) (optimization of the hydrodealkylation of toluene), Gebreslassie et al. (2009) (design of absorption cooling systems),Kikuchi et al (2010) (production of biomass-derived polypropylene), and the design of chemical supply chains (Hugo and Pistikopoulos 2005, Guillen-Gosalbez and Grossmann 2009), among some others.

In particular this thesis will focus on introducing a methodology for processes synthesis based on the combined use of process simulation, multi-objective optimization tools (MOO), economic analysis, life cycle assessment (LCA) and decision support systems (DSS). The developed strategy will lead to complex formulations, such as: mixed-integer non-linear programming (MINLP) and mixed-integer dynamic optimization (MIDO). New algorithms and decomposite strategies will be devised in order to expedite their solution. The capabilities of the methodology will be tested in different chemical process along the Ph.D Thesis; firstly it is study the optimal design of biotechnological facilities, the second part is focused in the study of thermodynamic cycles, then we move to the economic, environmental and enegetic balance of biofuel production process, the fourth part is focused in the optimization and heat intgreation

of basic chemicals manufacture process, and finally we optimize a wastewater treatment plant.

This thesis aims is providing a novel framework for the optimal design of sustainable chemical process, which will be useful for decision-makers in order to take chemical process operation and topological design. Therefore, such general aim can be formalized in four specific objectives as follows:

- Propose a novel framework based on the combined use of process simulation, multi-objective optimization tools (MOO), economic analysis, life cycle assessment (LCA) and decision support systems (DSS).
- Implement a method which is able to achieve significant reductions in their production costs along with the associated environmental impact.
- Developed new algorithms and decomposition strategies in order to expedite the solution of the problem.
- Use the approach presented in different type of chemical processes, such as: bioprocesses, thermodynamic cycles and biofuels.

1.2. Chemical process design

The main goal of a process chemical engineer is to create and design processes to manufacture chemicals. The process design task is very important for the company because it incurs in the 80% of the subsequent costs of the project. In the past, the major approaches in process design were based on rules of thumb and the major goal was to reduce the plant cost. However, more recent trend has been present more rigorous methods based on mathematical programming techniques. Additionally, we now focus in the design of environmentally conscious chemical process taken also into account the economic analyses of the plant.

Chemical plant

Chemical plants are a series of ordered operations that take raw materials and convert them into desired products, salable by-products and unwanted wastes. See Figure 1.

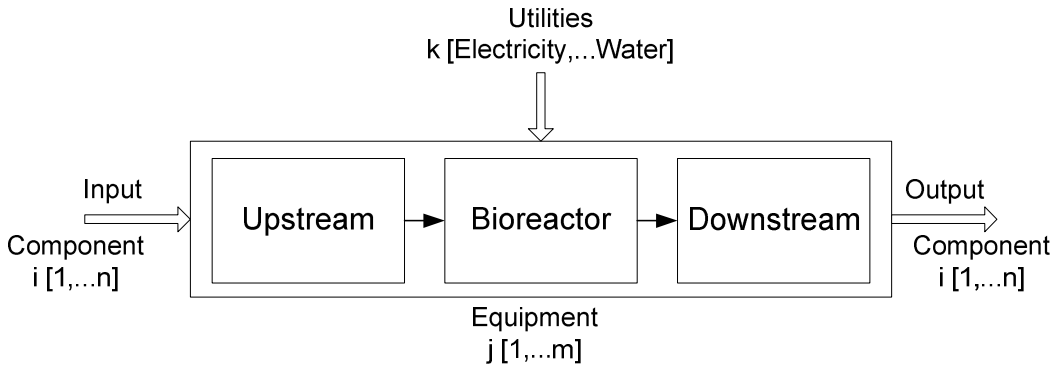

Figure 1. Chemical process

The main chemical processes operations are: feed storage, feed preparation, reaction, product purification and product packaging. However, among these main steps there are many different unit procedures and equipments, such as: tanks, mixers, splitters, separators, heat exchangers, columns, reactors, pumps, compressors, etc.

Classification of chemical processes

Normally, the chemical processes are classified based on the type of chemical component that you produce. The main chemical processes in the industry are: basic chemicals, fuel processing, biofuels processing, plastic processing, consumer goods, bioprocesses, waste water treatment, mineral processing, air pollution, pulp and paper, pharmaceutical, thermodynamic cycles and others. In this PhD dissertation we used three different types of chemical processes to test and present the systematic method developed. The processes that we used are: bioprocesses, thermodynamic cycles and biofuel processing:

- **Bioprocess** can be seen as a special type of chemical processes that employs microorganisms to produce a wide variety of biochemical products (antibiotics, proteins, amino acids, enzymes, etc). Although they share some common features with general chemical processes, typical bioprocesses differ in process structure and operating constraints when compared with the former ones (Heinzle et al., 2006a).

- **Energy,** we focused here in absorption cycles and Rankine power cycles. Absorption cycles use a mixture of a refrigerant and an absorbent. The most widely employed mixtures are water-lithium bromide (water as refrigerant) and ammonia-water (ammonia as refrigerant). Absorption cooling systems may use low grade heat sources as energy input in order to produce cooling thereby leading to less global warming emissions. Rankine power cycles most commonly uses water, although other types of inorganic (ammonia, ammonia/ water, etc) and organic fluids (hydrocarbons, fluorocarbons, siloxanes, etc) can be used. The main advantage of organic working fluids in Rankine cycles is that they can be driven at lower temperatures than similar cycles using water and also in many cases superheating is not necessary.

- **Biofuels are aimed at replacing mainly the conventional liquid fuels like diesel and petrol. The two most common and successful biofuels are biodiesel and bioethanol. They are classified as primary and secondary. The 1st generation biofuels are usually produced from sugars grains or seeds and requires a simple process to produce biofuel. The 2nd generation liquid biofuels are produced from lignocellulosic biomass, that means that are using non-edible residues of food crop production and non-edible whole plant biomass, so has the advantage to limit the direct food versus fuel competition, a problem associated to the 1st generation. The use of 3rd generation biofuels specifically derived from microbes and microalgae, therefore, is considered to be a viable alternative energy resource without the associated problems that using first and second-generation biofuels bring.**

1.3. Chemical process modeling and simulation

In PSE modeling is of paramount importance. Flexible modeling environments will be required that can accommodate a greater variety of models, ranging from molecular level to macroscopic systems. This implies being able to pose from the simple algebraic to the more complex partial differential algebraic models, both in pure equation form and with mixed procedures. The capability of automating problem formulation

through higher level physical descriptions should also be an area of potentially great impact.

Process simulation is used to determine the size of equipment in a chemical plant, the amount of energy needed, the overall yield, and the magnitude of the waste streams. Because the results of process simulation depend upon thermodynamics and transport processes, the mathematical models are complicated and would be time-consuming to solve without a computer.

1.3.1. Process simulators

Exist a wider variety of commercial process simulators, some of the with powerful tools for the calculation of industrial processes, with a large data base, equipment embedded models and libraries for the thermodynamic blanaces. Some of these process simulators are: Aspen Plus (Aspen Technologies, USA), Hysys (Hyprotech, Canada), SuperPro Desginer (Intelligen, USA), Chemcad (Chemistations, USA) and Pro II (Simulation Sciences, USA).

- **Aspen Plus** is a market-leading process modeling tool for conceptual design, optimization, and performance monitoring for the chemical, polymer, specialty chemical, metals and minerals, and coal power industries.

- **Aspen Hysys** is a market-leading process modeling tool for conceptual design, optimization, business planning, asset management, and performance monitoring for oil & gas production, gas processing, petroleum refining, and air separation industries.

- **SuperPro Designer** facilitates modeling, evaluation and optimization of integrated processes in a wide range of industries (Pharmaceutical, Biotech, Specialty Chemical, Food, Consumer Goods, Mineral Processing, Microelectronics, Water Purification, Wastewater Treatment, Air Pollution Control, etc.). The combination of manufacturing and environmental operation models in the same package enables the user to concurrently design and evaluate manufacturing and end-of-pipe treatment processes and practice waste minimization via pollution prevention

as well as pollution control. SuperPro Designer is a valuable tool for engineers and scientists in process development, process engineering, and manufacturing. It is also a valuable tool for professionals dealing with environmental issues (e.g., wastewater treatment, air pollution control, waste minimization, pollution prevention). SuperPro provides under a single umbrella modeling of manufacturing and end-of-pipe treatment processes, project economic evaluation, and environmental impact assessment.

1.4. Sustainability assessment

Sustainability has recently emerged as a key issue in PSE. Nowadays, three dimensions (economic, environmental, and social development) constitute sustainability.

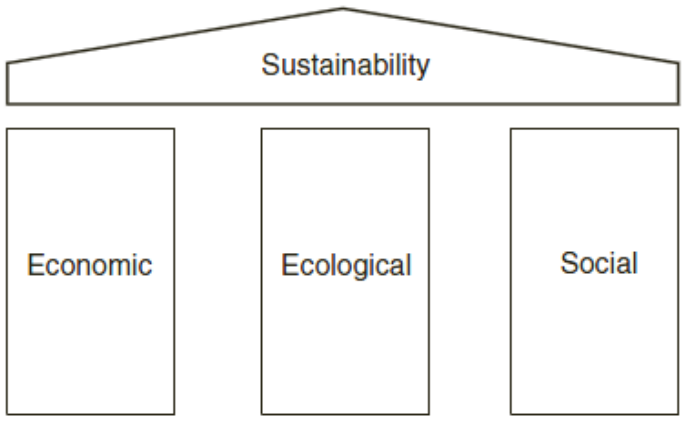

Figure 2. The three pillars of sustainability

1.4.1. Economic assessment

We provide a basic description of economic assessment and several tools for cost and profitability analysis that are usually applied during process development. There are already a number of books, especially in the chemical engineering field, that cover cost and profitability assessment in detail.

As the objective function for our problem, we normally use the maximization of the net present value (NPV) or the minimization of the total annualized cost (TAC). In both cases the first step is the estimation of the capital cost, which includes the plant investment and operating costs.

1.4.1.1. Capital-cost estimation

Capital cost is the total amount of money that has to be spent to supply the necessary plant, plus the working capital that is handed for the operation of the facility.

1.4.1.2. Capital Investment Costs

The capital investment cost estimation is based on the cost of the necessary equipment for the process. The most accurate estimate is to obtain a quote from a vendor, however for conceptual designs we normally use equipment correlations costs. Additionally to the price of the piece of equipment, sometimes we have also to add the cost of transportation and installation. Moreover we have also to take into account if there are auxiliary equipments that are necessary. Finally the estimation of the total includes part of the equipment costs, the installation, process piping, instrumentation/control, insulation, electrical systems, building, yard improvement and auxiliary facilites. And the engineering, construction and land.

Operating costs

Operating costs can divided into variable, fixed and plant overhead costs. Variable costs largely depend on the amount of product that is produced. In contrast, the fixed costs are largely independent of the production operations. However, there are additional expenses necessary to run a plant, e.g. storage facilities or safety measurements. These expenses are summarized under the plant overhead costs or factory expenses.

- *Raw materials:* The list of raw materials and the amounts consumed are obtained from the material balance of the process. The raw material cost is derived by multiplying the amount by its prices.
- *Utilities:* The energy is provided mainly by electricity, steam and cooling water.
- *Others:* Other operating costs are: consumables, labor, operating supplies, laboratory, waste treatment, royalty expenses.

1.4.1.3. Total annualized cost

The total annualized cost (TAC) accounts for the capital cost and operating cost.

1.4.1.4. Revenues

The revenue is the sum of all sales of the main and side products of a process within a certain time period. For a single-product facility.

1.4.1.5. Profitability analysis

There are a number of indices that are used to evaluate the profitability of a process.

- *Gross profit,* is the annual revenue r_j minus the annual total product cost c_j.

$$G_j = r_j - c_j$$

- *Net profit,* is the gross profit minus the income tax.

$$N_j = (r_j - c_j)\cdot(1-\phi) = G_j\cdot(1-\phi)$$

- *Net cash flow,* is the sum of net profit and the depreciation d_j.

$$A_j = N_j - d_j$$

- *Return of investment,* is the ratio of profit to investment and measures how effectively the company uses its invested capital to generate profit. It is usually calculated using the net profit and the total capital investment (TCI) and is shown as a percentage value:

$$ROI = \frac{N_j}{TCI}\cdot 100$$

- *Payback period (PBP),* is the length of time necessary to pay out the capital investment by using the annual net cash flow that returns to the company's capital reservoir.

$$PBP = \frac{DFC}{A_j}$$

- *Net present value (NPV),* considers the time-value of the earned money.

$$NPV = \sum_{j=1}^{n} \frac{A_j}{(1+i)^j}$$

1.4.2. Environmental assessment

The increased awareness of the importance of environmental protection, and the possible impacts associated with products, both manufactured and consumed, has increased interest in the development of methods to better understand and address these impacts. One of the techniques being developed for this purpose is life cycle assessment (LCA).

The LCA methodology serves two major purposes. The first one is to quantify and evaluate the environmental performance of a process from "cradle-to-grave" in order to help decision makers to choose between different processes and processing routes. The second one is to assist in the identification of alternatives for environmental improvements. This second goal is particularly important for process designers, as it helps to identify possible modifications to reduce the environmental impact of the system.

The LCA methodology (ISO 14040. 1997) that enables the computation of the environmental impact of the process is applied in four phases (Consoli et al. 1993):

1. Goal and scope definition. This is the first stage of the LCA. At this point, we must define the system boundaries of the system, the functional unit, the methodology used to quantify the impact and the data and assumptions required to perform the LCA. In this work we address the analysis of a bioprocess production plant. The functional unit of the system is a fixed amount of final product. The environmental impact is assessed according to the Eco-indicator 99 methodology (Consultants 2000), which follows LCA principles.

2. Life cycle inventory analysis (LCI). This phase quantifies the input and output flows (i.e., life cycle inventory, denoted by the continuous variable LCI_b) associated with the operation and construction of the cycles. The damage during the operation phase is given by the natural gas and electricity consumption rates, which are retrieved from the process simulation. This information is translated into the corresponding LCI using environmental databases. The LCI of the construction phase is approximated by the LCI

of the mass of steel contained in the process units. This LCI is determined from some variables of the simulation models using sizing correlations.

3. Life Cycle Impact Assessment (LCIA). This phase translates the LCI into the corresponding environmental damages (denoted by the continuous variable DAM_d). Damage factors (df_{bd}) for different environmental burdens (i.e., LCI entries) are available in the literature (Pre-consultants et al., 2000).

$$DAM_d = \sum_b df_{b,d} \cdot LCI_b \qquad \forall d$$

4. Life cycle Interpretation. In this phase, the LCA results are analyzed and a set of conclusions and recommendations are formulated. In this work, this step is carried out in the post optimal analysis of the optimal solutions found.

LCA does not provide any systematic procedure to generate alternatives for environmental improvements. To overcome this drawback, it has been proposed in the literature to couple LCA with optimization tools (Azapagic and Clift 1999a). One of the limitations of the combined use of LCA and optimization techniques is that the complexity of the solution methods for MOO grows rapidly in size with the number of objectives. In this paper, we explore the use of PCA in order to ameliorate the complexity of the problem.

1.4.3. Assessing social aspects

In order to identify relevant social and to compile a set of indicators, four basic perspectives on technology assessment have been taken into consideration. The typical indicators are: health and safety, quality of working conditions, employment, education training, knowledge management, innovation potential, product acceptance and societal benefit and societal dialogue.

However none of these indicators it is used yet in the optimization environment for plant design.

1.4.4. Interactions between the different sustainability dimensions

The plant capacity is defined for an expected market demand and development that many be interpreted in a societal context and has a strong impact on the economic success of process. The economic success is also influenced by the technological development of the company and its competitors. The general economic development influences product sales, which also has a strong social component. Furthermore, government policies and legal constraints have an effect on the process.

1.5. Optimization theory and methods

In this thesis, the decision making process for the optimal design of sustainable chemical process is tackled by means of optimization, also termed as mathematical programming. Indeed, optimization is a wide discipline which aims at systematically finding the best solution of a problem, represented as variable values, according to specified criteria, expressed in terms of objective functions, by fulfilling, if necessary, a given set of constraints. Therefore, the problem representation must be firstly formalized, specifically as a mathematical mode, and next optimized.

Regarding mathematical models, they can be classified according to different features. For example, deterministic models are those whose parameter values are assumed to know with certainty, whereas stochastic models involve quantities known only in probability. Additionally, models may be either lineal or non-lineal, in the former case the model equations are algebraic expressions which may contain constants and the product of a constant and a single variable, whereas in the latter, non-linear functions are also included. Moreover, they may be classified as dynamic or static, depending on whether the variables change over time or not, respectively.

Table 1. Classification of mathematical programming techniques

	Variables		Equations		Nº OF		Diff eq.
	Discrete	Continuous	Linear	Non linear	1	>1	
Linnear programming (LP)	N	Y	Y	N	Y	N	N
Mixed integer linear programming (MILP)	Y	Y	Y	N	Y	N	N
Non linear programming (NLP)	N	Y	O	Y	Y	N	N
Mixed integer non linear programming (MINLP)	Y	Y	O	Y	Y	N	N
Dynamic optimization (DO)	N	Y	O	O	Y	N	Y
Mixed integer dynamic optimization (MIDO)	Y	Y	O	O	Y	N	Y
Multi-objective optimization (MOO)	O	Y	O	O	N	Y	O

1.5.1. Features of mathematical programming

The general expression of mathematical programming problem is given by the following equation:

$$\begin{aligned} \min\ & Z = f(x,y) \\ s.t.\quad & h(x,y) = 0 \\ & g(x,y) \leq 0 \\ & x \in X, y \in \{0,1\}^m \end{aligned}$$

Where *f(x,y)* represents the objective function. Equations *h(x,y)=0* and *g(x,y)≤0* are explicit external constraints added to the problem. The continuous design variables are given by *x*, and *y* represents discrete variables.

In general, three basic steps may be identified when formulating a mathematical problem: (i) identifying all restrictions and formulating all corresponding constraints in terms of linear, non linear or dynamic equations equalities or inequalities; and (iii) identifying and formulating the objective(s) as function of the decision variables to be optimized (either minimized or maximized).

1.5.2. Rigorous optimization methods

Continuous optimization includes linear programming (LP) and non-linear programming (NLP). Discrete problems are classified into mixed-integer linear programming (MILP) and mixed-integer non-linear programming (MINLP).

Linear programming (LP)

LP problems are when all decision variables are continuous and the objective function and constrains of the problem are linear function of the decision variables.

$$\begin{aligned} \min\ & Z = c^T x \\ s.t.\ & Ax = b \\ & Cx \le d \\ & x \ge 0 \end{aligned}$$

The standard method to solve (LP) is the simplex method (Dantzing ,1963), although interior point methods have become quite advanced and competitive for highly constrained problems (Wright, 1996).

Many refinements have been developed over the last three decades for the simplex method, and most of the current commercial computer codes (e.g., OSL, CPLEX, LINDO) are based on this method.

Non linear programming (NLP)

In this case, the problem corresponds to equation 3.3, where in general f(x), h(x), g(x) are nonlinear functions.

$$\begin{aligned} \min\ & Z = f(x) \\ s.t.\ & h(x) = 0 \\ & g(x) \le 0 \\ & x \in R^n \end{aligned}$$

A key characteristic of problem (NLP) is whether it is convex or not. If NLP is a convex problem, than any local solution is also a global solution to NLP. If it is not convex the algorithm can only satisfies local solutions.

The more efficient NLP methods solve this problem by determining directly a point that satisfies the Karush-Kuhn-Tucker conditions. Within constrained nonlinear optimization programs, three main numerical algorithms can be distinguished:

- Sequential quadratic programming (SQP). It is one of the most popular NLP algorithm because it has fast convergence properties and can be tailored to a

wide variety of problem structures. Some examples of commercial codes which apply the SQP algorithm are fmincon or SNOPT.

- Interior point methods. This method relaxes the complmentary conditions and solves a set of relaxed problems. Some commercial codes are IPOPOT or KNITRO.
- Nested projection methods. These methods are useful for NLPs with nonlinear objectives and constraints where it is important for the solver to remain close to feasible over the course of iterations. MINOS, CONOPT or LANCELOT are available codes based on nested and gradient projection.

Mixed integer linear programming (MILP)

This is an extension of the LP problem where a subset of the variables is restricted to integer values (most commonly to 0-1). The general form of the MILP problem is given by, equation 3.3.

$$\begin{aligned} min \quad & Z = a^T x + b^T y \\ s.t. \quad & Ax + By = c \\ & Cx + Dy \leq e \\ & x \geq 0, y \in \{0,1\}^t \end{aligned}$$

Two powerful solution procedures for MILP are the Branch and Bound (B&B), and the Cutting Plane methods. Specifically, the B&B method consists of an implicit enumeration approach and it is the most effective and widely used technique for solving MILP. The B&B method starts with solving the LP relaxation. If the optimal solution to the relaxed LP is integer-valued, the optimal solution to the LP relaxation is also optimal to the MILP. However, such condition is mostly unlikely and the MILP is partitioned into a number of subproblems that are generally smaller in size or easier to solver than the original problem. In contrast, the basic idea of the Cutting Plane method consists of changing the boundaries of the convex set of the relaxed LP feasible region by adding cuts, i.e. additional linear constraints, so that the optimal extreme point becomes all-integer when all such cuts are added. Therefore, when enough such cuts are added, the new optimal extreme point of the sliced feasible region becomes all-integer, and is optimal to the MILP.

CPLEX is one of the most sophisticated existing packages for integer programming. Other computer packages are OSL, LINDO or ZOOM.

Mixed integer non-linear programming (MINLP)

MINLP models typically arise in synthesis and design problems, and in planning and scheduling problems. MINLP problems are usually the hardest to solve unless a special structure can be exploited. The following particular formulation, which is linear in the 0-1 variables and linear/nonlinear in the continuous variables.

$$\begin{aligned} \min\ & Z = f(x,y) \\ s.t.\ & h(x,y) = 0 \\ & g(x,y) \leq 0 \\ & x \in X, y \in \{0,1\}^m \end{aligned}$$

In these MINLP formulations, continuous variables are used to represent the materials and energy flows as well as operating conditions (temperatures, pressures, concentrations, etc.) whereas binary variables are employed to denote the existence of the equipment units. The resulting MINLP formulations can be solved by methods such as branch and bound (BB) (Borchers and Mitchell 1994), Generalized Benders Decomposition (GBD) (Geoffrion 1972), outer-approximation (OA) (Duran and Grossmann 1986), extended cutting planes (Westerlund and Petterson 1995) and LP/NLP based branch and bound (Quesada and Grossmann 1992).

1.5.3. Dynamic optimization

Chemical processes are modeled dynamically using DAEs, consisting of differential equations that describe the dynamic behavior of the system, such as mass and energy balances, and algebraic equations that ensure physical and thermodynamic relations. Typical applications include control and scheduling of batch processes; startup, upset, shutdown and transient analysis; safety duties and the evaluation of control schemes.

Mixed integer dynamic optimization (MIDO) problem

In mathematical terms, a MIDO problem can be posed as follows:

$$
\begin{aligned}
\min_{u(t),d,y} \quad & J\left(\dot{x}_d(t_f), x_d(t_f), x_a(t_f), u(t_f), d, y, t_f\right) \\
s.t. \quad & h_d\left(\dot{x}_d(t), x_d(t), x_a(t), u(t), d, y, t\right) = 0 && \forall t \in \left[t_0, t_f\right] \\
& h_a\left(x_d(t), x_a(t), u(t), d, y, t\right) = 0 && \forall t \in \left[t_0, t_f\right] \\
& h_0\left(\dot{x}_d(t_0), x_d(t_0), x_a(t_0), u(t_0), d, y, t_0\right) = 0 \\
& h_p\left(\dot{x}_d(t_i), x_d(t_i), x_a(t_i), u(t_i), d, y, t_i\right) = 0 && \forall t_i \in \left[t_0, t_f\right], i = 1,\ldots I \\
& g_p\left(\dot{x}_d(t_i), x_d(t_i), x_a(t_i), u(t_i), d, y, t_i\right) \le 0 && \forall t_i \in \left[t_0, t_f\right], i = 1,\ldots I \\
& h_q(d, y) = 0 \\
& g_q(d, y) \le 0
\end{aligned}
$$

In this formulation, $h_d=0$ and $h_a=0$ represent the system of differential-algebraic equations (DAEs) that describe the dynamic system whose initial conditions are $h_0=0$. $h_p=0$ and $g_p\leq 0$ enforce conditions that must be satisfied at specific time instances, whereas $h_q=0$ and $g_q \leq 0$ are time invariant equality and inequality constraints, respectively. $x_d(t)$ and $x_a(t)$ denote the differential state and algebraic variables of the dynamic system, $u(t)$ is the vector of time-varying control variables, d is the vector of time-invariant continuous search variables and y are the binary variables, which in our case are assumed to be time invariant.

1.5.3. Computer solving algorithms

One of the most important tools of this work is the computer solving algorithms used to solve the problems presented. Most of the algorithms used were implemented in Matlab (i.e. fmincon and fminsearch), in Tomlab but executed in Matlab (i.e. SNOPT, CONOPT, CPLEX) or in Gams (i.e. SNOPT, CONOPT and CPLEX).

In the 1st article is used an Outer-approximation (OA) strategy which decomposes the problem into levels a primal NLP and a master MILP. The primal NLP was solved using fmincon and the master MILP with CPLEX implementd in Gams. In the 2nd article similar OA strategy is used but in this case the NLP was solved using SNOPT and the MILP with CPLEX with CPLEX but implemented in this case in Tomlab. Similar strategy is used to solve the moMINLP in the 3rd article. In the 4th article we used SNOPT to solve

the moNLP problem and SNOPT and CPLEX for the moMINLP. Finally in the articles 5th and 6th is used CONOPT to solve the biNLP problems.

- **Fmincon attempts to find a constrained minimum of a scalar function of several variables starting at an initial estimate. This is generally referred to as constrained nonlinear optimization or nonlinear programming.**
- **Fminsearch** finds the minimum of a scalar function of several variables, starting at an initial estimate. This is generally referred to as *unconstrained nonlinear* optimization.
- **SNOPT** (for 'Sparse Nonlinear OPTimizer') is a software package for solving large-scale optimization problems written by Philip Gill, Walter Murray and Michael Saunders. It is especially effective for nonlinear problems whose functions and gradients are expensive to evaluate. The functions should be smooth but need not be convex.
- **CONOPT** has a fast method for _nding a _rst feasible solution that is particularly well suited for models with few degrees of freedom. If you have a model with roughly the same number of constraints as variable you should try CONOPT. CONOPT can also be used to solve square systems of equations without an objective function corresponding to the GAMS model class CNS - Constrained Nonlinear System.
- **CPLEX** Optimizer solves integer programming problems, very large linear programming problems using either primal or dual variants of the simplex method or the barrier interior point method, convex and non-convex quadratic programming problems, and convex quadratically constrained problems (solved via Second-order cone programming, or SOCP).

1.6. Decision support systems

In industry, decisions must be continuously taken under multiple and usually conflicting criteria. Precisely, multicriteria decision making (MCDM) is a discipline that deals with the methodology and theory to treat complex problems entailing conflicting objectives, such as cost, performance, reliability, safety, sustainability and productivity among other (Wiecek et al., 2008).

Multi-objective optimization (MOO) is an area of MCDM which aims at finding suitable solutions of mathematical programs with multiple objectives. This thesis applies multiobjective programming techniques to obtain solutions of multiobjective problems, and uses some criteria of multiple criteria decision analysis to reach objectively good solutions.

For the calculation of the Pareto set, two main methods exist in the literature. These are the Є-constraint and the weighted-sum methodology.

1.5.4.1. Є-constraint methodology

This method is based on formulating an auxiliary model (MA), which is obtained by transferring one of the objectives of the original problem (M) to additional constraints. This constraint imposes an upper limit on the value of the secondary objective. Model (MA) is then solved for different values of the auxiliary parameter ϵ in order to generate the entire Pareto set of solutions.

Thus, if (MA) is solved for all possible values of ϵ and the resulting solutions are unique, then these solutions represent the entire Pareto set of solutions of the original multi-objective problem. If the solutions to MA are not unique for some values of ϵ, then the Pareto points must be picked by direct comparison.

1.5.4.2. Weighting-sum methodology

The fundamental philosophy of the adaptive weighted sum method is to adaptively refine the Pareto front. In then first stage, the method determines a rough profile of the Pareto front. By estimating the size of each Pareto match (line segment in the case

of two-dimensional problems), the regions for further refinement in the objective space are determined. In the subsequent stage, only these regions are specified as feasible domains for sub-optimization by assigning additional constraints. In the bi-objective adaptive weighted sum method, the feasible domain for further exploration is determined by specifying two inequality constraints. The usual weighted sum method is then performed as sub-optimization in these feasible domains obtaining more Pareto optimal solutions. When a new set of Pareto optimal solutions are determined, the Pareto patch size estimation is again performed to determine the regions for further refinement.

Chapter 2. Articles

List of publications

1. **R. Brunet**, G. Guillén-Gosálbez, J.R. Pérez-Correa, J.A. Caballero, L. Jiménez. Hybrid Simulation-Optimization based approach for the Optimal Design of Biotechnological Processes. *Computers and Chemical Engineering,* 37(1):125-135, 2012.

2. **R. Brunet**, G. Guillén-Gosálbez, L. Jiménez. Cleaner design of single-product biotechnological facilities through the integration of process simulation, multi-objective optimization, LCA and principal component analysis. *Industrial & Engineering Chemistry Research*, 51(1):410-424, 2012.

3. **R. Brunet**, J.A. Reyes-Labarta, G. Guillén-Gosálbez, L. Jiménez, D. Boer. Combined simulation-optimization methodology for the design of environmental conscious absorption systems. *Computers and Chemical Engineering,*

4. **R. Brunet**, D. Cortés, G. Guillén-Gosálbez, L. Jiménez, D. Boer. Minimization of the LCA impact of thermodynamic cycles using a combined simulation-optimization approach. Applied Thermal Engineering,

5. **R. Brunet**, G. Guillén-Gosálbez, L. Jiménez. Reducing the environmental impact of biodeisel production from vegetable oil using a solar assisted steam generation system with heat storage. *Industrial & Engineering Chemistry Research*,

6. **R. Brunet**, E. Antipova, G. Guillén-Gosálbez, L. Jiménez. Minimization of the energy consumption in bioethanol production processes using a solar assisted steam generation system with heat storage. *AIChE Journal*,

Book chapters

1. **R. Brunet**, K. Kumar, G. Guillen-Gosalbez, L. Jiménez. Integrating process simulation, multi-objective optimization and LCA for the development of sustainable processes. *ESCAPE 21, Chalkidiki, Greece*. June 2011.

2. J.A. Reyes-Labarta, **R. Brunet**, J.A. Caballero, D. Boer, L. Jiménez. Integrating process simulation and MINLP methods for the optimal design of absorption cooling systems. *ESCAPE 21, Chalkidiki, Greece*. June 2011.

3. **R. Brunet**, D. Carrasco, E. Muñoz, G. Guillen-Gosalbez, I. Katakis, L. Jiménez. Economic and environmental analysis of microalgae biodiesel production using process simulation tools. *ESCAPE 22, London, England*. June 2012.

Congresses contributions

1. **R. Brunet**, J.A. Caballero, G. Guillén-Gosálbez, L. Jiménez. Hybrid optimization-simulation based approach for the optimal development of biotechnological processes. ESCAPE 20, Ischia, Napoles, Italy. June 2010.

2. R. Brunet, G. Guillén-Gosálbez, J.R. Pérez-Correa, J.A. Caballero, L. Jiménez. Hybrid Development of cleaner biotechnological facilities thorugh the integration of LCA, process simulation, multi-objective optimization. ICCOPT, Santiago de Chile, Chile. July 2010.

3. **R. Brunet**, J.A. Caballero, G. Guillén-Gosálbez, L. Jiménez. Optimal design of Bioprocesses with Economic and Environemtnal Concerns via a Combined Simulation-Optimization approach. AICHE Annual Meeting. Salt Lake City, USA. November 2010.

4. **R. Brunet**, K. Kumar, G. Guillen-Gosalbez, L. Jiménez. Integrating process simulation, multi-objective optimization and LCA for the development of sustainable processes. *ESCAPE 21, Chalkidiki, Greece*. June 2011.

5. J.A. Reyes-Labarta, **R. Brunet**, J.A. Caballero, D. Boer, L. Jiménez. Integrating process simulation and MINLP methods for the optimal design of absorption cooling systems. *ESCAPE 21, Chalkidiki, Greece*. June 2011.

6. **R. Brunet**, D. Cortes, D. Boer, G. Guillen-Gosalbez, L. Jiménez. Combined simulation-optimization and statistical tools for the optimal design of sustainable thermodynamic cycles. *AICHE Annual Meeting. Minneapolis, USA*. October 2011.

7. **R. Brunet**, M. Matos, A. Bleizeffer, G. Guillen-Gosalbez, L. Jiménez. Economical and environemtnal evaluation of different biocombustible production plants using process simulation and optimization tools. *12th Mediterranean congress. Barcelona, Spain*. November 2011.

8. **R. Brunet**, D. Carrasco, E. Muñoz, G. Guillen-Gosalbez, I. Katakis, L. Jiménez. Economic and environmental analysis of microalgae biodiesel production using process simulation tools. *ESCAPE 22, London, England*. June 2012.

9. **R. Brunet**, G. Guillen-Gosalbez, L. Jiménez. Reducing the environmental impact of biofuel production processes using a solar assisted steam generation system with heat storage. *AUNQUE, Sevilla, Spain*. June 2012.

10. **R. Brunet**, G. Guillen-Gosalbez, L. Jiménez. Reducing the energy consumption of biofuel production processes using a solar assisted steam generation system with heat storage. *AIChE Annual Meeting, Pittsburg, USA*. November 2012.

Article 1

Authors: **R. Brunet**, G. Guillén-Gosálbez, J.R. Pérez-Correa, J.A. Caballero, L. Jiménez.

Title: Hybrid Simulation-Optimization based approach for the Optimal Design of Biotechnological Processes.

Journal: *Computers and Chemical Engineering*

Volume: 37 **Pages:** 125-135 **Year:** 2012

ISI category: Computer Science **AIF:** 0.597

Impact Index: 2.235

Position in the category: 20/97 (Q1)

Cites: -

Hybrid Simulation-Optimization based approach for the Optimal Design of Single-Product Biotechnological Processes

Robert Brunet[1], Gonzalo Guillén-Gosálbez[1]*, J. Ricardo Pérez-Correa[2], José Antonio Caballero[3] and Laureano Jiménez[1]

[1] Departament d'Enginyeria Quimica, Escola Tecnica Superior d'Enginyeria Quimica, Universitat Rovira i Virgili, Campus Sescelades, Avinguda Paisos Catalans 26, 43007, Tarragona, Spain

[2] Departamento de Ingenieria Quimica y Bioprocesos, Pontificia Universidad Catolica de Chile, Casilla 306, Correo22, Santiago de Chile, Chile

[3] Departmento de Ingenieria Quimica, Universidad de Alicante, Aparatado de Correos 99. 03080 Alicante, Spain

*Corresponding author. E-mail: gonzalo.guillen@urv.cat, telephone: +34 977558618

Abstract

In this work, we present a systematic method for the optimal development of bioprocesses that relies on the combined use of simulation packages and optimization tools. One of the main advantages of our method is that it allows for the simultaneous optimization of all the individual components of a bioprocess, including the main upstream and downstream units. The design task is mathematically formulated as a mixed-integer dynamic optimization (MIDO) problem, which is solved by a decomposition method that iterates between primal and master sub-problems. The primal dynamic optimization problem optimizes the operating conditions, bioreactor kinetics and equipment sizes, whereas the master levels entails the solution of a tailored mixed-integer linear programming (MILP) model that decides on the values of the integer variables (i.e., number of equipments in parallel and topological decisions). The dynamic optimization primal sub-problems are solved via a sequential approach that integrates the process simulator SuperPro Designer with an external NLP solver implemented in Matlab. The capabilities of the proposed methodology are illustrated through its application to a typical fermentation process and to the production of the amino acid L-lysine.

Keywords: *hybrid simulation-optimization; mixed-integer dynamic optimization; biotechnological processes; L-lysine.*

1 INTRODUCTION

Because of their potential to produce high-value products in human health and care, bioprocesses have recently gained wider interest. The recent boost in competitiveness for customers and new products experienced in this sector has created a clear need for modeling and optimization tools to assist decision-makers in the early stages of the process development.

A bioprocess is a special type of chemical process that produces biochemical products (e.g. antibiotics, proteins, amino acids, etc.) from microorganisms or enzymes. Bioprocesses share some common features with general chemical processes, but differ in their kinetics of product formation, process structure (unit operations and procedures) and operating constraints (Heinzle et al. 2006a).

Optimization approaches devised so far in biotechnology have primarily focused on the bioreactor step. Cuthrell and Biegler (1989) optimized a fed-batch reactor for penicillin production with a solution strategy based on successive quadratic programming (SQP) and orthogonal collocation on finite elements. Carrasco and Banga (1997) addressed the dynamic optimization of batch and fed-batch reactors using stochastic optimization algorithms. More recently, Banga et al. (2005) introduced a new solution method for this problem based on control parameterization, whereas Sarkar and Modak (2005) proposed the use of genetic algorithms in this context. For an extensive review of dynamic optimization of bioreactors, the reader is referred to Banga et al. (2003).

Another area related with the bioreactor step that has received attention in the literature is the optimization of metabolic networks. Raghunathan et al. (2003) addressed the data reconciliation and parameter estimation problems in metabolic networks, whereas Guillen-Gosalbez and Sorribas (2009) and Pozo et al. (2010) have proposed deterministic global optimization techniques for kinetic models of metabolic networks that assist in biotechnological and evolutive studies.

In contrast to these approaches, the optimization of complete bioprocesses considering all their individual steps has received very little attention to date. This can be attributed to

the fact that these problems lead to complex formulations that integrate structural and operating decisions, some of which change over time. To the best of our knowledge, the work by Groep et al. (2000), is the only one that addressed the optimization of a entire bioprocess (i.e., production of an intracellular enzyme alcohol dehydrogenase). This pioneering work has two main limitations: (i) it assumed a fixed plant topology; and (ii) it applied a simple sensitivity analysis to optimize the operating variables of the process that is not guaranteed to converge to a local (or global) optimum.

Hence, it seems clear that the rich theory available for synthesizing standard chemical process flowsheets has not been applied to the same extent to their biochemical counterparts. In fact, the design of bioprocess flowsheets is nowadays typically accomplished by empirical and/or intuitive methods such as rules of thumb or simple heuristics (Petrides et al. 1996, Koulouris et al. 2000, Wong et al. 2004 and Petrides et al. 2006) that are likely to lead to sub-optimal process alternatives.

With this observation in mind, the aim of this paper is to present a systematic tool for the design of bioprocesses that relies on the combined use of simulation and optimization techniques. More precisely, the design task is formulated as a mixed-integer dynamic optimization (MIDO) problem, which is solved by a hybrid simulation-optimization decomposition method that exploits the complementary strengths of optimization tools (i.e., nonlinear programming, NLP, and mixed-integer linear programming, MILP) and commercial bioprocess simulators (i.e., SuperPro Designer). Our methodology has been tested using two different examples: a typical fermentation process and the production of the amino acid L-Lysine.

2 PROBLEM STATEMENT

The problem addressed in this article can be formally stated as follows. Given are the demand and prices of final products, cost parameters, including capital investment and operating cost data (i.e., raw materials and utilities cost), time horizon, thermodynamic properties and per-

formance models of the equipment units embedded in the flowsheet, including the bioreactor kinetics. The goal of the analysis is to determine the optimal process design, including type and size of process units (e.g., centrifuge, decanter, filtration, etc.), number of equipment units in parallel and operating conditions (concentrations, flow rates, temperatures, etc.) that maximize a given economic performance indicator over a specified time horizon.

In this work, we consider single-product batch plants that can operate with more than one equipment unit (in parallel) per stage. The equipment units in parallel are assumed to be of the same size and operating under the same process conditions. The unit yields are described through nonlinear process models that may require the solution of differential-algebraic equations (DAEs). The operating times and batch sizes are regarded as continuous variables to be optimized rather than as fixed parameters. It should be emphasized that many bioprocesses follow this general pattern, such as the production of penicillin, citric and pyruvic acid, vitamin riboflavin, human serum and insulin, monoclonal antibodies, and plasmid DNA, among many others. It is also important to clarify that in this work the emphasis is on the optimization of the operating conditions and topology of these processes, rather than on the solution of the scheduling problem associated with complex bioprocess batch facilities. The reader is referred to the review paper by Mendez et al. (2006) for more details on general scheduling approaches, the overwhelming majority of which assume fixed operating times and process yields.

3 MATHEMATICAL FORMULATION

Most bioreactors in commercial bioprocesses operate in batch or fed-batch mode. Thus, the reaction kinetics of the biochemical conversions, catalysed either by single enzymes or by cells, are the cornerstones of a bioprocess synthesis problem. The design task requires therefore the simultaneous solution of a mixed-integer non-linear programming (MINLP) synthesis models with embedded DAEs. This gives rise to mixed-integer dynamic optimiza-

tion (MIDO) problems, the solution of which is a highly difficult task (Bansal et al. 2003). So far, MIDO algorithms have been applied to the integrated design and control of process plants (Pistikopoulos et al. 2004), simultaneous scheduling and optimal control of reactors (Terrazas-Moreno et al. 2007) and optimization of hybrid systems (Allgor and Barton 1999). However, to our knowledge, they have never been applied to the optimization of a complete biotechnological process model.

In mathematical terms, the synthesis of biotechnological processes can be posed as a MIDO problem. In this work, we apply the following notation taken from Bansal et al. (2003), which may be simplified in some cases according to the features of the design problem being addressed.

$$
\begin{array}{lll}
\min\limits_{u(t),d,y} & J(\dot{x_d}(t_f), x_d(t_f), x_a(t_f), u(t_f), d, y, t_f) & \\
s.t. & h_d(\dot{x_d}(t), x_d(t), x_a(t), u(t), d, y, t) = 0 & \forall t \in [t_0, t_f] \\
& h_a(x_d(t), x_a(t), u(t), d, y, t) = 0 & \forall t \in [t_0, t_f] \\
& h_0(\dot{x_d}(t_0), x_d(t_0), x_a(t_0), u(t_0), d, y, t_0) = 0 & \\
& h_p(\dot{x_d}(t_i), x_d(t_i), x_a(t_i), u(t_i), d, y, t_i) = 0 & \forall t_i \in [t_0, t_f] \quad i = 1, ..., I \\
& g_p(\dot{x_d}(t_i), x_d(t_i), x_a(t_i), u(t_i), d, y, t_i) \leq 0 & \forall t_i \in [t_0, t_f] \quad i = 1, ..., I \\
& h_q(d, y) = 0 & \\
& g_q(d, y) \leq 0 &
\end{array}
\tag{1}
$$

In this formulation, $h_d = 0$ and $h_a = 0$ represent the set of differential-algebraic equations (DAEs) that describe the dynamic system whose initial conditions are $h_0 = 0$. $h_p = 0$ and $g_p \leq 0$ enforce conditions that must be satisfied at specific time instances, whereas $h_q = 0$ and $g_q \leq 0$ are time invariant equality and inequality constraints, respectively. $x_d(t)$ and $x_a(t)$ denote the differential state and algebraic variables of the dynamic system, $u(t)$ is the vector of time-varying control variables, d is the vector of time-invariant continuous search variables and y are the binary variables, which in our case are assumed to be time invariant.

Note that the embedded DAE system is required in order to model the bioreactor kinetics. The binary variables are necessary for representing the different topological decisions, such as the number of equipment units in parallel or the selection of different alternative units in the process. The vector y of binary variables contains $M{\cdot}N$ components, where M represents the different types of process units and N the maximum number of equipment units in parallel. The component $y_{m,n}$ of this vector takes the value of 1 if n equipment units in parallel of type m are selected, and 0 otherwise. Note that the logical relationships among the binary variables describing connections and interactions between the units in the superstructure are expressed also via constraints $h_q = 0$.

There are currently two major approaches to solve MIDO problems. The first type relies on converting the MIDO problem into a finite-dimensional MINLP by complete discretization using techniques such as orthogonal collocation on finite elements (Balakrishna and Biegler, 1993). The resulting MINLP can then be solved by classical MINLP methods. The second class of MIDO algorithms, to which the strategy presented in this work belongs, is based on the use of reduced space methods (Allgor and Barton, 1999). These techniques rely on decomposing the problem into a series of primal dynamic optimization sub-problems with fixed binary variables, and master MILP sub-problems that predict new values of the binary variables for the primal sub-problems.

In complete discretization approaches, the MINLP resulting from the discretization tends to be very large even for relatively small problems, as this approach requires a large number of variables and constraints in order to approximate the solution of the DAE system. On the other hand, in reduced space methods, the difficulty arises in the definition of the master MILP sub-problem. This master problem is typically created by either approximating the nonlinear objective function and constraints by first order linearizations (i.e., supporting hyperplanes) or by deriving Benders cuts from the solution of the primal problem and associated dual information. In the section that follows, we introduce a customized reduced space method for the solution of MIDO problems arising in the design of bioprocesses that

integrates optimization tools with a bioprocess simulator.

4 SOLUTION PROCEDURE

The solution strategy developed in this work is a reduced space method inspired by the works by Diwekar et al. (1992), Kravanja and Grossmann (1996) and Caballero et al. (2005). The key ideas of the approach presented are: (i) to integrate mathematical programming tools with a standard bioprocess simulator in the context of a reduced space method for MIDOs; and (ii) to derive a tailored master MILP formulation that exploits the structure of the problem.

The proposed algorithm iterates between master and primal sub-problems, as shown in Figure 1. The primal level entails the solution of a dynamic nonlinear programming sub-problem, in which the integer decisions, mainly the number of equipments in parallel, are fixed. As discussed in section 5, the solution of this sub-problem requires calculations performed by the bioprocess simulator. On the other hand, the task of the customized master problem is to decide on the value of the integer variables. The algorithm solves iteratively both sub-problems until a termination criterion is satisfied. A stopping criterion that tends to work very well in practice consists of stopping as soon as the primal sub-problems start worsening (i.e. the current primal sub-problem yields an optimal objective function that is worse than the previous one). The main features of these sub-problems are described in detail in the next sub-sections.

(Figure 1 could be placed here)

4.1 Primal sub-problem

The primal level entails the solution of a dynamic optimization problem at iteration k of the algorithm for fixed values of the binary variable k:

$$
\begin{array}{lll}
\min\limits_{u(t),d,y} & J(\dot{x_d}(t_f), x_d(t_f), x_a(t_f), u(t_f), d, \overline{y}, t_f) & \\
s.t. & h_d(\dot{x_d}(t), x_d(t), x_a(t), u(t), d, \overline{y}, t) = 0 & \forall t \in [t_0, t_f] \\
& h_a(x_d(t), x_a(t), u(t), d, \overline{y}, t) = 0 & \forall t \in [t_0, t_f] \\
& h_0(\dot{x_d}(t_0), x_d(t_0), x_a(t_0), u(t_0), d, \overline{y}, t_0) = 0 & \\
& h_p(\dot{x_d}(t_i), x_d(t_i), x_a(t_i), u(t_i), d, \overline{y}, t_i) = 0 & \forall t_i \in [t_0, t_f] \quad i = 1, ..., I \\
& g_p(\dot{x_d}(t_i), x_d(t_i), x_a(t_i), u(t_i), d, \overline{y}, t_i) \leq 0 & \forall t_i \in [t_0, t_f] \quad i = 1, ..., I \\
& h_q(d, \overline{y}) = 0 & \\
& g_q(d, \overline{y}) \leq 0 &
\end{array}
\tag{2}
$$

In the context of our algorithm, this primal sub-problem is solved by parameterizing the control variables, $u(t)$, in terms of time-invariant parameters (*reduced space discretisation* or *control vector parameterisation*). Then, for given $u(t)$ and values of the remaining search variables, d (e.g., equipment sizes, operating conditions, etc.) the DAE system is integrated by the process simulator, which in addition to solving the bioreactor kinetics, it calculates mass and energy balances and key economic parameters of the entire process. As will be discussed later on, in some cases it might be necessary to introduce an intermediate module that couples the model implemented in the bioprocess simulator with an external ODE solver algorithm (e.g., implicit Runge-Kutta method). This allows dealing with complex kinetic models that cannot be directly implemented in the process simulator. An external NLP solver is finally employed for searching the values of the control and design variables that maximize the NPV. To accomplish this task, it is necessary to obtain gradient information with respect to the objective function and constraints through finite difference perturbations.

(Figure 2 could be placed here)

Figure 2 outlines the solution procedure of the primal sub-problem. One of the main advantages of the approach presented is that it benefits from the unit operations models already implemented in the bioprocess simulator, which avoids having to define them in an explicit form (i.e., equation oriented). This issue facilitates to a large extent the implementation step, as it allows optimizing bioprocess models that are already implemented in the simulator without having to define the associated process and economic equations in an explicit way.

Note that due to the structure of the implicit models in a process simulator, the equations $h_q(d, \overline{y}) = 0$ are eliminated by expressing dependent variables z in terms of decision variables v, that is $h_q(v, z, \overline{y}) = 0 \Rightarrow z = \phi_q(v)$. Therefore, the NLP subproblem as it arises in a process simulator for fixed binary variables is indeed given as follows:

$$
\begin{aligned}
\min_{u(t),d,y} \quad & J(\dot{x_d}(t_f), x_d(t_f), x_a(t_f), u(t_f), v, \phi(v), \overline{y}, t_f) \\
s.t. \quad & h_d(\dot{x_d}(t), x_d(t), x_a(t), u(t), v, \phi(v), \overline{y}, t) = 0 && \forall t \in [t_0, t_f] \\
& h_a(x_d(t), x_a(t), u(t), v, \phi(v), \overline{y}, t) = 0 && \forall t \in [t_0, t_f] \\
& h_0(\dot{x_d}(t_0), x_d(t_0), x_a(t_0), u(t_0), v, \phi(v), \overline{y}, t_0) = 0 \\
& h_p(\dot{x_d}(t_i), x_d(t_i), x_a(t_i), u(t_i), v, \phi(v), \overline{y}, t_i) = 0 && \forall t_i \in [t_0, t_f] \quad i = 1, ..., I \\
& g_p(\dot{x_d}(t_i), x_d(t_i), x_a(t_i), u(t_i), v, \phi(v), \overline{y}, t_i) \leq 0 && \forall t_i \in [t_0, t_f] \quad i = 1, ..., I \\
& h_q(v, \phi(v), \overline{y}) = 0 \\
& g_q(v, \phi(v), \overline{y}) \leq 0
\end{aligned}
\tag{3}
$$

A very important point in the method is that the process simulator must converge at each time the solver sends a set of values for the design variables. Otherwise the overall procedure will fail. One way to ensure convergence consists of adding slack variables and a penalty to

the objective function (Viswanathan and Grossmann 1990). This gives rise to the following primal sub-problem:

$$
\begin{aligned}
\min_{u(t),d,y} \quad & J(\dot{x_d}(t_f), x_d(t_f), x_a(t_f), u(t_f), v, \phi(v), \overline{y}, t_f) \\
& + \prod^T (s^+_{hp} + s^-_{hp} + s_{gp} + s^+_{hq} + s^-_{hp} + s_{gq}) \\
s.t. \quad & h_d(\dot{x_d}(t), x_d(t), x_a(t), u(t), v, \phi(v), \overline{y}, t) = 0 && \forall t \in [t_0, t_f] \\
& h_a(x_d(t), x_a(t), u(t), v, \phi(v), \overline{y}, t) = 0 && \forall t \in [t_0, t_f] \\
& h_0(\dot{x_d}(t_0), x_d(t_0), x_a(t_0), u(t_0), v, \phi(v), \overline{y}, t_0) = 0 \\
& h_p(\dot{x_d}(t_i), x_d(t_i), x_a(t_i), u(t_i), v, \phi(v), \overline{y}, t_i) + s^+_{hp} - s^-_{hp} = 0 && \forall t_i \in [t_0, t_f] \quad i = 1, ..., I \\
& g_p(\dot{x_d}(t_i), x_d(t_i), x_a(t_i), u(t_i), v, \phi(v), \overline{y}, t_i) - s_{gp} \leq 0 && \forall t_i \in [t_0, t_f] \quad i = 1, ..., I \\
& h_q(v, \phi(v), \overline{y}) + s^+_{hp} - s^-_{hp} = 0 \\
& g_q(v, \phi(v), \overline{y}) - s_{gq} \leq 0
\end{aligned}
\tag{4}
$$

where $\prod$ is a penalty parameter vector whose value is finite but chosen to be sufficient large, whereas s^+_{hp}, s^-_{hp}, s_{gp}, s^+_{hq}, s^-_{hp} and s_{gq} are vectors of positive variables.

4.2 4.2. Master sub-problem

The goal of the master problem is to provide a new set of values for the binary variables that yield better results than the previous one. Here, we present a tailored master MILP that exploits the structure of the problem. Note that due to the presence of nonconvexities in the model, it is not guaranteed that this master MILP will provide a rigorous lower bound on the global optimal solution of the problem.

To generate the master MILP, the design variables are fixed to the optimal value obtained in the latest NLP solved at iteration k of the algorithm, and a series of simulation problems are calculated. The master MILP takes the following form:

$$
\begin{aligned}
\min_{u(t),d,y} \quad & \eta + \Pi^T \left(s_{gp} + s_{hq} + s_{gq}\right) \\
s.t. \quad & \eta \geq J^k + \left(\frac{\partial J}{\partial v}\right)|_k \left(v - \hat{v}^k\right) + \sum_j \left(\frac{\partial J}{\partial u_j}\right)|_k \left(u_j - \hat{u_j}^k\right) + \Delta J^k \cdot y \\
& 0 \geq T_p^k \left\{ h_p^k + \left(\frac{\partial h_p}{\partial v}\right)|_k \left(v - \hat{v}^k\right) + \sum_j \left(\frac{\partial h_p}{\partial u_j}\right)|_k \left(u_j - \hat{u_j^k}\right) + \Delta h_p^k \cdot y \right\} \\
& s_{gp} \geq g_p^k + \left(\frac{\partial g_p}{\partial v}\right)|_k \left(v - \hat{v}^k\right) + \sum_j \left(\frac{\partial g_p}{\partial u_j}\right)|_k \left(u_j - \hat{u_j}^k\right) + \Delta g_p^k \cdot y \\
& s_{hq} \geq T_q^k \left\{ h_q^k + \left(\frac{\partial h_q}{\partial v}\right)|_k \left(v - \hat{v}^k\right) + \Delta h_q^k \cdot y \right\} \\
& s_{gq} \geq g_q^k + \left(\frac{\partial g_q}{\partial v}\right)|_k \left(v - \hat{v}^k\right) + \Delta g_q^k \cdot y \\
& T_p^k = \begin{cases} -1 & \text{if } \lambda_p^k < 0 \\ 0 & \text{if } \lambda_p^k = 0 \\ 1 & \text{if } \lambda_p^k > 0 \end{cases} \quad T_q^k = \begin{cases} -1 & \text{if } \lambda_q^k < 0 \\ 0 & \text{if } \lambda_q^k = 0 \\ 1 & \text{if } \lambda_q^k > 0 \end{cases}
\end{aligned} \tag{5}
$$

The objective function is formed by the auxiliary variable η and a penalty for constraint violation Π that multiplies the slack variables. The linearizations of the objective function and time variant constraints contain three main terms corresponding to: the design variables ($\hat{v}^k$), control variables ($\hat{u_j}^k$) and the binary variables representing the topological alternatives (y). Note that the control variables u_j are parameterized by means of a piecewise constant profile defined on J sub-intervals. On the other hand, the time invariant constraints only consider, the design and topological decisions. In this formulation, λ_p^k and λ_q^k represent the Lagrangean multipliers associated with the time-invariant and time-variant equality constraints, respectively, of the NLP solved at in iteration k of the algorithm. These values are used to correctly relax the equalities into inequalities.

A key issue in this master MILP is how to obtain the derivatives of the objective function and constraints with respect to the decision variables. The derivatives of the continuous variables are approximated by perturbing them in the optimal solution of the NLP problem.

On the other hand, the partial derivatives with respect to the binary variables, which do not appear explicitly in the MIDO formulation, are determined by running several simulations for different topologies. Note that at each iteration, we need the derivatives of the objective function and the constraints with respect to all the components $y_{m,n}$ of the vector of binary variables. This requires performing at most (depending on the allowable interconections between the equipment units) *M·N-1* simulations, in each of which we concentrate on changing one single process unit, while keeping the remaining topological decisions fixed. More precisely, we select one process unit m at a time, and run several simulations, each corresponding to a different number n of equipment units in parallel (i.e., from zero, the unit does not exist, up to the maximum number of equipment units in parallel) and leaving the remaining topological decisions unchanged. In performing this step, we discard two types of topological alternatives: (i) those that violate the logical relationships among the binary variables describing allowable connections and interactions between the units, which are expressed via constraints $hq = 0$; and (ii) those that are likely to lead to sub-optimal alternatives. To identify topologies of type (ii), we apply a heuristic rule that removes those process alternatives that place equipments in parallel in units others than the bottleneck of the topology found in iteration k. Note that all these simulations can be performed very efficiently because the starting point is the optimal solution of the NLP^k. Note that to keep the production rate constant in all the simulations, which allows for a fair comparison between the different alternatives being assessed, it is necessary to adjust the input flow rates to the units according to the yields and number of equipment units in parallel. This step can be easily performed with the process simulator assuming that all the process yields remain the same as in the optimal solution of the NLP solved in the previous iteration of the algorithm. It should be noted that all the linear constraints are accumulated in the master MILP, this means that at iteration k, the problem includes the constraints generated at the k^{th} iteration plus all the constraints of all previous iterations. In all cases, after determining the new set of values of the binary variables, the primal problem is solved again, and the overall procedure

is repeated until the termination criterion is satisfied.

4.3 Remarks

- At this point, time varying binary variables are not considered.
- All the required parameters to simulate the bioprocess are initialized in the simulator environment (i.e., properties of the components, equipment parameters, economic parameters, etc.). Also, the number of equipment units in parallel must be specified every time the simulation model is solved.
- The problem addressed in this work can be seen as a special case of the design of single product multi-stage batch plants (see Biegler et al. 1997). Note, however, that in standard scheduling formulations the operating times are assumed to be constant and the process models linear, whereas our approach accounts for variable operating times and nonlinear process models, including the kinetics of the bioreaction.
- Integer cuts can be added to the master problem in order to avoid the repetition of solution explored so far in the primal problem.
- Note that in each iteration of the algorithm we generate linearizations for the process models of both, the existing and non-existing equipment units.

5 RESULTS

The capabilities of the proposed approach are illustrated through two case studies. The implementation of the overall method is discussed in first place, whereas the case studies are described next.

5.1 Computer architecture / implementation

The model of the biotechnological plant is developed using SuperPro Designer, (Intelligen, NJ), a process simulation tool in which the mass and energy balances as well as the calculation of the key economic indicators are implemented. Note, however, that any other process simulator could be used for the same purpose.

The capabilities of this process simulator are enhanced by coupling it with a dynamic model of the bioreactor coded in Matlab and connected with SuperPro Designer, using the Component Object Module (COM) technology implemented in the Pro-Designer COM Server. The kinetic model of the bioreactor is solved by the odefun function of Matlab. Most of the problems are solved using ode45, which is based on an explicit Runge-Kutta formula, the Dormant-Prince Pair (Forsythe et al. 1977). For stiff problem, the ode15s algorithm (Shampine, 1994) can be employed.

As NLP solvers, we use the fmincon function that implements a sequential quadratic programming (SQP) method. The Hessian of the Lagrangian is updated using the BFGS formula (Powell, 1978). The master MILP is implemented in GAMS and solved with CPLEX. The termination criterion applied in the numerical examples is the NLP worsening (i.e., the algorithm stops when the NLPs start to deteriorate). In order to communicate both software packages, we use the interface GAMS-Matlab developed by Ferris (2010).

Note that the function fmincon minimizes a given objective function. In our case, we reverse the sign of the NPV in order to pose the problem as a minimization one.

5.2 Case Study I. A basic fermentation process

We first consider a basic illustrative example of a hypothetical fermentation process (Figure 3). The process includes two steps: a reaction that takes place in a fermentor, and a separation that is performed in either a decanter, a centrifuge or a filter. In the reaction-phase, the initial substrate dissolved in water reacts with oxygen forming product A and by-products (waste). In the second stage, the product is separated to obtain pure A. The production

recipe involves the following operations: charge of water (time neglected), charge of substrate (time neglected), heating (60 min), charge of inoculum (time neglected), fermentation (time to be optimized), cooling (60 min) and transfer out (time neglected) carried out in the reactor; and a separation task whose time depends on the equipment used (decanting 120 min, centrifugation 100 min, and filtration 130 min).

Substrate and water are charged at 25ºC. Then the mixture is heated until the optimal growth temperature (i.e., 37ºC) using steam at 152ºC, with an efficiency of 80% in the heat transfer. The inocolum is added when the optimal temperature is reached. The reaction is an aerobic fermentation carried out at constant temperature that is modeled by a Monod-type kinetics of the following form:

$$\mu = \mu_{max} \frac{S}{K_M + S} \tag{6}$$

where μ is the rate of formation of biomass expressed in g/l·h, S is the concentration of substrate in g/l and K_M and μ_{max} are kinetic parameters that take a value of 0.2 h^{-1} and 35 g/l, respectively. The reaction requires an aeration stream of 0.5 VVM (i.e., volume of air per volume of liquid per min). Chilled water is used to remove the metabolic heat (reaction enthalpy equals -15,478 kJ/kg). The stoichiometry of the reaction is as follows:

100 kg Substrate + 70 kg O_2 → 28 kg Biomass + 70 kg CO_2 + 60 kg H_2O + 2 kg A + 10 kg waste

The final mixture is cooled down to 25ºC, using chilled water and assuming an efficiency of 90% in the heat transfer. The mixture is then transferred to the separation equipment, where a percentage of A is separated from the remaining compounds yielding a final product with a purity of 100%. The efficiency in the decanter and filter is 90% (i.e., 90% of A is

retained and 10% is lost), whereas that of the centrifuge is 92%.

(Figure 3 could be placed here)

The design objective is to maximize the NPV assuming a fixed demand of 2025 kg/year of A. The entire process is modeled using SuperPro Designer, the kinetic model and the NLP solver are implemented in Matlab, whereas the master MILP is coded in GAMS. The bioreactor is modeled as a stoichiometric reactor in SuperPro Designer, whose conversion is provided by Matlab after integrating the DAE system that describes the kinetic model. The NLP solver is also implemented in Matlab, whereas the master MILP is solved with CPLEX interfacing with GAMS. As NLP solver, we use a gradient based method (i.e., SQP). The continuous decision variables to be optimized are the initial substrate concentration and the reaction time. The integer decision variables represent the number of equipment units in parallel, as well as the selection of a specific separation unit (i.e., decanter, centrifuge and filter) in the downstream section. The NPV calculations are performed with the default parameters used in SuperPro Designer, and assuming that the facility dependent capital costs are zero.

A preliminary analysis of the process is performed prior to the application of the optimization algorithm. Figures fig:figure4a and fig:figure4b show the dependency of the concentration of A in the reactor and total number of batches with respect to the reaction time and initial substrate concentration for a demand of 2025 kg/year. As observed, by increasing the reaction time, higher concentrations of A per batch (but fewer number of batches) are obtained. Similarly, increasing the initial substrate concentration leads to higher concentrations of A in each batch. However, as shown in Figure fig:figure5, the completion time of the reaction (i.e., time required to achieve the total depletion of the substrate) increases with the initial substrate concentration. Hence, increasing the substrate concentration indirectly diminishes the total number of batches produced per year. The task of the optimization algorithm is

therefore to find the proper values of substrate concentration and reaction time and the plant topology that minimize the negative value of the NPV.

(Figure 4 could be placed here)

(Figure 5 could be placed here)

The algorithm is next applied to the problem. It converges after 2 major iterations and 12.46 CPU seconds on a computer AMD Phenom^{TM} 8600B, Triple-Core Processor 2.29GHz and 3.23 GB of RAM memory.

(Table 1 could be placed here)

Table 2 shows the starting point and the optimized values obtained. In the base case, the concentration of glucose is 53.47 g/l, the reaction time is 15.27 hours and only one single equipment is placed in each stage and the separation unit used is the decanter. In the optimized case, the initial concentration of glucose attains its upper bound (i.e. 80 g/l) and the reaction time is 16.18 hours. As observed, the NPV is maximized by increasing the initial substrate concentration up to its upper bound, and by making the reaction time equal to the completion reaction time. By doing so, the water added to the reactor is minimized, and hence its size. This solution does not imply the use of equipment units in parallel either, and the separation unit selected for the optimal design is the decanter. The reason for this is that the decanter is cheaper than the centrifuge (where two units have to be placed in parallel) and the filter. However, for smaller A production rates the centrifuge becomes the best alternative.

With these changes, the NPV is increased by 4.71% (i.e., from 20,870 M$ to 21,854 M$). Note that increasing the initial concentration of substrate leads to larger batch throughputs and lower volumes and capital investment. On the other hand, it also leads to larger cycle

times, and hence, fewer batches per year. Particularly, in the optimized solution the reactor volume is reduced by 29% (from 7,675 l in the base case, to 5,454 l in the optimal case) and the total capital investment by 4.5%.

(Table 2 could be placed here)

5.3 Case study II. Production of L-lysine

As second example, we study the production of the amino acid L-Lysine. This product is mainly used as an animal dees additive (for more details the reader is referred to Pfefferle et al. 2003).

This is indeed a more difficult problem that requires the solution of a complex kinetic bioreactor model. The associated flowsheet (see Figure 6) comprises ten major processing units that are aggregated into three different sections: upstream, fermentation and downstream. The upstream processing includes all unit operations required to prepare the feed streams. In this section, the nutrients are mixed in a blending tank and mixed with water before being sterilized and transferred to the fermentor. When the reaction is completed, the mixture is transferred to a stabilization vessel and then filtered. The permeate is pumped to an evaporation unit that removes most of the water content. The broth is finally spray-dried and processed to granules. For biomass removal, we consider the following process alternatives: a rotary vacuum filtration, a micro filtration and a centrifugation.

(Figure 6 could be placed here)

The bioprocess includes a fed-batch reactor that uses a genetically modified microorganism (i.e., *Corynebacterium glutamicum*). The main reactants are threonine, nutrients (glucose, NH_4OH and KH_2PO_4), and oxygen. The set of equations describing the reaction kinetics and the associated data are taken from the literature (Heinzle et al. 2006b and Büchs 1994).

A demand of 6,202 tones Lysine/ year is considered.

The application of our algorithm to this example follows the same implementation scheme discussed in previous sections. Particularly, the bioreactor model that accounts for the kinetics of the lysine production is implemented in Matlab and solved by the ODE solver ode15s. The decision variables are the initial concentrations of threonine and glucose, initial volume of the fermentor (i.e., amount of raw materials fed to the bioreactor) and reaction time, which are the ones with a larger impact on the performance of the process. The discrete variables represent the number of equipment units in parallel and process units used for the biomass removal.

Figures 7 and 8 show the results of coupling the bioreactor model with the process model for a fixed topology with one fermentor in parallel and a rotatory vacuum filter. Specifically, in Figure 7a, the unit production cost, the space-time-yield (STY) (i.e., mass of L-lysine produced per unit of volume and time in the bioreactor) and the overall yield (Y_{oa}) (mass of L-lysine produced per mass of glucose consumed) are plotted versus the initial concentration of threonine. In Figure 7b, the same variables are plotted versus the initial concentration of glucose, and in Figures 8a and 8b versus the initial fermentor volume and reaction time respectively.

In all cases, we only change one decision variable at a time maintaining the remaining ones constant (1.62 g/l Threonine, 48.72 g/l glucose, 310.34 m^3 initial fermentor volume and 71.01 h of reaction time). Let us clarify that all these points violate the demand satisfaction constraint (i.e., production equals the demand of 6,202 tones L-lysine/year).

(Figure 7 could be placed here)

(Figure 8 could be placed here)

As observed in Figures 7 and 8, the selected variables have a large impact on the bioreactor performance. Within the investigated range of the decision variables, the economical objec-

tive function is highly dependent on the STY and Y_{oa}. Note that the economic performance of the process depends to a large extent on the capital investment and operating costs. The former term is mainly influenced by the STY. Specifically, larger STY values lead to lower equipment sizes. On the other hand, the operating costs are mainly affected by the Y_{oa}, since this variable has a large impact on the amount of raw materials consumed.

Higher initial concentrations of threonine increase the STY, but decrease the Y_{oa}. With regard to the glucose, the maximum STY and Y_{oa} are both found at high initial glucose concentration. The initial reaction volume is the decision variable with the smallest effect on the STY and Y_{oa}. Finally, longer times lead to high values of STY and Y_{oa} and lower unit production costs.

We studied the effect of the integer decisions (number of reactors and separators for biomass removal) on the performance of the plant for a given set of initial conditions (1.62 g/l Threonine, 48.72 g/l glucose, 310.34 m3 initial fermentor volume and 71.01 h of reaction time). Increasing the number of reactor units leads to more batches, and hence smaller equipment units. For biomass removal, three options are presented: a rotary vacuum filter(RVF), a microfilter(MF) and a centrifuge(CF). For the RVF and MF, the operation time is 8h and for the centrifuge 6h. The efficiencies of these units are: 98.5% (RVF), 93.6% (MF) and 99.6% (CF).

The preliminary analysis presented above provides some insight into the problem but cannot lead in itself to optimal solutions. The task of the optimization algorithm is to perform an exhaustive search in the entire parameters space. Two constraints are considered: production less or equal than the demand and a specification on the final concentration of L-lysine (i.e., the mass fraction should be in the range 0.36-0.76 as suggested by Stevens and Blinder 1999).

The algorithm converged in 4 major iterations and 194.90 CPU seconds on the same computer as before.

(Table 3 could be placed here)

Table 4 summarizes the base case, which has been taken from Heinzle et al. (2006b), as starting point to initialize the overall solution procedure we use this base case solution but considering a different topology (i.e., no reactors in parallel and a rotary vacuum filtration for the biomass removal). As observed, NPV increases by 13.77% compared to the base case (195,688 M$ vs. 172,003 M$). This is accomplished by using two fermentors instead of three (as was the case in the base solution adapted from Heinzle et al. 2006b) and also by properly adjusting the operating conditions of the fed-batch reactor and the rest of the upstream and downstream equipment capacities. Particularly, in the optimal solution, the initial concentrations of glucose and threonine are higher than in the other cases. These new conditions increase both the STY and Y_{oa}. The increase in the STY leads to a reduction of the equipment sizes and the associated capital investment. On the other hand, increasing the Y_{oa} reduces the raw materials consumption, and therefore the operating cost. As a result, the total capital investment and operating costs are reduced by 21.5% (79.885M$ vs 101.766M$) and 16.9% (8.830M$/year vs. 10.631M$/year) respectively, while keeping the production rate constants (6,202 tones L-lysine/year).

(Table 4 could be placed here)

6 Conclusions

This work has introduced a systematic strategy to assist in the development of biotechnological processes that allows to optimize the operating conditions and topology of the entire bioprocess. The proposed method relies on a reduced space MIDO algorithm that integrates commercial process simulators (SuperPro Designer) with optimization tools (Matlab and GAMS).

The capabilities of the method presented have been tested in two biotechnological examples: a typical fermentation process, and the production of the amino acid L-lysine. From numerical results, we concluded that it is possible to significantly improve the economic performance of bioprocesses by optimizing them as a whole. Particularly, larger benefits can be attained by properly adjusting the operating conditions and equipment sizes of all the units embedded in the flowsheet. One of the main advantages of our approach is that it makes use of a standard bioprocess simulation package, that implements the main process and economic equations. This largely simplifies the modeling and economic analysis of the whole plant, allowing for the optimization of a wide range of bioprocess facilities.

Acknowledgements

The authors wish to acknowledge support from the Spanish Ministry of Education and Science (projects DPI2008-04099 and CTQ2009-14420-C02) and the Spanish Ministry of External Affairs (projects A/023551/09, A/031707/10 and HS2007-0006).

References

Allgor RJ, Barton PI. Mixed-integer dynamic optimization I: Problem formulation. *Computers and Chemical Engineering* 1999; 23: 567–584.

Balakrishna S, Biegler LT. A unified approach for the simultaneous synthesis of reaction, energy, and separation systems. *Industrial Engineering and Chemical Research* 1993; 32:1372–1382.

Banga JR, Moles CG, Balsa-Canto E, Alonso AA. Dynamic optimization of bioreactors-a review. *Proc. Ind. Natl. Sci. Acad.* 2003; 69:257–265.

Banga JR, Moles CG, Balsa-Canto E, Alonso AA. Dynamic optimization of bioprocesses: Efficient and robust numerical strategies. *Journal of Biotechnology* 2005; 117:407–419.

Bansal V. Perkins JD, Pistikopoulos EN, Sakizlis V, Ross R. New algorithms for mixed-integer dynamic optimization. *Computers and Chemical Engineering* 2003; 27:647–668.

Biegler, LT, Grossmann, IE, Westerberg, AW. Systematic methods of chemical process design. *Prentice Hall;* 1997.

Büchs J, Precise optimization of fermentation processes through integration of bioreaction. Process computations in biotechnology.*McGraw-Hill: New Delhi;* 1994; 194–237.

Caballero JA, Milan-Yañez D, Grossmann IE. Rigorous design of distillation columns.*Ind. Eng. Chem. Res.* 2005; 44:6760–6775.

Carrasco E, Banga JR. Dynamic optimization of batch reactors using adaptive stochastic algorithms.*Ind. Eng. Chem. Res.* 1997; 36:2252–2261.

Cuthrell JE, Biegler LT. Simultaneous optimization and solution methods for batch reactor control profiles.*Computers and Chemical Engineering* 1989; 13:49–62.

Diwekar UM, Grossmann IE, Rubin ES. An MINLP Process Synthesizer for a Sequential Modular Simulator. *Ind. Eng. Chem. Res.* 1992; 31:313–322.

Gill PE., Murray W, Saunders MA. SNOPT: An SQP algorithm for large-scale constrained optimization *SIAM Journal on Optimization* 2002;12(4):979-1006.

Forsythe G, Malcolm M, Moler C. Computer Methods for Mathematical Computations. *Prentice-Hall, New Jersey;* 1977.

Groep ME, Gregory ME, Kershenbaum LS, Bogle IDL.. Performance Modeling and Simulation of Biochemical Process Sequences with Interacting Unit Operations.*Biotechnology and Bioengineering* 2000; 67:300–311.

Guillen-Gosálbez G. Sorribas A. Identifying quantitative operation principles in metabolic pathways: a systematic method for searching feasible enzyme activity patterns leading to cellular adaptive responses. *BMC Bioinformatics* 2009; 32:1372-1382.

Heinzle E, Biwer AP, Cooney CL. Development of sustainable bioprocesses. modeling and assessment. *John Wiley and Sons;* 2006; 1–116

Heinzle E, Biwer AP, Cooney CL. Development of sustainable bioprocesses. modeling and assessment. *John Wiley and Sons;* 2006; 155–165

Kravanja Z, Grossmann I.E. Computational Approach for the Modeling/Decomposition Strategy in the MINLP Optimization of Process Flowsheets with Implicit Models. *Ind. Eng. Chem. Res.* 1996; 35:2065–2070.

Petrides DP, Calandris J, Cooney CL. Bioprocess optimization via CAPD and simulation for prodcut commercialization. *Genet. Eng. New.* 1996; 16:24–40.

Koulouris A, Calandranis J, Petrides DP. Throughput Analysis and Debottlenecking of Integrated Batch Chemical Processes.*Computers and Chemical Engineering* 2000; 24:1387–1394.

Mendez CA, Cerda J, Grossmann IE, Harjunkoski I, Fahl M. State-of-the-art review of optimization methods for shrt-term scheduling of batch processes. *Computers and Chemical Engineering* 2006; 30:913-946.

Petrides DP, Papavasileiou V, Kolouris A. Siletti C. Optimize manufacturing of pharmaceutical products with process simulation and production. *Chemical Engineering Research and Design* 2006; 85:1086-1097.

Pfefferle W, Moeckel B, Bathe B, Marx A. Biotechnological manufacture of Lysine *Adv. Biochem. Eng. Biotechnol* 2003; 79:59-112.

Pistikopoulos EN, Sakizlis V, Perkins JD. Recent advances in optimization-based simultaneous process and control design.*Computers and Chemical Engineering* 2010; 28:2069–2086

Pozo C. Sorribas A. Vilaprinyo E. Guillén-Gosálbez G. Jiménez L. Alves R. Optimization and evolution in metabolic pathways: global optimization techniques in Generalized Mass Action models.*Journal of biotechnology* 2010; 149:141–153

Powell MJD. A Fast Algorithm for Nonlinearly Constrained Optimization Calculations. Numerical Analysis. *Springer Verlag;* 1978.

Raghunathan AU, RPérez-Correa JR, Biegler LT. Data Reconciliation and Parameter Estimation in Flux-Balance Analysis. *Biotechnology and Bioengineering* 2003; 84:700–709.

Shampine LF. Numerical Solution of Ordinary Differential Equations. *Chapman and Hall, New York;* 1994.

Stevens J, Blinder T. Porcess for making granular L-lysine. *US Patent US 005 990 350A;* 1999.

Sarkar D, Modak JM. Pareto-optimal solutions for multi-objective optimization of fed-batch bioreactors using nondominated sorting genetic algorithms. *Chemcial Engineering Science* 2005; 60:481–492

Terrazas-Moreno S, Flores-Tlacuahuac A, Grossman IE. Simultaneous Cyclic Scheduling and Optimal Control of Polymerization Reactors. *AICHE Journal* 2007; 53:2301–2315

Viswanathan J, Grossman IE. A combined penalty function and outer approximation method for MINLP optimization. *Computers and Chemical Engineering* 1990; 14:769–782

Wong VVT, Oh SKW, Kuek KH. Design, simulation and optimization of a large scale monoclonal antibody production plant. *Pharmaceutical Engineering* 2004; 24:24–60

NOMENCLATURE

Abbreviatures

CF	centrifuge
COM	component Object Module
DAEs	differential-algebraic equations
MF	microfilter
MIDO	mixed-integer dynamic optimization
MILP	mixed-integer linear programming
MINLP	mixed-integer non-linear programming
NLP	non-linear programming
ODE	ordinary differential equation
RVF	rotary vacuum filter
SQP	successive quadratic programming
STY	space time yield (g/L·h)
Y_{oa}	overall yield (g/g)

Indices

a	algebraic
d	differential
f	final
i	intermedium
m	type unit selected
n	units in parallel
k	iterations
p	equality
q	inequality
0	intial

Variables

K_M	substrate concentration at half max. rate (g/l)
NPV	Net Present Value ($)
S	Substrate concentration (g/l)
STY	Space-time yield (g/l·h)
VVM	Volume of air per volume of liquid per min
Y_{oa}	Overall-yield (g/g)
μ	specific growth rate (g/l·h)
μ_{max}	maximum specific growth rate (g/l·h)

Bioreaction parameters

c_L	oxygen concentration (g/L)
c_P	product concentration (g/L)
c_S	substrate concentration (g/L)
c_{SF}	substrate concentration in the feed (g/L)
c_{sIN}	initial substrate concentration (g/L)
c_{Thr}	threonine concentration (g/L)
c_x	biomass concentration (g/L)
F	rate of feed (feed rate) (L/h) or (m3/h)
K_La	specific mass transfer coefficient (1/h)
K_{IP}	product inhibition constant (g/L)
K_{IThr}	threonine inhibition constant (g/L)
K_O	substrate oxygen affinity constant (g/L)
K_{PS}	product affinity constant (g/L)
K_s	substrate carbon source affinity constant (g/L)
K_{Thr}	substrate threonine affinity constant (g/L)
L_{O2}	oxygen solubility (mol/L/bar)
mo	specific oxygen consumption for maintenance (g/L)
ms	specific substrate consumption for maintenance (g/L)

OTR	oxygen transfer rate (mol/L·h)
P_R	reactor pressure (bar)
r_p	rate of lysine production (g/L·h)
STY	space time yield (g/L·h)
t	time (h)
V	fermenter filling volume (m3)
y_l	mole fraction of oxygen in the liquid phase (mol/mol)
y_{o2}	mole fraction of oxygen in the gas phase (mol/mol)
Y_{oa}	overall yield (g/g)
$Y_{P/O}$	product yield per amount of oxygen (g/g)
$Y_{P/S}$	product yield per amount of substrate (g/g)
$Y_{x/s}$	biomass yield per amount of substrate (g/g)
$Y_{x/o}$	biomass yield per amount of oxygen (g/g)
$Y_{x/Thr}$	biomass yield per amount of threonine (g/g)
a_p	growth-associated coefficient for product synthesis (g/g)
ßp	non-growth-associated coefficient for product synthesis (g/g·h)
μ	specific growth rate (1/h)
μ_{max}	maximum specific growth rate (1/h)

A Biochemical reaction model for a fed-batch reactor to produce L-lysine

Mass balance for glucose $\frac{dc_s}{dt} = -\frac{1}{Y_{X/S}} \cdot \mu \cdot c_x - \frac{1}{Y_{P/S}} \cdot r_p \cdot c_x - m_s \cdot c_x + \frac{F}{V}(c_{SF} - cs)$

Mass balance for oxygen $\frac{dc_L}{dt} = -\frac{1}{Y_{X/O}} \cdot \mu \cdot c_x - \frac{1}{Y_{P/O}} \cdot r_p \cdot c_x - m_s \cdot c_x + OTR$

Mass balance for threonine $\frac{dc_{Thr}}{dt} = -\frac{1}{Y_{X/Thr}} \cdot \mu \cdot c_x - \frac{F}{V}(c_{Thr})$

Mass balance for biomass $\frac{dc_x}{dt} = \mu \cdot c_x - \frac{F}{V} \cdot c_x$

Mass balance for lysine $\frac{dc_P}{dt} = r_P \cdot c_x - \frac{F}{V} \cdot c_P$

Mass balance for the fermenter volume $\frac{dV}{dt} = F$

Kinetic model for oxygen transfer $OTR = k_L a \cdot L_{O_2} \cdot p_R \cdot (y_{O_2} - y_L)$

Kinetic model for growth $\mu = \mu_{max} \cdot \frac{c_s}{c_s + K_s} \cdot \frac{c_L}{c_L + K_O} \cdot \frac{c_L}{c_L + K_T hr}$

Kinetic model for lysine formation $r_P = (\alpha_P \cdot \mu + \beta_P) \cdot \frac{c_s}{c_s + K_{PS}} \cdot \frac{c_L}{c_L + K_O} \cdot \frac{K_{IThr}}{c_{Thr} + K_{IThr}} \cdot \frac{K_{IP}}{c_P + K_{IP}}$

Overall yield $Y_{oa} = \frac{c_p}{c_{S_{IN}}}$

Space-time yield $STY = \frac{c_P}{t}$

List of Tables

Table 1: Progress of iterations of MIDO algorithm in the optimization of component A production plant

Iteration Number	NLP1	MILP1	NLP2
Discrete decisions			
Fermentors	1	2	2
Equipment separation phase	Decanter	Decanter	Decanter
Objective function			
J^k [\$]	$2.18{\cdot}10^7$	$2.79{\cdot}10^7$	$1.90{\cdot}10^7$
CPU time [s]	5.59	0.15	6.87

Table 2: Results of the optimization of component A production plant

	Initial Point	Optimal Point
Net present value [M$]	20,870	21,854
Total capital investment [M$]	6.164	5.874
Operating cost [M$/year]	2.962	2.758
Production rate [kg A/year]	2,025	2,025
Unit production cost [$/kg A]	1.462	1.362
Batch throughput [kg A/batch]	5.84	6.16
Recipe batch time [h]	19.27	20.18
Recipe cycle time [h]	17.27	18.18
Annual operating time [h]	5,994	5,984
Number of batches per year	347	329
Substrate concentration [g/l]	53.47	80.00
Reaction time [h]	15.27	16.18
Fermentors	1	1
Fermentor volume [l]	7675.89	5454.16
Separator	Decanter	Decanter
Volume separator [l]	97.32	56.47

Table 3: Progress of iterations of MIDO algorithm in the optimization of L-lysine production plant

Iteration Number	NLP1	MILP1	NLP2	MILP2	NLP3	MILP3	NLP4
Discrete decisions							
Fermentors	1	2	2	2	2	3	3
Equipment separation phase	MF	MF	MF	RVF	RVF	RVF	RVF
Objective function							
J^k [\$]	$7.01{\cdot}10^7$	$2.00{\cdot}10^8$	$1.66{\cdot}10^8$	$1.85{\cdot}10^8$	$1.95{\cdot}10^8$	$2.26{\cdot}10^8$	$1.82{\cdot}10^8$
CPU time [s]	55.34	0.21	44.04	0.17	41.20	0.19	53.75

Table 4: Results of the optimization of L-lysine production plant

	Base Case	Initial Point	Optimal Point
Net present value [M$]	172,003	59,276	195,688
Total capital investment [M$]	101.766	55.369	79.885
Operating cost [M$/year]	10.631	4.854	8.830
Production rate [tones L-lysine/year]	6,202	2,611	6,202
Unit Production cost [$/kg L-lysine]	1.71	1.86	1.42
Batch Throughput [tons L-lysine/batch]	29.674	27.783	44.300
Recipe Batch time [h]	111.07	110.46	137.67
Recipe Cycle time [h]	37.51	83.51	55.81
Number of batches per year	209	94	140
Concentration Threonine [g/l]	1.62	1.62	1.92
Concentration Glucose [g/l]	48.72	48.72	94.61
Initial Volume Ferment [m^3]	310.34	310.34	282.77
Reaction time [h]	71.01	71.01	97.16
Fermentors	3	1	2
Space-time yield [g/l·h]	1.022	1.022	1.103
Overall yield [g/g]	0.299	0.299	0.316
Separator	RVF	MF	RVF

List of Figures

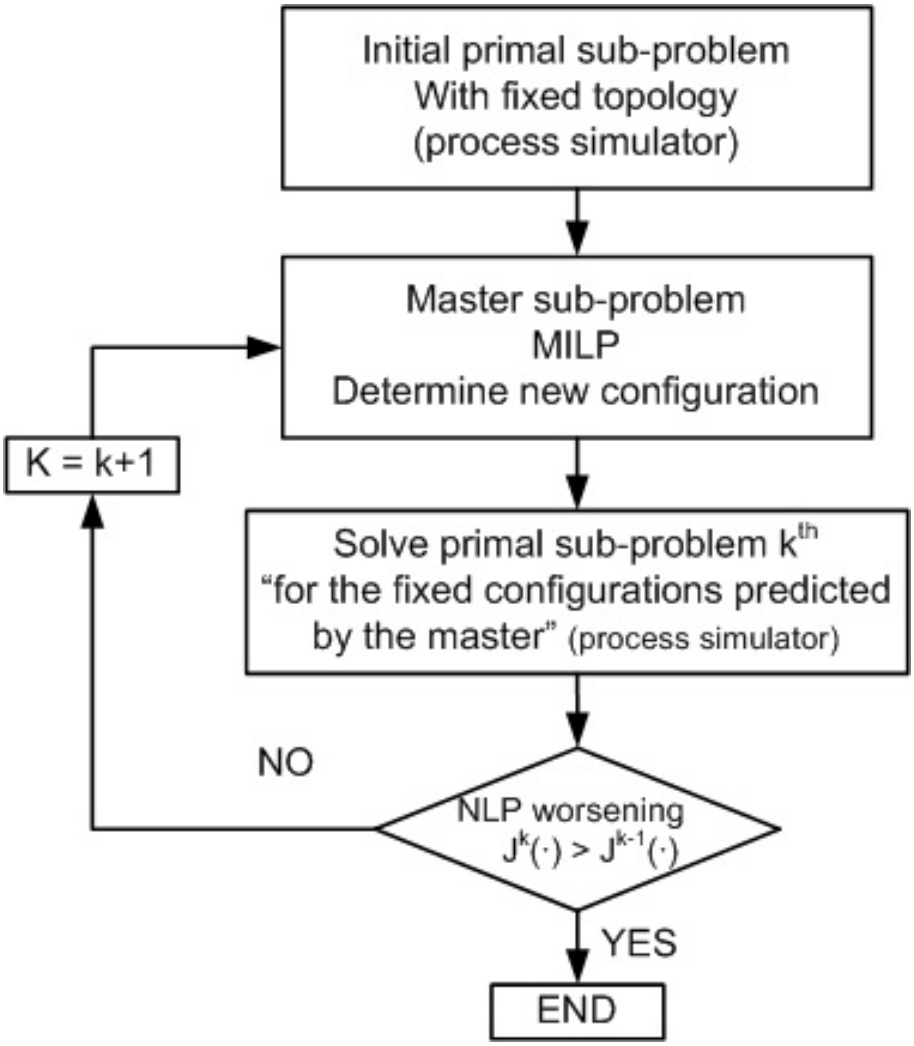

Figure 1: Flowchart of the proposed algorithm

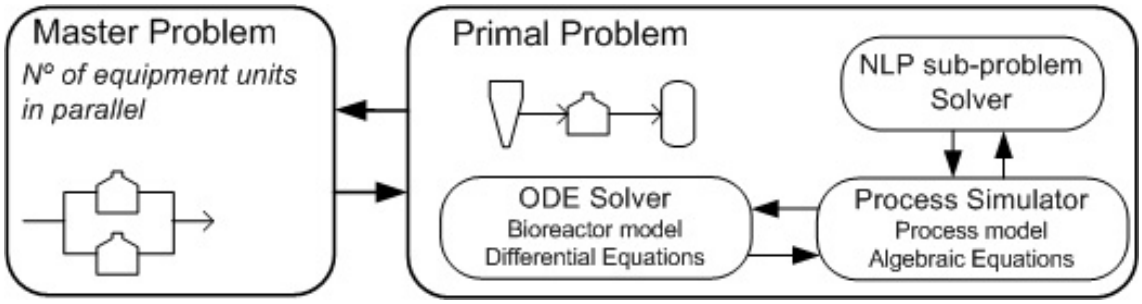

Figure 2: Main steps in the resolution of the NLP sub-problem

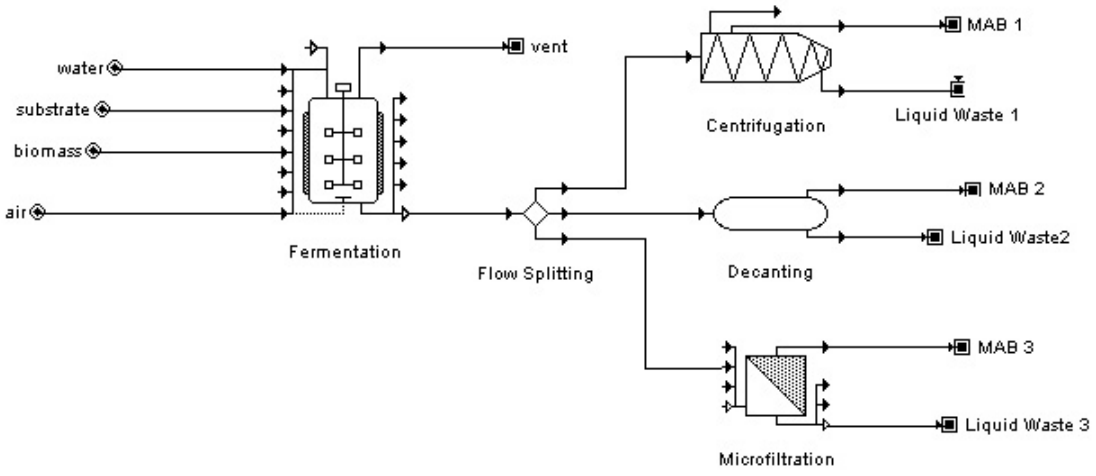

Figure 3: Process flow diagram of a typical ferementation process

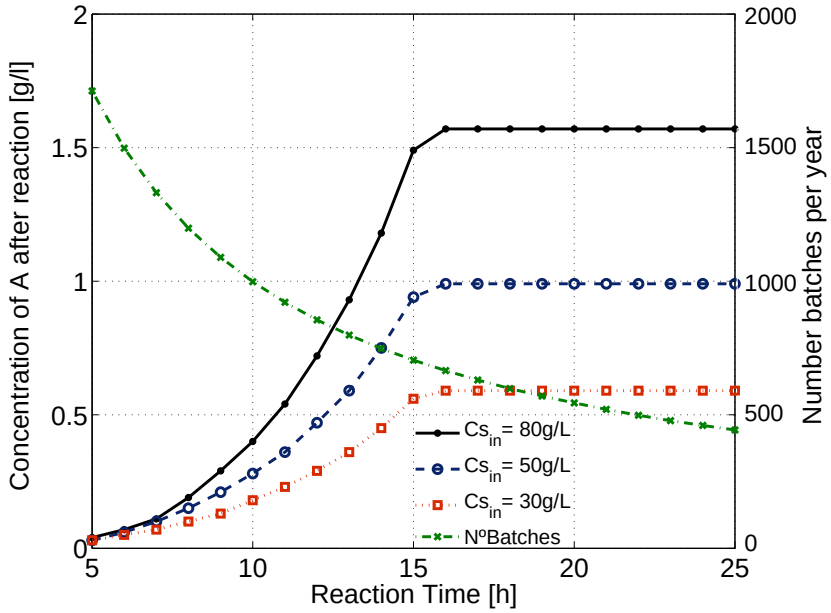

(a) Concentration of A and number of batches versus reaction time for a fixed demand of 2025 kg/yr

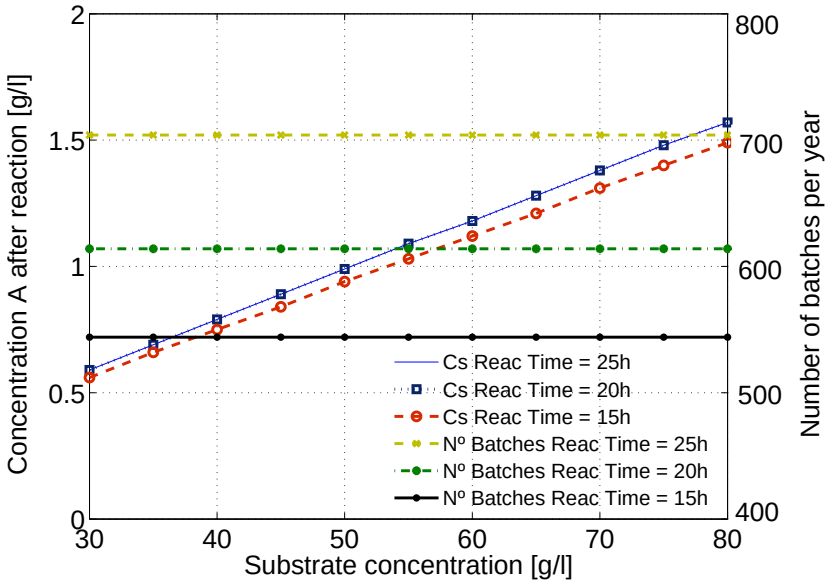

(b) Concentration of A and number of batches versus initial substrate concentration for a fixed demand of 2025 kg/yr

Figure 4: Preliminary analysis of the decision variables in the case study 1

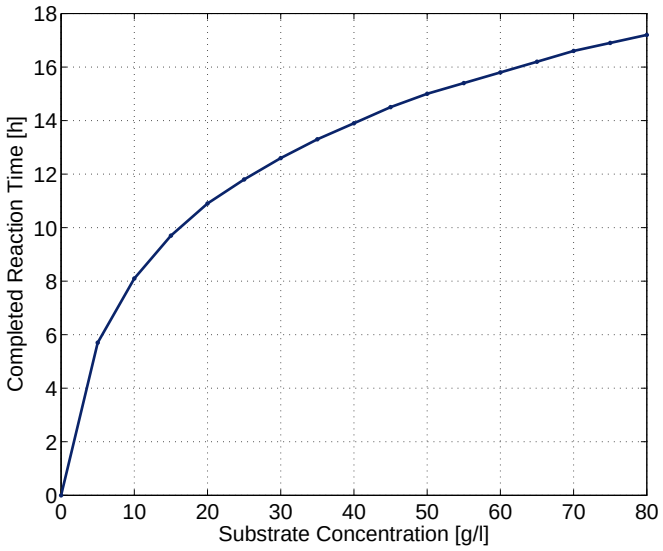

Figure 5: Completed reaction time (i.e., reaction time for which concentration of substrate is zero)versus substrate concentration

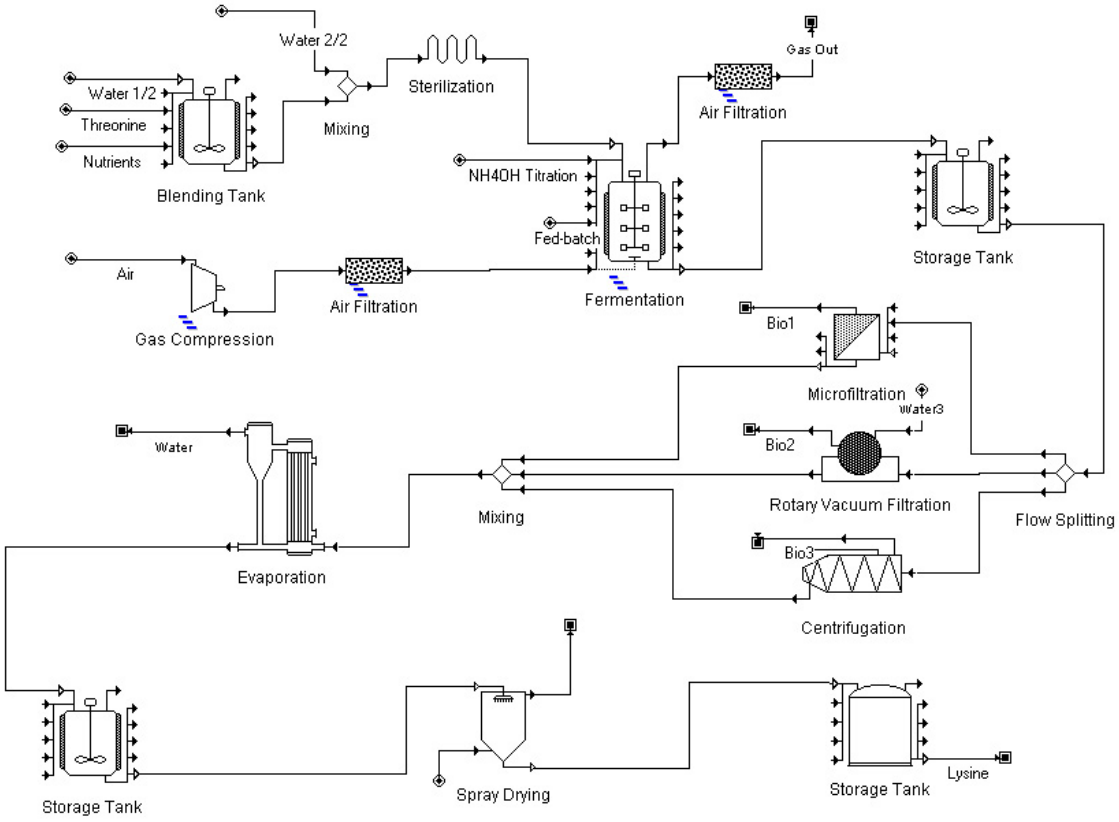

Figure 6: L-lysine production plant (adapted from Heinzle et al.,2006)

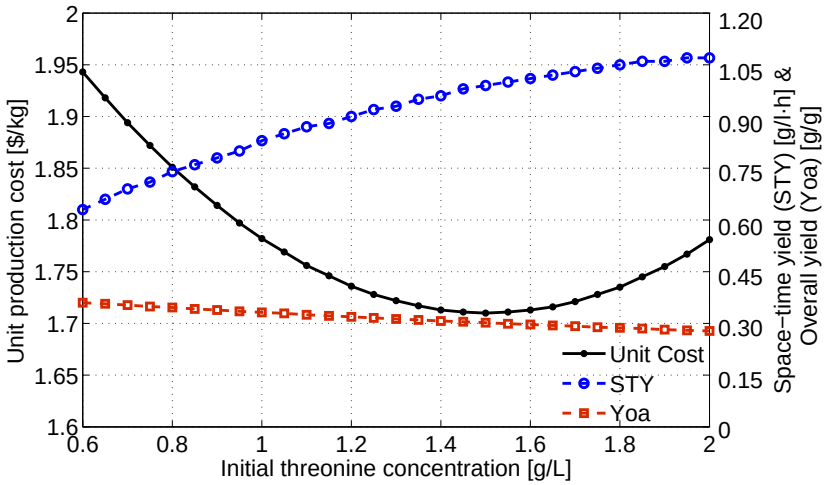

(a) Relationship between the unit production cost, STY and Y_{oa} and the initial threonine concentration (C_{Thr}), maintaining the rest of the decision variables constant

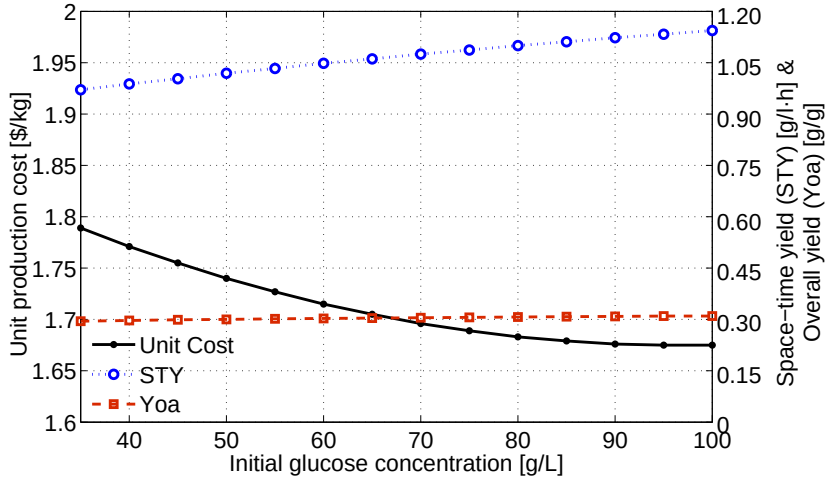

(b) Relationship between the unit production cost, STY and Y_{oa} and the initial glucose concentration (Cs_{in}), maintaining the rest of the decision variables constant

Figure 7: Preliminary analysis of the decision variables in case study 2

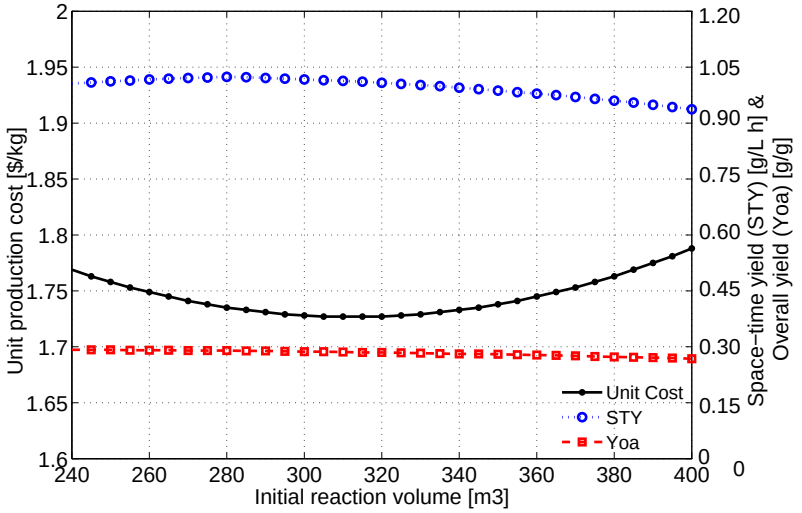

(a) Relationship between the unit production cost, STY and Y_{oa} and the initial reactor volume, maintaining the rest of the decision variables constant

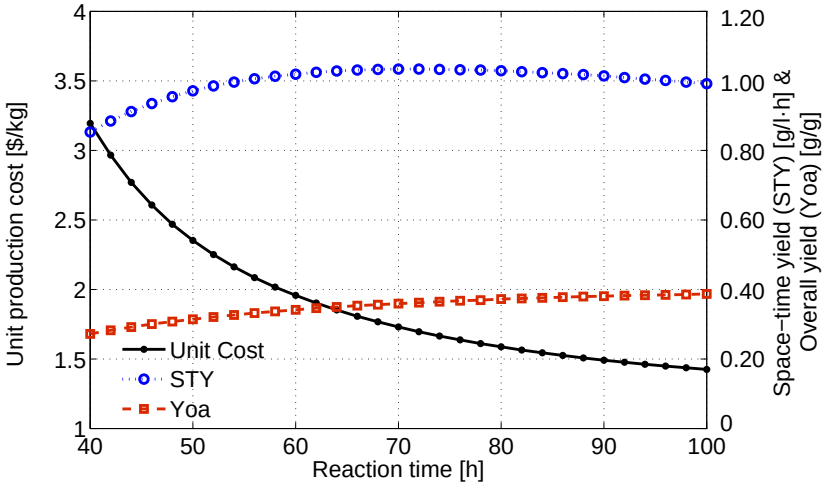

(b) Relationship between the unit production cost, STY and Y_{oa} and the initial reaction time, maintaining the rest of the decision variables constant

Figure 8: Preliminary analysis of the decision variables in case study 2

Article 2

Authors: **R. Brunet**, G. Guillén-Gosálbez, L. Jiménez.

Title: Cleaner design of single-product biotechnological facilities through the integration of process simulation, multi-objective optimization, LCA and principal component analysis.

Journal: *Industrial & Engineering Chemistry Research*

Volume: 51 (1) **Pages:** 410-424 **Year:** 2012

ISI category: Chemical Engineering **AIF:** 0.608

Impact Index: 2.071

Position in the category: 29/135 (Q1)

Cites: -

Cleaner design of single-product biotechnological facilities through the integration of process simulation, multi-objective optimization, LCA and principal component analysis

Robert Brunet, Gonzalo Guillén-Gosálbez*and Laureano Jiménez
Departament d'Enginyeria Quimica, Escola Tecnica Superior d'Enginyeria Quimica,
Universitat Rovira i Virgili, Campus Sescelades, Avinguda Paisos
Catalans 26, 43007, Tarragona, Spain

*Corresponding author. E-mail: gonzalo.guillen@urv.cat, telephone: +34 977558618

Abstract

Bioprocesses have been typically optimized according to their economic performance. In this work we present a novel framework for their optimal design that allows for the simultaneous consideration of economic and environmental concerns. Our approach relies on the combined use of simulation packages, multi-objective optimization (MOO), life cycle assessment (LCA) and principal component analysis (PCA). The capabilities of the proposed methodology are illustrated through its application to the production of the amino acid L-lysine.

Keywords: *combined simulation-optimization, biotechnological processes, multi-objective optimization, life cycle assessment, principal component analysis*

1 Introduction

Sustainability has recently gained wider interest in process systems engineering (PSE). As a result, intensive research effort is currently being devoted towards the incorporation of environmental criteria in the decision-making process. This general trend has motivated the development of systematic strategies for quantifying and minimizing the environmental impact of process industries [1].

An overwhelming majority of the methods that provide decision-support for environmentally conscious process design have focused on the chemical sector. In contrast, the optimization of biotechnological facilities with environmental concerns has received little attention to date. In the recent past, these processes have become increasingly important, due to their potential to produce high-value products in human health and care applications. Hence, there is a clear need for developing systematic tools to reduce their cost and environmental impact.

Optimization approaches devised so far in biotechnology have primarily focused on improving the economic performance, paying special attention to the bioreactor step. Cuthrell and Biegler [2] optimized a fed-batch reactor for penicillin production with a solution strategy based on successive quadratic programming (SQP) and orthogonal collocation on finite elements. Carrasco and Banga [3] addressed the dynamic optimization of batch and fed-batch reactors using stochastic optimization algorithms. More recently, Banga et al. [4] introduced a new solution method for this problem based on control parametrization, whereas Sarkar and Modak [5] proposed the use of genetic algorithms in the same context.

The optimization of complete bioprocesses considering all their individual steps has received less attention to date. Groep et al. [6] applied a simple sensitivity analysis to optimize a typical enzyme production process. Pinto et al. [7] proposed a model that simultaneously optimizes the process variables and structure of a multi-product batch plant that produces recombinant proteins. Montanga et al. [8] applied generalized disjunctive programming (GDP) in the synthesis of insulin plants.

The environmental impact of bioprocesses was traditionally neglected in all of these approaches, mainly because of their small scale in comparison with their petrochemical counterparts. It was not until the Environmental Protection Agency (EPA) increased the regulatory controls in the bioprocess industry, when authors such as Konopacz [9] started to highlight the importance of assessing their environmental performance. To the best of our knowledge, the work by Steffens et al. [10] was the first to address the optimal design of a biotechnological plant (penicillin manufacturing) with economic and environmental criteria. Dietz et al. [11] optimized also a multi-product batch plant for proteins production, using genetic algorithms. The aforementioned optimization works focused on assessing the environmental performance at the plant level. This approach can lead to solutions that shift environmental burdens from one echelon of the bioprocess supply chain to another, thereby increasing the overall damage. Further, these methods restrict the environmental analysis to one single environmental indicator, neglecting other damage categories. This simplification may eventually result in solutions in which one environmental impact is decreased at the expense of increasing other damages. To the best of our knowledge, there is one single contribution in the literature by Jimenez-Gonzalez and Woodley [12] that applies life cycle assessment (LCA) principles to bioprocess industries. This work, however, is somehow limited, as it focuses on assessing the envirnomental performance of a bioprocess but it does not include any systematic procedure to minimize it.

In this work we introduce a novel framework for the optimal development of biotechnological processes with economic and environmental concerns that overcomes the limitations mentioned above. More precisely, we present advances in the following two fronts: (i) the combined use of optimization tools (i.e., multi-objective mixed-integer nonlinear programming (moMINLP) techniques), commercial simulation packages (i.e., SuperPro Designer), and LCA principles within a unified framework; and (ii) the use of PCA as an effective tool to uncover and visualize the results of the multi-objective optimization (MOO) problem arising in the design of these facilities. Our method has been tested in a typical fermentation

process, the production of the amino acid L-Lysine.

2 Problem Statement

The problem addressed in this work can be formally stated as follows. Given are the annual production demand, final product prices, cost parameters (capital investment and operating cost), time horizon, thermodynamic properties, performance models of the equipment units embedded in the flowsheet and LCA data (i.e., life cycle inventory of emissions and feedstock requirements and parameters of the damage model). The goal is to determine the optimal process design, including equipment sizes, structural alternatives and operating conditions (concentrations, flow rates, temperatures, etc.) that maximizes a given economic performance indicator and minimizes the associated environmental impact.

We consider single-product batch plants that can operate with more than one equipment unit (in parallel) per stage. It is assumed that parallel equipment units have the same size and operating conditions and that they operate out of phase with respect to the first unit, that is, they start operating after the starting time of the first unit. This allows reducing the cycle time of the process. Further details on this topic can be found in Biegler et al. [14]. As opposed to standard scheduling models, we consider that the operating times and batch sizes are continuous variables to be optimized rather than fixed parameters. It should be emphasized that several bioprocesses follow this general pattern, such as the production of penicillin, citric acid, pyruvic acid, vitamin riboflavin, human serum and insulin, monoclonal antibodies, and plasmid DNA, among many others. Hence, the complexity of the design task largely comes from the need to optimize nonlinear process models describing the equipment units operation, some of which may involve systems of ordinary differential equations (ODEs), and not from the combinatorial nature of the batch facility itself.

3 Proposed approach: integration of process simulation, MOO, LCA and PCA

As mentioned before, our solution method integrates several engineering tools within a unified framework. In this section we first describe the MOO model. It is constructed combining explicit constraints defined in an algebraic modeling system with implicit equations implemented in the simulation package. We will then provide details on the inclusion of LCA principles within the mathematical formulation and present a method for its efficient solution. We end this section with a discussion on the use of PCA to analyze and interpret the results generated by the MOO.

3.1 3.1. Simulation-optimization model

Most MOO approaches used in process design rely on monolithic algebraic formulations that embed "short-cut" models. These methods cannot handle some unit operations, such as non-ideal distillation columns, reactors with complex kinetics, etc. In this work, we integrate process simulation packages with MOO tools to address the optimization of bioprocesses, including all their individual steps.

In mathematical terms, the synthesis of biotechnological processes with environmental concerns can be formulated as a moMINLP problem with the following form:

$$\begin{aligned} \min_{x_D} \quad & U = \{f_1(x,u,x_D),...,f_m(x,u,x_D)\} \\ \text{s.t.} \quad & h_I(x,u,x_D) = 0 \\ & h_E(x,u,x_D) = 0 \\ & g_E(x,u,x_D) \leq 0 \end{aligned}$$

Here f_1 represents the economic objective function, whereas f_2 to f_m denote the set of environmental metrics. Equations h_I are implicit constraints solved by the process simulator, whereas h_E and g_E are explicit external constraints. The continuous design variables corre-

spond to x_D, whereas x denotes the remaining process variables calculated by the simulator, and u represents fixed parameters not modified during the calculations. Note that x_D includes both, continuous variables (pressures, temperatures, flow rates, etc.), and discrete variables such as the type and number of equipment units in parallel.

Note that we assume herein that all model parameters can be perfectly known in advance (i.e., they are deterministic). Uncertainty sources could be however incorporated into the formulation in a manner similar as done before by the authors [15] [16].

3.2. Integration of life cycle assessment principles

In this work we follow a combined approach that integrates process simulation and MOO with LCA principles. Process simulation is employed to perform mass and energy balances that provide the amount of raw materials, energy consumed, emissions released and waste generated by the bioprocess. This information is further translated into life cycle emissions and feedstock requirements using an environmental database (i.e., Ecoinvent Database [17]) that stores information related to common industrial processes found in Europe. In the last step, these data are translated into impact using a damage assessment model.

Note that Life cycle assessment [18] is a well established methodology for environmental assessment. There is a research journal devoted entirely to LCA (International Journal of LCA) and there are many environmental studies reported in other journals that employ this methodology. In our work, we follow the Eco-indicator 99 methodology, an LCA-based metric that quantifies the impact considering all the stages in the life cycle of a process.

The combined use of MOO and LCA, which was formally introduced by Azapagic and Clift [19], has recently attracted an increasing attention in PSE. This methodology couples LCA principles, used to quantify the environmental performance of a process, with optimization tools. Examples of this general approach can be found in the works by Azapagic and Clift [20] (production of boron compounds), Alexander et al. [21] (design of a nitric acid plant), Khan et al. [22] (production of vinyl chloride monomer), Baratto et al. [23]

(design of auxiliary power units), Carvalho et al. [24] (design of a methyl tertiary butyl ether plant), Guillén-Gosálbez et al. [25] (optimization of the hydrodealkylation of toluene process), Gebreslassie et al. [26] (design of absorption cooling systems), Kikuchi et al. [27] (production of biomass-derived polypropylene) and Hugo et al. [28], Guillén-Gosálbez and Grossmann [16] and Puigjaner and Guillén-Gosálbez [29] (design of chemical supply chains), among some others. Further, case studies on the combined use of process simulation and LCA are available in Azapagic et al. [30] and Bojarski et al. [31].

The LCA methodology (ISO 14040:2006) that enables the computation of the environmental impact of the process is applied in four phases:

1. Goal and scope definition. This is the first stage of the LCA. At this point, we must define the system boundaries of the system, the functional unit, the methodology used to quantify the impact and the data and assumptions required to perform the LCA. In this work we address the analysis of a bioprocess production plant. The functional unit of the system is a fixed amount of final product. The environmental impact is assessed according to the Eco-indicator 99 methodology [32], which follows LCA principles.

2. Life cycle inventory analysis (LCI). To calculate the entries of the life cycle inventory of emissions and feedstock requirements (continuous variable LCI_b) we proceed as follows. We first extract from the simulation model the relevant streams crossing the boundaries of the system. Raw materials, energy and utilities consumed are regarded as inputs, whereas byproducts and waste generated are outputs from the system. In addition, the simulation package provides the amount of steel required for the construction of the equipment units embedded in the flowsheet. All this information is translated into the corresponding life cycle emissions and feedstock requirements using standard environmental databases [17].

3. Life Cycle Impact Assessment (LCIA). In this phase, the environmental burdens are translated into a set of impacts. Specifically, the damage caused in each impact category dam_d is determined from the life cycle inventory entries (i.e., emissions and feed-

stock requirements) (continuous variable LCI_b) and the corresponding set of damage factors (parameter $df_{b,d}$).

$$dam_d = \sum_b df_{b,d} \cdot LCI_b \qquad \forall d$$

The impact is assessed according to the Eco-Indicator 99 methodology (Eco-99) [32], which considers 10 environmental impacts that are further aggregated into the following damage categories: damage to human health (HH), damage to ecosystem quality (EQ) and depletion of resources (DR). Note that here we do not determine the final ECO-99 value with a specific normalization and weighting factors [32]. Instead we analyze each of its three damage categories separately.

4. Life cycle Interpretation. In the last LCA phase, the results are analyzed, and a set of conclusions and recommendations are formulated. In the context of our approach, this phase is carried out in the post-optimal analysis of the solutions of the MOO problem. One of the limitations of the combined use of LCA and optimization techniques is that the generation and interpretation of solutions become more complex as one increases the number of environmental objectives. In this work we explore the use of PCA to analyze the results of the MOO. As we will discuss later in the article, this technique allows uncovering relationships between environmental impacts, thereby facilitating the decision-making process.

4 Solution procedure

The solution of the MOO problem is given by a set of Pareto optimal process designs, each one achieving a unique combination of environmental and economic performance. In this work we solve this problem via the epsilon constraint method [33] although any other method could be used for the same purpose. This strategy is based on formulating an aux-

iliary model, where one objective is kept in the objective function (let us say objective one) and the remaining ones are transferred to auxiliary constraints.

$$
\begin{aligned}
\min_{x_D} \quad & z = f_1(x, u, x_D) \\
\text{s.t.} \quad & f_o(x, u, x_D) \leq \epsilon_o \qquad o = 2, ..., m \\
& \underline{\epsilon_o} \leq \epsilon_o \leq \overline{\epsilon_o} \qquad o = 2, ..., m \\
& h_I(x, u, x_D) = 0 \\
& h_E(x, u, x_D) = 0 \\
& g_E(x, u, x_D) \leq 0
\end{aligned}
$$

In this model, f_1 is the economic objective function, whereas f_2 to f_m denote the LCA metrics. Note that the environmental objectives have been transferred to a set of inequality constraints that include an auxiliary epsilon parameter ϵ. The original problem is first solved by optimizing each single scalar objective separately. This provides the lower and upper bounds of the epsilon interval. This interval is then split into a given number of sub-intervals, for which the original model is calculated. The solutions obtained following this procedure are finally filtered applying the dominance concept.

For solving each single-objective problem, we use an approach inspired by the works of Caballero et al. [34]. Our strategy relies on decomposing the problem into two hierarchical levels: a primal NLP and a master MILP, as shown in Figure 1 (more details can be found in the work by Brunet et al. [35]). The primal level entails the solution of a NLP sub-problem, in which the integer decisions (number of equipment units in parallel and topological decisions) are fixed. The solution of this sub-problem requires calculations performed by the bioprocess simulator. On the other hand, the task of the customized master problem is to decide on the value of the integer variables. The algorithm solves iteratively both sub-problems until a termination criterion is satisfied (e.g. the current primal sub-problem yields an optimal objective function that is worse than the previous one). We next describe each level of the algorithm in more detail.

(Figure 1 could be placed here)

4.1. Primal sub-problem

The primal level entails the solution of a NLP sub-problem at iteration k of the algorithm for fixed values of the binary variables. This NLP is calculated by coupling the NLP solver with a process simulator, which calculates mass, energy and economic balances. This approach takes advantage of the customized process unit models already implemented in the bioprocess simulator, thereby avoiding their definition in an explicit form (i.e. equation oriented).

If the process simulator does not converge when the solver sends a set of design variables, then the complete procedure fails. To avoid this, the problem is modified to properly handle infeasible solutions. This is done by adding slack variables and an exact penalty to the objective function, as shown in the following formulation:

$$
\begin{aligned}
\min_{x_D} \quad & z = f_1(x,u,x_D) + \prod(s + s_1 + s_2 + s_3) \\
\text{s.t.} \quad & f_o(x,u,x_D) \leq \ \epsilon_o + s_1 && o = 2,...,m \\
& \underline{\epsilon_o} \leq \ \epsilon_o \leq \ \overline{\epsilon_o} && o = 2,...,m \\
& h_I(x,u,x_D) = 0 \\
& h_E(x,u,x_D) + s_2 - s_3 = 0 \\
& g_E(x,u,x_D) \leq \ s \\
& s \geq \ 0; s_1 \geq \ 0; s_2 \geq \ 0; s_3 \geq \ 0;
\end{aligned}
$$

where $\prod$ is a penalty parameter vector, and s, s_1, s_2 and s_3 are vectors of positive slack variables.

All the required parameters to simulate the bioprocess are initialized in the simulation environment (i.e., properties of the components, equipment parameters, economic data, etc.). Also, the number of equipment units in parallel must be specified for each solution being

optimized.

4.2. Master sub-problem

The goal of the master problem is to provide a new set of values for the binary variables that lead to better results than the previous solution. Here, we present a tailored master MILP that exploits the problem structure. Note that due to the presence of nonconvexities in the NLP, the master MILP is not guaranteed to provide a rigorous lower bound on the optimal solution. We define the following sets at iteration k of the algorithm:

$T = \{i | i$ is a potential bioprocess configuration$\}$
$T_k = \{i | i$ is a potential bioprocess configuration that can be obtained by performing$\}$
one single structural modification on the design obtained at iteration k of the algorithm
$EQ = \{j | j$ is an external equality constraint (explicit constraint)$\}$
$IEQ = \{j | j$ is an external inequality constraint (explicit constraint)$\}$
$D = \{n | n$ is a design variable (independent variable)$\}$

To generate the master problem, the design variables x_D are fixed to the optimal value obtained in the latest k iteration of the algorithm and a series of simulation problems are solved. Particularly, we run i simulations, each one corresponding to a different possible topology. The following notation is used in the master problem:

$\Delta obj^k_{i,o}$ = Difference between the objective function o at iteration k of the NLP
and the objective function associated with the new topology i
$\Delta g^k_{i,j}$ = Difference between the values of the inequality constraint j for the
new topology i and its value in the original NLP^k problem
$\Delta h^k_{E_{i,j}}$ = Difference between the values of the external equality constraint j
in the new topology i and its value in the original NLP^k problem

Hence, the master MILP takes the following form:

$$\min \quad \alpha + \prod (\sum_{o=2}^{m} s_{1_o} + \sum_{j \in IEQ} s_{2_j} + \sum_{j \in EQ} s_{3_j})$$

$$\text{s.t.} \quad f_o(x^k, u^k, x_D^k) + \sum_n \left(\frac{\partial f_o}{\partial x_{D_n}} \right)_{x_{D_n}=x_D^i} (x_{D_n} - x_D^k) + \sum_{i \in T,k} W_i \cdot \Delta obj_{i,o}^k \leq \alpha \quad o = 1$$

$$f_o(x^k, u^k, x_D^k) + \sum_n \left(\frac{\partial f_o}{\partial x_{D_n}} \right)_{x_{D_n}=x_D^i} (x_{D_n} - x_D^k) + \sum_{i \in T,k} W_i \cdot \Delta obj_{i,o}^k \leq \epsilon_o + s_{1_o} \quad o = 2, ..., m$$

$$(x^k, u^k, x_D^k) + \sum_n \left(\frac{\partial g_j}{\partial x_{D_n}} \right)_{x_{D_n}=x_D^i} (x_{D_n} - x_D^k) + \sum_{i \in T,k} Wi \cdot \Delta g_{i,j}^k \leq s_{2_j} \quad \forall j \in IEQ$$

$$sign(\lambda_j^k) h_{E_j}(x^k, u^k, x_D^k) + \sum_n \left(\frac{\partial h_{E_j}}{\partial x_{D_n}} \right)_{x_{D_n}=x_D^i} (x_{D_n} - x_D^k) + \sum_{i \in T,k} Wi \cdot \Delta h_{E_{i,j}}^k$$

$$\leq s_{3_j} \quad \forall j \in EQ$$

$$k = 1, 2, 3, ..., K$$

$$\begin{bmatrix} s_{1_o} \geq 0 \qquad s_{2_j} \geq 0 \qquad s_{3_j} \geq 0 \\ \sum_i Wi = 1 \quad i \in T \\ W_i \in \{0, 1\} \end{bmatrix}$$

The objective function of the master problem is formed by an auxiliary variable α and a penalty for constraint violation $\prod$ that multiplies the slack variables s_1, s_2 and s_3. The first inequality constraint is formed by three terms: (i) the objective function value at iteration k of the algorithm, (ii) the linearizations of the objective function with respect to the design variables (iii) and the contribution of changing the current topology, by either adding an extra equipment unit in parallel or replacing an existing unit by another one. This last term is the product of binary variable W_i that is one if topology modification i is implemented and zero otherwise, with the the parameter Δobj_i^k, which accounts for the change in the objective function value when topology i is implemented. External inequality (IEQ) and equality (EQ) constraints are handled following a similar procedure. $sign(\lambda_j^k)$ refers to the

sign of the Lagrange multiplier of the NLP solved at iteration k of the algorithm. This value is used to correctly relax the equalities into inequalities.

It should be noted that linear constraints are accumulated in the master MILP, this means that at iteration k, the problem includes constraints generated at the current and past iteration. In all cases, after determining the new set of values for the binary variables, the primal problem is solved again, and the overall procedure is repeated until the termination criterion is satisfied. Integer cuts can be added to the master problem in order to avoid repetition of solutions explored so far in the primal problem.

Regarding the implicit constraints, it is important to remark that these sets of equations are solved by the process simulator and their derivatives are calculated using finite differences.

4.3. Interpretation of results: principal component analysis

Most approaches based on MOO applied in green engineering restrict the environmental analysis to two objectives (economic vs environmental performance). This is mainly due to the large computational cost and difficulty in visualization of the objective space when more than two environmental metrics are optimized. The use of PCA allows uncovering relationships between environmental metrics thereby facilitating the task of decision-makers during the analysis and calculation of the Pareto set.

PCA is a multivariate technique that allows to reduce the dimensionality of a data set without disturbing its main features. Here we will concentrate on using this technique to shed light on the Pareto structure of MOO problems where several environmental metrics are simultaneously minimized. The application of PCA in LCA studies was first introduced in the context of waste water treatment plants and mussel cultivation by Gutierrez et al. [36], who investigated the relationships between different LCA metrics. Deb and Saxena [37] proposed the use of PCA for reducing the dimensionality of MOO problems by identifying redundant objectives using the coefficients of the objectives in the principal components calculated from the PCA. Despite these contributions, to the best of our knowledge, PCA, has been never

used together with MOO in the context of environmental problems. PCA is particularly appealing for our purposes because it reduces the complexity of the MOO results, thereby facilitating the decision-making process. This provides a sound basis to identify redundant environmental metrics that can be left out of the problem without significant changes in its structure. This makes it easier to generate and analyze the Pareto set of solutions, tasks that are difficult to accomplish when many LCA metrics are simultaneously optimized.

Hence, the solutions of the MOO model generated using the algorithm described above are further analyzed using PCA. Note that the number of points in the PCA corresponds to the number of Pareto solutions, whereas the number of variables is given by the number of objectives. The goal of PCA is to identify a set of uncorrelated variables (i.e., objectives) from a wider set of correlated variables. Different methods have been proposed so far to accomplish this task (see Gutierrez et al. [36]). In this work, without loss of generality, we will use the approach introduced by Deb and Saxena [37], who proposed several rules to identify redundant objectives based on the analysis of the eigenvectors of the correlation matrix calculated from the efficient solutions of the MOO problem (further details on these rules are available in the original work).

The application of PCA to the results of the MOO allows to focus our attention on a reduced number of environmental metrics, thereby facilitating the post-optimal analysis of the Pareto set. Note that the integration of PCA and MOO can also be done in an iterative manner, as suggested by Deb and Saxena [37]. That is, generating Pareto solutions in a high dimensional space and gradually decreasing the number of objectives until no further reductions in the dimensionality of the problem is possible. We should remark that our methodology is general enough to be applied to any chemical plant, so it is not restricted only to bioprocesses. Hence, our approach can be easily adapted to other processes by selecting a suitable process simulator capable of reproducing the unit operations of the system in an accurate manner.

5 Results and discussion

The capabilities of the proposed approach are illustrated through the production of the amino acid L-lysine. The implementation of the overall method is discussed first before presenting the case study.

5.1. Computer implementation

The model of the biotechnological plant is developed using SuperPro Designer (Intelligen, NJ), a process simulation tool in which mass and energy balances as well as economic calculations are implemented. The process simulator is coupled with external modules that implement the bioreactor model and the LCA calculations. These modules are coded in Matlab and connected with SuperPro Designer using the Component Object Module (COM) technology available in the Pro-Designer COM Server. Note that the models embedded in the simulation include detailed equations of the system, so they are not approximated shortcut models. In practice, it would be necessary to validate these models with plant data by means of parameter estimation techniques in order to obtain an accurate representation of the system.

As NLP solver, we used SNOPT, which is accessed via the Tomlab modeling system supported by Matlab. This solver is especially effective for nonlinear problems whose functions and gradients are expensive to evaluate [38]. The master MILP problem is implemented in GAMS and solved with CPLEX. In order to communicate both software packages, we use the interface GAMS-Matlab developed by Ferris et al. [39]. The PCA analysis is implemented in the statistical toolbox available in Matlab.

(Figure 2 could be placed here)

5.2. Case study: L-lysine process production

5.2.1. General description of the process

The process chosen for illustrative purposes is the production of the amino acid L-lyisine. This product is mainly used as an animal feed additive (an extensive overview of this process can be found in Pfefferle et al. [40]).

The associated flowsheet (see Figure 3) comprises ten major process units that are aggregated into three different sections: upstream, fermentation and downstream. The upstream processing includes all unit operations required to prepare the feed streams. In this section, the nutrients are mixed with water in a blending tank before being sterilized and transferred to the fermentor. When the reaction is completed, the mixture is transferred to a stabilization vessel and then filtered. The permeate is pumped to an evaporation unit that removes most of the water content. The broth is finally spray-dried and processed to granules. For biomass removal, we consider the following process alternatives: a rotary vacuum filtration (RVF), a micro filtration (MF) and a centrifuge (CF).

(Figure 3 could be placed here)

The bioprocess includes a fed-batch reactor that uses a genetically modified microorganism (*Cornyebacterium glutamicum*). The reactants are threonine, nutrients (glucose, KH_2PO_4 and NH_4OH) and oxygen. In the first reaction-step, glucose is consumed for L-lysine production, microorganism growth and maintenance. In this stage, threonine is consumed only for microorganism growth. After glucose depletion, the fed-batch operation starts with the addition of new glucose feed-rate controlled by the dissolved oxygen (DO_2) (fixed at 25% of air saturation). When all threonine is consumed, the cell growth stops and L-lysine synthesis is enhanced. The set of equations describing the reaction kinetics and the associated data are taken from the literature [41] [42]. A demand of 6,202 tones L-lysine/year

with a given desired purity is considered.

For the sake of brevity, details on the LCA calculations required to assess the environmental performance are given in Appendix A.

5.2.2. Preliminary analysis

A preliminary analysis of the process is performed prior to the application of the optimization algorithm. This analysis is aimed at enhancing our understanding on how the operating variables influence the economic and environmental performance (i.e, NPV, HH, EQ and DR). The decision variables selected for the analysis are the initial concentrations of threonine and glucose, initial volume of the fermentor (i.e., amount of raw materials fed to the bioreactor) and reaction time. Discrete variables model the number of equipment units working in parallel, as well as the selection of a specific equipment unit for biomass removal.

Figures 4 and 5 show the results of the process model for a fixed topology with one fermentor in parallel and a rotary vacuum filter for biomass removal. Specifically, the unit production cost, environmental impact per kg of L-lysine produced (EI), space-time-yield (STY) (i.e., mass of L-lysine produced per unit of volume and time in the bioreactor) and Overall yield (Y_{oa}) (mass of L-lysine produced per mass of glucose consumed) are plotted versus the continuous decisions variables. In all these cases, one decision variable is changed at a time, keeping the remaining ones constant (i.e., 1.62 g/l of threonine, 48.72 g/l of glucose, 310.34 m^3 of initial fermentor volume and 71.01 h of reaction time). Let us clarify that these points do not satisfy the demand satisfaction constraint (i.e., production equals the demand of 6,202 tones L-lysine/year), but are generated to gain insight into the process.

(Figure 4 could be placed here)
(Figure 5 could be placed here)

Within the investigated range of the decision variables, it is noticed that the economic

objective functions are highly dependent on the STY and Y_{oa}. The economic performance is given by the capital investment and operating costs. The capital investment is influenced by the STY. Larger STY values lead to lower equipment sizes. On the other hand, the operating costs are mainly affected by the Y_{oa}, since this variable has a large impact on the amount of raw materials consumed. Regarding the environmental objective, it is mainly affected by the Y_{oa}. Particularly, larger Y_{oa} values lead to lower consumption rates of raw materials for a fixed amount of L-lysine produced, and therefore to less impact.

Higher initial concentrations of threonine increase the STY and decrease the Y_{oa}. With regard to the glucose, the maximum STY and Y_{oa} values are both found at high initial glucose concentration levels. The initial reaction volume is the decision variable with the smallest effect on the STY and Y_{oa}. Finally, longer reaction times lead to high values of STY and Y_{oa} and small production costs.

Figure 6 shows the relationship between the STY and Y_{oa} and the economic and environmental performance. The figure confirms that at higher STY values the cost per unit produced is decreased while the environmental impact is increased. The opposite situation occurs when the Y_{oa} is increased.

(Figure 6 could be placed here)

The preliminary analysis presented above provides some insight into the problem, but does not lead to optimal solutions. The section that follows describes how our approach takes a step forward by identifying the values of the decision variables that simultaneously optimize the economic and environmental performance.

5.2.3. Multi-objective optimization

We first solve the problem maximizing the NPV as single objective. We use the base case configuration and operating conditions provided by Heinzle et al. [41] as starting point to

initialize the overall solution procedure and also for comparison purposes. This solution entails three reactors in parallel and the use of the RVF for the separation. Recall that the decision variables to be optimized are the initial concentrations of threonine and glucose, initial volume of the fermentor, and reaction time (continuous variables) and number of equipment units working in parallel, and selection of a specific equipment unit for biomass removal (discrete variables).

Table 1 displays the values of the main variables associated with each design. As observed, our final solution increases by 13.77% the NPV as compared to the base case (195,688M$ vs. 172,003M$). This is accomplished by using two fermentors in parallel instead of three, and also by adjusting the operating conditions of the plant. Particularly, in the optimal solution, the initial concentrations of glucose and threonine are higher than in the base case. These new conditions increase both the STY and Y_{oa}. Increasing the STY has the effect of reducing the equipment sizes and associated capital investment. On the other hand, by increasing the Y_{oa} it is possible to reduce the raw materials consumption, and therefore the operating cost. As a result, the total capital investment and operating costs are reduced by 21.5% (79,885M$ vs. 101,766M$) and 16.9% (8,830M$/year vs. 10,631M$/year) respectively, keeping the production rate constant (6,202 tones L-lysine/year). In addition, the environmental impact in all the damage categories is also reduced (6.79% in HH, 0.05% in EQ and 11.52% in DR).

(Table 1 could be placed here)

Figure 7 shows, for the maximum NPV solution, the main sources of impact affecting each damage category. Particularly, we consider the following contributors to the environmental impact (see Appendix A for details): (1) water, (2) glucose, (3) threonine, (4) KH_2PO_4, (5) NH_4OH, (6) steam, (7) process water, (8) CO_2, (9) biomass, (10) electricity and (11) steel.

(Figure 7 could be placed here)

As seen, glucose is the major source of impact in all of the cases. Note that bioprocesses are characterized by small consumption rates of utilities. Because of this, the main source of impact is typically given by a raw material, like glucose in our case. This is an interesting observation, since the impact associated with raw materials is typically neglected in many environmental assessment methodologies that focus on evaluating the emissions released and waste generated at the plant level. Hence, decreasing the glucose consumption allows to diminish the impact in all damage categories. This can be accomplished by increasing the overall yield (Y_{oa}) in the reaction step. Particularly, in the damage to ecosystem quality (EQ) and depletion of resources (DR), the percentages of impact associated with raw materials consumption are 93.48% and 87.69%, respectively. For the damage to human health (HH), the consumption of raw materials has a percentual impact of 75.06%.

We generate next a set of Pareto solutions for the 4-objective problem that will be used for the PCA study. For simplicity, we obtain these solutions by solving three bi-objective problems, in which we optimize the NPV versus each individual damage category separately. Note, however, that other Pareto solutions could also be generated by imposing different epsilon limits on the environmental objectives. It takes around 3,500 to 4,000 CPU seconds to generate 10 Pareto solutions of each 2-dimensional Pareto set on a computer AMD PhenomTM 8600B, with a Triple-Core Processor 2.29GHz and 3.23 GB of RAM.

We should clarify that simulations fail mainly when there are recycle streams or unit operations that cannot fulfill the required specifications. The case studies addressed in this work did not have these features, and for this reason convergence was not an issue. In general, however, recycled streams can be partitioned into two streams, forcing the properties of both sub-streams to match using equality constraints that are handled by the external NLP solver. Note that it is always better to handle the specifications externally by the NLP in order to avoid convergence difficulties in the process simulator.

The results of the aforementioned bi-criteria problems are shown in Figures 8-10. As observed, there is a clear trade-off between the economic indicator and each of the environmental categories, since reductions in the environmental impact can only be attained at the expense of decreasing the NPV.

Figure 8 represents the Pareto solutions of the bi-objective optimization problem NPV vs HH. The HH index is reduced by 6.69% (19,589 kpoints vs 20,382 kpoints) along the Pareto curve. This is accomplished by reducing the concentrations of threonine and glucose, which in turn increases the Y_{oa} of the reaction and decreases the consumption of raw materials. On the other hand, the NPV is decreased by 3.89% (187,396M$ vs 195,517M$). Low concentrations of threonine and glucose lead to slower reaction rates. Hence, to satisfy the total production, the model is forced to select larger volumes in the equipment units, which results in a higher capital investment. The initial concentrations of glucose and threonine for the maximum NPV solution are 94.63 g/l and 1.92 g/l, respectively, and 87.28 g/l and 1.16 g/l for the minimum HH. In addition, the reactor volume is increased from 283.52m^3 to 398.76m^3 and the reaction time is reduced from 97.16 h to 91.82 h as we move from the maximum NPV to the minimum HH solution. Note that all the Pareto solutions involve the same configuration (2 reactors in parallel and a rotary vacuum filtration).

In Figure 9, the EQ is reduced by 10.10% (8,549 kpoints vs 9,509 kpoints) along the Pareto curve, whereas the NPV is decreased by 11.32% (173,383M$ vs 195,517M$). Similarly, as in the previous case, we find that solutions with large NPV values involve higher glucose and threonine concentrations, smaller bioreactor sizes and longer reaction times, whereas lower environmental impacts are obtained doing the opposite. In this case, two different configurations of the plant are identified: one implying 2 reactors in parallel for solutions with higher NPV, and another one with 3 reactors in parallel for solutions with lower environmental impact. Hence, lower concentrations of threonine and glucose are compensated by placing more reactors in parallel, which allows to decrease the cycle time of the plant. All Pareto solutions use a rotary vacuum filtration for the biomass removal.

Finally Figure 10 shows the Pareto solutions that trade-off NPV vs DR. In this MOO problem the DR is decreased by 8.17% (25,613 kpoints vs 26,893 kpoints) and the NPV by 11.32% (173,383M$ vs 195,517M$). Further inspection of the results reveals similar insights, regarding the operating conditions, as in the previous cases.

(Figure 8 could be placed here)
(Figure 9 could be placed here)
(Figure 10 could be placed here)

Table 2 summarizes the main features of the maximum NPV and minimum HH, EQ and DR solutions. Note that the plant topology in the minimum EQ and DR solutions entails 3 reactors in parallel. In contrast, the minimum HH leads to 2 reactors in parallel. This is due to the fact that the stainless steel production has a large contribution in damage category HH and a small one in EQ and DR.

(Table 2 could be placed here)

Figure 11 depicts all Pareto solutions in a parallel coordinates plot, which is a useful graphical tool to display data sets of large dimension. The figure shows in the x axis the set of objective functions and in the y axis the normalized value attained by each solution in every criterion. The normalization is performed by dividing each objective function value by its maximum value attained over the entire data set. Note that each line in the plot represents a different Pareto solution, entailing a topology and set of operating conditions, that connects the performance obtained by that design in each objective. As observed, all environmental impacts are somehow equivalent, since they tend to behave in a similar manner. Moreover, the largest reductions in environmental impact are attained in the EQ category (10.10%), followed by DR (8.17%) and finally by HH (3.59%). These environmental savings

are obtained at the expense of reducing the NPV by 11.32%. Further, it is clearly shown how there is a trade-off between the NPV and LCA impacts since alternatives with better NPV values lead in turn to larger LCA impacts.

(Figure 11 could be placed here)

5.2.4. Principal component analysis

PCA is applied next to the Pareto solutions obtained in the previous section. The 3 bi-objective problems provides a total of 30 solution points that are stored in matrix M (see Table 3).

(Table 3 could be placed here)

The correlation matrix is first computed in order to reveal whether there exists correlation between objectives (see Table 4). This information is valuable in assessing whether a reduction in the number of objectives is possible using PCA methodology.

(Table 4 could be placed here)

The correlation between the environmental metrics is particularly strong. Henceforth, it is expected that the PCA will allow significant reductions in the number of objectives.

We next standardize matrix $M1$ so that its centroid equals zero. This is accomplished by subtracting the mean from each measurement. At this point, the principal components are computed together with the associated eigenvalues by solving an eigenvector-eigenvalue problem. The results are given in Table 5.

(Table 5 could be placed here)

Figure 12 depicts the objectives (vectors) and Pareto points (dots) in the space of the two first PCs. Note that the projections of the vectors representing the environmental impact categories onto the PC1 axis are all negative, whereas that of the NPV is positive, confirming the existence of a clear trade-off between them. In addition, the projections of the vectors associated with the environmental metrics fall within the same region, which indicates a strong correlation between them. The coefficient of HH in PC3 has opposite sign than those associated with EQ and DR. A possible explanation for this is that, as already mentioned, the minimization of HH produces a different topological alternative (i.e., two reactors in parallel) than that associated with the minimum EQ and DR solutions (i.e., three reactors in parallel).

(Figure 12 could be placed here)

The heuristic proposed by Deb and Saxena [37] is next applied to the PCA results. We start by analyzing the first principal component, identifying the objectives with the most positive (NPV) and most negative (EQ) values. These objectives will be kept in the analysis. Since with this first PC we do not achieve the threshold cut of 95.00% (as suggested by the same authors), we continue with the analysis of the second PC. In this case, all the components of the eigenvector are positive, so we select the objective with the most positive value (NPV). Since, the cumulative variance of PC2 (99.73%) exceeds the TC, no further PCs are analyzed.

The outcome of the PCA analysis therefore suggests to keep NPV and EQ as main objectives and discard the others. This result is consistent with what we observed in the parallel coordinates plot. This reduction in environmental objectives simplifies to a large extent the analysis of the Pareto set, since decision-makers can now focus on optimizing and analyzing the system on the basis of a single environmental indicator.

Regarding the number of points required by the PCA, there are different rules to determine the minimum number of samples for stable PCA results. Note that when the variables (i.e., objectives) are highly correlated, like in our case, it is possible to use PCA even when the number of samples is small.

6 CONCLUSIONS

This work has introduced a novel framework to assist the development of biotechnological processes . The proposed algorithm integrates process simulation, multi-objective optimization (MOO) tools, life cycle assessment (LCA) and principal component analysis (PCA).

The capabilities of this method have been tested in a typical fermentation process and the production of the amino acid L-lysine. From numerical results, we concluded that it is possible to significantly improve the economic and environmental performance of bioprocesses by optimizing them as a whole. Particularly, larger benefits can be attained by properly adjusting the operating conditions and equipment sizes of all units embedded in the flowsheet. The main contributions of our approach are the use of a bioprocess simulation package, in which the process performance and economic equations are already implemented, the integration of LCA analysis in this context and the use of dimensionality reduction techniques based on PCA for identifying redundant LCA metrics. Future work will focus on exploring the use of surrogate or short-cut modeling to optimize the process model, thereby reducing the associated complexity.

Acknowledgements

The authors wish to acknowledge support from the Spanish Ministry of Education and Science (projects DPI2008-04099 and CTQ2009-14420-C02) and the Spanish Ministry of External Affairs (projects A/023551/09 and HS2007-0006).

References

[1] Grossmann, I.E.; Guillén-Gosálbez, G. Scope for the application of mathematical programming techniques in the synthesis and planning of sustainable processes.*Computers and Chemical Engineering.* **2010**,34,1365-1376.

[2] Cuthrell, J.E.; Biegler, L.T. Simultaneous optimization and solution methods for batch reactor control profiles.*Computers and Chemical Engineering.* **1989**,13,49-62.

[3] Carrasco, E.F.; Banga, J.R. Dynamic optimization of batch reactors using adaptive stochastic algorithms.*Ind.Eng.Chem.Res.* **1997**,36,2252-2261.

[4] Banga, J.R.; Balsa-Canto, E.; Moles C.G.; Alonso, A.A. Dynamic optimization of bioprocesses: Efficient and robust numerical strategies.*Journal of Biotechnology.* **2005**,117,407-419.

[5] Sarkar, D.; Modak, J.M. Pareto-optimal solutions for multi-objective optimization of fed-batch bioreactors using nondominated sorting genetic algorithm.*Chemical Engineering Science.* **2005**,60,481-492.

[6] Groep M,E.; Gregory M,E.; Kershenbaum L,S.; Bogle, D. Performance modeling and simulation of biochemical process sequences with interacting unit operations.*Biotechnology and bioengineering.* **2000**,67,300-311.

[7] Pinto, J.M.; Montagna, J.M. Vecchietti, A.R.; Iribarren, O.A.; Asenjo. J.A. Process performance models in the optimization of multiproduct protein production plants.*Biotechnology and bioengineering.* **2001**,74,451-465.

[8] Montagna J,M.; Iribarren, O.A. Vecchietti, A.R.; Synthesis of biotechnological processes using generalized disjunctive programming.*Ind.Eng.Chem.Res.* **2004**,43,4220-4232.

[9] Konopacz, R.F. Environmental impacts upon biotechnology facility design. A review of

Chiron's recent environmental impact report for a biotechnology facility.*Annals of the New York Academy of Sciences.* **1991**,646,381-384.

[10] Steffens, M.A.; Fraga, E.S.; Bogle, D. Multicriteria process synthesis for generating sustainable and economic bioprocesses.*Computers and Chemical Engineering.* **1999**,23,1455-1467.

[11] Dietz, A.; Azzaro-Pantel, C.; Pibouleau, L.; Domenech, S. Multiobjective optimization for multiproduct batch plant design under economic and environmental considerations.*Computers and Chemical Engineering.* **2006**,30,599-613.

[12] Jimenez-Gonzalez, C. Woodley, J.M.; Bioprocesses: Modeling needs for process evaluation and sustainability assessment. *Chem.Eng.Res.Des.* **2010**,34,1009-1017.

[14] Biegler, L.T.; Grossmann I.E.; Westerberg A.W. Systematic Methods of Chemical Process Design.*Prentice Hall.* **1999**.

[14] Biegler, L.T.; Grossmann I.E.; Westerberg A.W. Systematic Methods of Chemical Process Design.*Prentice Hall.* **1999**.

[15] Guillén, G.; Mele, F.D.; Espuña, A.; Puigjaner, L. Addressing the design of chemical supply chains under demand uncertainty.*Ind.Eng.Chem.Res.* **2006**,45,7566-7581.

[16] Guillén-Gosálbez, G.; Grossmann, I.E. Optimal design and planning of sustainable chemical supply chains under uncertainty.*AIChE Journal.* **2009**,55,99-121.

[17] Swiss Center for Life Cycle Inventories (http://www.ecoinvent.ch/).

[18] Consoli F., Allen D., Boustead I., Fava J., Franklin W., Jensen A.A. (1993) A code of practice. Guidelines for life-cycle assessment. Pensacola, USA:SETAC.

[19] Azapagic, A.; Clift, R. Application of life cycle assessment to process optimisation.*Computers and Chemical Engineering.* **1999**,23,1509-1526.

[20] Azapagic, A.; Clift, R. Life cycle assessment and multiobjective optimisation.*Journal of Cleaner Production.* **1999**,7,135-143.

[21] Alexander, B.; Barton, G.; Petrie, J.; Romagnoli, J. Process synthesis and optimisation tools for environmental design: Methodology and structure.*Computers and Chemical Engineering.* **2000**,24,1195-2000.

[22] Khan, F.I.; Natrajan, B.R.; Revathi, P. A new methodology for cleaner and greener process design.*Journal of Loss Prevention in the Process Industries.* **2001**,14,307-328.

[23] Baratto, F.; Diwekar, U.M.; Manca, D. Impacts assessment and tradeoffs of fuel cell based auxiliary power units Part II. Environmental and health impacts, LCA, and multi-objective optimization.*Journal of Power Sources.* **2005**,139,214-222.

[24] Carvalho, A.; Gani, R.; Matos, H. Design of sustainable processes: Systematic generation and evaluation of alternatives.*Computer Aided Chemical Engineering.* **2006**,21,817-822.

[25] Guillén-Gosálbez, G.; Caballero, J.A.; Jiménez, L.; Application of life cycle assessment to the structural optimization of process flowsheets.*Ind.Eng.Chem.Res.* **2008**,47,777-789.

[26] Gebreslassie, B.H.; Guillén-Gosálbez, G.; Jiménez, L.; Boer, D. Design of environmentally conscious absorption cooling systems via multi-objective optimization and life cycle assessment.*Applied Energy.* **2009**,86,1712-1722.

[27] Kikuchi, Y.; Mayumi, K.; Hirao, M. Integration of CAPE and LCA tools in environmentally-conscious process design: A case study on biomass-derived resin.*Computer Aided Chemical Engineering.* **2010**,28,1051-1056.

[28] Hugo, A.; Rutter, P.; Pistikopoulos, S.; Amorellib, A.; Zoia, G. Hydrogen infrastructure

strategic planning using multi-objective optimization.*International Journal of Hydrogen Energy.* **2005**,30,1523-1534.

[29] Puigjaner, L.; Guillén-Gosálbez, G. Towards an integrated framework for supply chain management in the batch chemical process industry.*Computers and Chemical Engineering.* **2008**,32,650-670.

[30] Azapagic A.; Millington A.; Collett A. Optimal design and planning of sustainable chemical supply chains under uncertainty.*Chem.Eng.Res.Des.* **2006**,84,439-452.

[31] Bojarski A.D.; Guillén-Gosálbez G.; Jiménez L.; Espuña A.; Puigjaner L. Life cycle assessment coupled with process simulation under uncertainty for reduced environmental impact: Application to phosphoric acid production.*Ind.Eng.Chem.Res.* **2008**,47,8286-8300.

[32] PRé-Consultants. The Eco-indicator 99A damage oriented method for life cycle impact assessment. methodology report and manual for designers.*Technical Report, PRé Consultants.* **2000**,Amersfoort, The Netherlands.

[33] Haimes, Y.; Lasdon, L.; Wismer, D. On a bicriterion formulaiton of the problems of integrated system identification and system optimization.*IEEE Transaction on systems.* **1971**,1,296-297.

[34] Caballero, J.A.; Milán-Yañez, D.; Grossmann, I.E. Rigorous design of distillation columns: Integration of disjunctive programming and process simulators.*Ind.Eng.Chem.Res.* **2005**,44,6760-6775.

[35] Brunet,R.; Guillen-Gosalbez, G.; Perez-Correa, R.; Caballero, J.A.; Jimenez, L. Hybrid optimization-simulation based approach for the optimal development of biotechnological processes.*Computers and Chemical Engineering.* **2011**,doi:10.1016.

[36] Gutierrez, E.; Lozano, S.; Moreira, M.T.; Feijo, G. Assessing relationships among life-cycle environmental impacts with dimension reduction techniques.*Journal of environmental management.* **2010**,91,1002-1011.

[37] Deb, K.; Saxena, D.K. On finding Pareto-optimal solutions through dimensinality reduction for certain large-dimensional multi-objective optimization problems. *KanGal Report.* **2005**.

[38] Gill, P.E.; Murray, W.; Saunders, M.A. SNOPT: An SQP algorithm for large-scale constrained optimization *SIAM Journal on Optimization.* **2002**,12,979-1006.

[39] Ferris, M.C.; Jain, R.; Dirkse, S.; GDXMRW: Interfacing GAMS and MATLAB. *Computer Sciences Department, University of Wisconsin.* **2010**.

[40] Pfefferle, W.; Moeckel, B.; Bathe, B.; Marx, A. Biotechnological manufacture of lysine. *Adv. Biochem. Eng. Biotechnol.* **2003**,79,59-112.

[41] Heinzle, E.; Biwer, A.P.; Cooney, C.L. Development of sustainable bioprocesses: modeling and assessment. *John Wiley and Sons.* **2006**,155-167.

[42] Büchs, J. Precise optimization of fermentation processes through integration of bioreaction. Process computations in biotechnology. *McGraw-Hill,New Delhi.***1994**,194-237.

[43] Miyawaki, I.; Kaneko, K. Process for the production of glucose. *United States Patent* 5,534,075, 1996.

[44] Furukawa, S.; Nakanishi, T. Process for producing L-threonine by fermentation. *United States Patent* 4,996,147, 1991.

[45] Rubin, E.; Szpruch, E.; Orell, A. Production of KH2PO4 from KCl and H3PO4 in an organic liquid medium.*Ind. Eng. Chem.Proc.* **1978**,17,460-468.

[46] Mulle WH. Process for manufacture of ultra-high purity ammonium hydroxide. *United States Patent* 5,746,993, 1998.

NOMENCLATURE

Abbreviatures

CF	Centrifuge
COM	Component Object Module
DR	Depletion of Resources
EQP	Environmental Protection Agency
EQ	Damage to Ecosystem Quality
EI	Environmental impact
GDP	Generalized Disjunctive Programming
HH	Damage to Human Health
LCA	Life-Cycle Assessment
MF	microfilter
MILP	Mixed-Integer Linear Programming
MINLP	Mixed-Integer Non-Linear Programming
moMINLP	Multi-Objective Mixed-Integer Non-Linear Programming
MOO	Multi-Objective Optimization
NLP	Non-Linear Programming
NPV	Net Present Value
ODEs	Ordinary differential equations
RVF	Rotary Vacuum Filtration
PC	Principal Component
PCA	Principal Component Analysis
PSE	Process Systems Engineering
SQP	Successive Quadratic Programming
STY	Space Time Yield
Y_{oa}	Overall yield

A Life Cycle Assessment of the L-lysine production plant

The environmental performance of the L-lysine production is quantified according to the LCA methodology (ISO 14040), which is combined with process simulation and MOO in a way similar as done before by the authors (Bojarski et al. [31]) . The method is applied in four phases:

1. *Goal and scope definition:*

- The functional unit was set to 76.470 tones of L-lysine produced over a time horizon of 15 years.

- The system under study comprises the three stages of the bioprocess: upstream, bioreaction and downstream. Every stream crossing this boundary is regarded as an input or output of our system.
  (Figure 12 could be placed here)

- We perform a cradle to gate study that covers all the activities from the extraction of raw materials to the production of L-lysine.

- The environmental impact is determined using the Eco-Indicator 99 (Eco99) framework, which includes 10 impact categories that are divided into 3 specific damage categories: damage to human health (carcinogenics, climate change, ionizing radiation, ozone depletion and respiratory effects), damage to ecosystem quality (acidification and eutrophication, ecotoxicity and land occupation) and damage to natural resources (fossil fuels and mineral extraction).

- We consider the following sources of impact:

  Raw materials (inputs): threonine, nutrients (glucose, KH_2PO_4 and NH_4OH) and water.

Utilities (inputs): electricity, steam and cooling water.

Stainless steel contained in the equipment units (input).

Waste and emissions generated (outputs): biomass, CO_2 and water.

2.*Life cycle inventory analysis (LCI):*

- The quantification of the mass and energy streams crossing the boundaries of the system is performed using the bioprocess simulator. The input streams of energy and mass are translated into the corresponding emissions and feedstock requirements using the Eco-invent database [17]. For those components that are not in the database, it is necessary to move one step backward and analyze their production process. Particularly, individual LCA analysis are performed on the following components: glucose, threonine, KH2PO4 and NH4OH. The following assumptions are made:

  Glucose is produced by saccharifying liquefied starch (see Miyawaki et al. [43]).

  Threonine is obtained by the aerobic fermentation of glucose using Escherichia Coli (see Furukawa et al. [44]).

  KH_2PO_4 is produced from KCl and H_3PO_4 (see Rubin et al. [45]).

  NH_4OH is obtained from ammonia and ultra-pure water (see Mulle et al. [46]).

3.*Life cycle impact assessment (LCIA):*

- The damage caused in each impact category (dam_d) is determined from the entries of the life cycle inventory of emissions and feedstock requirements (LCI_b) and corresponding set of damage factors (df_{bd}) as follows.

$$dam_d = \sum_b df_{b,d} \cdot LCI_b \qquad \forall d$$

- The damage factors have been retrieved from the Eco-Indicator 99 methodology report [32]. The results of the LCIA are shown in Tables 6 to 8.

(Table 6 could be placed here)

(Table 7 could be placed here)

(Table 8 could be placed here)

4.*Life cycle interpretation:* As mentioned previously, the interpretation is performed in the post-optimal analysis of the Pareto solutions. This step is assissted by the use of PCA.

List of Tables

Table 1: Results of the economic optimization of L-lysine production plant

Variables	Base Case	Optimal Point
Net present value [M$]	172,003	195,688
Total capital investment [M$]	101,766	79,885
Operating cost [M$/year]	10,631	8,830
Production rate [tones MP/year]	6,202	6,202
Unit Production cost [$/kg MP]	1.71	1.42
Batch Throughput [tons MP/batch]	29.67	44.30
Recipe Batch time [h]	111.07	137.67
Recipe Cycle time [h]	37.51	55.81
Number of batches per year	209	140
Concentration Glucose [g/l]	48.72	94.61
Concentration Threonine [g/l]	1.61	1.92
Initial Volume Ferment [m^3]	310.34	282.77
Reaction time [h]	71.01	97.16
Fermentors [equip.]	3	2
Separator	RVF	RVF
Space-time yield [g/l·h]	1.022	1.103
Overall yield [g/g]	0.299	0.316
Separator	RVF	RVF
Human Health [Kpoints]	21,866	20,382
Ecosystem Quality [Kpoints]	9,514	9,509
Depletion Resources [Kpoints]	31,526	27,893

Table 2: Results of the optimization of the L-lysine production plant for different objective functions

Variables	max NPV	min HH	min EQ	min DR
Net present value [M$]	195,688	187,396	173,383	173,494
Human Health [Kpoints]	20,382	19,589	19,747	19,751
Ecosystem Quality [Kpoints]	9,509	8,778	8,549	8,557
Depletion Resources [Kpoints]	27,893	26,154	25,613	25,605
Concentration Glucose [g/l]	94.61	87,28	89,98	89.05
Concentration Threonine [g/l]	1.92	1.16	0.96	0.96
Initial Volume Ferment [m^3]	282.77	398.76	398.66	396.79
Reaction time [h]	97.162	91.82	95.89	95.97
Fermentors [equip.]	2	2	3	3
Separator	RVF	RVF	RVF	RVF
Space-time yield [g/l·h]	1.103	0.914	0.859	0.859
Overall yield [g/g]	0.316	0.348	0.372	0.371

Table 3: Solutions matrix of the original 2-dimensional problems

NPV [$]	HH [Points]	EQ [Points]	DR [Points]
195,517,044	20,382,538	9,509,658	27,893,721
195,395,664	20,237,840	9,391,320	27,586,280
195,385,792	20,230,751	9,411,804	27,643,591
195,357,969	20,244,053	9,403,678	27,619,686
194,979,665	20,135,339	9,311,688	27,383,932
194,894,646	20,127,492	9,293,449	27,338,871
194,837,412	20,119,418	9,285,589	27,318,468
194,353,704	20,045,055	9,217,483	27,153,293
194,111,849	20,007,873	9,183,431	27,070,706
194,111,849	20,007,873	9,183,431	27,070,706
193,369,855	19,948,318	9,102,053	26,879,839
193,368,848	19,926,575	9,089,258	26,847,424
193,368,848	19,926,575	9,089,258	26,847,424
192,756,629	19,892,174	9,031,156	26,718,450
191,718,388	19,849,783	8,986,662	26,615,911
190,862,157	19,801,882	8,918,681	26,460,176
190,067,928	19,772,992	8,884,066	26,384,397
189,233,790	19,712,545	8,848,803	26,304,523
188,137,027	19,648,861	8,805,609	26,207,369
187,871,528	19,624,164	8,803,842	26,198,934
187,493,393	19,607,484	8,779,456	26,148,359
187,396,749	19,589,390	8,778,137	26,154,129
176,940,713	19,797,523	8,755,592	26,060,850
176,098,812	19,803,393	8,722,428	25,981,318
174,935,488	19,781,882	8,648,755	25,832,539
174,267,079	19,776,669	8,613,143	25,756,435
173,493,733	19,751,395	8,557,266	25,605,575
173,383,255	19,747,784	8,549,283	25,613,317

Table 4: Correlation matrix

	NPV	HH	EQ	DR
NPV	1.0000	-0.6201	-0.8617	-0.8599
HH	-	1.0000	0.9241	0.9248
EQ	-	-	1.0000	0.9997
DR	-	-	-	1.0000

Table 5: PCs (presented in decreasing order of their eigenvalues) and other relevant data computed from the correlation matrix

PC	NPV	HH	EQ	DR	Variance	Percentage	Cumulative
1	0.4612	-0.4812	-0.5272	-0.5271	3.5873	89.680	89.68
2	0.7643	0.6421	0.0390	0.0436	0.4020	10.050	99.73
3	0.4504	-0.5966	0.4503	0.4883	0.0105	0.262	99.99
4	-0.0146	0.0140	-0.7195	0.6942	0.0003	0.007	100.00

Table 6: Results of the LCIA using eco-indicator 99, (H/A)/ Human health

Components	Carcinogenics	Climate Change	Ionising Radiation	Ozone Depletion	Respirator
	Points/kg	Points/kg	Points/kg	Points/kg	Po
Water	$2.87 \cdot 10^{-6}$	$4.35 \cdot 10^{-6}$	$4.17 \cdot 10^{-6}$	$1.63 \cdot 10^{-8}$	1.3
Glucose	$7.28 \cdot 10^{-3}$	$1.89 \cdot 10^{-2}$	$1.89 \cdot 10^{-3}$	$3.40 \cdot 10^{-5}$	1.6
Threonine	$4.90 \cdot 10^{-2}$	$1.26 \cdot 10^{-1}$	$1.27 \cdot 10^{-2}$	$2.29 \cdot 10^{-4}$	1.0
KH_2PO_4	$1.36 \cdot 10^{-2}$	$1.06 \cdot 10^{-1}$	$1.05 \cdot 10^{-3}$	$5.27 \cdot 10^{-5}$	2.8
NH_4OH	$1.20 \cdot 10^{-3}$	$5.59 \cdot 10^{-3}$	$2.76 \cdot 10^{-5}$	$4.14 \cdot 10^{-6}$	1.1
CO_2	0	$5.45 \cdot 10^{-3}$	0	0	
Biomass	0	$1.06 \cdot 10^{-2}$	0	0	
Steam	$1.04 \cdot 10^{-4}$	$1.27 \cdot 10^{-3}$	$1.91 \cdot 10^{-6}$	$7.78 \cdot 10^{-7}$	1.5
Process Water	$2.87 \cdot 10^{-6}$	$4.35 \cdot 10^{-6}$	$4.17 \cdot 10^{-7}$	$1.63 \cdot 10^{-8}$	1.3
Electricity *kWh	$1.29 \cdot 10^{-3}$	$4.07 \cdot 10^{-3}$	$8.94 \cdot 10^{-5}$	$5.41 \cdot 10^{-7}$	1.0
Steel	$6.32 \cdot 10^{-3}$	$1.31 \cdot 10^{-2}$	$4.51 \cdot 10^{-4}$	$4.55 \cdot 10^{-6}$	8.0

Table 7: Results of the LCIA using eco-indicator 99,(H/A)/ Ecosystem quality

Components	Acidification	Ecotoxicity	Land Occupation
	Points/kg	Points/kg	Points/kg
Water	$9.52 \cdot 10^{-7}$	$1.80 \cdot 10^{-6}$	$1.70 \cdot 10^{-6}$
Glucose	$1.88 \cdot 10^{-2}$	$9.71 \cdot 10^{-3}$	$2.37 \cdot 10^{-3}$
Threonine	$1.26 \cdot 10^{-1}$	$6.51 \cdot 10^{-2}$	$1.60 \cdot 10^{-2}$
KH_2PO_4	$2.16 \cdot 10^{-2}$	$3.40 \cdot 10^{-2}$	$6.21 \cdot 10^{-2}$
NH_4OH	$7.20 \cdot 10^{-4}$	$3.22 \cdot 10^{-3}$	$7.51 \cdot 10^{-4}$
CO_2	0	0	0
Biomass	0	0	0
Steam	$1.21 \cdot 10^{-4}$	$2.85 \cdot 10^{-4}$	$8.60 \cdot 10^{-5}$
Process Water	$9.52 \cdot 10^{-7}$	$1.80 \cdot 10^{-6}$	$1.70 \cdot 10^{-6}$
Electricity *kWh	$9.88 \cdot 10^{-4}$	$2.14 \cdot 10^{-4}$	$4.64 \cdot 10^{-4}$
Steel	$2.71 \cdot 10^{-3}$	$7.45 \cdot 10^{-2}$	$3.73 \cdot 10^{-3}$

Table 8: Results of the LCIA using eco-indicator 99, (H/A)/ Damage resources

Components	Fossil Fuels	Mineral Extraction
	Points/kg	Points/kg
Water	$1.55 \cdot 10^{-5}$	$1.27 \cdot 10^{-6}$
Glucose	$3.67 \cdot 10^{-2}$	$7.75 \cdot 10^{-3}$
Threonine	$2.47 \cdot 10^{-1}$	$5.19 \cdot 10^{-2}$
KH_2PO_4	1.87	$1.50 \cdot 10^{-2}$
NH_4OH	$6.20 \cdot 10^{-2}$	$7.04 \cdot 10^{-4}$
CO_2	0	0
Biomass	0	0
Steam	$1.24 \cdot 10^{-2}$	$8.87 \cdot 10^{-6}$
Process Water	$1.55 \cdot 10^{-5}$	$1.27 \cdot 10^{-6}$
Electricity *kWh	$1.01 \cdot 10^{-2}$	$5.85 \cdot 10^{-5}$
Steel	$5.93 \cdot 10^{-2}$	$7.42 \cdot 10^{-2}$

List of Figures

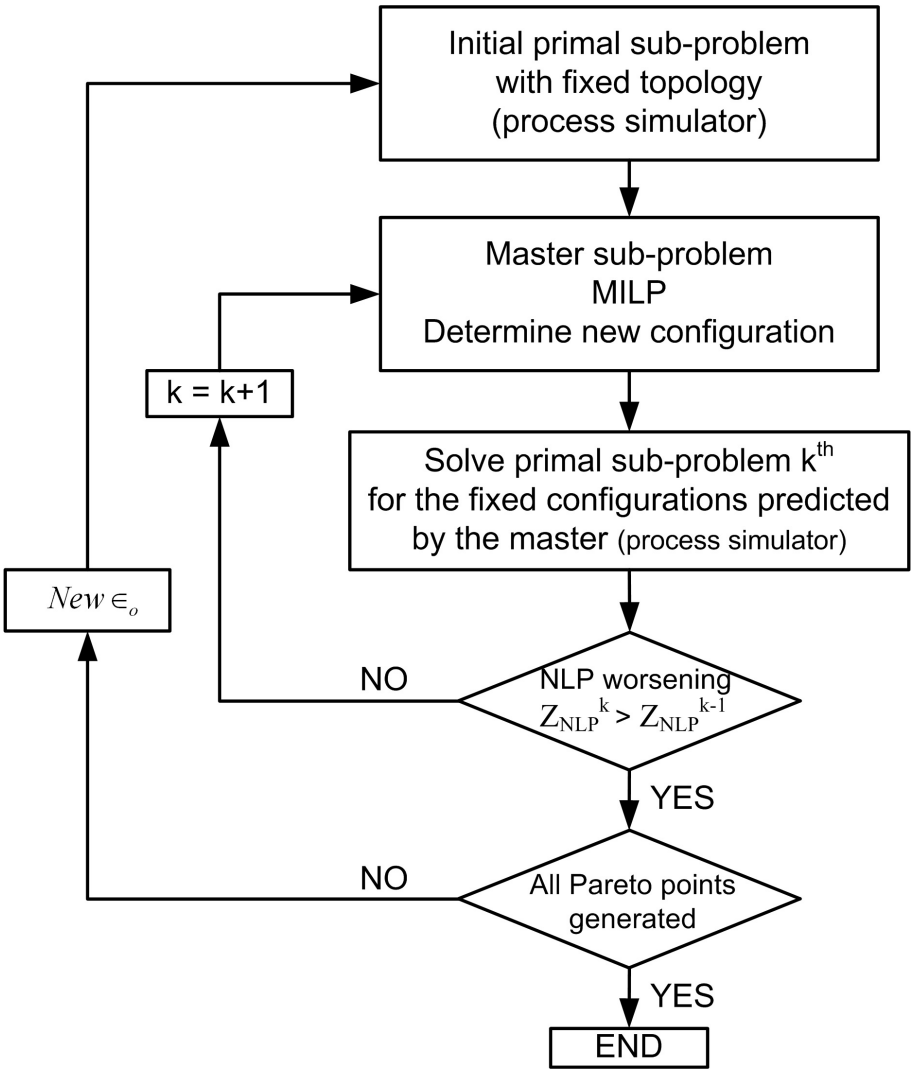

Figure 1: Flowchart of the proposed algorithm

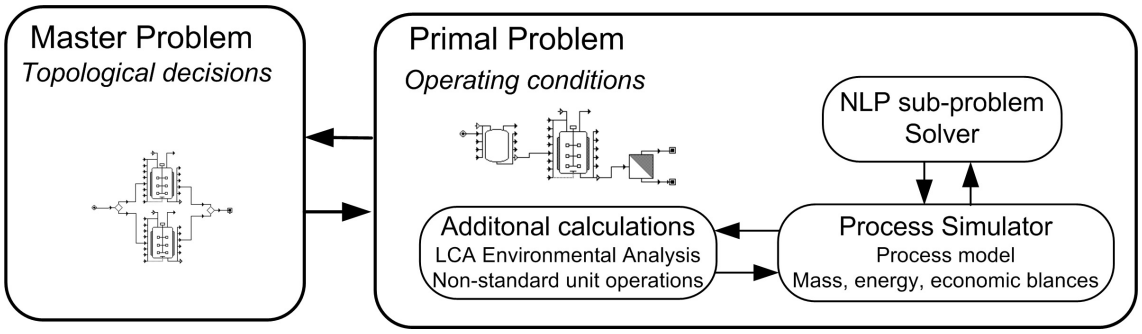

Figure 2: Details on the implementation details of the algorithm

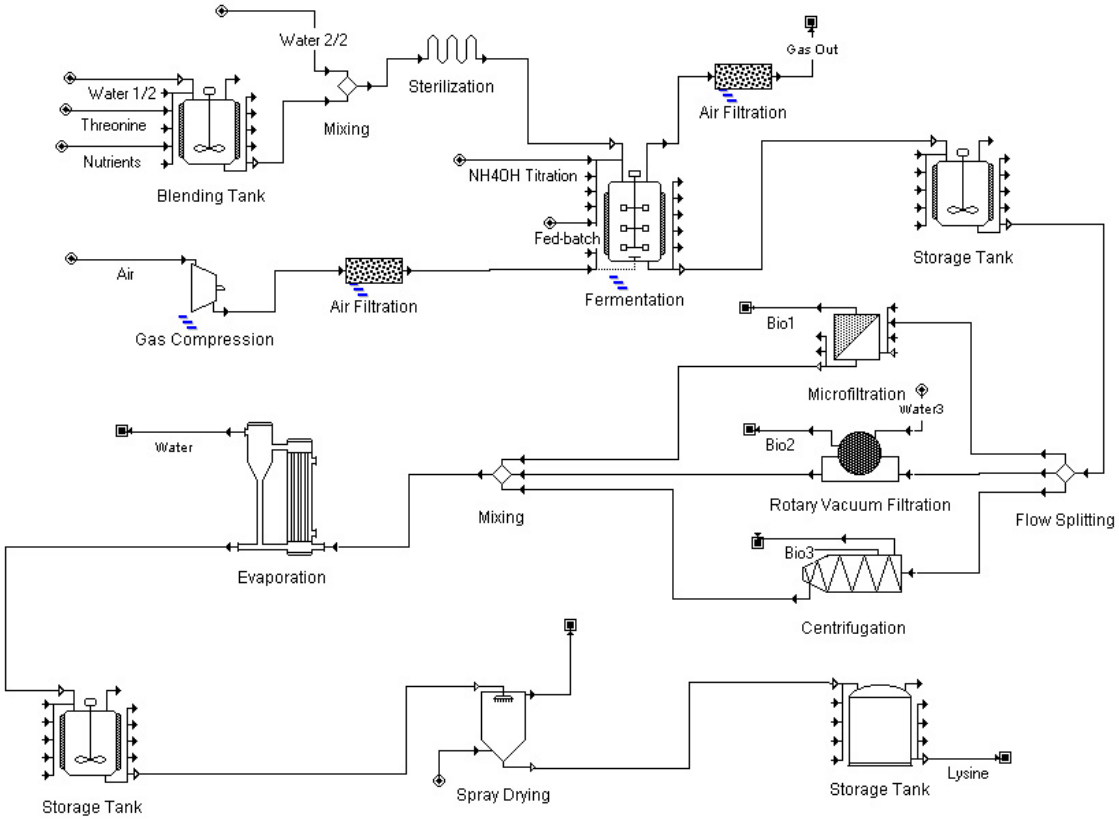

Figure 3: L-lysine production plant (adapted from Heinzle et al.,2006)

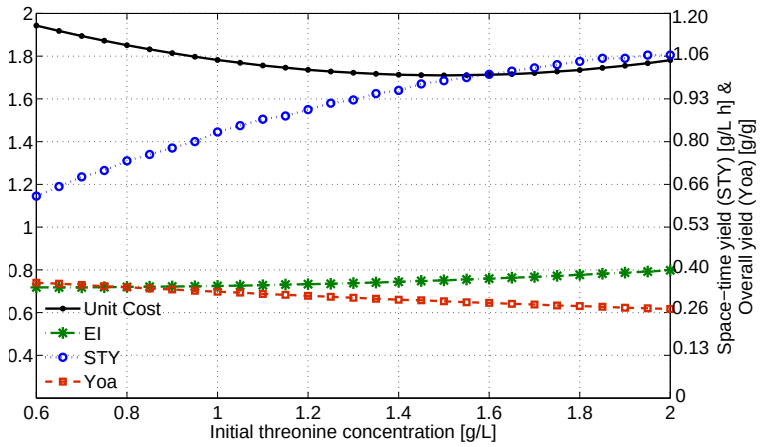

(a) Relationship between the unit production cost, the environmental impact, STY and Y_{oa} and the initial threonine concentration (C_{Thr}), maintaining the rest of the decision variables constant

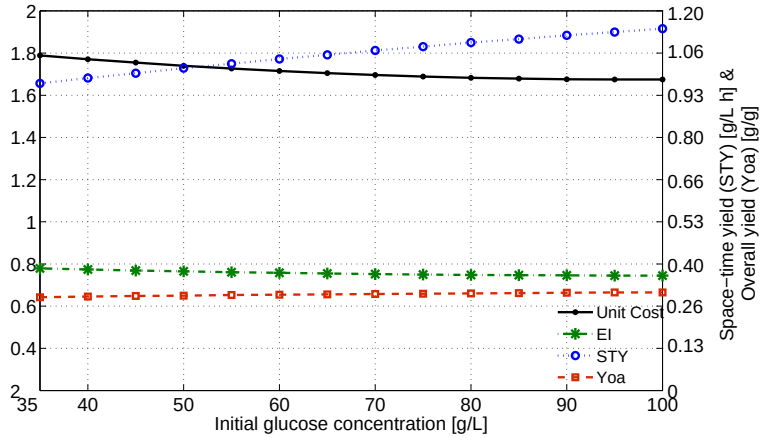

(b) Relationship between the unit production cost, the environmental impact, STY and Y_{oa} and the initial glucose concentration ($C_{S_{in}}$), maintaining the rest of the decision variables constant

Figure 4: Preliminary analysis of the decision variables

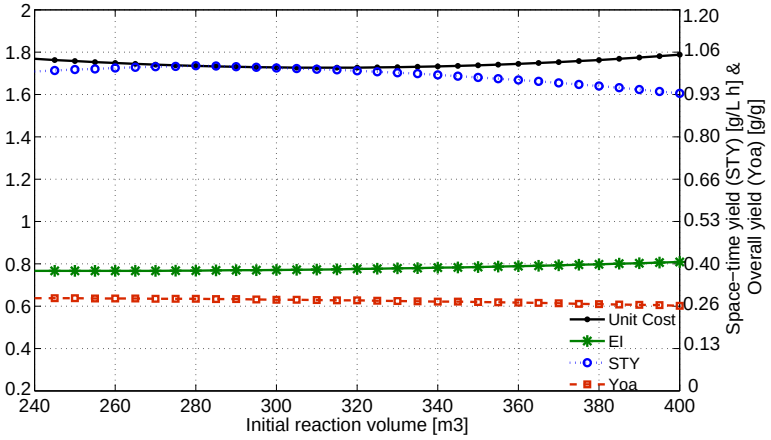

(a) Relationship between the unit production cost, the environmental impact, STY and Y_{oa} and the initial reactor volume, maintaining the rest of the decision variables constant

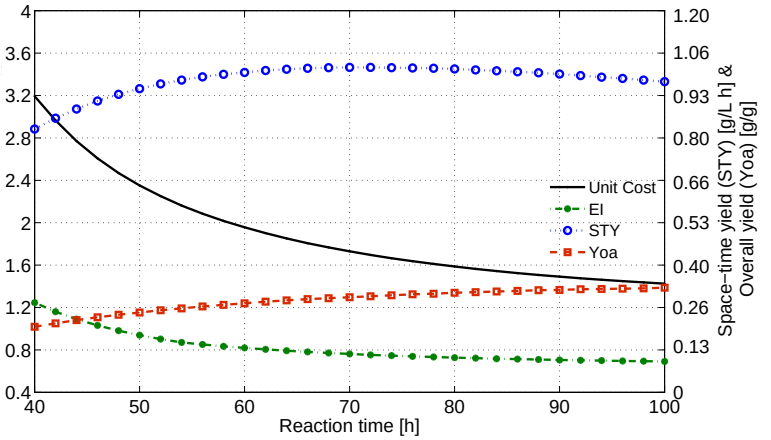

(b) Relationship between the unit production cost, the environmental impact, STY and Y_{oa} and the reaction time, maintaining the rest of the decision variables constant

Figure 5: Preliminary analysis of the decision variables

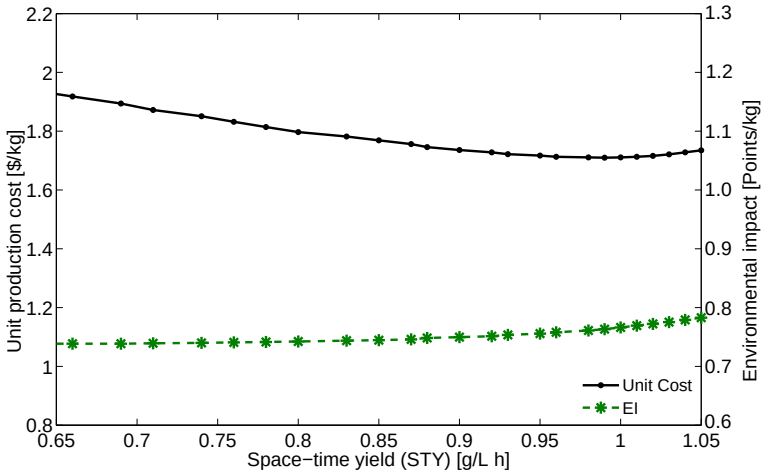

(a) Space-time yield versus the unit production cost and the environmental impact

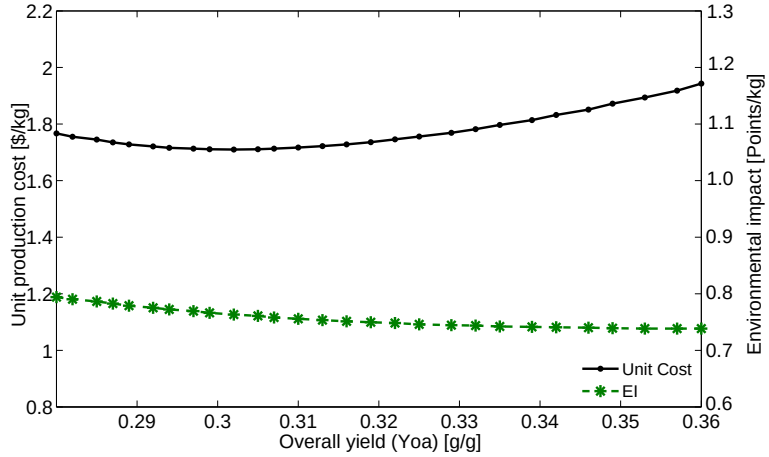

(b) Overall-yield versus the unit production cost and the environmental impact

Figure 6: Relationship between the reaction output variables and the economic and environmental performance

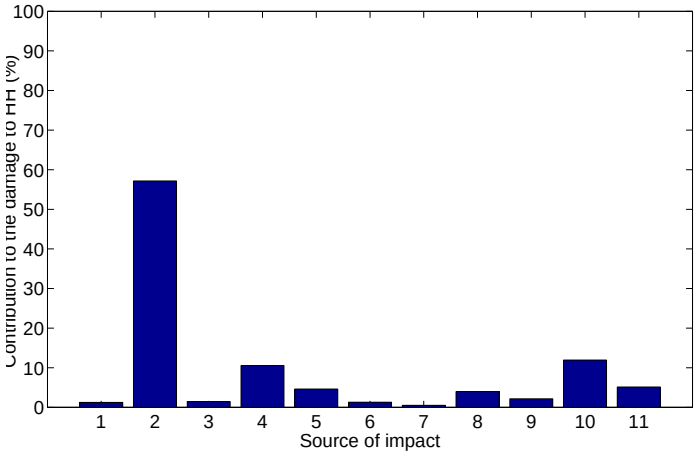

(a) Breakdown of the main sources of impact contributing to the Damage to Human Health

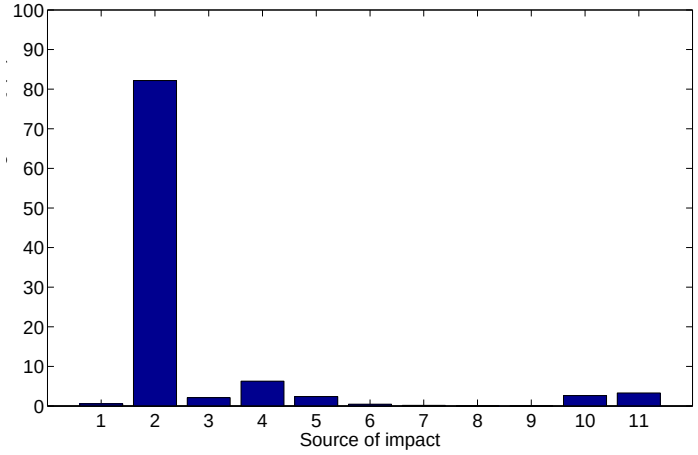

(b) Breakdown of the main sources of impact contributing to the Damage to Ecosystem

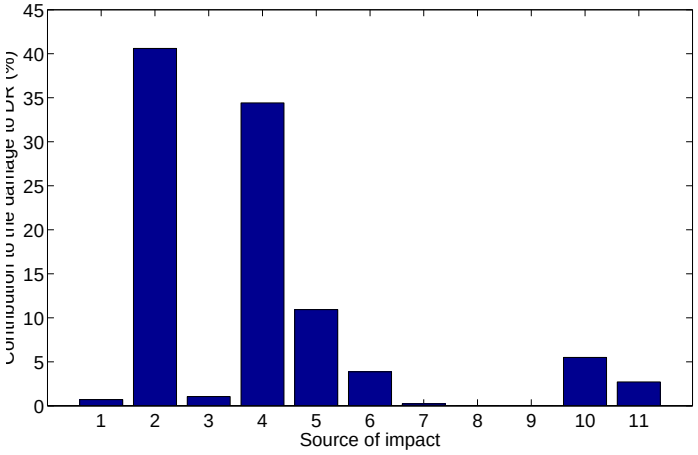

(c) Breakdown of the main sources of impact contributing to the Damage to Depletion of resources

Figure 7: Breakdown of the main sources of impact contributing to the different environmental impact categories

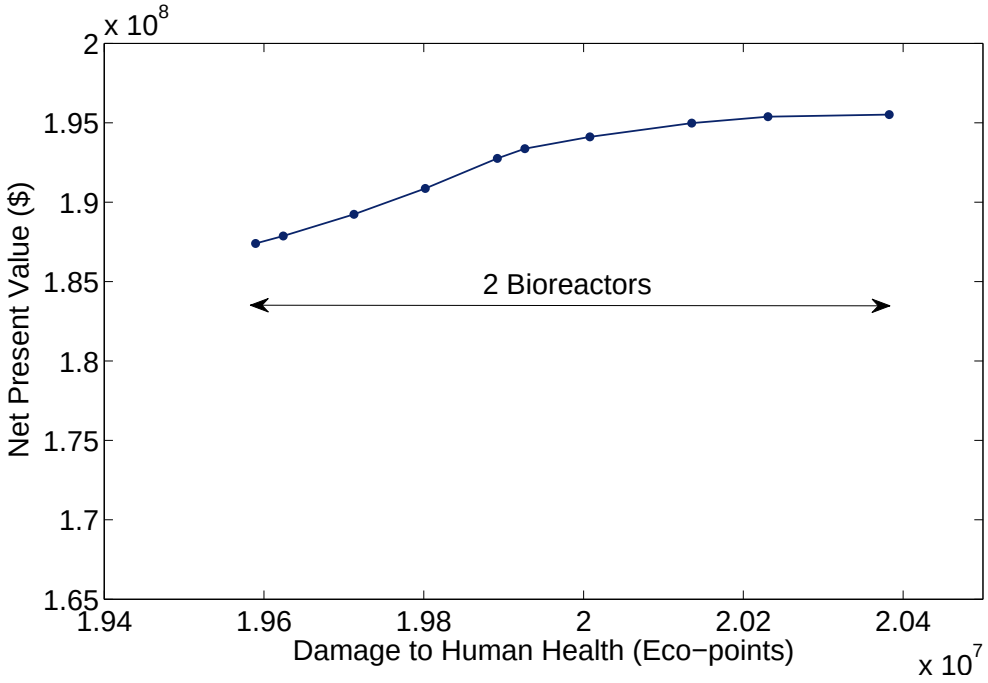

Figure 8: 2-dimensional Pareto set: Net Present Value vs Damage to Human Health

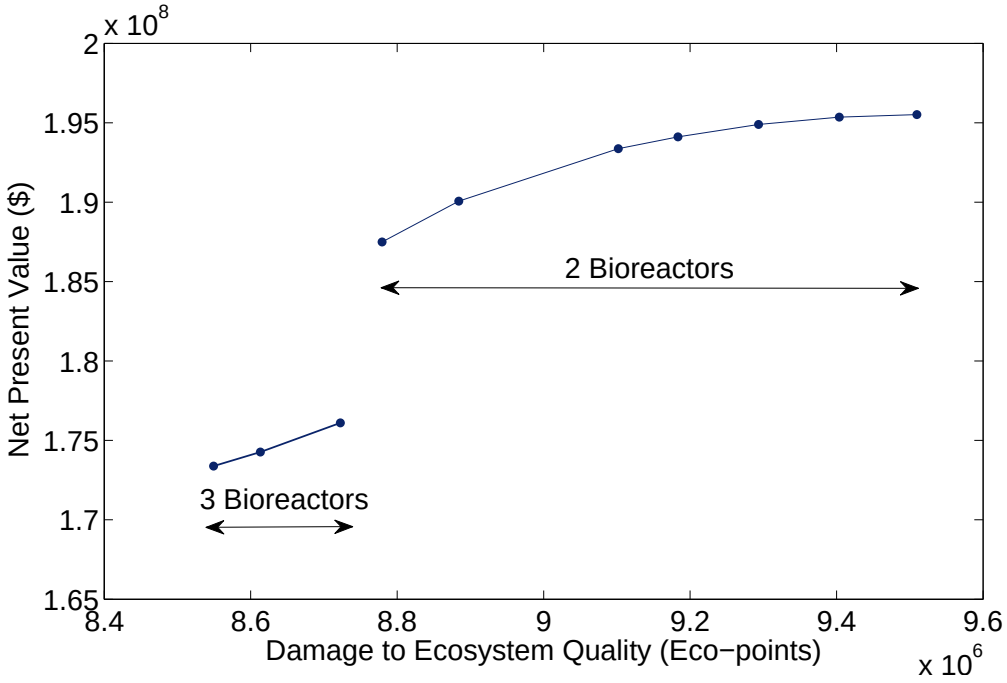

Figure 9: 2-dimensional Pareto set: Net Present Value vs Damage to Ecosystem Quality

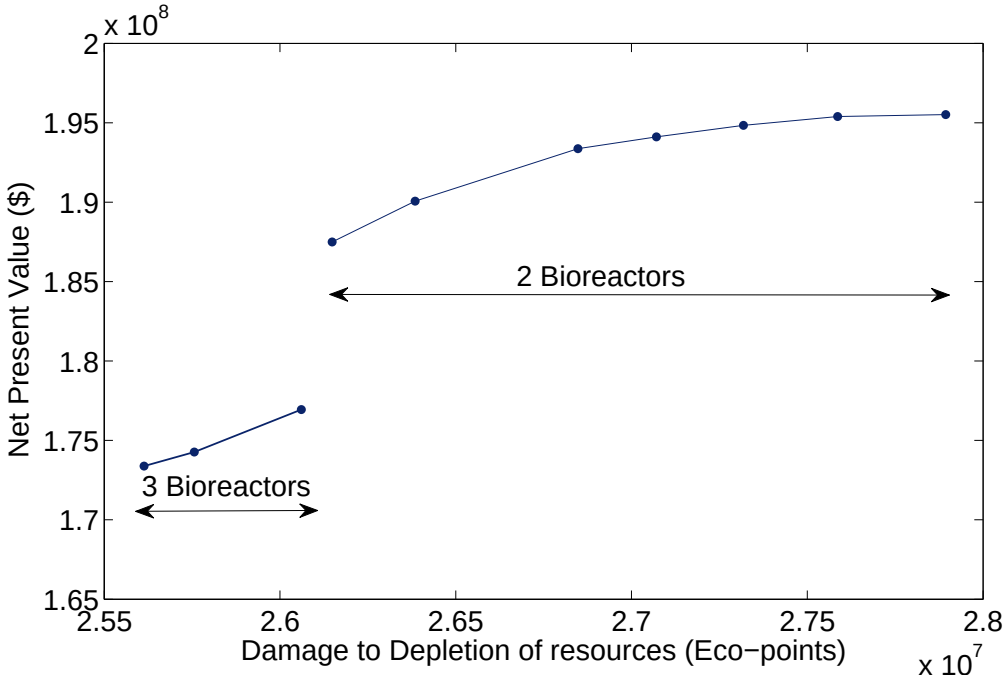

Figure 10: 2-dimensional Pareto set: Net Present Value vs Damage to Natural Resources

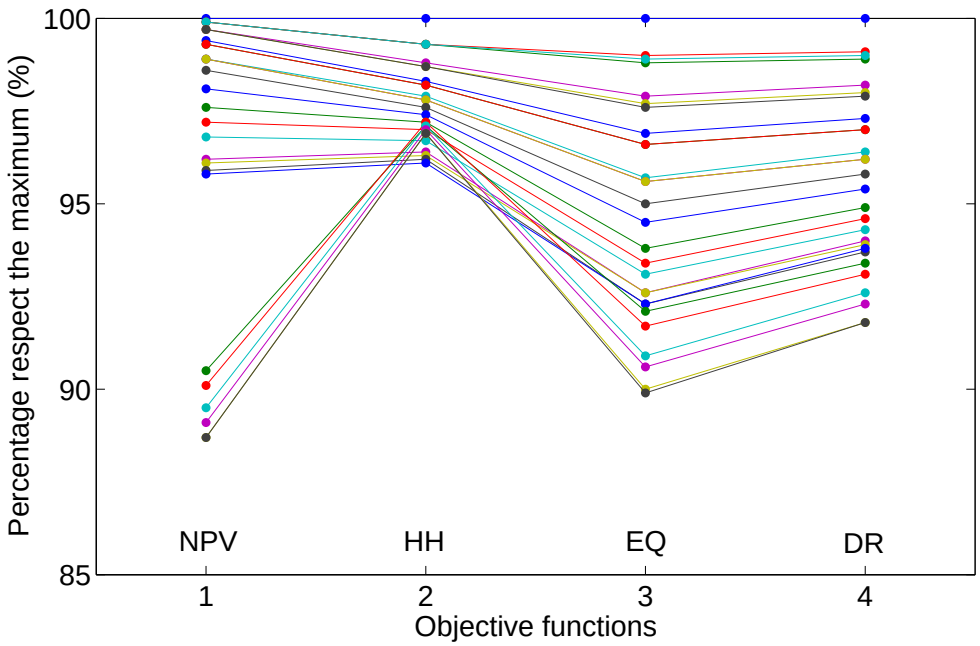

Figure 11: Parallel coordinates of the 2-dimensional Pareto sets

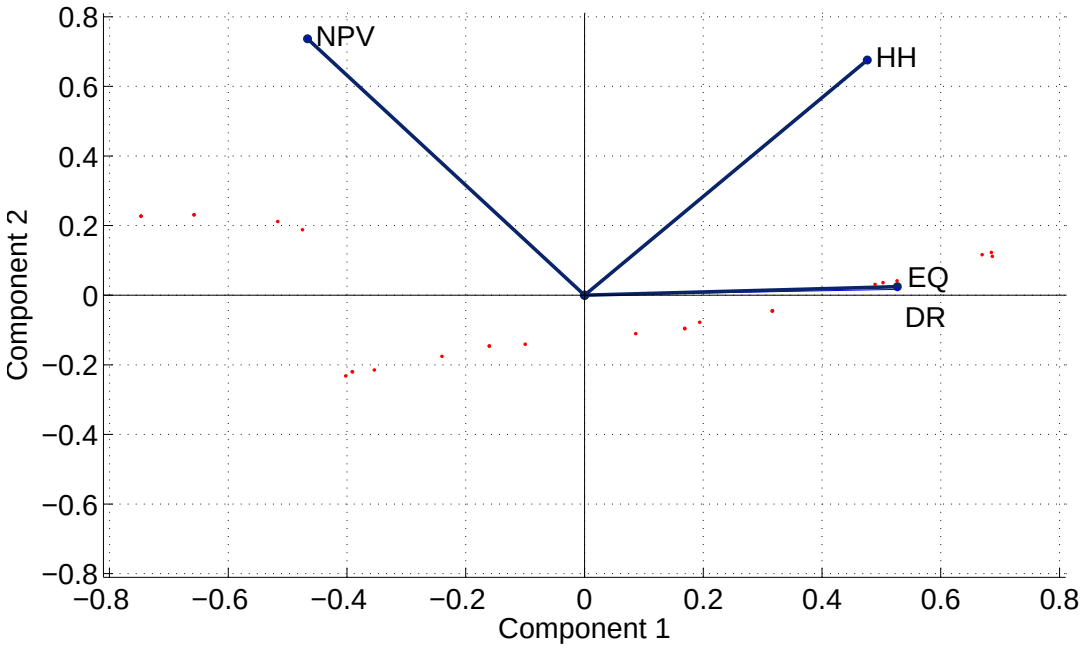

Figure 12: Components of the two first PCs (note that for simplicity, the sign of the coefficients in the first PC has been reversed)

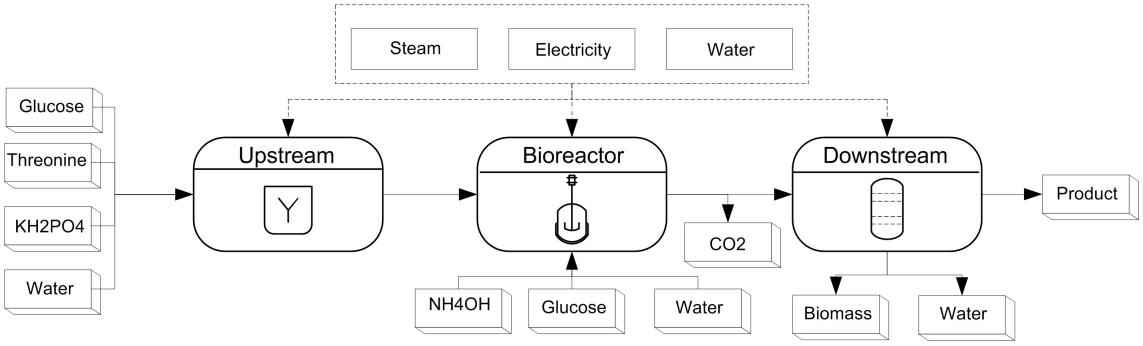

Figure 13: Inputs/outputs of mass and energy considered in the LCA analysis

Article 3

Authors: **R. Brunet**, J.A. Reyes-Labarta, G. Guillén-Gosálbez, L. Jiménez, D. Boer.
Title: Combined simulation-optimization methodology for the design of environmental conscious absorption systems.
Journal: *Computers and Chemical Engineering*
Volume: **Pages:** **Year:** 2012
ISI category: Computer Science **AIF:** 0.597
Impact Index: 2.235
Position in the category: 20/97 (Q1)
Cites: -
Observations Under review

Combined simulation-optimization methodology for the design of environmental conscious absorption systems

Robert Brunet[1], Juan A. Reyes-Labarta[2], Gonzalo Guillén-Gosálbez[1]*, Laureano Jiménez[1] and Dieter Boer [3]

[1] Departament d'Enginyeria Quimica, Escola Tecnica Superior d'Enginyeria Quimica, Universitat Rovira i Virgili, Campus Sescelades, Avinguda Paisos Catalans 26, 43007, Tarragona, Spain.

[2] Departamento de Ingenieria Quimica, Universidad de Alicante, Apartado de Correos 99, 03080, Alicante, Spain.

[3] Departament d'Enginyeria Mecanica, Escola Tecnica Superior d'Enginyeria, Universitat Rovira i Virgili, Campus Sescelades, Avinguda Paisos Catalans 26, 43007, Tarragona, Spain.

*Corresponding author. E-mail: gonzalo.guillen@urv.cat, telephone: +34 977558618

Abstract

This work addresses the optimal design of ammonia-water absorption cycles for cooling and refrigeration applications with economic and environmental concerns. Our approach combines the capabilities of process simulation, multi-objective optimization (MOO), cost analysis and life cycle assessment (LCA). The design task is posed in mathematical terms as a multi-objective mixed-integer nonlinear programming (moMINLP) that seeks to minimize the total annualized cost and environmental impact of the cycle. This moMINLP is solved by an outer-approximation strategy that iterates between primal nonlinear programming (NLP) subproblems with fixed binaries and a tailored mixed-integer linear programming (MILP) model. The capabilities of our approach are illustrated through its application to an ammonia-water absorption cycle used in cooling and refrigeration applications.

Keywords: *Process simulation; multi-objective optimization; absorption cycle; cost analysis; life cycle assessment*

1 INTRODUCTION

The worldwide cooling demand has drastically increased over the last few years, which has led to the installation of a large number of air conditioning systems (Balaras et al. 2007 and Henning 2007). This has resulted in a dramatic rise in electricity consumption, which is nowadays mostly generated from fossil fuels. This trend has caused important environmental problems such as: ozone layer depletion and global warming. In this general context, there is a clear need to develop environmentally friendly and energy efficient technologies in order to minimize the environmental impact of cooling applications. Particularly, absorption systems have emerged as a promising alternative to conventional compression cycles (Herold 1996, McMullan 2002 and Florides et al. 2002), since they can use low grade energy sources that are environmentally friendlier.

Absorption machines use a mixture of a refrigerant and an absorbent. The most widely employed mixtures are ammonia-water (ammonia as refrigerant) and water-lithium bromide (water as refrigerant). An important difference between absorption and compression refrigeration systems lies in the energy source. Compression systems require electrical energy for its operation, whereas absorption systems can use low grade heat sources as energy input. Therefore solar energy or waste heat (Keil et al., 2008), can be used for saving up to 50% of the primary energy required for the provision of useful heat (Ziegler et al., 1993). Energy conservation via waste heat recovery has been the focus of increasing interest in the literature (Erickson et al., 2004). These systems can reduce global warming emissions (Darwish et al., 2008) and mitigate as well to the ozone layer depletion. They show a high reliability and a silent and vibration free operation. Unfortunately, absorption cycles require more units than compression cycles, which leads to larger capital investments.

Finding ways to improve the efficiency of absorption systems has recently attracted an increasing interest (Darwish et al., 2008). In order to promote the use of absorption systems and to ensure their competitiveness with respect to conventional compression systems, it is still necessary to find ways to further improve their performance and reduce their cost. This

can be accomplished by developing systematic strategies to assist in their design. Thermoeconomic optimization is well suited to address this problem, since it allows performing energy and economic analysis for different configurations and operating conditions in a systematic and rigorous manner (Misra et al. 2005, Misra et al. 2006, Selbas 2006 and Kizilkan et al. 2007).

Particularly, methods based on mathematical programming have recently gained wider interest in the optimization of cooling systems. Most of these approaches have focused on optimizing the economic performance of ammonia-water absorption refrigeration systems (AWRS). One of the first optimization models for absorption cycles was the one introduced by Fernandez-Seara et al. (2003). More recently, Chavez-Islas & Heard (2009a) and (2009b) presented an equation-oriented method and a mixed-integer nonlinear programming (MINLP) model for the economical optimization of these systems. The same authors introduced a MINLP that considers different types of heat exchangers Chavez-Islas et al. (2009c). Gebreslassie et al. (2009a) addressed the optimization of a simplified AWRS considering uncertainties in the economic parameters.

These works focused on optimizing the economic performance as unique criterion. New trends have motivated the development of systematic strategies for optimizing the environmental impact of thermodynamic cycles along with their economic performance. Particularly, a promising strategy to accomplish this task relies on combining multi-objective optimization (MOO) tools with economic analysis and life cycle assessment (LCA) principles. This approach allows automating the search for alternatives leading to life cycle environmental savings (see Azapagic & Clift 1999a). The overwhelming majority of this type of strategies that provide decision-support for environmentally conscious process designs have focused on the chemical sector. In contrast, these techniques have not been used to the same extent in energy applications. Particular examples on the combined use of LCA and MOO can be found in the works by Azapagic & Clift (1999b) (production of boron compounds), Alexander et al. (2000) (design of a nitric acid plant), Carvalho et al. (2006) (design of a methyl tertiary

butyl ether plant), Guillen-Gosalbez et al. (2008) (optimization of the hydrodealkylation of toluene) among some others.

Hence, the optimization of energy systems, and in particular, of cooling and refrigeration cycles with environmental concerns has received little attention to date. To the best our knowledge, Gebreslassie et al. (2009b) were the first ones to address the multi-objective optimization of absorption cycles with economic and environmental concerns. The main limitation of this work is that it relies on "short-cut" models of the process units, that is, on simplified equations used to predict their performance. This simplification was originally aimed at avoiding the numerical difficulties associated with the nonlinearities and nonconvexities resulting from the detailed formulation of the thermodynamic equations of the process units of the cycle. These simplified models work reasonably well within a given range of operating conditions, but may perform poorly outside these intervals. Particularly, the generator of the cycle is a key unit that requires the use of complex thermodynamic packages for predicting the liquid-vapor equilibrium and stream properties (e.g., enthalpies, vapor pressures, etc.). Attempting to model this unit by short-cut formulations may lead to poor predictions, especially when working under refrigeration conditions.

This work introduces a systematic tool for the optimal design of absorption systems that aims to overcome the limitations mentioned above. Our approach is based on the combined use of process simulation and optimization tools (Diwekar et al., 1992; Reneaume et al., 1995; Kravanja & Grossmann, 1996; Diaz and Bandoni, 1996; Caballero et al., 2005; Kim et al., 2010; Brunet et al., 2012a). One of the main advantages of our strategy is the use of detailed process models of the cycle, including a rigorous tray-by-tray formulation of the rectification column, all of which are implemented in a commercial process simulator (i.e., Aspen Plus). This avoids the definition of the underlying equations of the process units in an explicit form, taking advantage of the customized unit operations models and tailored solution algorithms already implemented in the process simulator. Further, our method improves the robustness and numerical performance of the optimization algorithm, which is

likely to fail even in identifying an initial feasible solution when using a simultaneous (i.e., equation oriented) approach.

The design task is posed in mathematical terms as a multi-objective mixed-integer nonlinear programming (moMINLP) problem that accounts simultaneously for the minimization of the total annualized cost (TAC) and environmental impact (EI). The environmental impact is quantified by applying LCA principles, an approach that provides solutions in which the overall damage to the environment is globally minimized.

The methodology presented is intended to promote a more sustainable design of absorption cycles. Our method has been tested using an AWRS at cooling and refrigeration conditions. Numerical results demonstrate that the method presented can identify solutions in which the environmental impact is reduced at a marginal increase in cost. The remainder of this article is organized as follows. We formally introduce the problem of interest first. The model is then presented and the solution procedure is described afterwards. Some numerical results are then provided, and the conclusions are finally drawn in the last section of the paper.

2 PROBLEM STATEMENT

We consider a single effect AWRS. We describe the system first and then formally state the problem of interest.

2.1 System description

Figure 1 depicts the single effect AWRS under study. The system can either be used to provide chilled water for cooling applications (10ºC to 5ºC), or a solution with 95% of ethylene glycol for refrigeration applications (-5ºC to -10ºC). The basic components are the absorber (A), condenser (C), rectification column (RC), and evaporator (E). The cycle also includes the refrigerant subcooler (SC), refrigerant expansion valve (VLV1), solution heat exchanger (SHX), solution pump (P), and solution expansion valve (VLV2). The cycle works at two

pressure levels. The equipment units operating at a high pressure are the solution heat exchanger, rectification column and condenser. In contrast, the refrigerant subcooler, the evaporator and absorber work at a low pressure.

The system operation is as follows. The refrigerant in the vapor phase (12) coming from the subcooler (SC) is mixed with the expanded stream (6) coming from the solution heat exchanger (SHX). The resulting stream (13) is absorbed in the absorber (A) by the weak solution (W1). The strong solution (1) leaving the absorber is preheated in the solution heat exchanger (SHX). The solution (3) enters the rectification column (RC). Vapor refrigerant (7) from the top of the rectification column (RC) condenses completely in the condenser (C). The liquid refrigerant (8) from the condenser is then subcooled (9) in the subcooler (SC) by the superheating stream (11) that comes from the evaporator (E). The refrigerant (10) passes through the refrigerant expansion valve (VLV1) and enters the evaporator (E). The weak liquid solution (4) from the bottom of the rectification column (RC) is cooled in the heat exchanger (SHX) and sent to the expansion valve (VLV2). The resulting stream (6) is mixed with the refrigerant vapor (12). Note that streams W1-W6 are external heat transfer fluids. The useful output energy is given by the heat extracted from the evaporator (E). The driving energy is the heat supplied to the generator. Heat is dissipated in the absorber (A), the condenser (C), and in the partial condenser of the rectification column (RC).

(Figure 1 could be placed here)

It is assumed that the system works under steady state conditions. Pressure losses are neglected. Adiabatic valves are considered. The refrigerant is assumed to leave the condenser, absorber and bottom of the rectification column as saturated liquid. Heat losses are supposed to reduce the coefficient of performance (COP) by 10%. Note, COP is a term that represents the ratio of the heat delivered divided by the energy input to the system.

2.2 Problem definition

The problem addressed in this article can be formally stated as follows. Given are the cooling capacity of the system, inlet and outlet temperatures of the external fluids, overall heat transfer coefficients of the heat exchangers, cost parameters (capital investment and operating cost data), time horizon, thermodynamic properties, performance models of the equipment units embedded in the system and LCA related information (i.e., life cycle inventory of emissions and feedstock requirements, and parameters of the damage model). The goal of the analysis is to determine the optimal process design, including equipment sizes, structural alternatives (i.e., number of trays) in the rectification column and operating conditions that minimize the total annualized cost and associated environmental impact of the system. Note that the problem is multi-objective in nature. Hence, we expect to obtain a set of alternative solutions representing the optimal trade-off between the economic and environmental performance rather than a single point.

3 MATHEMATICAL FORMUALTION

The design of the absorption cooling and refrigeration system with economic and environmental concerns can be formulated as a moMINLP problem with the following form:

$$\begin{aligned} (M)\min_{x_D} \quad & U = \{f_1(x,u,x_D),...,f_n(x,u,x_D)\} \\ s.t. \quad & h_I(x,u,x_D) = 0 \\ & h_E(x,u,x_D) = 0 \\ & g_E(x,u,x_D) \leq 0 \end{aligned} \tag{1}$$

In model (M), f_1 represents the economic objective function, whereas f_2 to f_n denote the set of environmental metrics. Equations h_I are implicit equations solved by the process simulator, whereas h_E and g_E are explicit external equality and inequality constraints. The

continuous design variables are given by x_D, whereas x denotes the remaining process variables calculated by the simulator, and u represents fixed parameters not modified during the calculations. Note that x_D includes both continuous variables (pressures, temperatures, flow rates, etc.) and discrete variables. The latter denotes the number of trays and the feed stage selected for the rectification column.

3.1 Objective functions

Model (M) seeks to optimize simultaneously the TAC and EI of the absorption cycle. Details on the calculation of each objective function are provided next.

3.1.1 Economic objective function (Total annualized cost)

The TAC accounts for the annual capital cost (CF) and operating costs (CO).

$$TAC = CO + CF \tag{2}$$

The annual capital cost cost (CF) includes the cost of the rectification column (C_{RC}), heat exchangers (C_{HX}), and the pump (C_P). The valves and mixer cost are neglected. The total equipment cost is multiplied by the capital recovery factor (crf) (see equation 3), which is a function of the interest rate (parameter i) and life time (parameter t) of the absorption cycle expressed in years. (see equation 4).

$$CF = (C_{RC} + C_{HX} + C_P)crf \tag{3}$$

$$crf = \left(\frac{i(1+i)^t}{(1+i)^t - 1} \right) \tag{4}$$

The rectification column cost (equation 5) is determined using the correlations developed by Guthrie (1996). The heat exchangers cost (equation 6) is estimated according to the work by Kizilkan et al. (2007), whereas the pump cost (equation 7) is calculated as proposed by

Siddiqui (1997).

$$C_{RC} = \left(\frac{M\&S}{280}\right)(101.9Diam^{1.066}H^{0.802})(2.18 + 2F_c)\chi_{euro} \tag{5}$$

$$C_{HX} = \sum_{u \in HX}(c_1 \cdot Am_u + c_2) \tag{6}$$

$$C_P = c_3 \cdot Wp^{0.4} \tag{7}$$

Where $M\&S$ is a cost factor, $Diam$ is diameter of the column and H is the height of the column both in ft, F_c is a cost factor that depends on the type of column and χ_{euro} is the conversion from dollars to euros. HX denotes the set of equipment units m that are heat exchangers, c_1 and c_2 are cost parameters, Am is the area of heat exchanger m. C_P denotes de cost of the pump, Wp is the power of the pump and c_3 is a cost parameter.

The area of a heat exchanger u ($u \in HX$) is calculated from the logarithmic mean temperature difference (ΔT_u^{lm}), the overall heat transfer coefficient (Uh_u) and the heat duty (Q_u) as follows:

$$Am_u = \left(\frac{Q_u}{Uh_u \Delta T_j^{lm}}\right) \qquad \forall u \in HX \tag{8}$$

The operating cost (CO) accounts for the cost of the steam used in the rectification column as well as the electricity consumed by the pump. The cooling water cost is neglected.

$$CO = \sum_{u \in U}(Q_u \cdot cq + W_u \cdot cw) \cdot top \tag{9}$$

In equation 9 Q_u [MW] is the thermal power supplied to equipment unit u, W_u [MW] is the electrical power required by the equipment unit, top [h] is the total annual operation time and cq [€/MWh] and cw [€/MWh] are the unit costs for heat and electricity respectively. Note that Q_u and W_u are provided by the process simulator.

3.1.2 Environmental objective function (Eco-indicator 99)

The environmental impact is quantified following LCA principles, similarly as done before by the authors in other works (Puigjaner & Guillen-Gosalbez, 2008; Guillen-Gosalbez et al., 2008; Guillen-Gosalbez & Grossmann , 2009, 2010; Brunet et al., 2012b). Further details on the calculations are provided in the Appendix.

4 SOLUTION PROCEDURE

Our approach integrates process simulators, MOO, cost analysis and LCA within a single framework. Figure 2 summarizes the solution procedure proposed to tackle the problem.

The moMINLP is solved via the ϵ-constraint method (Haimes et al. 1971; Mavrotas 2009). This strategy is based on formulating an auxiliary model where one objective is kept in the objective function (without loss of generality, say objective 1) and the remaining ones are transferred to auxiliary constraints. This single objective problem is then iteratively solved for different values of the auxiliary epsilon parameters.

$$\begin{aligned} (MA)\ \min_{x_D}\quad & z = \{f_1(x,u,x_D)\} \\ s.t.\quad & f_o(x,u,x_D) \leq \epsilon_o \qquad o = 2,...,n \\ & h_I(x,u,x_D) = 0 \\ & h_E(x,u,x_D) = 0 \\ & g_E(x,u,x_D) \leq\ 0 \end{aligned} \tag{10}$$

In model (MA), f_1 is the economic objective function, whereas f_2 to f_n denote the LCA metrics. As observed, the LCA metrics have been transferred to auxiliary inequality constraints bounded by ϵ parameters. The original problem is first solved by optimizing each single scalar objective separately. This provides the lower and upper bounds of each epsilon interval. This interval is split into a number of sub-intervals, for which the original model is calculated.

Each single-objective problem is solved following a decomposition approach inspired by the work by Caballero et al. (2005). More precisely, we make use of an outer-approximation solution procedure that decomposes the original problem into two hierarchical levels: a primal non-linear programming (NLP) model and a master mixed-integer linear programming (MILP) problem, between which the algorithm iterates until a termination criterion is satisfied. Particularly, a termination criterion that works well in practice is to stop when the NLP of the primal level starts worsening. Note that there are two nested loops in the algorithm. The inner loop solves the auxiliary single objective epsilon constraint problems, whereas the outer loop proposes iteratively new values for the epsilon parameter and finally ends the overall procedure when the desired number of Pareto points are generated. One of the main advantages of this approach is that it ensures that the solution found are at least locally optimally, as oppose to other meta-heuristic approaches that do not show this property. Besides, the overall solution procedure takes advantage of the thermodynamic packages and mass and energy equations defined in the process simulator, avoiding their definition in an explicit form. We provide next details on each level of the algorithm.

(Figure 2 could be placed here)

4.1 Primal sub-problem

The primal level entails the solution of a NLP sub-problem at iteration k of the algorithm for fixed values of the binary variables. The NLP is solved by integrating the process simulator (Aspen Plus) with a gradient-based solver. This approach exploits the benefits of the customized process unit models implemented in the process simulator, which avoids their definition in an explicit form (i.e. equation oriented). At each iteration, the gradient based NLP solver calculates the derivatives of the objective function and constraints with respect to the design decision variables. At the optimal solution of the NLP, this information is used

to generate the master problem.

A key issue in the method proposed is that the process simulator must converge at each time the solver sends a set of design variables. To ensure this, the NLP is modified to handle infeasible solutions by adding slack variables and an exact penalty to the objective function. Hence, the modified NLP takes the following form:

$$\begin{aligned}
\min_{x_D} \quad & z = f_1(x,u,x_D) + \prod(s_1+s_2+s_3+s_4) \\
s.t. \quad & f_o(x,u,x_D) \leq \ \epsilon_o + s_1 && o = 2,...,n \\
& \underline{\epsilon_o} \leq \ \epsilon_o \leq \ \overline{\epsilon_o} && o = 2,...,n \\
& h_I(x,u,x_D) = 0 \\
& h_E(x,u,x_D) + s_2 - s_3 = 0 \\
& g_E(x,u,x_D) \leq \ s_4 \\
& s_1 \geq \ 0; s_2 \geq \ 0; s_3 \geq \ 0; s_4 \geq \ 0;
\end{aligned} \tag{11}$$

Where $\prod$ is a penalty parameter vector, and s_1, s_2, s_3 and s_4 are vectors of positive slack variables. All the required parameters to simulate the absorption cycle are initialized in the simulation environment: properties of the components, equipment parameters and binary variables (i.e., number of trays and feed stage in the rectification column).

4.2 Master sub-problem

The master problem provides a new set of values for the binary variables that are likely to yield better results than the previous one. Due to the presence of nonconvexities in the NLP, it is not guaranteed that the master MILP will provide a rigorous lower bound on the global optimal solution.

The master MILP is derived in each iteration by linearizing the objective function and constraints of the NLP at its optimal solution. The resulting MILP subproblem can be solved by standard MIP solution algorithms that implement efficient branch and cut methods (e.g, CPLEX, GUROBI, etc.).

To generate the master problem, the design variables x_D are fixed to the optimal value obtained in the latest NLP^k iteration of the algorithm, and a series of simulation problems are solved. We define the following sets at iteration k of the algorithm that will be used in the MILP formulation:

$T = \{i|i$ is a potential column configuration$\}$

$T_k = \{i|i$ is a rectification column configuration, entailing a given number of trays and a specific feed stage$\}$

$EQ = \{j|j$ is an external (explicit) equality constraint$)\}$

$IEQ = \{j|j$ is an external (explicit) inequality constraint$\}$

In addition, the following notation is used in the master problem:

$\Delta obj^k_{i,o}$ = Difference between the objective function o at iteration k of the NLP and the objective function associated with the new rectification column design i

$\Delta g^k_{i,j}$ = Difference between the values of the inequality constraint j for the new rectification column design i and the constraint j in the original NLP^k problem

$\Delta h^k_{E_{i,j}}$ = Difference between the values of the external equality constraint j new rectification column design i and the constraint j in the original NLP^k problem

The master MILP takes the following form:

$$
\begin{aligned}
\min \quad & \alpha + \prod (\sum_{o=2}^{n} s_{1_o} + \sum_{j \in IEQ} s_{2_j} + \sum_{j \in EQ} s_{3_j}) \\
s.t. \quad & f_o(x^k, u^k, x_D^k) + \sum_n \left(\frac{\partial f_o}{\partial x_{D_n}} \right)_{x_{D_n} = x_{D_n}^i} (x_{D_n} - x_{D_n}^k) + \sum_{i \in T_k} y_i \cdot \Delta obj_{i,o}^k \leq \ \alpha \quad o = 1 \\
& f_o(x^k, u^k, x_D^k) + \sum_n \left(\frac{\partial f_o}{\partial x_{D_n}} \right)_{x_{D_n} = x_{D_n}^i} (x_{D_n} - x_{D_n}^k) + \sum_{i \in T_k} y_i \cdot \Delta obj_{i,o}^k \leq \ \epsilon_o + s_{1_o} \quad o = 2, ..., n \\
& g_j(x^k, u^k, x_D^k) + \sum_n \left(\frac{\partial g_j}{\partial x_{D_n}} \right)_{x_{D_n} = x_{D_n}^i} (x_{D_n} - x_{D_n}^k) + \sum_{i \in T_k} y_i \cdot \Delta g_{i,j}^k \leq \ s_{2_j} \quad \forall j \in IEQ \\
& sign(\lambda_j^k) h_{E_j}(x^k, u^k, x_D^k) + \sum_n \left(\frac{\partial h_{E_j}}{\partial x_{D_n}} \right)_{x_{D_n} = x_{D_n}^i} (x_{D_n} - x_{D_n}^k) + \sum_{i \in T_k} y_i \cdot \Delta h_{E_{i,j}}^k \\
& \leq \ s_{3_j} \quad \forall j \in EQ \\
& k = 1, 2, 3, ..., K \\
& \begin{bmatrix} s_{1_o} \geq 0 \quad s_{2_j} \geq 0 \quad s_{3_j} \geq 0 \\ \sum_{i \in T} y_i = 1 \\ y_i \in \{0, 1\} \end{bmatrix}
\end{aligned}
\tag{12}
$$

The objective function of the master problem is formed by an auxiliary variable α and a penalty for constraint violation $\prod$ that multiplies the slack variables. The first constraint is formed by three terms: (i) the objective function value at iteration k of the algorithm, (ii) the linearization with respect to design variables and (iii) the contribution topological modification by changing the current rectification column by either adding or removing stages in the column or changing the feed stage. This last term makes use of binary variable y_i, which is 1 if topological modification i in the rectification column is implemented and 0 otherwise. In addition, parameter $\Delta obj_{i,o}^k$ accounts for the change in objective function o when topology i is implemented. External inequality (IEQ) and equality (EQ) constraints are handled following a similar procedure. Parameter $sign(\lambda_j^k)$ denotes the sign of the Lagrange multiplier of the NLP solved at iteration k of the algorithm. This value is used to correctly relax the

equalities into inequalities. Note that the values of $\Delta obj_{i,o}^{k}$, $\Delta g_{i,j}^{k}$ and $\Delta h_{E_{i,j}}^{k}$ are obtained by fixing design variables x_D to their optimal value in the latest k iteration and then solving a series of i simulations, each one corresponding to a different possible rectification column configuration. Figure 3 provides an illustrative example on how these terms are defined.

(Figure 3 could be placed here)

It should be noted that all the linear constraints are accumulated in the master MILP, which means that at iteration k, the problem includes the constraints generated at this iteration and all the constraints from previous iterations. The primal problem is solved again for the new set of values of binary variables predicted by the master MILP and the overall procedure is repeated until the termination criterion is satisfied. Integer cuts can be also added to the master problem in order to avoid the repetition of solutions explored so far in the primal problem. Note, W_i are structural rectification column combinations if the value is 1, we select that structural topology is selected.

Regarding the implicit constraints, it is important to remark that these sets of equations are solved by the process simulator. Their derivatives, which are used to construct the master problem, are calculated via finite differences.

5 RESULTS AND DISCUSSION

The capabilities of our approach are illustrated through its application to the design of an absorption cooling system. We describe first the implementation details of the overall procedure and then present some numerical results.

5.1 Computer implementation

The mathematical model of the ammonia-water absorption system is based on that introduced by (Gebreslassie et al., 2009a). We use the process simulator Aspen Plus (2011) to simulate the AWRS. This software package allow an easy modeling of the system, as it implements thermodynamic correlations, built-in models for a variety of unit operations and mass and energy balances. This approach has been already followed by other authors in literature. Particularly, Zhang & Lior (2007) developed a model in Aspen Plus of a combined power and refrigeration cycle and validated it with the International Institute of Refrigeration (1994). In the same line, Vidal et al. (2006) simulated a combined power and refrigeration cycle using the RKS-EOS in Aspen Plus, finding good agreement with other results available in the literature (Kalina & Leibowitz, 1998; Zheng et al., 2002; Zhang & Lior, 2004, 2005) as well as with experimental data (Gomez et al., 2005).

Specifically, we simulate the generator of the absorption cycle as a multistage rectification column with a partial condenser using a rigorous tray-by-tray model of the rectification column, as proposed by (Darwish et al., 2008). The absorber (A), condenser (C), evaporator (E), refrigerant subcooler (SC) and solution heat exchanger (SHX) are simulated in Aspen Plus using the MheatX model. The RadFrac model was selected for the rectification column. The working fluid is a water-ammonia mixture. The Redlich-Kwong-Soave equation of state was employed to calculate the thermodynamic properties of the ammonia-water mixture in vapour phase. For the simulation of the liquid mixture, the Non-Random Two Liquid model (NRTL) was employed.

The process simulators is connected with Matlab (2011), in which the main code of the algorithm was implemented. This software gets the values of the dependent variables (e.g., temperature, pressure, mass and energy flows) from the process simulator at each iteration of the algorithm. Note, the SNOPT solver and Aspen Plus-Matlab were linked by a COM interface. The GAMS and Matlab connection were developed using text files.

As NLP solver, we used SNOPT (Holmström et al., 2009a), which was accessed via the

Tomlab (2009) modeling system supported by Matlab. This solver is particularly suited for nonlinear problems whose functions and gradients are expensive to evaluate (Gill et al., 2002). The master MILP sub-problem was solved using the MIP solver CPLEX (Holmström et al., 2009b), accessed via Tomlab. Figure 4 outlines the computer architecture of the solution algorithm proposed.

(Figure 4 could be placed here)

5.2 Numerical results

The design problem aims to determine the optimal operating conditions of the cycle (mainly external and internal fluids flow rates, equipments sizing and system pressures) and rectification column characteristics (number of trays, the feed tray, reboiler duty and reflux ratio) that minimize simultaneously the total annualized cost and environmental impact given a fixed cooling capacity of 90kW. Two different sets of working conditions (corresponding to cooling and refrigeration applications) were studied. The ammonia-water absorption system provides 90 kW of cooling power using chilling water that is cooled down from 10ºC to 5ºC in the evaporator at cooling conditions. The same cooling demand is provided at refrigeration conditions, using in this case a solution of 95% ethyleneglycol that is cooled down from -5ºC to -10ºC.

The moMINLP features 10 design variables: 8 continuous and 2 discrete. In addition, it includes 5 nonlinear inequality constraints. Recall that the remaining process variables and constraints are defined in an implicit form using the process simulator Aspen Plus. The algorithm takes around 2,500 to 3,000 CPU seconds to generate 10 Pareto solutions on a computer AMD PhenomTM 8600B, Triple-Core Processor 2.29GHz and 3.23 GB of RAM. The same design decision variables are optimized at cooling and refrigeration conditions. The degrees of freedom (i.e., external continuous variables of the model) are the rectification

column reboiler duty, the high and low pressures of the system, mass flow rate and mass fraction of stream 1, temperature at the outlet of the hot side of the SHX (temperature 5), temperature at the outlet of the hot side of the SC (temperature 9) and reflux ratio in the rectification column. Discrete decision variables correspond to the number of trays and feed stage in the rectification column. Hence, the model has in total 10 degrees of freedom. The economic data used in the analysis are shown in Table 1.

(Table 1 could be placed here)

In addition, Table 2 displays the environmental data, which have been retrieved from the Ecoinvent database. Recall that the LCA impact is assessed using the Eco-Indicator 99 methodology (see Apendix A).

(Table 2 could be placed here)

Figure 5 depicts the Pareto curves obtained for the absorption machine at cooling and refrigeration conditions. Particularly, 10 Pareto solutions were generated for each case. Note that each point entails different values for the design and operating conditions.
As observed, the slope of the Pareto curve is smooth from point 1 (minimum EI) to point 4, and then increases from point 4 to point 10 (minimum cost). Hence, it seems convenient to choose optimal trade off solutions close to point 4, in which significant environmental savings can be obtained at a marginal increase in cost.

(Figure 5 could be placed here)

Table 3 shows the decision variables values corresponding to the extreme points (i.e., minimum environmental impact and minimum cost) at cooling and refrigeration conditions. Both

designs primarily differ in the duty provided to the system. Particularly, the reboiler duty in the minimum environmental impact design is significantly lower than in the minimum cost solution in both cases: at cooling (130.5 kW vs. 142.3 kW) and refrigeration conditions (173.3kW vs. 197.7kW). This is because the environmental impact is highly dependent on the steam supplied to the reboiler. As observed, the minimum impact solution shows better COP, that is, the energy is used more efficiently, thereby leading to less environmental impact. These low reboiler duties are obtained at the expense of larger exchange areas that increase the total cost. In the first case (at cooling conditions), all Pareto points involve a rectification column with one single stage. In the second case (at refrigeration conditions) all the solutions lead to a rectification column with 3 stages, with the feed stage placed in the first tray starting from the bottom of the column.

(Table 3 could be placed here)

As observed in Table 4, in the first case (at cooling conditions) the TAC is reduced by 9.35% (23,445 €/year vs 21,916 €/year) along the Pareto curve by reducing the total equipment area by 31.0% (129.23 m^2 vs 89.13 m^2). This is accomplished by providing more duty to the system, which decreases the COP and the areas of the heat exchangers (i.e., absorber, condenser and evaporator). In this second case, (at refrigeration conditions) the TAC is reduced by 10.90% (32,293 €/year vs 28,771 €/year). Similar observations are obtained in this second case. Particularly, the total equipment area is reduced by 41.2% (175.9 m^2 vs 103.5 m^2). More duty is in turn provided to the system, and the COP is decreased. Further, the environmental impact is reduced by 7.82% (16,926 points vs 15,453 points) at cooling conditions and by 11.27% (23,451 points vs. 20,807 points) at refrigeration conditions. In both cases, the minimum cost design leads to lower COP, requiring more steam than the minimum EI design. This leads to higher operational cost. The total area of the equipment units, however, is reduced by 31.1% (129.3 m^2 vs 89.1 m^2) resulting in a significantly lower

capital cost and total TAC.

(Table 4 could be placed here)

Figures 6 and 7 provide a breakdown of the environmental impact for the Pareto extreme solutions (min TAC and min EI) at cooling and refrigeration conditions. As can be seen, most of the environmental impact is due to the steam consumption. This is consistent with the results obtained previously, in which the total impact was minimized by reducing the reboiler duty. Furthermore, it is also noticed that the environmental indicator with the largest contribution to the total impact is the extraction of fossil fuels.

(Figure 6 could be placed here)
(Figure 7 could be placed here)

As observed in the Pareto curves as well as in Tables 3 and 4, both the cost and environmental impact are larger at refrigeration conditions. The minimum TAC is 23.8% higher (28,771 €/year vs. 21,916 €/year) and the environmental impact is 25.02% higher (20,807 Points vs. 15,601 Points). This is due to the fact that refrigeration conditions require more duty and larger areas of the equipment units.

6 CONCLUSIONS

This work has introduced a systematic method to assist decision makers in the design of environmentally conscious ammonia-water absorption machines for cooling and refrigeration applications. The approach presented shows three main advantages compared to other methods available in the literature: (1) it uses detailed process models implemented in a process simulator that are optimized with an external solver, (2) it applies rigorous deterministic

mathematical programming techniques that ensure the (local) optimality of the solutions found, and (3) it quantifies the environmental impact of the system over its entire life cycle by applying LCA principles.

A rigorous solution approach has been presented that decomposes the model into two hierarchical levels between which the algorithm iterates. The capabilities of this method have been tested in an ammonia-water absorption machine for cooling and refrigeration purposes. Numerical results demonstrate that it is possible to significantly improve the environmental performance of thermodynamic cycles by compromising the cost to a certain extent. This is accomplished by properly adjusting the operating conditions and equipment sizes of all their units.

Acknowledgements

The authors wish to acknowledge support from the Spanish Ministry of Education and Science (projects ENE 2011-28269-CO3-03), the Spanish Ministry of External Affairs (projects PHB 2008-0090-PC)and the Conselleria de Educacion of the Generalitat Valenciana (BEST/2010/085).

References

Aspen Plus, version 7.1 (0.0.7119). Aspen Technology, Inc., Cambridge, www.aspentech.com.

Alexander, B., Barton, G., Petrie, J., & Romagnoli, J. (2000). Process synthesis and optimisation tools for environmental design: Methodology and structure. *Computers and Chemical Engineering,24* ,1195-2000.

Azapagic, A., & Clift, R. (1999). Application of life cycle assessment to process optimisation. *Computers and Chemical Engineering,23*, 1509-1526.

Azapagic, A., & Clift, R. (1999). Life cycle assessment and multiobjective optimisation. *Journal of Cleaner Production,7*, 135-143.

Balaras C.A., Gaglia A.G., Georgopoulou E., Mirasgedis S., Sarafidis Y., & Lalas D.P.(2007). European residential buildings and empirical assessment of the Hellenic building stock, energy consumption, emissions and potential energy savings. *Building and environment,42*, 1298-1314.

Brunet, R., Guillen-Gosalbez, G., Pérez-Correa, J.R., Caballero, J.A., & Jimenez, L. (2012). Hybrid simulation-optimization based approach for the optimal design of single-product biotechnological processes. *Computers and Chemical Engineering,37*, 125-135.

Brunet, R., Guillen-Gosalbez, G., & Jimenez, L. (2012). Cleaner Design of Single-Product Biotechnological Facilities through the Integration of Process Simulation, Multiobjective Optimization, Life Cycle Assessment, and Principal Component Analysis. *Industrial & Egineering Chemistry Research,51*, 410-424.

Caballero, J.A., Milán-Yañez, D., & Grossmann, I.E. (2005). Rigorous design of distillation columns: Integration of disjunctive programming and process simulators.*Industrial & Egineering Chemistry Research,44*, 6760-75.

Carvalho, A., Gani, R., & Matos, H. (2006). Design of sustainable processes: Systematic generation and evaluation of alternatives. *Computer Aided Chemical Engineering,21*, 817-22.

Chavez-Islas, L.M., & Heard, C.L. (2009). Design and analysis of an ammonia-water absorption refrigeration cycle by means of an equation-oriented method.*Industrial & Egineering Chemistry Research,48*, 1944-1956.

Chavez-Islas, L.M., & Heard, C.L. (2009) Optimization of a simple ammonia-water absorption refrigeration cycle by application of mixed-integer nonlinear programming.*Industrial & Egineering Chemistry Research,48*, 1957-1962.

Chavez-Islas, L.M., Heard, C.L., & Grossmann, I.E. (2009). Synthesis and optimization of an ammonia-water absorption refrigeration cycle considering different types of heat exchangers by application of mixed-integer nonlinear programming. *Industrial & Egineering Chemistry Research,48*, 2927-2990.

Consoli, F., Allen, D., Boustead, I., Fava, J., Franklin, W., & Jensen A.A. (1993). A code of practice. Guidelines for life-cycle assessment. Pensacola, USA:SETAC.

Darwish, N.A., Al-Hashimi, S.H., & Al-Mansoori, A.S. (2008) Performance analysis and evaluation of a commercial absorption-refrigeration water-ammonia (ARWA) system. *International Journal of Refrigeration,7*, 1214-1223.

Diaz, M.S., & Bandoni J.A. 1996. A mixed integer optimization strategy for a large chemical plant in operation. *Computers & Chemical Engineering,20*,531-545.

Diwekar, U.M., Grossmann, I.E., & Rubin, E.S. (1992) An MINLP Process Synthesizer for a Sequential Modular Simulator. *Industrial & Engineering Chemistry Research,31*,313-322.

Erickson, D.C., Anand, G., & Kyung, I. (2004). Heat-activated dual-function absorption cycle *ASHRAE Transactions,110*, 515-524.

Fernandez-Seara, J., Sieres, J., & Vazquez, M. (2003). Distillation column configurations in ammonia-water absorption refrigeration systems. *International Journal of Refrigeration,26* 28-34.

Florides, G.A., Kalogirou, S.A., Tassou, S.A., & Wrobel L.C. (2002). Modelling, simulation and warming impact assessment of a domestic-size absorption solar cooling system. *Applied Thermal Engineering,22*, 1313-1325.

Gebreslassie, B.H., Guillén-Gosálbez, G., Jiménez, L., & Boer D. (2009). Design of environmentally conscious absorption cooling systems via multi-objective optimization and life cycle assessment. *Applied Energy,86*, 1712-1722.

Gebreslassie, B.H., Guillén-Gosálbez, G., Jiménez, L., & Boer D. (2009). Economic performance optimization of an absorption cooling system under uncertainty. *Applied Thermal Engineering,29*, 3491-3500.

Gill, P.E., Murray, W., & Saunder, M.A. (2002). SNOPT: An SQP algorithm for large-scale constrained optimization. *SIAM Journal on Optimization,12*, 979-1006.

Gomez, V.H., Vidal, A., Garcia, C., Garcia-Valladares, O., Best, R., Hernandez, J., & Velazquez, N. (2005). Evaluation of an indirect-fired gas cycle cooling system. *International sorption heat pump conference, Denver, Colorado*. Paper ISHPC-004-2005.

Guillen-Gosalbez, G., Caballero, J.A., Jiménez, L. (2008). Application of life cycle assessment to the structural optimization of process flowsheets. *Industrial & Egineering Chemistry Research,47*, 777-789.

Guillen-Gosalbez, G., & Grossmann I.E. (2009). Optimal design and planning of sustainable chemical supply chains under uncertainty. *AIChE Journal,55*, 99-121.

Guillen-Gosalbez, G., & Grossmann I.E. (2010). A global optimization strategy for the envi-

ronmentally conscious design of chemical supply chains under uncertainty in the damage assessment model. *Computers and Chemical Engineering,34*, 42-58.

Guthrie, K.M. (1996). Data and techniques for preliminary capital cost estimating. *Chemical Engineering,24*, 114-142.

Haimes, Y., Lasdon, L., & Wismer D. (1971). On a bicriterion formulaiton of the problems of integrated system identification and system optimization. *IEEE Transaction on systems,1*, 296-297.

Henning, H.M. (2007). Solar assisted air conditioning of buildings - an overview. *Applied Thermal Engineering,27*, 1734-1749.

Herold, K.E., Radermacher, R., & Klein S.A. (1996). Absorption chillers and heat pumps. *CRC Press*.

Holmström, K., Göran, A.O., & Edvall, M.M. (2009). User's guide for Tomlab/SNOPT v12.1.

Holmström, K., Göran, A.O., & Edvall, M.M. (2009). User's guide for Tomlab/CPLEX v12.1.

Hugo, A., Rutter, P., Pistikopoulos, S., Amorellib, A., & Zoia G. (2005). Hydrogen infrastructure strategic planning using multi-objective optimization. *International Journal of Hydrogen Energy,30*, 1523-1534.

Kalina, A.I., & Leibowitz H. (1988). The design of a 3MW Kalina cycle experimental plant. *American Society of Mechanical Engineers Paper*. Amsterdam 88-Gt-140.

Keil, C., Plura, S., Radspieler, M., & Schweigler, C. (2008). Application of customized absorption heat pumps for utilization of low-grade heat sources. *Applied Thermal Engineering,28*, 2070-2076.

Kim, H., Kim, I.H., & Yoon, E.S. (2010). Multiobjective design of calorific value adjustment process using process simulators. *Industrial & Egineering Chemistry Research,49*, 2841-2848.

Kizilkan, O., Sencan, A., & Kalogirou, S.A. (2007). Thermoeconomic optimization of a LiBr absorption refrigeration system. *Chemical Engineering and Processing: Process Intensification,46*, 1376-1384.

Kravanja, Z., & Grossmann, I.E. (1996). Computational Approach for the Modelling/Decomposition Strategy in the MINLP Optimization of Process Flowsheets with Implicit Models. *Industrial & Egineering Chemistry Research,35*, 2065-2070.

Matlab 2011, The MathWorks, Software (2011). Available from: www.mathworks.com.

Mavrotas, G. (2009). Effective implementation of the ϵ-constraint method in multi-objective mathematical programming problems. *Applied mathematics and computation,213*, 455-465.

McMullan J.T. (2002). Refrigeration and the environment-Issues and strategies for the future. *International Journal of Refrigeration,25*, 89-99.

Misra R.D., Sahoo P.K., Gupta A. (2005). Thermoeconomic evaluation and optimization of a double-effect H 2O/LiBr vapour-absorption refrigeration system. *International Journal of Refrigeration,28*, 331-343.

Misra R.D., Sahoo P.K., Gupta A. (2006). Thermoeconomic evaluation and optimization of an aqua-ammonia vapour-absorption refrigeration system. *International Journal of Refrigeration,29*, 47-59.

PRe-Consultants. (2000) The Eco-indicator 99A damage oriented method for life cycle impact assessment. methodology report and manual for designers. Technical Report, PR´e Consul-tants Amersfoort, The Netherlands.

Puigjaner, L., & Guillén-Gosálbez, G. (2008). Towards an integrated framework for supply chain management in the batch chemical process industry. *Computers and Chemical Engineering,32*, 650-670.

Reneaume, J.M., Koehret, B., & Joulia, X.L. (1995). Optimal process synthesis in a modular simulator environment: New formulation of the mixed-integer nonlinear programming problem. *Industrial & Egineering Chemistry Research,34*, 4378-4394.

Selbas R., Kizilkan O., & Sencan A. (2006). Thermoeconomic optimization of subcooled and superheated vapor compression refrigeration cycle. *Energy,31*, 1772-1792.

Siddiqui, M.A. (1997). Economic analyses of absorption systems: Part A - Design and cost evaluation. *Energy Conversion and Management,38*, 889-904.

TOMLAB Optimization (2009), Avaliable from: www.tomopt.com.

Vidal, A., Best, R., Rivero, R., & Cervantes J. (2006). Analysis of a combined poer and refrigeration cycle by the exergy method. *Energy,31*, 3401-3414.

Zhang, N., & Lior, N. (2004). A novel ammonia-water cycle for power and refrigeration cogeneration. *Proceedings of IMECE04, ASME international mechanical engineering congress and exposition*, Anaheim, CA, USA. Paper IMECE 2004-60692.

Zhang, N., & Lior, N. (2005) Configuration selection methodology for combined power/refrigeration generation ammonia-water cycles. *Proceedings of ECOS Trondheim*, Norway.

Zhang, N., & Lior, N. (2007). Methodology for thermal design of novel combined refrigeration/power binary fluid systems. *International Journal of Refrigeration,30*, 1072-1085.

Zheng, D., Chen, B., & Qi, Y. (2002). Thermodynamic analysis of a novel absorption power/cooling combined cycle. *International sorption heat pump conference*, Shanghai, China.

Ziegler, F., Kahn, R., Summerer, F., & Alefeld G. (1993). Multi-effect absorption chillers. *International Journal of Refrigeration,15*, 301-311.

NOMENCLATURE

Sets/Indices

B	environmental burdens (i.e., feedstock requirements, emissions and waste)
D	decision variables
E	equality constrains
I	inequality constraints
i	topology
j	external equality and inequality constraints
j∈ EQ	external (explicit) equality constraint
j∈ IEQ	external (explicit) inequality constraint
k	iteration
o	objective functions
u∈HX	heat exchangers
u∈U	equipment units

Abbreviations

A	Absorber
AWRS	Ammonia-water absorption refrigeration system
C	Condenser
COP	Coefficient of performance
E	Evaporator
Eco99	Eco-Indicator 99
EI	Environmental Impact
LCA	Life cycle assessment
LCI	Life cycle inventory
MILP	Mixed-integer linear programming
MINLP	Mixed-integer non-linear programming
moMINLP	Multi-objective mixed-integer non-linear programming

MOO	Multi-objective optimization
NLP	Non-linear programming
P	Pump
RC	Rectification column
SC	Refrigerant subcooler
SHX	Solution heat exchanger
TAC	Total annualized cost
VLV1	Refrigerant expansion valve
VLV2	Solution expansion valve

Variables

Am	Area heat exchanger of unit u (m^2)
C_{HX}	Cost heat exchanger (€)
C_P	Cost pump (€)
C_{RC}	Cost rectification column (€)
CF	Annual capital cost (€)
Cb	Exchange are (m^2)
C_u	Cost of the unit (€)
CO	Operating cost (€/yr)
DAM_d	Environmental damages (Points)
$Diam$	Diameter of rectification column (m)
DAM_d	Damage in a given category d (Points)
$df_{b,d}$	Damage in category d per unit of b (Points/kg)
EI	Environmental impact (Points)
H	Height of the rectification column (m)
LCI_b	Life cycle inventory entry associated with b (kg)
Q_u	Heat transfer of unit m (kW)
W_u	Mechanical power of unit u (kW)

δT_m^{lm}	Logarithmic mean temperature difference of unit m (K)
α	Auxiliary variable
$\prod$	Penalty value for the constraint violation

Parameters

c_1	Cost parameter (€/m^2)
c_2	Cost parameter (€)
c_3	Cost parameter (€/kW)
cq	Unitary cost of steam (€/MJ)
cw	Unitary cost of electricity (€/MW h)
crf	Capital recovery factor
Fc	Cost factor that depends on the type of column
fd	Coefficient of the design type
fp	Coefficient of the design type
fm	Coefficient of the material construction
$M\&S$	Marshal & Swift equipment cost index
n	Number of objective functions
t_{op}	Operational hours (h/yr)
Uh_u	Overall heat transfer coefficient of unit m (kW/m^2K)
χ_{euro}	Conversion from dollars to euros (€/$)

A Life Cycle Assessment of the thermodynamic cycles

We use, the LCA methodology (ISO 14044. 2006) to determine the environmental impact of the cycle. This methodology is applied in four phases. Next, we describe these phases in the context of our approach.

1. Goal and scope definition. In this first stage, we define the system boundaries, the functional unit, and the impact categories. The system under study in this work is the absorption cycle shown in Figure 1, which is used for cooling and/or refrigeration applications. The functional unit is a given cooling capacity. The environmental impact is measured according to the Eco-Indicator 99 methodology (Eco-99) PRé-Consultants (2000).

2. Inventory analysis. This second LCA phase provides an output the life cycle inventory (LCI) of emissions and feedstock requirements associated with the process under study. To this end, we first quantify the mass and energy streams crossing the system boundaries. In our case, these streams are provided by the process simulator, and are further translated into the corresponding emissions, waste and feedstock requirements using standard environmental databases.

Particularly, we consider three main sources of impact: generation of natural gas (used in the boiler), electricity (consumed in the pumps), and stainless steel (employed in the construction of the equipment units). The consumption rates of natural gas and electricity are retrieved from Aspen Plus. The capacity of the equipment units is used to estimate the mass of stainless steel they contain (see (**?**)). Hence, the impact associated with the construction of an equipment unit is approximated by that associated with the generation of the corresponding amount of steel. Data retrieved from eco-invent PRé-Consultants (2000) is used to perform these calculations.

3. Impact assessment. The Life Cycle Impact Assessment (LCIA) phase translates the LCI data into the corresponding environmental impacts. The damage in a given category (DAM_d) is determined from the life cycle inventory entries (LCI_b) and corresponding set of damage factors (df_{bd}). Therefore, Eco-indicator 99 is the sum of the 10 impact categories.

$$DAM_d = \sum_{b \in d} df_{bd} \cdot LCI_b \qquad \forall d \in D$$

4. Interpretation. In the last LCA phase, the results are analyzed and a set of conclusions and recommendations are formulated. Our approach provides as output a set of Pareto optimal solutions that trade-off the economic and environmental performance. The interpretation phase is therefore performed in the post-optimal analysis of these solutions.

B Operating values in the extreme points

Tables 5 and 6 summarize the solutions of the extreme Pareto points (minimum cost and minimum environmental impact) at cooling and refrigeration conditions. The information given includes the thermodynamic properties of each state point of the cycle, the pressure, temperature, ammonia composition, mass flow rates and enthalpy.

(Table 5 could be placed here)

(Table 6 could be placed here)

List of Tables

Table 1: Economic data of the absorption cooling cycle Gebreslassie et al. (2009a)

Heat transfer coefficient U (kW/m^2 K)	
Absorber	800
Condenser	500
Evaporator	1100
Rectification column	1300
Subcooler	1000
Solution heat exchanger	700
Absorber	800
Cost parameters	
M&S (-)	1092
$F_c(\$/ft^2)$	5.97
$c_1(e/m^2)$	561.62
$c_2(e)$	268.45
$c_3(e/kW)$	630.00
$d_{euro}(e/\$)$	0.704
Cost data	
Unitary cost of heat (e/MWh)	27.00
Unitary cost of electricity (e/MWh)	100.00
Interest rate (%)	10
Operation time per year (h)	4000
Amortization period (yr)	15

Table 2: Environmental data of the absorption cooling cycle Gebreslassie et al. (2009a)

	Impact category	Steam [Points/kg]	Electricity [Points/kWh]	Steel [Points/kg]
1	Carcinogencis	$1.18 \cdot 10^{-4}$	$4.36 \cdot 10^{-4}$	$6.32 \cdot 10^{-3}$
2	Climate change	$1.60 \cdot 10^{-3}$	$3.61 \cdot 10^{-6}$	$1.31 \cdot 10^{-2}$
3	Ionising radiation	$1.13 \cdot 10^{-3}$	$8.24 \cdot 10^{-4}$	$4.51 \cdot 10^{-4}$
4	Ozone depletion	$2.10 \cdot 10^{-6}$	$1.21 \cdot 10^{-4}$	$4.55 \cdot 10^{-6}$
5	Respiratory effects	$7.87 \cdot 10^{-7}$	$1.35 \cdot 10^{-6}$	$8.01 \cdot 10^{-2}$
6	Acidification	$1.21 \cdot 10^{-4}$	$2.81 \cdot 10^{-4}$	$2.71 \cdot 10^{-3}$
7	Ecotoxicity	$2.80 \cdot 10^{-3}$	$1.67 \cdot 10^{-4}$	$7.45 \cdot 10^{-2}$
8	Land occupation	$8.58 \cdot 10^{-5}$	$4.68 \cdot 10^{-4}$	$3.73 \cdot 10^{-3}$
9	Fossil fuels	$1.25 \cdot 10^{-2}$	$1.20 \cdot 10^{-3}$	$5.93 \cdot 10^{-2}$
10	Mineral extraction	$8.82 \cdot 10^{-6}$	$5.70 \cdot 10^{-6}$	$7.42 \cdot 10^{-2}$

Table 3: Comparison between the decision variables in the base case and the optimal solution

Design	Reb.Duty [kW]	P_{High} $[bar]$	P_{Low} $[bar]$	m_1 $[kg/s]$	x_1 $[kg_{NH_3}/kg_{tot}]$	ΔT_{SHX} $[^oC]$	ΔT_{SC} $[^oC]$	RR $[-]$
Cooling								
ECO99	130.5	12.94	5.00	0.330	0.545	38.05	21.77	0.042
Cost	142.3	13.32	4.42	0.309	0.510	41.53	20.20	0.057
Refrigeration								
ECO99	173.3	12.91	2.75	0.580	0.400	37.25	0.00	0.233
Cost	197.6	13.89	2.53	0.454	0.391	43.52	5.68	0.235

Table 4: Comparison between the output variables in the base case and the optimal solution

Design	COP [-]	TAC [€/$year$]	CF [€/$year$]	CO [€/$year$]	A_T [m^2]	$Steam$ [$kg/year$]	$Electricity$ [$MJ/year$]	$ECO99$ [$Points/year$]
Cooling								
ECO99	0.686	23,445	13,334	10,105	129.3	829,668	10,453	15,453
Cost	0.629	21,916	14,534	7,382	89.1	904,972	10,790	16,926
Refrigeration								
ECO99	0.516	32,293	18,262	14,031	175.9	1,101,775	15,577	20,807
Cost	0.453	28,771	20,133	8,537	103.5	1,256,111	13,548	23,451

Table 5: Thermodynamic properties and mass flow rates of the minimum cost and minimum environmental impact design at cooling conditions

State Point	$P[bar]$	$T[^oC]$	$x[kg/kg]$	$m[kg/s]$	$h[kJ/kg]$
1	4.48//5.00	33.77//33.59	0.514//0.545	0.309//0.330	-88.28//-86.75
2	13.28//12.94	34.11//33.89	0.514//0.545	0.309//0.330	-86.02//-84.69
3	13.28//12.94	82.21//74.88	0.514//0.545	0.309//0.330	256.5//217.5
4	13.28//12.94	120.30//107.23	0.316//0.360	0.219//0.240	429.3//326.8
5	13.28//12.94	41.15//38.05	0.316//0.360	0.219//0.240	-19.81//-47.57
6	4.48//5.00	41.24//38.23	0.316//0.360	0.219//0.240	-20.19//-47.92
7	13.28//12.94	56.08//49.27	0.997//0.997	0.090//0.090	1358//1340
8	13.28//12.94	34.62//33.68	0.997//0.997	0.090//0.090	1293//1293
9	13.28//12.94	20.20//21.77	0.997//0.997	0.090//0.090	94.75//102.2
10	4.48//5.00	1.27//4.33	0.997//0.997	0.090//0.090	1270//1273
11	4.48//5.00	3.78//6.00	0.997//0.997	0.090//0.090	1276//1278
12	4.48//5.00	30.44//30.14	0.997//0.997	0.090//0.090	1342//1338
13	4.48//5.00	55.46//52.49	0.514//0.545	0.309//0.330	308.4//290.0
w1	1.00//1.00	27.00//27.00	-	3.730//3.534	113.3//113.3
W2	1.00//1.00	35.00//35.00	-	3.730//3.534	146.8//146.7
W3	1.00//1.00	27.00//27.00	-	3.085//3.047	113.3//113.3
W4	1.00//1.00	35.00//35.00	-	3.085//3.047	146.8//146.8
W5	1.00//1.00	10.00//10.00	-	4.770//4.770	41.88//41.88
W6	1.00//1.00	5.00//5.00	-	4.770//4.770	20.83//20.83

Table 6: Thermodynamic properties and mass flow rates of the minimum cost and minimum environmental impact design at refrigeration conditions

State Point	$P[bar]$	$T[^oC]$	$x[kg/kg]$	$m[kg/s]$	$h[kJ/kg]$
1	2.54//2.75	33.35//34.48	0.391//0.400	0.455//0.580	-77.78//-74.93
2	13.89//12.91	33.60//34.70	0.391//0.400	0.455//0.580	-75.67//-73.07
3	13.89//12.91	111.65//104.01	0.391//0.400	0.455//0.580	427.8//365.3
4	13.89//12.91	148.70//125.93	0.242//0.291	0.365//0.491	698.6//468.2
5	13.89//12,.91	43.52//37.25	0.242//0.291	0.365//0.491	27.23//-24.2
6	2.54//2.75	43.66//37.36	0.242//0.291	0.365//0.491	26.84//-24.63
7	13.89//12.91	64.14//49.55	0.999//0.999	0.090//0.089	1382//1342
8	13.89//12.91	36.24//33.60	0.999//0.999	0.090//0.089	694.4//1063
9	13.89//12.91	5.68//0.00	0.999//0.999	0.090//0.089	23.84//-0.218
10	2.54//2.75	-13.21//-11.32	0.999//0.999	0.090//0.089	-63.19//516.7
11	2.54//2.75	-11.74//-11.03	0.999//0.999	0.090//0.089	1180//1164
12	2.54//2.75	34.72//32.18	0.999//0.999	0.090//0.089	1369//1358
13	2.54//2.75	53.48//47.59	0.391//0.400	0.455//0.580	220.0//112.7
W1	1.00//1.00	27.00//27.00	-	4.398//3.852	113.3//113.3
W2	1.00//1.00	35.00//35.00	-	4.398//3.852	146.8//146.8
W3	1.00//1.00	27.00//27.00	-	3.090//3.022	113.3//113.3
W4	1.00//1.00	35.00//35.00	-	3.090//3.022	146.8//146.8
W5	1.00//1.00	-5.00//-5.00	-	8.591//8.591	-21.38//-21.38
W6	1.00//1.00	-10.01//-10.01	-	8.591//8.591	-42.58//-42.58

List of Figures

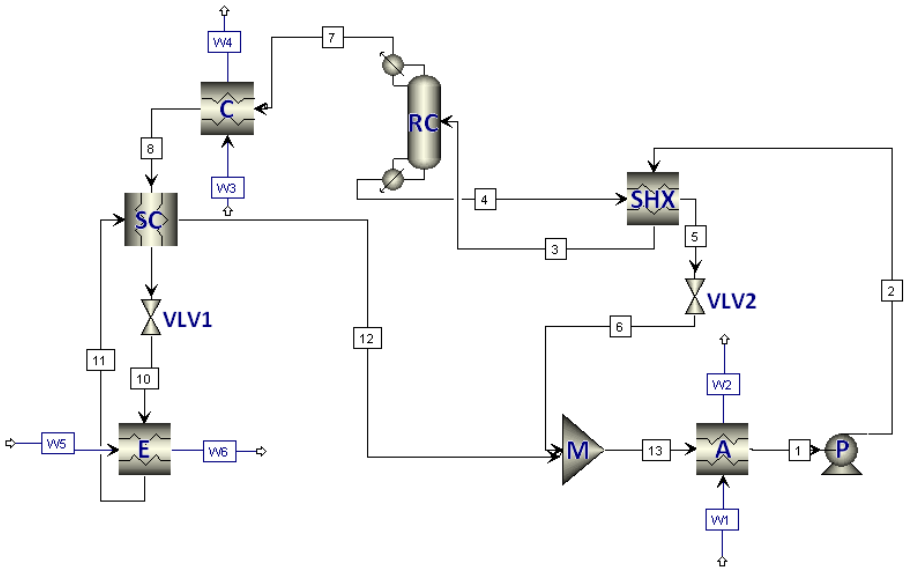

Figure 1: Ammonia-water absorption cycle

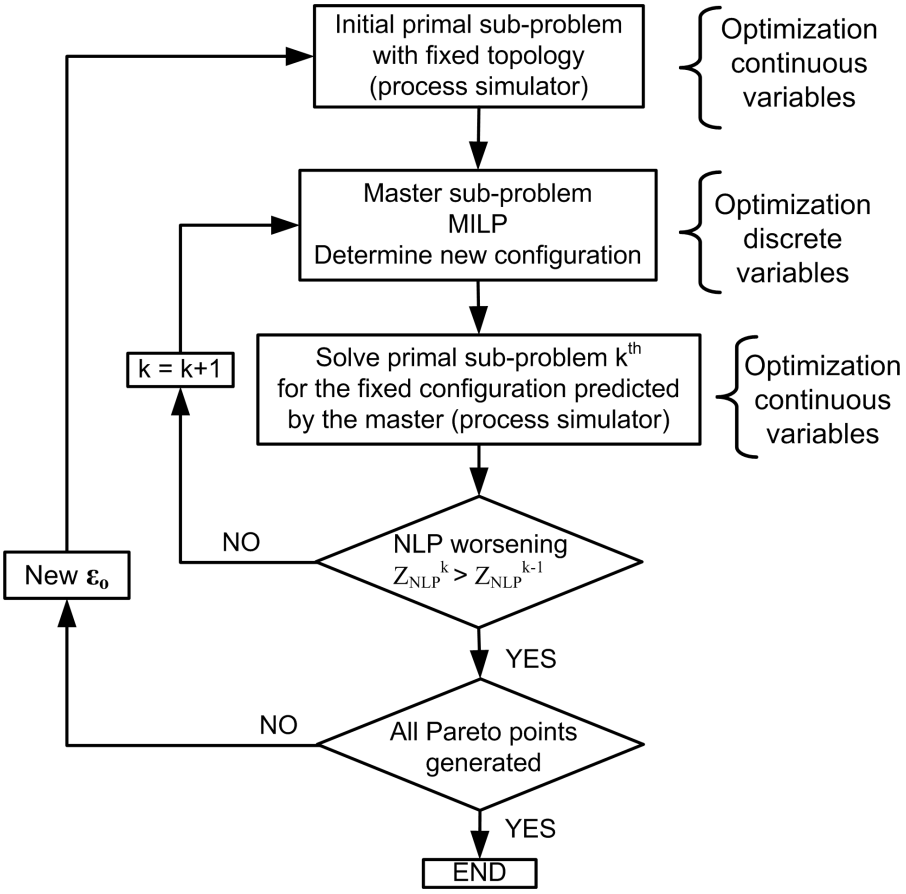

Figure 2: Flowchart of the proposed algorithm

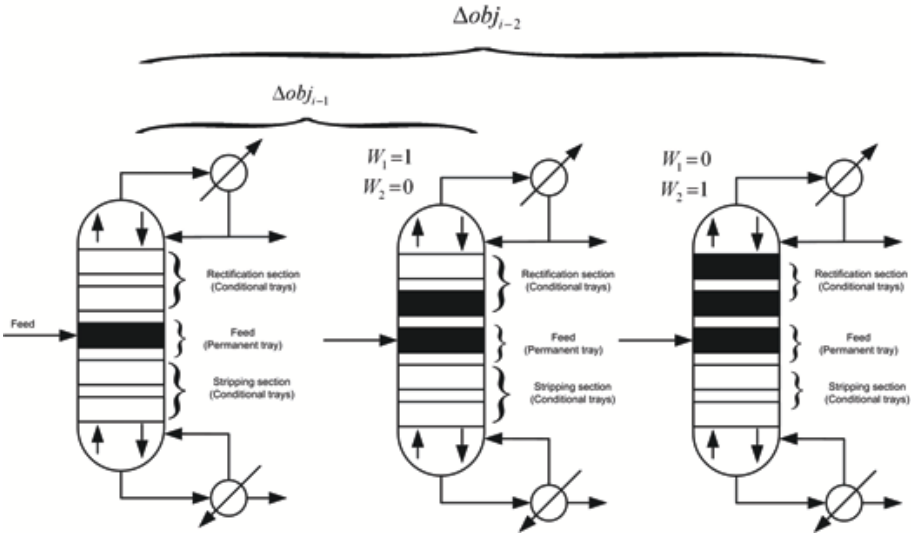

Figure 3: Details on the definition of binary variables in the MILP (inspired in the work by Caballero et al.(Caballero et al., 2005))

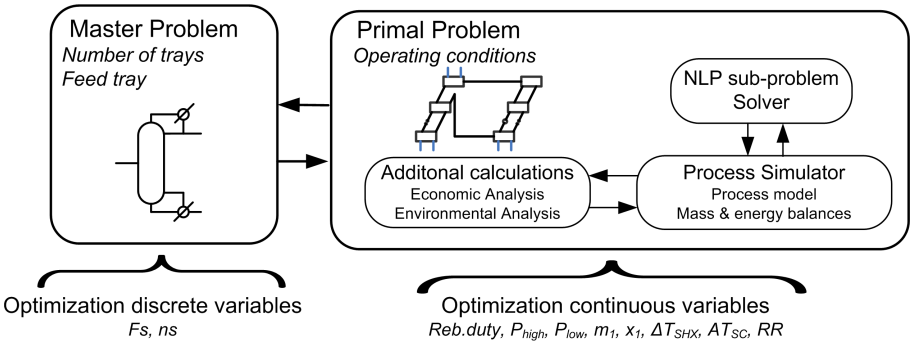

Figure 4: Main steps of the solution algorithm proposed

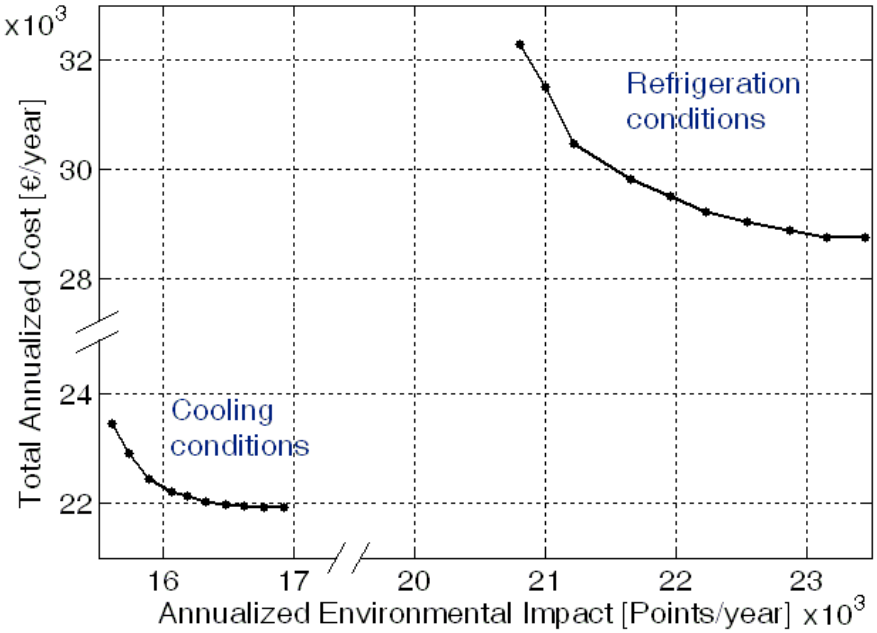

Figure 5: Pareto set of solutions for the absorption cycle

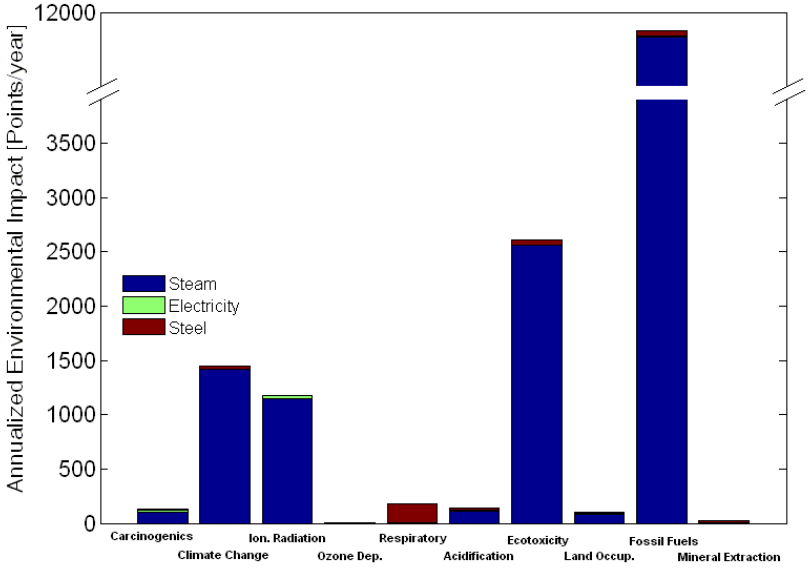

(a) Breakdown of the Annualized Environmental Impact for the solutions of the minimum TAC at cooling conditions

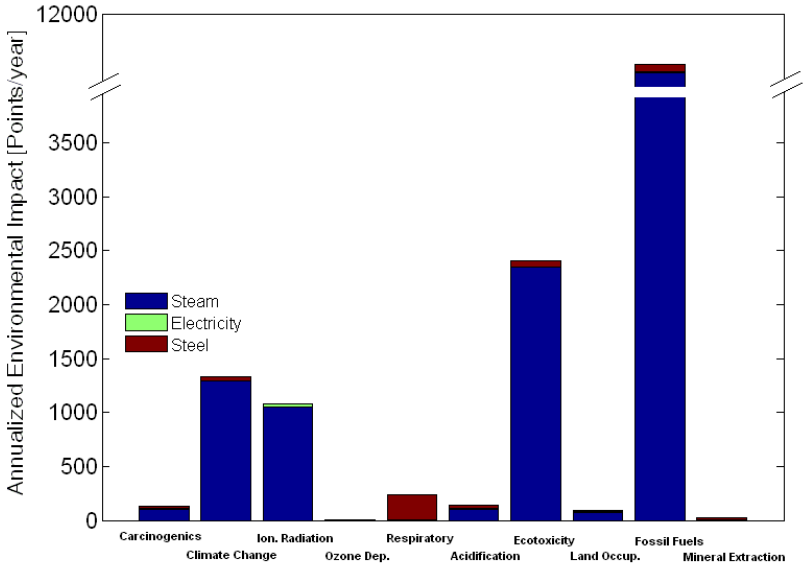

(b) Breakdown of the Annualized Environmental Impact for the solutions of the minimum EI at cooling conditions

Figure 6: Breakdown of the Annualized Environmental Impact at cooling conditions

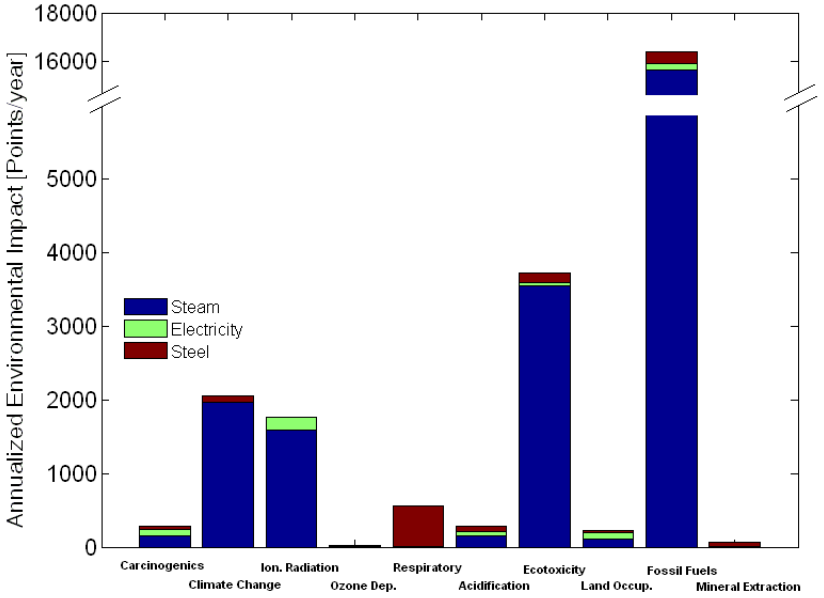

(a) Breakdown of the Annualized Environmental Impact for the solutions of the minimum TAC at refrigeration conditions

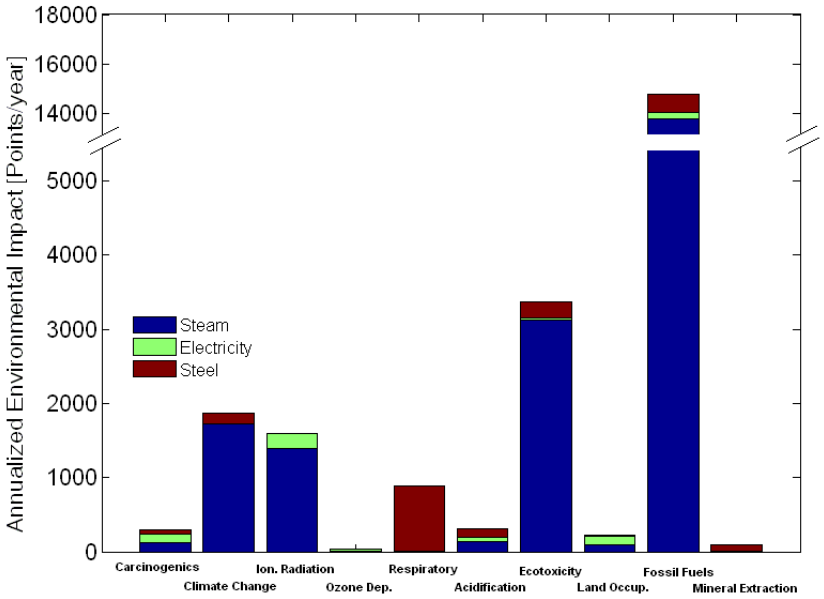

(b) Breakdown of the Annualized Environmental Impact for the solutions of the minimum EI refrigeration conditions

Figure 7: Breakdown of the Annualized Environmental Impact at refrigeration conditions

Article 4

Authors: **R. Brunet**, D. Cortés, G. Guillén-Gosálbez, L. Jiménez, D. Boer.
Title: Minimization of the LCA impact of thermodynamic cycles using a combined simulation-optimization approach.
Journal: *Applied Thermal Engineering*
Volume: **Pages:** **Year:** 2012
ISI category: Mechanical Engineering **AIF:** 0.645
Impact Index: **1**.823
Position in the category: 9/122 (Q1)
Cites: -
Observations: *Accepted doi:10.1016/j.applthermaleng.2012.04.032*

Minimization of the LCA impact of thermodynamic cycles using a combined simulation-optimization approach

Robert Brunet[1], Daniel Cortés[1], Gonzalo Guillén-Gosálbez[1]*, Laureano Jiménez[1] and Dieter Boer [2]

[1] Departament d'Enginyeria Quimica, Escola Tecnica Superior d'Enginyeria Quimica, Universitat Rovira i Virgili, Campus Sescelades, Avinguda Paisos Catalans 26, 43007, Tarragona, Spain

[2] Departament d'Enginyeria Mecanica, Escola Tecnica Superior d'Enginyeria, Universitat Rovira i Virgili, Campus Sescelades, Avinguda Paisos Catalans 26, 43007, Tarragona, Spain

*Corresponding author. E-mail: gonzalo.guillen@urv.cat, telephone: +34 977558618

Abstract

This work presents a computational approach for the simultaneous minimization of the total cost and environmental impact of thermodynamic cycles. Our method combines process simulation, multi-objective optimization and life cycle assessment (LCA) within a unified framework that identifies in a systematic manner optimal design and operating conditions according to several economic and LCA impacts. Our approach takes advantages of the complementary strengths of process simulation (in which mass, energy balances and thermodynamic calculations are implemented in an easy manner) and rigorous deterministic optimization tools. We demonstrate the capabilities of this strategy by means of two case studies in which we address the design of a 10MW Rankine cycle modeled in Aspen Hysys, and a 90kW ammonia-water absorption cooling cycle implemented in Aspen Plus. Numerical results show that it is possible to achieve environmental and cost savings using our rigorous approach.

Keywords: *Process simulation; Optimization; Rankine cycle; Absorption cycle; Cost analysis; Life cycle assessment*

1 INTRODUCTION

The energetic and economic analysis of industrial processes has gained wider interest in recent years. This has been motivated by the need to use the resources available nowadays more efficiently. In this context, process optimization has emerged as an effective tool for reducing energy consumption and improving efficiency in process industries. Multi-objective optimization (MOO), in particular, offers decision makers a suitable framework to identify the set of operating conditions and design variables that simultaneously improve the economic and environmental performance of a system[1].

Thermodynamic cycles are widely used in energy conversion processes. They are often found in daily life, but have the drawback of requiring large amounts of energy to operate. By optimizing power generation cycles, (e.g Rankine cycle) it is possible to increase their efficiency and reduce the associated global warming emissions [2]. Cooling cycles can also benefit from the application of rigorous optimization tools. Increments of up to 50% in their coefficient of performance (COP) have been reported [3], which leads to significant savings in primary energy sources [4].

A variety of optimization approaches have been applied to thermodynamic cycles. Some studies in power cycles focus on the minimization of a single indicator, such as the net present value (NPV), total plant cost (TPC) [5, 6], and cycle efficiency [7–10]. In cooling cycles, some models were devised to optimize the COP and cooling load [3]. The application of MOO to thermodynamic cycles, however, has been quite scarce. The simultaneous optimization of the exergetic efficiency and the TPC in power generation systems was studied by Becerra-Lopez and Golding [11] and Dipama et al. [2]. Pelet et al. [12] optimized a superstructure of energy systems considering the cost and CO_2 emissions. In the context of cooling cycles, Gebreslassie et al. [13, 14] proposed a multi-objective non-linear programming (moNLP) problem for the design of an ammonia-water absorption cycle considering the cost and life cycle assessment (LCA) performance [15, 16].

The overwhelming majority of the works mentioned above follow the so called simultaneous

approach, which relies on formulating algebraic optimization models described in an explicit form. For simplicity, most of these formulations contain short-cut models that avoid the numerical difficulties associated with handling nonlinear equations. These simplified formulations provide "good" approximations when certain assumptions hold, but can lead to large numerical errors otherwise. Sequential process simulation models are more difficult to optimize due to the presence of nonconvexities of different types, but provide more accurate results. Another limitation of the works mentioned above is that those that account for environmental concerns restrict the analysis to a single environmental indicator, neglecting the effects caused in other environmental damages.

This work applies a combined approach that takes advantage of the complementary strengths of sequential modular process simulators (e.g. Aspen Hysys and Aspen Plus), optimization tools (e.g. SNOPT and CPLEX) and LCA. The pivotal idea of our method is to optimize modular simulation models of thermodynamic cycles using an external deterministic optimizer that is guaranteed to converge to an optimal solution. Our approach is inspired by other simulation-optimization methods used in a variety of chemical engineering applications, including the design of systems such as: heat exchangers and chemical reactions [17–19], chemical plants [20, 21], distillation columns [22], and biotechnological processes [23]. An efficient solution method is presented for tackling these problems based on decomposing them into two sub-levels between which an algorithm iterates until a stopping criterion is satisfied. This algorithm performs the calculations using both a process simulation and an external optimizer.

The final goal of our analysis is to identify the design and operating conditions of different thermodynamic cycles that simultaneously minimize the total annualized cost (TAC) and environmental impact (EI). We demonstrate the capabilities of this methodology through its application to the design of two cycles: a steam Rankine cycle and an ammonia-water absorption cycle. The optimization of the steam Rankine cycle is formulated as a moNLP problem, which is optimized with a Successive Quadratic Programming (SQP) solver that interacts at

each iteration with the process simulator of choice. The optimization of the absorption cycle gives rise to a multi-objective mixed-integer non-linear programming (moMINLP) problem, in which binary variables are employed to model the number of trays in the desorber.

2 PROBLEM STATEMENT

As previously mentioned, we will focus herein on two energy conversion cycles: a steam Rankine cycle for power generation and an ammonia-water absorption cooling cycle. Note, however, that the approach presented is general enough to be adapted to any other energy system. We provide next a brief description of each of these systems before immersion into a detailed mathematical formulation.

Rankine Cycle

We consider a reheat-regenerative power cycle with one closed and one open feedwater heater (see Figure 1). The system contains one boiler, one turbine, a condenser, two pumps, and two shell-tube heat exchangers. Water is used as working fluid in the cycle. The boiler is assumed to operate with natural gas. The combustion gases behave as air. For the condenser as well as the heat exchangers, we use shell-tube heat exchangers.

(Figure 1 could be placed here)

Absorption cycle

We consider the single effect ammonia-water absorption cooling cycle described by Gebreslassie et al. [13, 14] (see Figure 2). The absorption cycle provides chilled water at 5 ^{o}C. The equipment units are the absorber (A), condenser (C), rectification column (RC), evaporator (E), subcooler (SC), refrigerant expansion valve (VLV1), solution heat exchanger (SHX), solution pump (P), and solution expansion valve (VLV2). It is assumed that the system works

under steady state conditions. Heat and pressure losses are neglected. Adiabatic valves are considered. The refrigerant leaves the condenser, absorber and bottom of the generator as saturated liquid.

(Figure 2 could be placed here)

Problem definition

The problems can be formally stated as follows. In the case of the Rankine cycle, we are given the flowsheet arrangement, net power yield, turbines and pumps efficiencies, overall heat transfer coefficients, thermodynamic properties, cost estimation correlations, economic parameters and environmental indicators. For the absorption cycle, we need to specify as well the cooling capacity, and inlet and outlet temperatures of the external fluids.
The goal of our study is to identify the optimal design and operating conditions that simultaneously minimize the TAC and the following damage impact indicators: damage to human health (HH), damage to ecosystem quality (EQ) and depletion of resources (DR).

3 METHODOLOGY

This section describes the approach proposed to tackle the problems described above. A general mathematical formulation is first presented. We then describe how the economic and environmental objective functions are calculated. The solution procedure and the computer implementation are finally discussed.

3.1 Mathematical formulation

The design of thermodynamic cycles with economic and environmental concerns can be expressed in mathematical terms as a moMINLP. We solve this model using the ϵ constraint method [24, 25]. This technique is based on calculating a set of single-objective models

in which one objective is kept in the objective function while the others are transferred to auxiliary constraints and forced to be lower than a set of epsilon parameters:

$$\begin{aligned} \min_{x_D} \quad & z = \{f_1(x, u, x_D)\} \\ s.t. \quad & f_o(x, u, x_D) \leq \epsilon_o \qquad\qquad o = 2, ..., n \\ & h_I(x, u, x_D) = 0 \\ & h_E(x, u, x_D) = 0 \\ & g_E(x, u, x_D) \leq \ 0 \end{aligned} \tag{1}$$

Where f_1 is the economic objective function, and f_2 to f_n denote the LCA metrics. ϵ is an auxiliary parameter that bounds the values of the objectives transferred to the auxiliary inequality constraints. Equations h_I are implicit equations implemented in the process simulator, whereas h_E and g_E are explicit constraints that ensure certain process conditions. The form of these equations depends on the system under study.

The design variables are denoted by x_D, while other process variables are represented by x. Finally, u denotes parameters not modified during the calculations. It is important to note that x_D include only continuous variables in the case of the Rankine cycle, while in the case of the absorption cycle it includes both, continuous and integers (i.e., number of trays and feed tray in the absorber).

3.2 Objective functions

The model presented, seeks to optimize simultaneously the TAC and environmental impact. We describe next how these indicators are calculated.

3.2.1 Economic indicator (Total annualized cost)

The TAC of the thermodynamic cycles is given by equation 2.

$$TAC = CO + CF \cdot crf \tag{2}$$

Where CO and CF are the operating and fixed costs, and crf is the capital recovery factor, which is a function of the interest rate (parameter i) and the lifetime of the cycle (parameter t) expressed in years (see equation 3).

$$crf = \left(\frac{i(1+i)^t}{(1+i)^t - 1} \right) \tag{3}$$

The operation cost, denoted by CO, accounts for the cost of the energy and electricity required to operate the cycle.

$$CO = \sum_{u \in U} (Q_u \cdot cq + W_u \cdot cw) \cdot top \tag{4}$$

In this equation, Q_u [MW] is the thermal power supplied to equipment unit U, W_u [MW] is the electrical power required by equipment unit, top [h] is the total annual operation time and cq [€/MWh] and cw [€/MWh] are the unit costs for heat and electricity respectively. Note that Q_u and W_u are provided by the process simulator.

Equation 5 determines the total fixed cost (CF) which accounts for the cost of the main equipment units of the cycle (C_u) which includes the equipment and maintenance cost, which are determined using the costing correlations described in sections 4.1 and 4.2.

$$CF = \sum_{u \in U} C_u \tag{5}$$

3.2.2 Environmental indicator (Damage categories)

The environmental impact is quantified following LCA principles, similarly as done before by the authors in other works [23]. Further details on the calculations are provided in the Appendix.

3.3 Solution procedure

3.3.1 ϵ-constraint methodology

The solution of model is given by a set of Pareto points representing the optimal compromise between the objectives considered in the model. These points are generated combining the ϵ-constraint method [24, 25] with a tailored decomposition algorithm that integrates simulation and optimization tools.

The solution method proposed is shown in Figure 3. It comprises two nested loops: an outer loop in which epsilon values on the environmental impacts are defined, and an inner loop that solves each single-objective problem. We provide next details on the inner loop of the algorithm.

3.3.2. Simulation-optimization approach

The solution strategy for solving each single-objective problem relies on an outer approximation [26] scheme that decomposes each model into two hierarchical levels: a primal non-linear programming (NLP) sub-problem and a master mixed-integer linear programming (MILP) sub-problem. The algorithm iterates between these levels until a termination criterion is satisfied.

The master MILP is constructed using information provided by the primal NLP. This primal NLP is solved integrating a deterministic gradient-based method with the process simulator. The binary variables are thus handled by the MILP, while the NLP provides the optimal values of the continuous variables for a fixed set of binaries. This strategy is inspired by

previous simulation-optimization approaches applied in chemical engineering [17–23]. The main advantage of this method is that it ensures convergence to a local (or global) optimum, as opposed to heuristic-based approaches that are unable to guarantee the optimality of the solutions calculated.

(Figure 3 could be placed here)

Primal NLP sub-problem

This level optimizes the continuous decision variables of the NLP sub-problem for fixed values of the binary variables predicted by the master sub-problem (equation 6). This procedure is repeated iteratively for different values of the binary variables until a termination criterion is met. The NLP sub-problems are solved using a gradient-based SQP solver that iterates with the simulation package in order to obtain information on the derivatives of the decision variables with respect the objective function and constraints.

Slack variables are used to relax the external equality and inequality constraints, which avoids unconvergencies in the slave problem. Potential intermediate unfeasible points are thus handled externally by the optimization algorithm. These slacks are penalized in the objective function. This approach avoids unfeasible simulation runs, preventing the algorithm from

ending prematurely. The modified objective function is expressed as follows.

$$
\begin{aligned}
\min_{x_D} \quad & z = f_1(x,u,x_D) + \prod(s_1+s_2+s_3+s_4) \\
s.t. \quad & f_o(x,u,x_D) \leq \ \epsilon_o + s_1 && o = 2,...,n \\
& \underline{\epsilon_o} \leq \ \epsilon_o \leq \ \overline{\epsilon_o} && o = 2,...,n \\
& h_I(x,u,x_D) = 0 \\
& h_E(x,u,x_D) + s_2 - s_3 = 0 \\
& g_E(x,u,x_D) \leq \ s_4 \\
& s_1 \geq \ 0; s_2 \geq \ 0; s_3 \geq \ 0; s_4 \geq \ 0;
\end{aligned}
\tag{6}
$$

Where $\prod$ is a penalty parameter vector, and s_1, s_2, s_3 and s_4 are vectors of positive slack variables.

Master MILP sub-problem

The master sub-problem provides new values for the binary variables that are expected to yield better results than previous solutions. Note that this master MILP is only required in the case of the absorption cycle, in which the number of trays of the desorber must be decided. In contrast, the optimization of the Rankine cycle can be solved as an NLP.

To construct the master MILP, we use the derivatives of the objective function and constraints of the NLP sub-problem at the optimal NLP solution of the previous iteration. Due to the presence of non-convexities in the NLP, the master MILP is not guaranteed to provide a rigorous lower bound on the global optimum. The following notation is defined in the MILP at iteration k of the algorithm:

$T = \{i | i$ is a potential column configuration$\}$

$T_k = \{i | i$ is a rectification column configuration, entailing a given number of trays and a specific feed stage$\}$

$EQ = \{j | j$ is an external (explicit) equality constraint$)\}$

$IEQ = \{j | j$ is an external (explicit) inequality constraint$\}$

$\Delta obj^k_{i,o}$ = Difference between the objective function o at iteration k of the NLP and the objective function associated with the new rectification column design i

$\Delta g^k_{i,j}$ = Difference between the values of the inequality constraint j for the new rectification column design i and the constraint j in the original NLP^k problem

$\Delta h^k_{E_{i,j}}$ = Difference between the values of the external equality constraint j new rectification column design i and the constraint j in the original NLP^k problem

The master MILP takes the following form:

$$
\begin{aligned}
\min \quad & \alpha + \prod (\sum_{o=2}^{n} s_{1_o} + \sum_{j \in IEQ} s_{2_j} + \sum_{j \in EQ} s_{3_j}) \\
s.t. \quad & f_o(x^k, u^k, x^k_D) + \sum_n \left(\frac{\partial f_o}{\partial x_{D_n}} \right)_{x_{D_n} = x^i_{D_n}} (x_{D_n} - x^k_{D_n}) + \sum_{i \in T_k} y_i \cdot \Delta obj^k_{i,o} \leq \ \alpha \quad o = 1 \\
& f_o(x^k, u^k, x^k_D) + \sum_n \left(\frac{\partial f_o}{\partial x_{D_n}} \right)_{x_{D_n} = x^i_{D_n}} (x_{D_n} - x^k_{D_n}) + \sum_{i \in T_k} y_i \cdot \Delta obj^k_{i,o} \leq \ \epsilon_o + s_{1_o} \quad o = 2, ..., n \\
& g_j(x^k, u^k, x^k_D) + \sum_n \left(\frac{\partial g_j}{\partial x_{D_n}} \right)_{x_{D_n} = x^i_{D_n}} (x_{D_n} - x^k_{D_n}) + \sum_{i \in T_k} y_i \cdot \Delta g^k_{i,j} \leq \ s_{2_j} \quad \forall j \in IEQ \\
& sign(\lambda^k_j) h_{E_j}(x^k, u^k, x^k_D) + \sum_n \left(\frac{\partial h_{E_j}}{\partial x_{D_n}} \right)_{x_{D_n} = x^i_{D_n}} (x_{D_n} - x^k_{D_n}) + \sum_{i \in T_k} y_i \cdot \Delta h^k_{E_{i,j}} \\
& \leq \ s_{3_j} \quad \forall j \in EQ \\
& k = 1, 2, 3, ..., K \\
& \begin{bmatrix} s_{1_o} \geq 0 \quad s_{2_j} \geq 0 \quad s_{3_j} \geq 0 \\ \sum_{i \in T} y_i = 1 \\ y_i \in \{0, 1\} \end{bmatrix}
\end{aligned}
\tag{7}
$$

The objective function of the MILP contains an auxiliary variable (α) and a penalty value for constraint violation ($\prod$) that multiplies the slack variables. The first constraint is formed by three terms: (i) the objective function value at iteration k of the algorithm, (ii) the linearization performed on the design variables, and (iii) the contribution of changing the current distillation column characteristics, by either adding or removing stages in the column or changing the feed stage. This last term is the product of the binary variable y_i (that is 1 if topological modification i is implemented and 0 otherwise) with the parameter $\Delta obj^k_{i,o}$. The latter accounts for the change in the objective function value when topology i is implemented. Figure 4 provides an illustrative example on how these terms are defined.

(Figure 4 could be placed here)

External inequality (IEQ) and equality (EQ) constraints are handled following a similar procedure. $sign(\lambda^k_j)$ refers to the sign of the Lagrange multiplier of constraint j at iteration k. This value is used to correctly relax equalities into inequalities [27]. Note that linear constraints are accumulated in the master MILP, so at iteration k, the problem includes constraints from current and previous iterations.

After determining the new set of values for the binary variables, the primal problem is solved again, and the overall procedure is repeated until the termination criterion is satisfied. Integer cuts can be added to the master MILP in order to avoid repetition of solutions explored so far in previous iterations. Implicit constraints are handled by the process simulator and their derivatives are obtained by finite differences.

Note that the complexity of the overall solution procedure grows rapidly with the number of environmental objectives. In cases with a large number of objectives, we might be interested in applying dimensionality reduction methods to keep the problem in a manageable size [28–30].

3.4. Computational implementation

We use the process simulators Aspen Hysys [31] and Aspen Plus [32] to simulate the thermodynamic cycles. These software packages allow an easy modeling of the cycles, as they implement thermodynamic correlations, built-in models for a variety of unit operations and mass and energy balances. These process simulators were connected with Matlab [33], in which the main code of the algorithm was implemented. This software gets the values of the dependent variables (e.g., temperature, pressure, mass and energy flows) from the process simulators at each iteration of the algorithm.

As NLP solver, we used SNOPT [34], which was accessed via the Tomlab [35] modeling system supported by Matlab. This solver is particularly suited for nonlinear problems whose functions and gradients are expensive to evaluate [36]. The master MILP sub-problem was solved using the MIP solver CPLEX [37], accessed via Tomlab. Figure 5 outlines the computer architecture of the solution algorithm proposed.

(Figure 5 could be placed here)

4 Case studies

Two thermodynamic cycles were studied, a steam Rankine cycle and an ammonia-water absorption cycle. Both systems were simulated using standard commercial process simulators, thereby avoiding the definition of the thermodynamic equations in an explicit form.

4.1 Case study I: Steam Rankine cycle

System description

The first case study addresses the design of a 10 MW steam Rankine cycle (see Figure 6) taken from Moran and Shapiro [38]. The cycle was simulated in Aspen Hysys under steady state

conditions. Heat and pressure losses were neglected. Adiabatic efficiencies in turbines and pumps were set to 75% [39]. An adiabatic expansion valve was considered in the calculations.

(Figure 6 could be placed here)

System modeling

The properties of water, selected as the working fluid of the cycle, were calculated using the ASME steam tables. The boiler and reboiler operate with natural gas. The composition of the combustion gases in the boiler and reboiler is unknown, but we assume that they behave as air, which was modeled using UNIQUAC. For the condenser, heat exchanger, boiler and reboiler simulation, we considered shell-tube heat exchangers, which were modeled using the weighted model built-in Aspen Hysys. The boiler and reboiler were simulated as separated heat exchangers. The same approach was applied to the turbine. The mixer was modeled as an open flow heat exchanger that mixes streams at different temperatures.

Objective functions

The heat cost was set to 25 €/MWh, and the operation time was 4,000 hours per year. The energy flows in the boiler and reboiler were retrieved from Aspen Hysys. The cost of the expansion valves and mixer were neglected. Table 1 shows the cost estimation correlations used for the remaining equipment units [39–41].

(Table 1 could be placed here)

The environmental impact of the operation phase was determined from the energy flows imported from Aspen Hysys. To calculate the environmental impact of the construction phase, we considered only the turbine and heat exchangers (heat exchanger, condenser, boiler and reboiler). The mass of steel from tubes, pumps, valves and other equipments in

the cycle were neglected. The amount of stainless steel contained in the heat exchangers was determined from the exchange area assuming a thickness of 1/4 inches. The weight of the turbine was assumed to be equal to 10 tons (typical weight of a 10 MW turbine [42]).

4.2. Case Study II: Absorption cooling cycle

System description

The second example studies a 90 kW single effect ammonia-water absorption cooling cycle (see Figure 7). This cycle is discussed in detail in Gebreslassie et al. [13, 14]. The absorption cycle provides water at 5°C.

(Figure 7 could be placed here)

System modeling

The Redlich-Kwong-Soave equation of state was selected to model the ammonia-water mixture in vapor phase [43]. For the simulation of the liquid mixture, the Non-Random Two Liquid model was employed. The absorber, condenser, evaporator, subcooler and solution heat exchanger were simulated using the MheatX model. The desorber was simulated with a rigorous tray-by-tray distillation column model.

Objective functions

The operational costs were calculated with equation 4, assuming an electricity cost of 100 €/MWh, a heat cost of 25 €/MWh, and an operation time of 4,000 hours per year. The energy flows (electricity and heat) in the pump and desorber were retrieved from Aspen Plus. The cost correlations are given in Table 2 [44–46].

(Table 2 could be placed here)

The energy flows were retrieved from the process simulator (in this case Aspen Plus). The mass of steel contained in the pipes, valves and other equipments in the cycle were neglected. The mass of steel contained in the heat exchangers was calculated following the same approach as in case study 1. The mass of steel from the desorber was determined approximating the distillation column by a cylinder. The dimensions of the desorber were imported from the process simulator.

5 RESULTS AND DISCUSSION

The design problem aims to determine the optimal operating conditions of the cycle (fluid flow rates, equipment sizing and system pressures and temperatures) that minimize simultaneously the economic indicator (TAC) and different impact categories (HH, EQ and DR) given a fixed energy capacity of the cycle.

We generated in both cases a set of Pareto solutions that we obtained for simplicity minimizing the TAC versus each individual damage category separately.

5.1. Case study I: Steam Rankine cycle

We first studied a 10MW Rankine cycle. The problem was solved as a moNLP with the following 11 design continuous variables: mass flow passing through the cycle (mass flow 1), temperatures of streams 1 and 4, pressure of stream 1, outlet pressure of the turbines (pressures 2, 3, 5 and 6) and outlet temperature of the heat exchangers (temperature B1 and B2). In addition, the model includes 5 nonlinear inequality constraints: power equal or higher than 10MW, and a minimum temperature difference of 10^{o}C in the heat exchangers. The remaining process variables and constraints are defined in an implicit form using the process simulator (Aspen Hysys). The algorithm takes around 600 to 1,000 CPU seconds to generate 10 Pareto solutions of each 2-dimensional Pareto set on a computer AMD PhenomTM 8600B, with a Triple-Core Processor 2.29GHz and 3.23 GB of RAM.

Three bi-criteria Pareto sets were generated optimizing the TAC against each single damage impact category separately (see Figure 8). Figure 8 represents the Pareto solutions of the three bi-objective optimization problem TAC vs HH, TAC vs EQ and TAC vs DR. As observed, the impact in damage category HH was reduced by 2.40% (334.89 kPoints vs 342.93 kPoints) along the Pareto curve. This was accomplished by increasing the heat exchanger areas, thereby reducing the natural gas consumption. This led in turn to an increase of 3.65% in the TAC (3,491 M€/yr vs. 3,619 M€/yr). In addition, the EQ was reduced by 2.38% (336.52 kPoints vs 344.55 kPoints) along the Pareto curve at the expense of increasing the TAC by 3.84% (3,491 M€/yr vs. 3,625 M€/yr). Note that in both cases, solutions with lower TAC entail larger natural gas consumption rates and smaller equipments. Finally we analyze the trade-off solutions between TAC vs DR. Here, the DR was decreased by 2.22% (2,873.06 kPoints vs 2,941.19 kPoints) while the TAC was increased by 4.44% (3,491 M€/yr vs 3,646 M€/yr). Further inspection of the results reveals similar insights, regarding operating conditions and design characteristics, as in the previous cases.

(Figure 8 could be placed here)

Figure 9 depicts the Pareto solutions in a parallel coordinates plot, which is a useful graphical tool to display data sets of large dimension. The figure shows in the x axis the set of objective functions (TAC, HH, EQ and DR) and in the y axis the normalized value attained by each solution in every criterion. The normalization was performed by dividing each objective function value by its maximum over the entire set. Note that each line in the plot represents a different Pareto solution, entailing a set of operating conditions. As observed, all environmental impacts are somehow equivalent, since they tend to behave similarly. Moreover, all of the impacts are conflictive with the TAC of the cycle. This is because reductions in the environmental impact are achieved at the expenses of increasing the cost.

(Figure 9 could be placed here)

Table 3 shows the details of the corresponding extreme points (i.e., minimum TAC and minimum environmental damage). First is presented the decision variables values in the extreme solutions, which differ mainly in the mass flow rate and temperature of stream 1, and the pressure in the turbines. The mass flow rate of stream 1 in the minimum cost solution is greater than in the minimum environmental impact. This is because larger mass flow rates require more natural gas to evaporate water in the boiler and reboiler. The temperature of stream 1 in the economic optimum is lower than in the environmental optimum. Moreover, the pressure drop in the turbine is lower in the minimum cost solution, which leads to smaller turbines and investment costs. Table 3 also displays the heat exchangers areas and the energy consumption (heat and electricity) of the extreme solutions. As observed, the heat exchangers area in the economic optimum is between 5 and 11% smaller than in the minimum environmental impact solutions. Regarding the use of energy, the use of heat and electricity in the minimum impact designs is between 1 and 3.5% smaller than in the economic optimum.

(Table 3 could be placed here)

The objective function values of the extreme designs are compared in Table 4. Note that impacts HH, EQ and DR were decreased by up to 2.40%, 2.38% and 2.22% respectively.

(Table 4 could be placed here)

5.2. Case study II: Absorption refrigeration cycle

A moMINLP model of the 90 kW absorption cycle was developed. This formulation featured 10 design variables, 8 continuous and 2 discrete, and 4 nonlinear inequality constraints. The continuous variables denote the reboiler duty in the desorber, the high and low pressure of the system, the mass flow and mass fraction of stream 1, the temperature at the outlet of the hot side of unit SHX (temperature 5), the temperature at the outlet of the hot side of the SC unit (temperature 9), and the reflux ratio in the desorber. Discrete variables model the number of trays and the feed tray in the desorber. Inequality constraints impose a minimum cooling capacity and minimum temperature difference between the inlet and outlet external flows. The remaining process variables and constraints were implemented in the process simulator, in this case Aspen Plus. The algorithm took around 2,500 to 3,000 CPU seconds to generate 10 Pareto solutions on the same computer as before.

Figure 10 depicts the Pareto solutions of the three bi-objective optimization problems: TAC vs HH, TAC vs EQ and TAC vs DR. The HH index is reduced by 5.84% (2,734 points vs 2,584 points) along the Pareto curve. This is accomplished by reducing the steam provided to the cycle. On the other hand, the TAC is increased by 4.66% (21,917 €/yr vs. 22,940 €/yr). The steam consumption is reduced by increasing the heat exchanger areas, which leads to larger capital investments. Concerning the EQ, this is reduced by 6.82% (2,740 points vs 2,565 points) along the Pareto curve, whereas the TAC is increased by 4.71% (21,917 €/yr vs. 22,951 €/yr). Finally, DR is decreased by 7.03% (10,497 points vs 11,228 points), while the TAC is increased by 4.73% (21,917 €/yr vs 22,954 €/yr). Note that all the Pareto solutions involve the same configuration in the rectification column (1 single stage).

(Figure 10 could be placed here)

The Pareto solutions obtained in the bi-criteria problems were plotted in a parallel coordinates plot (see Figure 11). Similar conclusions as in the Rankine cycle are obtained.

(Figure 11 could be placed here)

As observed, the environmental impacts are somehow redundant, since when one is minimized the others are also decreased. This is because all the damages are highly dependent on the steam consumption. Further, they are all conflictive with the cost as their minimization increases the cost of the cycle.

Table 5 shows the details corresponding to the extreme points (i.e., minimum TAC and minimum environmental damage indicators). As in the previous case, the minimum TAC design differs considerably from the minimum environmental impact alternatives. The main difference concerns the duty provided to the system (140kW vs. 131kW). The explanation for this is that the environmental impacts are highly dependent on the steam supplied to the reboiler. The extreme designs differ also in the reflux ratio of the rectification column and the temperatures of stream 5 and 9. With regard to the discrete variables, all of the designs lead to a rectification column with one single stage. In the minimum TAC, the energy consumption rate in the reboiler and reflux ratio in the rectification column are larger than in the minimum impact one. The coefficient of performance (COP), exchange area of the heat exchangers (and mass of stainless steel), electricity consumed in the pumps and amount of steam consumed by the reboiler in each solution.

(Table 5 could be placed here)

As observed, solutions with minimum impact show larger COP values and greater exchanger areas. The exchange area in these solutions is approximately 31% greater than in the minimum TAC design. This is due to the fact that the contribution of the mass of steel to the total impact is rather small. Regarding the use of energy, the minimum TAC solution consumes approximately 8% more steam and 4% more electricity than the minimum

environmental impact one. Hence, the impact caused during the operation phase is more significant than that associated with the construction phase. Particularly, the construction of the equipment units contributes around 4% to the total EI. As observed in Table 6, the TAC in the minimum cost solution is 4.67%, 4.71% and 4.73% lower than in the optimal HH, EQ and DR solutions, respectively. Moreover, HH, EQ and NR can be reduced by up to 5.80%, 6.82%, and 6.96%, respectively, compared to the minimum TAC solution.

(Table 6 could be placed here)

6 CONCLUSIONS

This work has introduced a computational approach for the optimal design of thermodynamic cycles considering economic and environmental concerns. Our approach combines simulation packages with rigorous deterministic mathematical programming tools and LCA analysis. The capabilities of this approach were tested in two thermodynamic cycles: a steam power cycle and an ammonia-water absorption cooling cycle, for which we minimized the total annualized cost and a set of environmental impacts measured in three LCA damage categories.

Numerical results showed that the environmental performance of thermodynamic cycles can be improved by compromising their economic performance. We also found that the main contribution to the total impact is the operation phase. The optimization of the individual damage categories produces similar results, indicating redundancies between them.

Acknowledgements

The authors wish to acknowledge support from the Spanish Ministry of Education and Science (projects DPI2008-04099 and CTQ2009-14420-C02) and the Spanish Ministry of External Affairs (projects A/023551/09 and HS2007-0006).

References

[1] Grossmann, I.E.; Guillen-Gosalbez, G. Scope for the application of mathematical programming techniques in the synthesis and planning of sustainable processes. Computers and Chemical Engineering 34(9) (2010) 1365-1376.

[2] J.Dipama, A.Teyssedou, F.Aubé, L. Lizon-Lugrin. A grid based multi-objective evolutionary algorithm for the optimization of power plants. Applied Thermal Engineering 30(8-9) (2010) 807-816.

[3] A.T.Bulgan, Optimization of the thermodynamic model of aqua-ammonia absorption refrigerations systems. Energy Conversion and Management 36(2) (1995) 135-143.

[4] J.C.Bruno, J.Miquel, F.Castells, Modeling of ammonia absorption chillers integration in energy systems of process plants. Applied Thermal Engineering 19(12) (1999) 1297-1328.

[5] C.Wu, L.Chen, F.Sun, Optimization of solar absorptions refrigerator. Applied Thermal Engineering 17(2) (1997) 203-208.

[6] G.Q.Zhang, L. Wang, L. Liu, Z. Wang, Thermoeconomic optimization of small size central air conditioner. Applied Thermal Engineering 24 (4) (2004) 471-485.

[7] J.C.Bruno, A.Valero, A.Coronas, Performance analysis of combined microgas turbines and gas fired water/LiBr absorption chillers with post-combustion. Applied Thermal Engineering 25(1) (2005) 87-89.

[8] M.Pouraghaie, K.Atashkari, S.M.Besarati, N.Nariman-Zadeh, Thermodynamic performance optimization of a combined power/cooling cycle. Energy Conversion and Management 51(1) (2010) 204-211.

[9] A. Huicochea, W.Rivera, G. Gutiérrez-Urueta, J.C. Bruno, A. Coronoas, Thermody-

namic analysis of a trigeneration system consisting of a micro gas turbine and a double effect absorption chiller. Applied Thermal Engineering 31(6) (2011) 3347-3353.

[10] A.Sapienza, I.S.Glaznev, S.Santamaria, A.Freni, Y.I.Aristov, Adsorption chilling driven by low temperature heat: New adsorbent and cycle optimization. Applied Thermal Engineering 32(1) (2012) 141-146.

[11] H.Becerra-Lopez, P.Golding, Multi-objective optimization for capacity expansion of regional power-generation systems: Case study of far west Texas. Energy Conversion and Management 49(6) (2008) 1433-1445.

[12] X.Pelet, D.Fevrat, G.Leyland, Multiobjective optimisation of integrated energy systems for remote communities considering economics and CO2 emissions. International Journal of Thermal Sciences 44(12) (2005) 1180-1189.

[13] B.H.Gebreslassie, G.Guillén-Gosálbez, L.Jiménez, D.Boer, Design of environmentally conscious absorption refrigeration systems via multi-objective optimization and life cycle assessment. Applied Energy 86(9) (2009) 1712-1722.

[14] B.H.Gebreslassie, G.Guillén-Gosálbez, L.Jiménez, D.Boer, Economic performance optimization of an absorption cooling system under uncertainty. Applied Thermal Engineering 29(17-18) (2009) 3491-3500.

[15] Eco-Indicator 99.The Netherlands, The Eco-indicator 99, Manual for designers. The Hague, The Netherlands, (2000).

[16] PRé consultants. Damage Oriented Method for Life Cycle Assessment. Methodology Report and Manual for Designers; Technical Report; PRé consultants: Amersfoort, The Netherlands, (2000).

[17] U.M.Diwekar, I.E.Grossmann, E.S.Rubin, An MINLP Process Synthesizer for a Se-

quential Modular Simulator. Industrial & Egineering Chemistry Research 31(1) (1992) 313-322.

[18] J.M.Reneaume, B.Koehret, X.L.Joulia, Optimal process synthesis in a modular simulator environment: New formulation of the mixed-integer nonlinear programming problem. Industrial & Egineering Chemistry Research 34(12) (1995) 4378-4394.

[19] Z.Kravanja, I.E.Grossmann, Computational Approach for the Modelling/Decomposition Strategy in the MINLP Optimization of Process Flowsheets with Implicit Models. Industrial & Egineering Chemistry Research 35(6) (1996) 2065-2070.

[20] M.S.Díaz, J.A.Bandoni, A mixed integer optimization strategy for a large chemical plant in operation. Computer and Chemical Engineering 20(5)(1996)531-545.

[21] H. Kim, I.H.Kim, E.S.Yoon, Multiobjective design of calorific value adjustment process using process simulators. Industrial & Egineering Chemistry Research 49(6) (2010) 2841-2848.

[22] J.A.Caballero, D.Milan-Yañez, I.E.Grossmann, Rigorous design of distillation columns: Integration of disjunctive programming and process simulators. Industrial & Egineering Chemistry Research 44(17) (2005) 6760-6775.

[23] R. Brunet, G.Guillen-Gosalbez, J.R.Pérez-Correa, J.A.Caballero, L.Jimenez, Hybrid simulation-optimization based approach for the optimal design of single-product biotechnological processes. Computers and Chemical Engineering 37(1) (2012) 125-135.

[24] Y.Y.Haimes, Integrated systems identification and optimization in control and dynamic systems: Advances in theory and applications, vol.10, Academic Press, Inc.1973.

[25] G.Mavrotas, Effective implementation of the ϵ-constraint method in multi-objective mathematical programming problems. Applied mathematics and computation. 213(2)(2009)455-465.

[26] M.A.Duran, I.E.Grossmann, An outer-approximation algorithm for a class of mixed-integer nonlinear programs. Mathematical Progress 36(3) (1986) 307-339.

[27] G.R.Kocis, I.E.Grossmann, Relaxation strategy for the structural optimization of process flow sheets. Industrial & Egineering Chemistry Research 26(9) (1987) 1869-1880.

[28] R. Brunet, G.Guillen-Gosalbez, L.Jimenez, Cleaner Design of Single-Product Biotechnological Facilities through the Integration of Process Simulation, Multiobjective Optimization, Life Cycle Assessment, and Principal Component Analysis. Industrial & Egineering Chemistry Research 51(1) (2012) 410-424.

[29] G. Guillen-Gosalbez, A novel MILP-based objective reduction method for multi-objective optimization: Application to environmental problems. Computers and Chemical Engineering 35(8) (2012) 1469-1477.

[30] C.Pozo, R.Ruíz-Femenia, J.A.Caballero, G.Guillen-Gosalbez, L.Jiménez, On the use of Principal Component Analysis for reducing the number of environmental objectives in multi-objective optimization: Application to the design of chemical supply chains. Chemical Engineering Science 69(1) 2012 146-158.

[31] Aspen HYSYS Version 7.1 (23.0.4507). Aspen Technology, Inc., Cambridge, www.aspentech.com.

[32] Aspen Plus, version 7.1 (0.0.7119). Aspen Technology, Inc., Cambridge, www.aspentech.com.

[33] Matlab 2011b, The MathWorks, Software (2011). Available from: www.mathworks.com.

[34] K.Holmström, A.O.Göran, M.M.Edvall, User's guide for Tomlab/SNOPT v12.1. (2009).

[35] TOMLAB Optimization (2009), Avaliable from: www.tomopt.com.

[36] P.E.Gill, W.Murray, M.A.Saunder, SNOPT: An SQP algorithm for large-scale constrained optimization. SIAM Journal on Optimization 12(4) (2002) 979-1006.

[37] K.Holmström, A.O.Göran, M.M.Edvall, User's guide for Tomlab/CPLEX v12.1. (2009).

[38] M.J.Moran, H.N.Shapiro, Fundamentals of engineering thermodynamics. 2nd ed. SI Version. Wiley. New Jersey, United States, (1993).

[39] A.S.Nafey, M.A.Sharif, Combined solar organic Rankine cycle with reverse osmosis desalination process: Energy, exergy and cost evaluations. Renewable Energy 35(11) (2010) 2571-2580.

[40] S.M.Walas, Chemical process equipment selection and design, Butterworth-Heinemann, Washington, United States, (1990).

[41] A.Mulet, L.B.Evans, A.B.Corripio, K.S.Chretien, Estimate costs of pressure vessels via correlations. Chemical Engineering 88(20) (1981) 148-150.

[42] Mitsubishi AT64C. Catalogue Steam Turbine Generator. Mitsubishi Heavy Industries, LTD.

[43] A.Vidal, R.Best, R.Rivero, J.Cervantes, Analysis of a combined power and refrigeration cycle by the exergy method. Energy 31(15) (2006) 3401-3414.

[44] K.M.Guthrie, Data and techniques for preliminary capital cost estimating. Chemical Engineering, 24 (1969) 114-142.

[45] O.Kizilkan, A.Sencan, S.A.Kalogirou, Thermoeconomic optimization of a LiBr absorption refrigeration system. Chemical & Engineering Processing 46(12) (2007) 1376-84.

[46] M.A.Siddiqui, Economic analyses of absorption systems: Part A-Design and cost evaluation. Energy Conversion Management 38(9) (1997) 889-904.

[47] Towards an integrated framework for supply chain management in the batch chemical process industry L.Puigjaner, G.Guillén-Gosálbez, Towards an integrated framework for supply chain management in the batch chemical process industry. Computers and Chemical Engineering 32(4-5) (2008) 650-670.

[48] G.Guillen-Gosalbez, J.A.Caballero, L.Jiménez, Application of life cycle assessment to the structural optimization of process flowsheets. Industrial & Egineering Chemistry Research 47(3) (2008) 777-789.

[49] G.Guillen-Gosalbez, I.E.Grossmann, Optimal design and planning of sustainable chemical supply chains under uncertainty. AIChE Journal 55(1) (2009) 99-121.

[50] G.Guillen-Gosalbez, I.E.Grossmann, A global optimization strategy for the environmentally conscious design of chemical supply chains under uncertainty in the damage assessment model. Computers and Chemical Engineering 34(1) (2010) 42-58.

[51] ISO 14040:(2006). Environmental management. Life cycle assessment: Principles and framework. International Organisation for Standardisation(ISO). Geneve, Switzerland, (2006).

Nomenclature

Sets/Indices

D	decision variables
E	equality constrains
I	inequality constraints
i	topology
j	external equality and inequality constraints
j∈ EQ	external (explicit) equality constraint
j∈ IEQ	external (explicit) inequality constraint
k	iteration
o	objective functions
u∈HX	heat exchangers
u∈U	equipment units

Abbreviations

A	Absorber
C	Condenser
COP	Coefficient of performance
DR	Depletion natural resources
E	Evaporator
EI	Environmental impact
EQ	Damage to ecosystem quality
HH	Damage to human health
LCA	Life cycle assessment
LCI	Life cycle inventory analysis
MILP	Mixed-integer linear programming
moMINLP	Multi-objective mixed-integer non-linear programming
moNLP	Multi-objective non-linear programming

MOO	Multi-objective optimization
NLP	Non-linear programming
NPV	Net present value
P	Pump
RC	Rectification column
SC	Refrigerant subcooler
SHX	Solution heat exchanger
SQP	Successive quadratic programming
TAC	Total annualized cost
TPC	Total plant cost
VLV1	Refrigerant expansion valve
VLV2	Solution expansion valve

Variables

Am	Area heat exchanger of unit m (m^2)
CF	Fixed cost (€)
Cb	Exchange are (m^2)
C_u	Cost of the unit (€)
CO	Operating cost (€/yr)
DAM_d	Environmental damages (Points)
$Diam$	Diameter of rectification column (m)
H	Height of the rectification column (m)
LCI_b	Input and output flows (kg/yr)
Q_u	Heat transfer of unit u (kW)
TAC	Total annualized cost (€/year)
W_u	Mechanical power of unit u (kW)
α	Auxiliary variable
$\prod$	Penalty value for the constraint violation

Parameters

c_1	Cost parameter (€/m^2)
c_2	Cost parameter (€)
c_3	Cost parameter (€/kW)
cq	Unitary cost of steam (€/MJ)
cw	Unitary cost of electricity (€/MW h)
crf	Capital recovery factor
df_{bd}	Damage factors (Points/kg)
d_{euro}	Conversion from dollars to euros (€/$)
F_c	Cost factor that depends on the type of column
fd	Coefficient of the design type
fp	Coefficient of the design type
fm	Coefficient of the material construction
$M\&S$	Cost factor
t_{op}	Operational hours (h/yr)

A Life Cycle Assessment of the thermodynamic cycles

The environmental impact is quantified following LCA principles, in a similar manner as done before by the authors in other works [47–50]. The LCA comprises four phases [51]: **1. Goal and scope definition.** This phase defines the system boundaries, functional unit, assumptions made and type of impact assessed. The system boundaries correspond to the limits of the energy system. The functional unit is a given amount of power/cool generated. We quantify the impact in three categories: damage to human health (HH), damage to ecosystem quality (EQ), and damage due to depletion of natural resources (DR).

2. Life cycle inventory analysis (LCI). This phase quantifies the input and output flows associated with the operation and construction of the cycles. The damage during the operation phase is given by the natural gas and electricity consumption rates, which are retrieved from the process simulation. This information is translated into the corresponding LCI using environmental databases. The LCI of the construction phase is approximated by the LCI of the mass of steel contained in the process units.

3. Life Cycle Impact Assessment. This phase translates the LCI into the corresponding environmental damages (denoted by the continuous variable DAM_d) using damage factors ($df_{b,d}$) available in the literature [16].

$$DAM_d = \sum_{b \in B} df_{b,d} \cdot LCI_b \qquad \forall d \in D \tag{8}$$

4. Life Cycle Interpretation. In this phase, the LCA results are analyzed and a set of conclusions and recommendations are formulated. In this work, this step is carried out in the post optimal analysis of the optimal solutions found.

List of Tables

Table 1: Cost correlations used in the Rankine cycle

Equipment	Correlation	Reference
Boiler and reboiler	$C_B = fm(1 + fd + fp) \cdot (Q_B)^{0.86}$	Walas [40]
Condenser and heat exchanger	$C_{HX} = fd \cdot fm \cdot fp \cdot Cb$	Evans et al. [41]
Turbine	$C_T = 4750 \cdot (W_T)^{0.75}$	Nafey [39]
Pumps	$C_P = 3500 \cdot (W_P)^{0.47}$	Nafey [39]

Table 2: Cost correlations used in the absorption cooling cycle

Equipment	Correlation	Reference
Desorber	$C_{RC} = \left(\frac{M\&S}{280}\right)(101.9 Diam^{1.066} H^{0.802})(2.18 + 2F_c) d_{euro}$	Guthrie [44]
Heat exchangers	$C_{HX2} = \sum_{u \in HX} (c_1 Am_{u \in HX} + c_2)$	Kizilkan et al. [45]
Pump	$C_P = c_3 W_P^{0.4}$	Siddiqui [46]

Table 3: Details of the extreme solutions. Case study I: Rankine cycle

Variable	min TAC	min HH	min EQ	min DR
Mass flow stream 1 [kg/s]	9.33	8.78	8.82	8.90
Temperature of stream 1 [°C]	516.43	587.30	577.85	571.55
Pressure of stream 1 [kPa]	8,550.08	8,878.49	8,860.25	8,805.51
Pressure of stream 2 [kPa]	2,300.00	2,269.70	2,274.19	2,276.43
Pressure of stream 3 [kPa]	737.29	698.34	703.54	707.00
Pressure of stream 5 [kPa]	329.92	301.20	304.74	307.58
Pressure of stream 6 [kPa]	8.80	7.00	7.23	7.40
Temperature of stream 4 [°C]	496.09	493.99	494.39	494.46
Temperature of stream 11 [°C]	205.19	215.15	214.66	212.94
Temperature of combustion gases B1 [°C]	250.00	249.90	249.91	249.92
Temperature of combustion gases B2 [°C]	278.69	300.00	295.56	295.26
Area of the boiler and reboiler [m^2]	160.82	165.47	165.73	166.59
Area of the condenser [m^2]	133.14	149.11	149.96	152.63
Area of the Heat Exchangers [m^2]	60.41	63.44	63.60	64.17
Steam [tones]	$3.96 \cdot 10^8$	$3.89 \cdot 10^8$	$3.89 \cdot 10^8$	$3.88 \cdot 10^8$
Electricity [MJ]	$1.48 \cdot 10^6$	$1.43 \cdot 10^6$	$1.43 \cdot 10^6$	$1.42 \cdot 10^6$

Table 4: Extreme solutions. Case study I: Rankine cycle

Objective function	min TAC	min HH	min EQ	min DR
TAC [€/yr]	3,491,584	3,619,084	3,625,842	3,646,903
HH [Points]	342,931	334,887	334,952	334,987
EQ [Points]	344,555	336,547	336,518	336,586
DR [Points]	2,941,189	2,877,357	2,876,312	2,873,056

Table 5: Details of the extreme solutions. Case study II: Absorption cycle

Variable	min TAC	min HH	min EQ	min DR
Reboiler duty [kW]	140.39	131.79	131.05	131.11
High pressure [bar]	13.28	12.95	12.96	12.95
Low pressure [bar]	4.48	4.82	4.97	4.93
Mass flow of stream 1 [kg/s]	0.32	0.33	0.33	0.33
Ammonia fraction of stream 1	0.51	0.53	0.54	0.54
Temperature of stream 5 [°C]	41.15	38.27	38.20	38.16
Temperature of stream 9 [°C]	20.20	21.45	22.80	22.08
Reflux ratio (mass)	0.055	0.043	0.042	0.042
Number of trays	1	1	1	1
Feed tray	1	1	1	1
COP	0.63	0.67	0.68	0.68
Total exchange Area [m2]	89.13	119.77	120.26	120.34
Steam [kg]	904,972	838,389	837,074	836,897
Electricity [MJ]	10,895	10,454	10,544	10,542

Table 6: Extreme solutions. Case study II: Absorption cycle

Objective function	min TAC	min HH	min EQ	min DR
TAC [€/yr]	21,917	22,940	22,951	22,954
HH [points]	2,734	2,584	2,593	2,593
EQ [points]	2,740	2,582	2,565	2,578
DR [points]	11,228	10,568	10,552	10,497

List of Figures

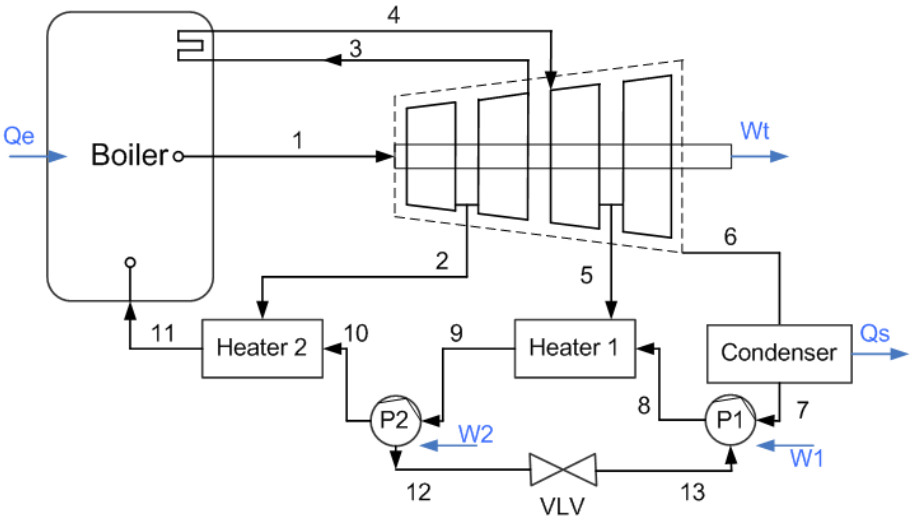

Figure 1: Steam Rankine cycle

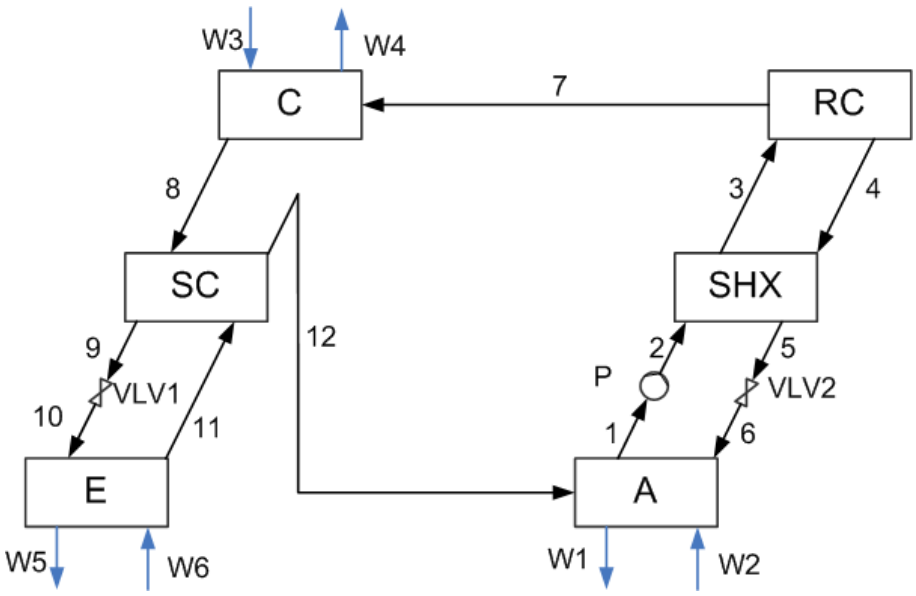

Figure 2: Ammonia-water absorption cycle

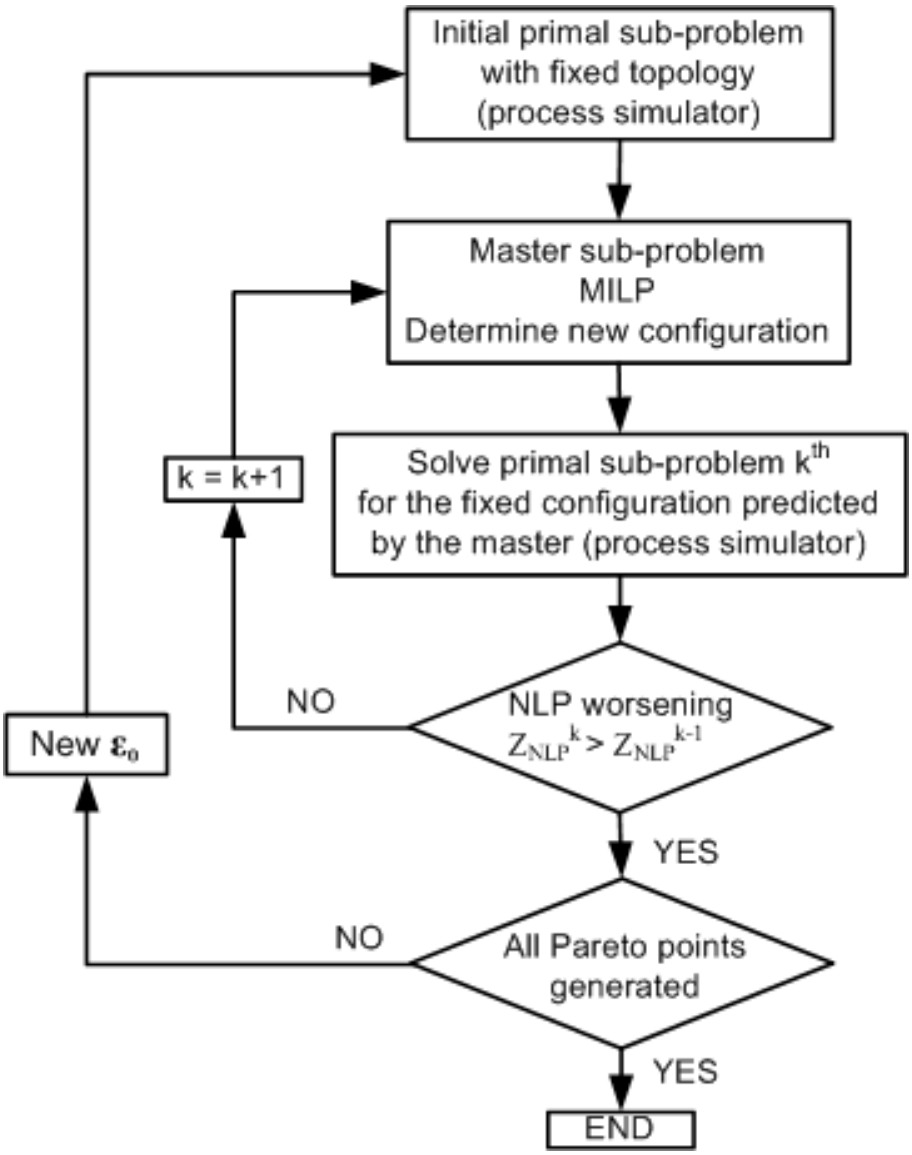

Figure 3: Flowchart of the proposed outer-approximation algorithm

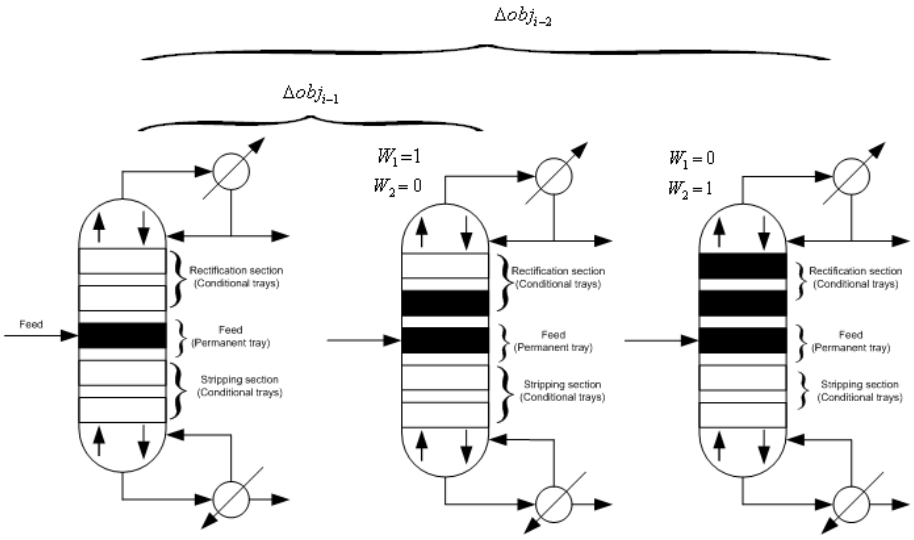

Figure 4: Details on the definition of binary variables in the MILP (inspired in the work by Caballero et al.[22])

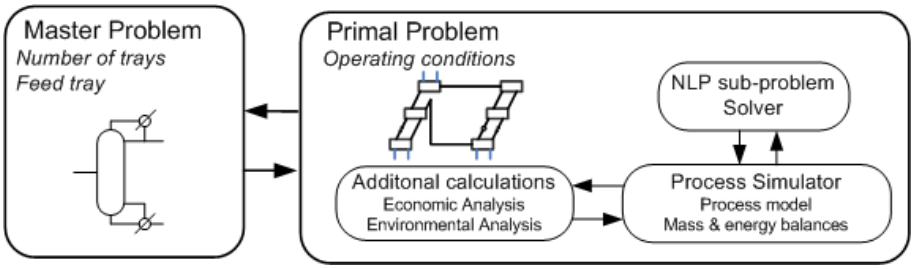

Figure 5: Main steps of the solution algorithm proposed

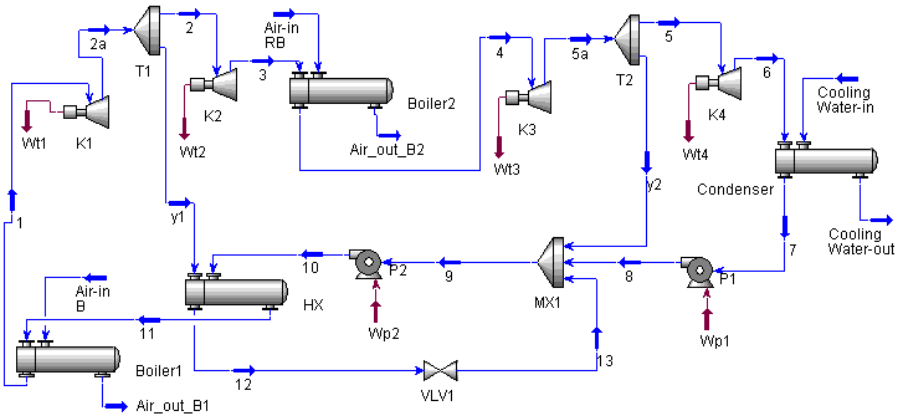

Figure 6: Steam Rankine cycle simulated in Aspen Hysys

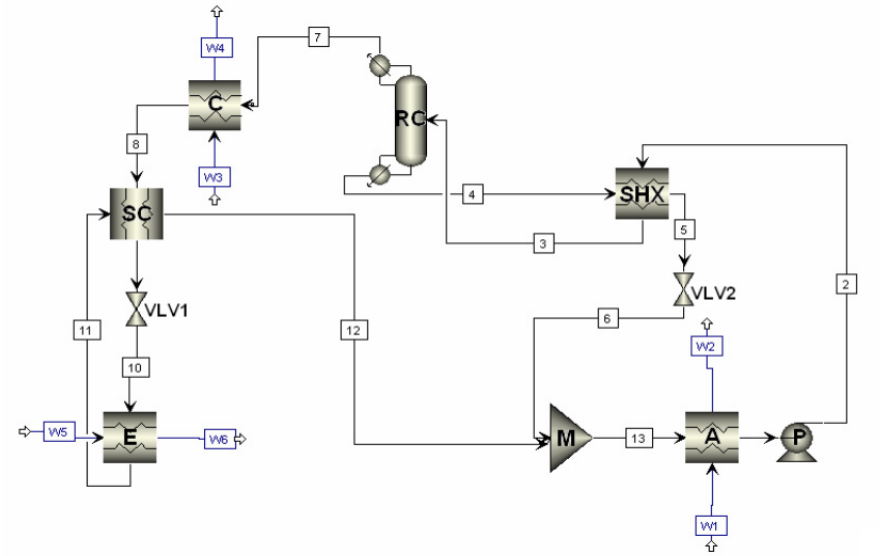

Figure 7: Ammonia-water absorption cycle simulated in Aspen Plus

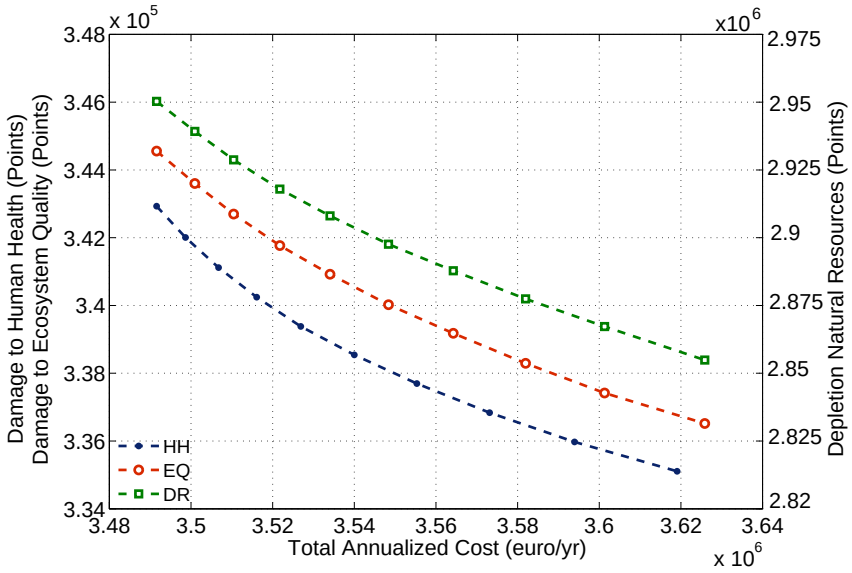

Figure 8: Total annualized cost vs impact damage categories. Case study I: Rankine Cycle

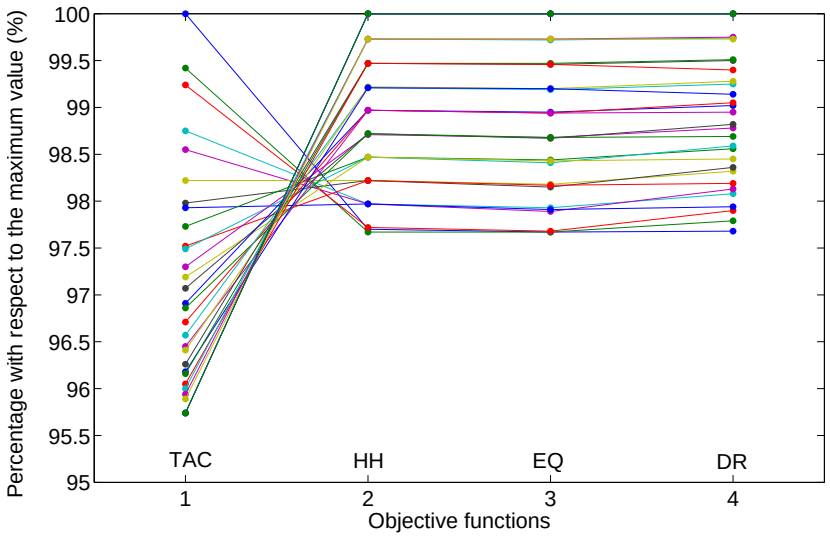

Figure 9: Parallel coordinates plot. Case study I: Rankine Cycle. Objective functions: Total annualized cost (TAC), damage to human health (HH), damage to ecosystem quality (EQ), and depletion of natural resources (DR).

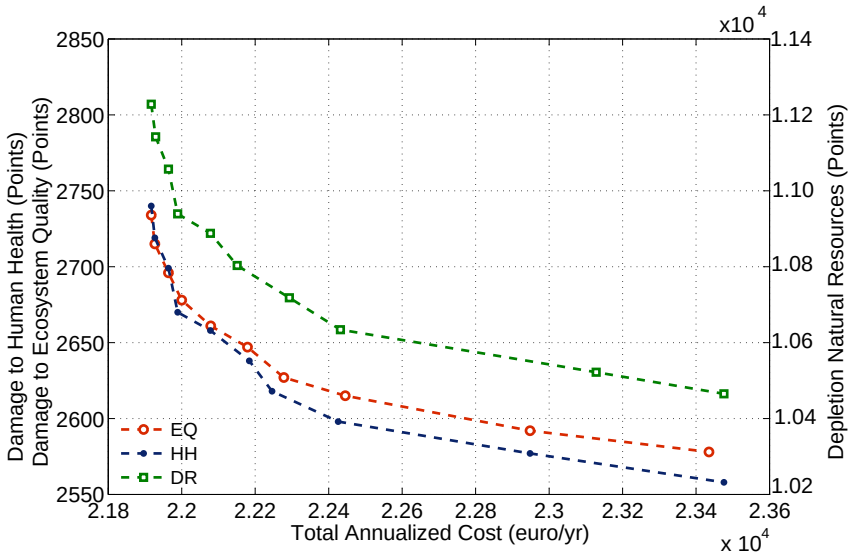

Figure 10: Total Annualized cost vs impact damage categories. Case study II: Absorption cycle

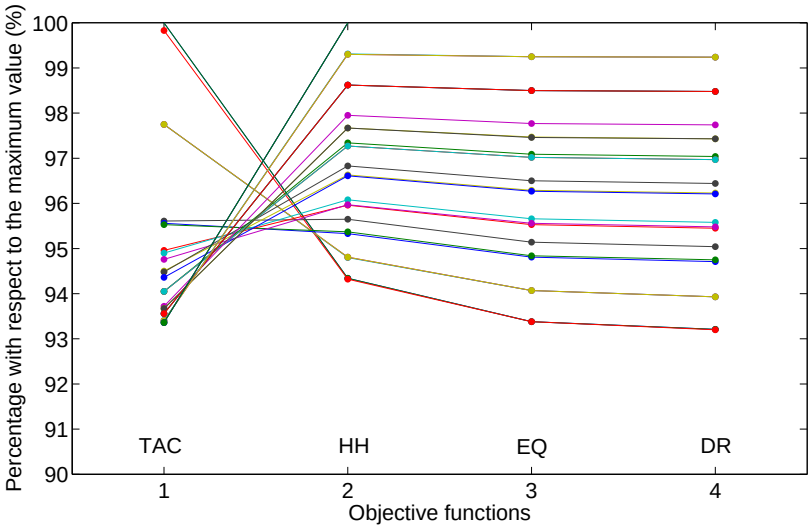

Figure 11: Parallel coordinates plot. Case study II: Absorption Cycle. Objective functions: Total annualized cost (TAC), damage to human health (HH), damage to ecosystem quality (EQ), and depletion of natural resources (DR).

Article 5

Authors: **R. Brunet**, G. Guillén-Gosálbez, L. Jiménez.

Title: Reducing the environmental impact of biodeisel production from vegetable oil using a solar assisted steam generation system with heat storage.

Journal: *Industrial & Engineering Chemistry Research*

Volume: **Pages:** **Year:** 2012

ISI category: Chemical Engineering **AIF:** 0.608

Impact Index: 2.071

Position in the category: 29/135 (Q1)

Cites: -

Observations: Under review

Reducing the environmental impact of biodiesel production from vegetable oil using a solar assisted steam generation system with heat storage

Robert Brunet, Ekaterina Antipova, Gonzalo Guillén-Gosálbez*and Laureano Jiménez

Departament d'Enginyeria Quimica, Escola Tecnica Superior d'Enginyeria Quimica,

Universitat Rovira i Virgili, Campus Sescelades, Avinguda Paisos

Catalans 26, 43007, Tarragona, Spain

September 3, 2012

*Corresponding author. E-mail: gonzalo.guillen@urv.cat, telephone: +34 977558618

Abstract

In this work, we address the problem of reducing the environmental impact of biodiesel plants through their integration with a solar thermal energy system that generates steam. A mathematical model of the solar energy system that includes energy storage is constructed and coupled with a rigorous simulation model of the biodiesel facility developed in Aspen Plus. The solar energy system model takes the form of a bi-criteria nonlinear programming (biNLP) formulation that accounts for the simultaneous minimization of cost and global warming potential (GWP). A detailed cost and environmental analysis of the integrated facility is presented based on data available in the literature. The environmental impact is quantified in terms of contribution to GWP using the CML2001 methodology, a framework based on life cycle assessment (LCA) principles. Numerical results indicate that it is possible to reduce the current natural gas consumption required in the biodiesel facility by more than 94.87% compared to the initial basic design, which results in an improvement of 19.88% in green house gases (GHG) emissions.

Keywords: *Biodiesel; Vegetable oil; Solar panels; Economic analysis; Life cycle assessment.*

UNIVERSITAT ROVIRA I VIRGILI
OPTIMAL DESIGN OF SUSTAINABLE CHEMICAL PROCESSES VIA A COMBINED SIMULATION OPTIMIZATION APPROACH
Robert Brunet Solé
Dipòsit Legal: T. 458-2013

1 INTRODUCTION

Petroleum-based fuels play a vital role in industrial development, transportation, agricultural sector and many other human needs [1]. Unfortunately, they contribute to global warming and related environmental problems. This has boosted research over the last few decades on the development of fuel production processes based on renewable biological materials as feedstock [2].

One of these alternatives that has recently gained wider interest is biodiesel. This fuel, which contains mostly fatty acid methyl (or ethyl) esters, is usually obtained from oils or fats via transesterification [3]. Feedstocks for biodiesel include animal fats, vegetable oils, soy, rapeseed, jatropha, mahua, mustard, flax, sunflower, palm oil, hemp, field pennycress, pongamia pinnata and algae [4]. Biodiesel is nowadays the most common biofuel in Europe. Its main advantage is that it shows similar composition and properties (viscosity and volatility) than fossil/mineral diesel. Because of this, it can be used in standard diesel engines without the need of making any modification [5]. As a result of these advantageous characteristics, biodiesel has become a serious candidate to substitute fossil fuels. However, the final adoption of this fuel in the market place still depends on whether it can be economically and environmentally competitive [6].

Process simulation has been used in the literature to assess the potential economic and environmental benefits of biodiesel production. Zhang et al. [7] were the first to use process simulators (Aspen Plus) to estimate the production costs of four different biodiesel processes. More recently, Haas et al. [8], West et al. [9], Apostolakou et al. [10], and Sotoft et al. [11] compared the economical benefits of different biodiesel production processes from vegetables and waste oils using Aspen Hysys and Aspen Plus. Morais et al. [12] used process simulation and life cycle assessment (LCA) to perform an environmental evaluation of three process design alternatives for biodiesel production from waste vegetable oils. Pokoo-Aikins et al. [13] presented an analysis of biodiesel production from algae grown through carbon sequestration. Chouinard-Dussault et al. [14] presented a method which is enable to considerate of

several levels of process integration while tracking the process economics and the reduction of the net greenhouse gas emissions.

Very few studies have addressed the optimization of biodiesel facilities using mathematical programming. Panichelli and Gnansounou [15] developed a non-linear programming (NLP) model for the reduction of green house gas (GHG) effects in biodiesel plants. Sanchez et al. [16] presented a heat integration strategy based on pinch analysis to reduce the energy consumed in biodiesel production from microalgae. Other works on optimization of biofuels facilities have focused on bioethanol plants. Karuppiah et al. [17] were the first to propose a superstructure optimization approach for the optimal design of corn-based ethanol plants. Grossmann and Martin [18] presented a general approach based on mathematical programming techniques for energy and water optimization in biofuel plants. More recently, Martin and Grossmann [19] and Martin and Grossmann [20] presented an optimization approach for the energy reduction in bioethanol production processes via gasification and hydrolosis of switchgrass. Ojeda et al. [21] presented a combined process engineering and exergy analysis to evaluate different routes of bioethanol production from lignocellulosic biomass.

The aforementioned works focused on improving the biofuel production process by changing the operating conditions and structural configuration of the plant. We investigate herein an alternative approach to improve the performance of biodiesel plants that consists of coupling them with renewable energy sources. In a recent work, Lewis and Nocera [22] highlighted the benefits of integrating solar energy with other technologies. Shinnar and Citro [23] claimed that solar thermal energy can be an environmentally friendly and economically competitive electric source. More recently, Gebresslassie et al. [24] addressed the minimization of the life cycle impact of cooling systems using solar collectors, while Salcedo et al. [25] developed a model for the optimization of reverse osmosis desalination plants coupled with solar Rankine cycles. Tora and El-Halwagi [26] presented an integration of solar energy into absorption refrigerators and industrial processes and also, Tora and El-Halwagi [27] presented an integrated conceptual design of solar-assisted trigeneration systems

Despite being a promising alternative, to the best of our knowledge, no work has addressed the use of renewable energy sources in the production of biofuels. In this work we fill this research gap by proposing a systematic framework to assess the potential economic and environmental benefits of using solar thermal energy in a biofuel production facility. Numerical results show that it is possible to reduce the impact of these facilities by coupling them with a renewable energy source.

2 PROCESS DESCRIPTION

2.1. Biodiesel production from vegetable oil

We consider a standard facility for biodiesel production from vegetable oil. The most common way to produce biodiesel is by transesterification, which involves a catalyzed chemical reaction using vegetable oil and an alcohol (e.g. methanol) that yields fatty acid alkyl esters (i.e. biodiesel) and glycerol. Transesterification reactions can be alkali-catalyzed, acid-catalyzed or enzyme-catalyzed. Particularly, we focus here on the alkali-catalysed production of biodiesel from vegetable oil [7].

The associated flowsheet (see Figure 1) comprises 7 major processing units that are aggregated into three different sections: upstream, transesterification and downstream. The upstream processing includes all unit operations required to prepare the feed streams. In this section, the alcohol (methanol), catalyst (sodium hydroxide) and water are mixed in a tank before being transferred to the reactor in which the oil is added (vegetable oil).

The reaction of oil with methanol takes place in a continuous stirred-tank reactor (TRANS) at 60°C and 400 kPa. The catalyst contains 1.78% (w/w) of sodium hydroxide, and the alcohol used is methanol. The molar ratio of the reaction is 6:1 (A:O). We assume that a 95% of the oil is converted to FAME, producing glycerol as by-product.

The output stream from the reactor (REACOUT) is fed to the methanol distillation column (MEOHCOL). In MEOHCOL, pure methanol containing 94% of the total methanol is ob-

tained in the top. This stream (MEOHREC) is then recycled and mixed with fresh make-up methanol before being charged into the reactor.

Stream EST1 obtained in the bottom of the distillation column MEOHCOL, is introduced in a water washing unit. The goal of this step is to separate the FAME from the glycerol, methanol and catalyst by adding water.

The resulting FAME stream EST4 is purified in a FAME distillation column (ESTCOL) to reach the final FAME purity specifications (purity greater than 99.6%). Water and methanol are removed as vent gases (stream MEOHWAT). FAME product is obtained as a liquid distillate (194°C and 10kPa). In the bottom of the distillation column, stream OILREC1, is recycled to be treated again in the reactor (TRANS).

Stream AQU1 leaving unit WASHCOOL is fed to the neutralization reactor NEUTR where sodium hydroxide is removed by adding phosphoric acid. The resulting Na_3PO_4, stream (AQU2) is removed in a gravity separator (FILTER). Stream AQU3 with a purity of 85% in glycerol is purified in the distillation column (GLYRCOOL) to reach the specification (weight content greater than 92%).

(Figure 1 could be placed here)

2.2. Integrated solar assisted steam generation system

To decrease the energy needed to generate the necessary amount of steam consumed by the plant. We propose to couple the biodiesel facility with a solar assisted steam generation system with heat storage. Figure 2 shows a sketch of the steam generation system proposed, in which the biodiesel plant is coupled with the solar thermal system.

(Figure 2 could be placed here)

The solar thermal unit provides heat to the evaporator in order to satisfy the energy demand of the biodiesel plant. Parabolic trough collectors are employed to transfer solar energy to the heating mineral oil. A gas fire heater (GFH) is coupled with the solar collectors and used as a back up system in order to cope with the intermittent radiation and maintain the oil temperature constant. This oil is used in the boiler to generate steam.

Thermal energy storage (TES) is integrated in the system to use the solar energy more efficiently. A molten-salt thermocline is considered for the thermal storage system. Molten salt is thus used as heat transfer fluid (HTF) that transports thermal energy between the storage unit and the remaining parts of the power system (e.g., collector field, GFH and boiler).

3 MODELING APPROACH

The design of the integrated facility could be accomplished following a superstructure optimization approach. This methodology relies on formulating a mixed-integer nonlinear programming (MINLP) model, where continuous variables represent process conditions (i.e., temperature, pressures, concentrations, etc.), while integers denote the existence of equipment units. Most MINLP models used in process design make use of short-cut methods to describe the performance of the process units. Hence, the ability to screen a large number of potential designs and identify the best one comes at the cost of using approximated models. Simulation-optimization tools aim at overcoming this limitation [28–34]. This second approach relies on optimizing a rigorous process model, which is implemented in a process simulator, using an external optimization tool. While this strategy has proved efficient for handling processes with complex unit operations, it still shows some limitations. Particularly, one major problem is that the process simulator may fail to convergence during the optimization task.

To surmount this difficulty to the extent possible, in this work we follow a two-step approach

in which the optimization of the integrated system is performed in two sequential phases. A rigorous simulation model is first constructed using a standard process simulator (i.e. Aspen Plus). The steam generation system is then optimized in a later step. The outcome of the optimization is combined afterwards with the simulation results, which provides the performance of the overall integrated system. In our approach the emphasis is therefore on the optimization of the solar system, rather than on obtaining an optimal flowsheet configuration. The goal is to enhance the performance of existing biodiesel facilities for which accurate process models fitted with real process data might be available, by coupling them with a solar system. The interest here is therefore on assessing the economic and environmental performance of the integrated facility rather than on developing an efficient solution method for the optimization of such a system. The sections that follow describe the modeling tools applied to each part of the process.

3.1. Process model of the biodiesel plant

The commercial simulator Aspen Plus is used to solve the steady state material and energy balances of a biodiesel production process plant with a capacity of 9,141,561 kg/year.
Some thermodynamic properties not available in the component library of Aspen Plus were estimated based on the molecular structure. Due to the presence of highly polar components, we used a combination of the NRTL (Non-Random Two Liquid) and UNIQUAC (Universal QUAsiChemical) thermodynamic/activity models to predict the activity coefficients. Some components not directly available in the process simulator were approximated by other similar chemicals available in the database. The vegetable oil was modeled as triolein, the biodiesel product (FAME) as methyl-oleate, and the by-product glycerol as glycerol. Sodium hydroxide, phosphoric acid and sodium phosphate were modeled using the physical properties of water. We made this assumption, because the reaction kinetics and electrolyte chemistry are not modeled in details and the best alternative was using physical property data for water, but with their correct molecular weights.

The transesterification process was modeled using a stoichiometric reactor (RStoic). The methanol recovery, catalyst removal and glycerol purification were modeled using a rigorous multi-stage distillation model (RadFrac), while for the water washing we used a liquid-liquid extractor, and for the catalyst removal we use firstly a neutralizer modeled as a RStoic and a filter modeled as a Flash.

3.2. Mathematical formulation of the solar energy system

The model of the energy system is based on mass and energy balances. These equations, which ensure mass and energy conservation, are applied to each unit of the system. The mass balance is defined by equation 1:

$$\sum_{i \in IN_k} m_{i,t} \cdot \chi_{i,p,t} - \sum_{i \in OUT_k} m_{i,t} \cdot \chi_{i,p,t} = 0 \qquad \forall k, p, t \tag{1}$$

where IN_k and OUT_k are the sets of streams entering and leaving unit k respectively, $m_{i,t}$ is the mass flow rate of stream i in period t, and $\chi_{i,p,t}$ is the mass fraction of component p in stream i in period t. The total summation of the mass fractions of components p in every stream i must equal 1 (see equation 2):

$$\sum_{p} \chi_{i,p,t} = 1 \qquad \forall i, t \tag{2}$$

The energy balance is defined by equation 3:

$$\sum_{i \in IN_k} m_{i,t} \cdot h_{i,t} - \sum_{i \in OUT_k} m_{i,t} \cdot h_{i,t} + Q_{k,t} - W_{k,t} = 0 \qquad \forall k, t \tag{3}$$

where $h_{i,t}$ is the enthalpy of stream i in period t, $Q_{k,t}$ is the thermal power supplied to unit

k in period t, and $W_{k,t}$ is the mechanical power output of unit k in period t.

In the model of the solar assisted steam generation system with heat storage, we use the following energy balance (see Figure 3):

(Figure 3 could be placed here)

$$Q_{k,t} + Q_{k',t} + Q_{k'',t-1} = Q_{k'',t} + Q_{k''',t} \qquad k = COL, k' = GFH, k'' = TES, k''' = E, \qquad \forall t \tag{4}$$

where $Q_{COL,t}$ is the thermal energy captured by the collectors, $Q_{GFH,t}$ is the energy provided by the fossil fuel combusted in the GFH, $Q_{TES,t}$ is the thermal energy accumulated in the storage at the end of period t and $Q_{B,t}$ is the energy required by the evaporator.

The maximum amount of thermal energy that can be accumulated is given by the maximum storage capacity CAP:

$$Q_{TES,t} \leq CAP \qquad \forall t \tag{5}$$

The heat captured in the solar collectors is calculated from equation 6:

$$Q_{k,t} = G_t \cdot A_k \cdot \eta_{k,t} \qquad k = COL, \qquad \forall t \tag{6}$$

where G_t represents the solar radiation, which depends on the time period of the day and month. The daily solar radiation expressed in MJ/m^2 day is available for different locations in Catalonia [38]. The efficiency of the medium-high temperature parabolic trough collectors

η_{col} is calculated according to the work by Bruno et al. [39] (equation 7):

$$\eta_{k,t} = \eta_t^0 - a_1(T_t^{av} - T_t^{amb}) - a_2(\frac{T_t^{av}-T_t^{amb}}{G_t}) - a_3(\frac{T_t^{av}-T_t^{amb}}{G_t}) \qquad k = COL, \qquad \forall t \quad (7)$$

where η_t^0 is the collector optical efficiency, a_1, a_2, a_3 are coefficients, T_t^{amb} is the ambient temperature in time period t, and T_t^{av} is the average temperature of the solar collector, which is determined by equation 8:

$$T_t^{av} = \frac{T_{OUT_k} - T_{IN_k}}{2} \qquad k = COL, \qquad \forall t \quad (8)$$

The heat produced by the combustion of natural gas in the heater is given by equation 9:

$$Q_{k,t} = m_k \cdot LHV \cdot \eta_k \qquad k = GFH, \qquad \forall t \quad (9)$$

In this equation, m_{NG} is the mass flow rate of natural gas, LHV is the lower heating value of natural gas, and η_{GFH} is the thermal efficiency of the natural gas heater.

3.3. Economic and environmental assessment

The economic objective function is the Net Present Value (NPV), which is obtained from the sum of the net profit in year j plus the depreciation. The economic assessment is based on the costs analysis of Haas et al. [8], Apostolakou et al. [10], Zhang et al. [40]. Further information on this issue is presented in section 4.1 and Appendix A.

With regard to the environmental impact, it is assessed following LCA principles similarly

as done in other works [41–45].

$$CML = \sum_{b \in B} df_b \cdot LCI_b \tag{10}$$

Where, parameter b represents each component of the system, LCI_b is the life cycle and df_b are the damage factors. Further details on the LCA analysis of the biodiesel plant are given in Appendix B.

3.4. Bi-criteria nonlinear programming (biNLP) model

The design of the integrated system with economic and environmental concerns can be expressed in mathematical terms as a biNLP. We solve this model using the ε constraint method [46, 47]. This technique is based on calculating a set of single-objective models in which one objective is kept in the objective function while the others are transferred to auxiliary constraints and forced to be lower than a set of epsilon parameters:

$$\begin{aligned} \min_{x_D} \quad & z = f_1(x,y) \\ s.t. \quad & f_2(x,y) \leq \varepsilon \\ & f_1(x,y) = f_1^P(x^P,y^P) + f_1^S(x^S) \\ & f_2(x,y) = f_2^P(x^P,y^P) + f_2^S(x^S) \\ & h^P(x^P,y^P) = 0 \\ & h^S(x^S) = 0 \\ & g_P(x^P,y^P) \leq 0 \\ & g_S(x^S) \leq 0 \end{aligned} \tag{11}$$

The economic objective function, represented by f_1, is quantified using the NPV while f_2 quantifies the impact according to the CML2001 methodology. ε is an auxiliary parameter

that bounds the values of the objectives transferred to the auxiliary inequality constraints, while x and y represent continuous and discrete variables defined for the plant and solar assisted system (x^P, y^P and x^S, respectively). For simplicity, in this formulation, we fully decouple the optimization of the plant and the steam generating system. Furthermore, we consider that the plant will not be modified, so variables x^P and y^P are fixed, while variables x^S are optimized using a gradient-based method.

4 NUMERICAL RESULTS

We study the design of a solar assisted biodiesel from vegetable oil production plant considering weather data of Tarragona (Spain). We first present the economic and environmental analysis of the base case, a biodiesel plant in which the heat capacity is generated by a gas fire heater. We will then analyze the alternative system in which the solar assisted steam generation with heat storage is used to cover the steam required for the plant. Finally, we present the Pareto curve of the biodiesel plant integrated with the solar assisted steam generation system.

4.1. Case Study: Biodiesel production from vegetable oil

Economic analysis

For the sake of brevity, details on the economic calculations are given in Appendix A.
In the base case, we assumed that all the energy required is generated by the GFH, as in conventional steam generation systems. The capital costs of the plant are summarized in Table 1. The estimated total capital cost of the 9,233,040 kg/year biodiesel production plant is 3,323 M$. The cost of the process equipments is 1,095 M$, with the most expensive equipments being the 4 distillation columns and the transesterification reactor.

(Table 1 could be placed here)

The projected annual operating costs are shown in Table 2. The raw materials purchases are the most significant contribution to the total cost, and in particular the oil purchases (2,856 M$/year), which represents a 88.5% of the raw materials cost (3,226 M$/year), and a 54.2% of the total operating costs (5,273 M$/year). The utilities cost is 692 M$/year, which represents a 13.1% of the total cost .

(Table 2 could be placed here)

With the cost and the incomes we can finally determine the NPV (see Appendix A). Table 3 shows the NPV value and the most significant items related with the economic analysis.

(Table 3 could be placed here)

Environmental analysis

Details on the environmental calculations are given in Appendix B. The CML2001 GWP 100a methodology has been applied considering a lifetime of the plant of 25 years. The results are shown in Table 4. The total environmental impact is 232,608,592 kgCO_2eq, most of which (70.2%) comes from the vegetable oil consumption. Additionally, the consumption of methanol, steam and natural gas contribute significantly to the total impact. The natural gas used for steam generation represents 21.0% of the total impact, which confirms that there is a large potential for environmental improvements using solar energy. The main sources of impact in this LCA analysis are: (1)vegetable oil, (2)methanol, (3)NaOH, (4)H_3PO_4, (5)water, (6)electricity, (7)steam, (8)natural gas and (9)steel.

(Table 4 could be placed here)

4.2. Optimal design of the solar assisted biodiesel production from vegetable oil

In this section we present the optimal results of the biodiesel production plant from vegetable oil coupled with a solar assisted steam generation system with heat storage. We first describe the biNLP optimization of the solar assisted steam generation system and then we present the Pareto set of solutions of the integrated system.

The model of the solar system was coded in GAMS and solved with CONOPT3. The solver algorithm took around 23.5 seconds to generate 10 Pareto solutions on a computer AMD PhenomTM 86000B, with Triple-Core Processor 2.29GHz and 3.23 GB of RAM.

Solar assisted steam generation system

We first solved the optimization problem of the steam generation system by minimizing the specific total cost (STC) of the system against the environmental impact of the natural gas (EING) used for the steam generation. Each objective function (STC and EING) was firstly optimized separately, which provided the limits of the ε interval. This interval was divided into a set of sub-intervals, and the model was then calculated for the limits of each of them. Figure 4 shows the Pareto set of optimal solutions of the steam generation system. Every point of this set represents an optimal design and associated operating conditions that leads to a specific economic and environmental performance. Note that an improvement in one criterion can only be achieved at the expense of worsening the other. Particularly, the maximum economic profitability solution shows the worst impact (design A) and vice versa (design B). The STC is equal to 27,247,466 $ in point A, and 714,250,600 $ in design B (i.e., 25 times larger) whereas the EING is reduced by 94.88% from 2,215,654 kgCO_2eq to 113,429 kgCO_2eq when moving from A to B. The specific cost of intermediate design C is

1.31% higher than that of design A (30,835,420 $ vs 27,247,466 $), while the environmental impact is reduced by 86.70% (294,587 $kgCO_2eq$ vs 2,215,654 $kgCO_2eq$), thereby making this solution quite appealing.

(Figure 4 could be placed here)

Further analysis of the Pareto set reveals that the environmental impact is reduced by increasing the solar collectors area, as shown in Figure 5. The minimum STC design uses only the GFH, and for this reason the environmental impact is so high. Design B implies a larger collector area (i.e., 625,773 m^2). This larger area leads to significant reductions in energy consumption, but at the expense of compromising the STC. Design C leads to a solar collector area of 19,539 m^2 and a natural gas consumption of 322,751 kg/year, 86% lower than the natural gas consumption in the design A (2,427,475 kg/year).

(Figure 5 could be placed here)

Solar assisted biodiesel production from vegetable oil

Figure 6 shows the Pareto curve of the NPV of the whole plant. The EI index is reduced by 19.88% (232,608,592 $kgCO_2eq$ vs. 186,356,418 $kgCO_2eq$) along the Pareto curve. This is accomplished by reducing the consumption of natural gas. However, the NPV is decreased drastically from design A to B (24,683,025 $ vs -99,271,720 $), this is because the solar collector area in the minimum EI is very large and the total capital investment required to produce all the steam for the plant just using solar collectors is very expensive. In contrast, design C has similar plant profitability as design A (23,293,750 $ vs 24,683,025 $), but the environmental impact in C is 17.02% lower than the environmental impact in A (193,018,984 $kgCO_2eq$ vs 232,608,592 $kgCO_2eq$). This is because in design C, we use 15,857 m^2 of solar

collectors and we save a 81.21% of natural gas compared to design A.

(Figure 6 could be placed here)

Figure 7 shows, for the maximum NPV and minimum EI solutions, the main sources of GHG emissions. Particulary we consider the following contributors to the environmental impact (see Appendix B for details): vegetable oil, methanol, NaOH, H_3PO_4, water, electricity, steam, natural gas and steel. As seen all the impact indicators remain constant but the natural gas is reduced by 94.88%

(Figure 7 could be placed here)

Finally, Table 5 summarizes the main characteristics of designs A, B and C. As observed, in design A, the NPV takes the maximum value. Mainly, because the total capital investment is the lowest (no collectors are installed). In design B the NPV is dramatically decreased, since generating the steam with just solar collectors leads to a very large area up to 500,000 m^2 and therefore to a prohibitive capital investment. In design C the NPV is very similar as in design A because the increase in capital cost is offset by the decrease in operating cost. Concerning the environmental impact, design B leads to the best results but at the expense of a large drop in NPV. In contrast, design C attains similar reductions in impact while still showing a good NPV value.

(Table 5 could be placed here)

5 Conclusions

In this work we have proposed a systematic method based on the combined used of process simulation and mathematical programming techniques, for the optimal design of biodiesel processes with economic and environmental concerns. The design task was formulated as biNLP that minimizes simultaneously the net present value (NPV) and the environmental impact (EI). The latter criterion was quantified over the entire life cycle of the plant using the CML2001 methodology, which follows LCA principles.

The capabilities of the approach presented were tested in the design of a 9,233,040 kg/year alkali-catalyzed biodiesel process using vegetable oil and considering weather data of Tarragona. A set of Pareto solutions were generated using the ε constraint methodology. The results obtained show that is possible to achieve reductions in CO_2 emissions of up to 19.88 % with respect to the maximum profitability design. This is achieved at the expense of reducing the NPV. In the Pareto set obtained we identified three designs of particular interest: the maximum (NPV) design, the minimum (EI) design, and an intermediate design with similar plant profitability as maximum NPV design (23,293,750 $ vs 24,683,025 $) but lower environmental impact (193,018,984 kgCO_2eq vs 232,608,592 kgCO_2eq).

As seen, our method provides a comprehensive framework for the design of biodiesel plants integrated with solar energy that systematically identifies the best process alternatives in terms of economic and environmental performance. This information is valuable for decision-makers, as it allows them to adopt more sustainable technological alternatives for biodiesel processes. We also want to remark that the method presented in this paper, can be used for the optimal design of other chemical processes.

Acknowledgements

The authors wish to acknowledge support from the Spanish Ministry of Education and Science (projects DPI2008-04099 and CTQ2009-14420-C02) and the Spanish Ministry of

362 External Affairs (projects PHB 2008-0090-PC).

A Appendix A. Economic balance of the biodiesel production plant coupled with solar assisted steam generation system

To assess the economic performance of the biodiesel production plant; the first step is to estimate the total cost (CT), equation 12. This is divided in two parts, the capital investment (CI), which is usually based on the cost of the equipments, and the operating costs (CO), which can be calculated from different items such as: raw materials, energy, etc.

$$CT = CI + CO \tag{12}$$

The correlations used for the calculation of the equipments investment costs are given in terms of different design variables. For most of the equipments (reactors, centrifuges, mixers, flash, heat exchangers, distillation columns and storage tanks) the correlations are based on the volumetric flowrates (Vq_e). Other equipments embedded in the process flow diagram such as expansion valves or pumps were not considered in the cost estimation because of its low impact in the total cost of the process. The cost correlations were taken from Haas et al. [8], Zhang et al. [40] and Apostolakou et al. [10].

(Table 6 could be placed here)

Table 6 summarizes the calculations of the equipment costs. C_e is the equipment cost, e represents an equipment unit, BM_e is a cost factor of the equipment, V_e is the volume of the equipment, A_{HX} is the area of the heat exchangers, Q_{FF} is the volumetric flow rate of the centrifuge, c represents a distillation column, H_c is the height of the distillation column, D_c is the diameter of the distillation column and N_c is the number of stages in the distillation

column.

Along with the cost of the equipments, other factors have to be included into the estimated CI. These include items such as installation, process piping, instrumentation/control, insulation, electrical systems, buildings and auxiliary facilities and safety features. The sum of these, plus the cost of the purchased equipment are added together to make the total plant direct cost TPDC. Finally, components such as the cost of engineering, construction, the contingency, and the land are applied to the total plant indirect cost TPIC.

$$CI = TPDC + TPIC \tag{13}$$

The CO refers to the cost of the raw materials and utilities required to operate the cycle. The raw materials cost (Crm) is the cost of vegetable oil, methanol, catalyst, HCL, NaOH and water (equation 14). The cost of the utilities (Cut) is the cost of cold water, electricity and natural gas (equation 15).

$$Crm = \sum_{rm}(c_{rm} \cdot m_{rm}) \cdot top \tag{14}$$

$$Cut = \sum_{ut}(c_{ut} \cdot m_{ut}) \cdot top \tag{15}$$

In equation 15, c_{rm} is the price of the raw material and m_{rm} is the mass flowrate in kg/year of the raw materials, c_{ut} is the price of the utilities, m_{ut} is the annual utility consumption and *top* is the total annual operation time in hours. Note that m_{rm} and m_{ut} are provided by the process simulator. Table 7 lists the cost values of the raw materials and utilities of the system:

(Table 7 could be placed here)

In addition to the raw materials (Crm) and utilities cost (Cut), the operational cost also includes the cost of labor (Cl), supplies (Cs) and general work (Cgw).

$$CO = Crm + Cut + Cl + Cs + Cgw \tag{16}$$

The annual total product cost ctp_j is the operating cost (CO) plus the capital cost of the (CI) of the year j:

$$ctp_j = CI_j + CO_j \tag{17}$$

The annual revenues (r_j) is the sum of all sales of the main and by-products of a the biodiesel process in the year j:

$$r_j = m_j \cdot pr_j \tag{18}$$

where m_j is the amount of product sold in year j and pr_j is the price of the product in year j.

Then, it is calculated the net profit in year j (N_j), which is the annual revenue r_j minus the annual total cost ctp_j including the depreciation and minus the income tax determined by the tax rate ϕ:

$$N_j = (r_j - ctp_j) \cdot (1 - \phi) \tag{19}$$

Finally, the economic objective function is the net present value (NPV), this parameter measures the profitability of the plant and it is equal to the sum of the net profit in year j plus the depreciation d_j.

$$NPV = \sum_{j=1}^{J} \frac{N_j + d_j}{(1+ir)^j} \tag{20}$$

B Appendix B. Environmental analysis of the biodiesel production plant coupled with solar assisted steam generation system

The environmental performance of the biodiesel production is quantified according to the LCA methodology (ISO 14040), which is combined with process simulation and MOO in a way similar as done before by the authors (Bojarski et al. [48]) . The method is applied in four phases:

1. *Goal and scope definition:*

- We perform a cradle to gate study that covers all the activities from the extraction of raw materials to the production of alkali-catalyzed biodiesel.
- The functional unit was set to 9.233.040 kg/year alkali-catalyzed biodiesel produced over a time horizon of 25 years.
- The system under study comprises three stages: upstream, transesterification and downstream. Every stream crossing this boundary is regarded as an input or output of our system.
- The environmental impact is determined using the CML2001 framework.
- We consider the following sources of impact:

  Raw materials (inputs): vegetable oil, methanol, NaOH, H_3PO_4 and water.

  Utilities (inputs): electricity, cooling water and natural gas.

  Stainless steel contained in the equipment units (input).

2. *Life cycle inventory analysis (LCI):*

- The quantification of the mass and energy streams crossing the boundaries of the system is performed using the process simulator (Aspen Plus). The input streams

of energy and mass are translated into the corresponding emissions and feedstock requirements using the Eco-invent database.

3.*Life cycle impact assessment (LCIA):*

- The global warming potential (GWP) is determined from the entries of the life cycle inventory of emissions and feedstock requirements (LCI_b) and corresponding set of damage factors (df_{bd}) as follows.

$$CML = \sum_{b \in B} df_b \cdot LCI_b \tag{21}$$

4.*Life cycle interpretation:* As mentioned previously, the interpretation is performed in the post-optimal analysis of the Pareto solutions.

References

[1] Agrawal, AK. Biofuels applications as fuels for internal combustion engines. *Progress in Energy and Combustion Science.* **2007**,33,233-271.

[2] Nigam, P.S.; Singh, A. Production of liquid biofuels from renewable resources. *Progress in Energy and Combustion Science.* **2010**,37,52-68.

[3] Ma, F.; Hanna, M.A. Biodiesel production: A review. *Bioresource Technology.* **1999**,70, 1-15.

[4] Sharma, Y.C.; Singh, B.; Upadhyay, S.N. Advancements in development and characterization of biodiesel: A review. *Fuel.* **2008**,87,2355-2373.

[5] Shahid, E.M.; Jamal, Y. A review of biodiesel as vehicular fuel. *Renewable and Sustainable Energy Reviews.* **2007**,12, 2484-2494.

[6] Hill, J.; Nelson, E.; Tilman, D.; Polasky, S.; Tiffany, D. Environmental, economic and energetic costs and benefits of biodiesel and ethanol biofuels. *Proceedings of the National Academy of Science.* **2006**,103,11206-11210.

[7] Zhang, Y.; Dube, M.A.; McLean, D.D.; Kates,M. Biodiesel production from waste cooking oil: 1. Process design and technological assessment. *Bioresource Technology.* **2003**,89,1-16.

[8] Haas, M.A.; Mcaloon, A.; Yee, W.; Foglia, T. A process model to estimate biodiesel production costs. *Bioresource Technology.* **2005**,97,671-678.

[9] West, A.H.; Posarac, D.; Ellis, N. Assessment of four biodiesel production processes using HYSYS.Plant. *Bioresource Technology.* **2007**,99,6587-6601.

[10] Apostolakou, A.A.; Kookos, I.K.; Marazioti, C.; Angelopoulos, K.C. Techno-economic analysis of a biodiesel production process from vegetable oils. *Fuel Processing Technology.* **2009**,90,1023-1031.

[11] Sotoft, L.F.; Rong, B.G.; Christensen, K.V.; Norddahl, B. Process simulation and economical evaluation of enzymatic biodiesel production plant. *Bioresource Technology.* **2010**,101,5266-5274.

[12] Morais, S.T.; Mata, A.; Martins, G.; Pinto, G.A.; Costa, C. Simulation and LCA of Process Design Alternatives for Biodiesel Production from Waste Vegetable Oils. *Journal of Cleaner Production.* **2010**,18,1251-259.

[13] Pokoo-Aikins, G.;Nadim, A.; Mahalec, V.; El-Halwagi, M.M. Design and Analysis of Biodiesel Production from Algae Grown through Carbon Sequestration. *Clean Technologies and Environmental Policy.* **2010**,12,239-254.

[14] Chouinard-Dussault, P.; Bradt, J.; Ponce-Ortega, J.M.; El-Halwagi, M.M. Incorporation of Process Integration into Life Cycle Analysis for the Production of Biofuels. *Clean Technology Environmnetal Policy.* **2011**,13(5),673-685.

[15] Panichelli, L.; Gnansounou, E. Estimating greenhouse gas emissions from indirect land-use change in biofuels production: Concepts and exploratory analysis for soybean-based biodiesel production. *Journal of Scientific and Industrial Research.* **2008**,67,1017-1030.

[16] Sanchez, E.; Ojeda, K.; El-Halwagi, M.; Kafarov, V. Biodiesel from microalgae oil production in two sequential esterification/transesterification reactors: Pinch analysis of heat integration. *Chemical Engineering Journal.* **2011**,176-177.

[17] Karuppiah, R.; Peschel, A.; Grossmann, I.E.; Martín, M.; Martinson, W.; Zullo, L. Energy optimization for the design of corn-based ethanol plants. *AIChE Journal.* **2008**,54,1499-1525.

[18] Grossmann, I.E.; Martin, M. Energy and water optimization in biofuel plants. *Chinese Journal of Chemical Engineering.* **2010**,18,914-922.

[19] Martin, M.; Grossmann, I.E. Energy optimization of hydrogen production from lignocellulosic biomass. *Computers and Chemical Engineering.* **2011a**,35,1798-1806.

[20] Martin, M.; Grossmann, I.E. 2011b. Process optimization of FT-diesel production from lignocellulosic switchgrass. *Industrial & Engineering Chemistry Research.* **2011b**50,13485-13499.

[21] Ojeda, K.A.; Sanchez E.L.;Suarez, J.; Avila, O.; Quintero, V.; El-Halwagi, M.M.; Kafarov, V. 2011. Application of Computer-Aided Process Engineering and Exergy Analysis to Evaluate Different Routes of Biofuels Production from Lignocellulosic Biomass. *Industrial & Engineering Chemistry Research.* **2011**50,2768-2772.

[22] Lewis, N.S.; Nocera, D.G. Powering the planet: Chemical challenges in solar energy utilization. *Proceedings of the National Academy of Sciences.* **2006**,103,15729-15735.

[23] Shinnar, R.; Citro, F. Solar thermal energy: The forgotten energy source. *Technology in Society.* **2007**,29,261-270.

[24] Gebresslassie, B.; Guillen-Gosalbez, G.; Jimenez, L.; Boer, D. A systematic tool for the minimization of life cycle impact of solar assisted absorption cooling systems. *Energy.* **2010**,35,3849-3862.

[25] Salcedo, R.; Antipova, E.; Boer, D.; Jiménez, L.; Guillén-Gosálbez, G. Multi-objective optimization of solar Rankine cycles cupled with reverse osmosis desalination considering economic and life cycle environmental concerns. *International Journal of Desalination.* **2011**,286,358-371.

[26] Tora, E.A.; El-Halwagi, M.M. Integration of Solar Energy into Absorption Refrigerators and Industrial Processes. *Chemical Engineering & Technology.* **2010**,33,1495-1505.

[27] Tora, E.A.; El-Halwagi, M.M. Integrated Conceptual Design of Solar-Assisted Trigeneration Systems. *Computers & Chemical Engineering.* **2011**,35,1807-1814.

[28] Diwekar, U.M.; Grossmann, I.E.; Rubin, E.S. An MINLP Process Synthesizer for a Sequential Modular Simulator. *Industrial & Engineering Chemistry Research.* **1992**,31,313-322.

[29] Reneaume, J.M.F; Koehret, B.; Joulia X.L. Optimal process synthesis in a modular simulator environment: New formulation of the mixed-integer nonlinear programming problem. *Industrial & Engineering Chemistry Research.* **1995**,34,4378-4394.

[30] Kravanja, Z.; Grossmann, I.E. Computational approach for the modelling/decomposition strategy in the MINLP optimization of process flowsheets with implicit models. *Industrial & Engineering Chemistry Research.* **1996**35,2065-2070.

[31] Diaz, M.S.; Bandoni J.A. A mixed integer optimization strategy for a large chemical plant in operation. *Computers & Chemical Engineering.* **1996**,20,531-545.

[32] Caballero, J.A.; Milan-Yañez, D.; Grossmann, I.E. Rigorous design of distillation columns. *Industrial & Engineering Chemistry Research.* **2005**,44,6760-6775.

[33] Brunet, R.; Guillen-Gosalbez, G.; Jimenez, L. Cleaner Design of Single-Product Biotechnological Facilities through the Integration of Process Simulation, Multiobjective Optimization, Life Cycle Assessment, and Principal Component Analysis. *Industrial & Engineering Chemistry Research.* **2012a**,51,410-424.

[34] Brunet, R.; Cortes, D.; Guillen-Gosalbez, G.; Jimenez, L.; Boer, D. Minimization of the LCA impact of thermodynamic cycles using a combined simulation-optimization approach. *Applied Thermal Engineering.* **2012b**.

[35] Matlab 2011b, The MathWorks, Software (2011). Available from: www.mathworks.com.

[36] GAMS 2008, A user's guide. GAMS Development Corporation: Washington. Available from: www.gams.com.

[37] Aspen Plus, version 7.1 (0.0.7119). Aspen Technology, Inc., Cambridge, www.aspentech.com.

[38] Generalitat de Catalunya Departament d'Indústria, Comerç i Turisme, 2000. Atlas 543 de radiacio solar a Catalunya.

[39] Bruno, JC.; Lopez-Villada, J.; Letelier, E.; Romera, S.; Coronas, A. Modelling and optimisation of solar organic rankine cycle engines for reverse osmosis desalination. *Applied Termal Engineering.* **2008**,28,2212-2226.

[40] Zhang, Y.; Dube, M.A.; McLean, D.D.; Kates,M. Biodiesel production from waste cooking oil: 2. Economic assessment and sensitivity analysis. *Bioresource Technology.* **2003**,90,229-240.

[41] Azapagic, A.; Clift, R. Application of life cycle assessment to process optimisation.*Computers & Chemical Engineering.* **1999**,23,1509-1526.

[42] Azapagic, A.; Clift, R. Life cycle assessment and multiobjective optimisation.*Journal of Cleaner Production.* **1999**,7,135-143.

[43] Alexander, B.; Barton, G.; Petrie, J.; Romagnoli, J. Process synthesis and optimisation tools for environmental design: Methodology and structure.*Computers & Chemical Engineering.* **2000**,24,1195-2000.

[44] Carvalho, A.; Gani, R.; Matos, H. Design of sustainable processes: Systematic generation and evaluation of alternatives.*Computer Aided Chemical Engineering.* **2006**,21,817-822.

[45] Guillen-Gosalbez, G.; Caballero, J.A.; Jimenez, L.; Application of life cycle assessment to the structural optimization of process flowsheets.*Ind.Eng.Chem.Res.* **2008**,47,777-789.

[46] Haimes, Y.; Lasdon, L.; Wismer, D. On a bicriterion formulaiton of the problems of integrated system identification and system optimization.*IEEE Transaction on systems.* **1971**,1,296-297.

[47] Mavrotas, G. Effective implementation of the ε-constraint method in multi-objective mathematical programming problems. *Applied mathematics and computation.* **2009**,212,455-465.

[48] Bojarski A.D.; Guillen-Gosalbez G.; Jimenez L.; Espuña A.; Puigjaner L. Life cycle assessment coupled with process simulation under uncertainty for reduced environmental impact: Application to phosphoric acid production.*Industrial & Engineering Chemistry Research.* **2008**,47,8286-8300.

Nomenclature

Sets/Indices

B	environmental burdens indexed by b
i	streams
j	year
k	units
P	plant variables
p	components
rm	raw materials
S	solar system variables
t	time period
ut	utilities

Abbreviatures

biNLP	bi-criteria nonlinear programming
COL	solar collectors
E	evaporator
EI	environmental impact
EING	environmental impact natural gas
GWP	global warming potential
LCA	life cycle assessment
GFH	gas fire heater
GHG	green house gases
HTF	heat transfer fluid
MINLP	mixed-integer nonlinear programming
NLP	non-linear programming
NPV	net present value
STC	specific total cost

TES	Thermal energy storage

Variables

A	solar collector area
c	cost
CI	capital investment
Cl	cost labor
Cgw	cost general work
CML	environmental impact CML2001
Crm	Raw materials cost
CO	operating cost
Cs	cost supplies
ctp	total product cost
CT	total cost
Cut	utilities cost
d	depreciation
df	damage factors of component b
G	solar radiation
LCI	component inventory
m	mass flow
N	annual net profit
NPV	Net present value
pr	price of the product
Q	thermal power
r	annual revenues
T^{amb}	ambient temperature
T^{av}	average temperature
TPDC	total plant direct cost

TPIC	total plant indirect cost
V	volume of the equipment
Vq	volumetric flowrates
W	mechanical power
x	continuous variables
y	integer variables
η	collector optical efficiency
ε	auxiliary parameter
χ	mass fraction

Parameters

a_1	solar collector coefficient
a_2	solar collector coefficient
a_3	solar collector coefficient
CAP	maximum storage capacity
LHV	lower heating value of natural gas
ir	interest rate
top	operation time

List of Tables

Table 1: Capital costs summary of the biodiesel production process

Item	**Costs[$]**
Process equipment	
Tanks	235,977
Mixers	68,532
Transesterification Reactor	106,066
Methanol distillation tower	121,305
Glycerol distillation column	104,901
Biodiesel distillation column	131,126
Pumps	42,000
Heat Exchangers	81,132
Others	159,137
Utility equipment	230,806
Installation & Other costs	1,996,567
Total Capital Investment	**3,323,190**

Table 2: Operating costs summary of biodiesel production process

Item	**Costs[$/yr]**
Raw materials	
Methanol	243,776
NaOH	49,360
Oil	2,856,000
H3PO4	52,800
Water	254
	3,202,190
Utilities	
Cold water	5,725
Electricity	457
Wastewater treatment	50,000
Natural gas	636,054
	692,237
Other costs	1,354,302
Operating Costs	**5,248,729**

Table 3: Executive economic summary of biodiesel production process

Item	**Biodiesel process**
Net Present Value [$]	24,683,026
Total Capital Investment [$]	3,323,190
Operating Cost [$/yr]	5,248,729
Production Rate [kg/ yr]	9,233,040
Unit Production Cost [$/kg]	0.59
Unit Selling Price [$/kg]	0.91
Total revenues[$]	145,841,164

Table 4: Results of the LCA of biodiesel production process using CML2001

Source	**Mass kg/25years**	**GWP100a kgCO2eq/kg**	**Impact kgCO2eq/25years**
Vegetable Oil	166,320,000	0.9815	166,256,386
Methanol	20,627,200	0.7373	15,207,816
NaOH	1,760,000	1.2432	2,188,032
H3PO4	8,800,000	0.3289	2,894,232
Water	15,840,000	0.0007	10,746
Electricity [kWh]	92,928	0.6180	57,427
Natural Gas	53.404.450	0.9127	48,744,378
Steel [m^2]	800	311.97	249,576
Total			**232,608,592**

Table 5: Economic and environmental summary of the different design alternatives proposed

Item	Design A	Design B	Design C
Net Present Value [$]	24,683,025	-99,271,729	23,293,750
CML-2001 [kgCO_2eq]	232,608,592	186,356,418	193,018,984
Total Capital Investment [$]	3,213,600	27,522,639	4,095,862
Operating Cost [$/yr]	5,284,729	17,792,926	5,211,284
Production Rate [kg/ yr]	9,233,040	9,233,040	9,233,040
Unit Production Cost [$/kg]	0.59	1.32	0.61
Unit Selling Price [$/kg]	0.91	0.91	0.91
Total revenues[$]	145,841,164	145,841,164	145,841,164
Area solar panels [m^2]	0	625,773	19,539
Natural gas consumed [kg/yr]	2,427,475	124,112	433,996

Table 6: Equipment cost correlations used in the biodiesel production

Equipment	Correlation
Storage tanks	$C^0_{ST} = BM_{ST} \cdot (250000 + 94.2 \cdot V_{ST})$
Mixers	$C^0_M = BM_M \cdot (12080 \cdot V_M^{0.525})$
Reactors	$C^0_R = BM_R \cdot (1500_R^{0.55})$
Heat exchangers	$C^0_{HX} = BM_{HX} \cdot (2320 \cdot A_{HX}^{0.65})$
Centrifuges	$C^0_{FF} = BM_{FF} \cdot (28100 \cdot Q_{FF}^{0.574})$
Flash	$C^0_D = BM_D \cdot (6500 \cdot V^{0.62})$
Distillation columns	$C^0_T = BM_T \cdot (4555 \cdot H_C^{0.81} \cdot D_C^{1.05} + 380 \cdot N_C^{0.81} \cdot D_C^{1.55})$

Table 7: Raw materials and utility price used in the biodiesel production

Item	Cost
Vegetable Oil	0.420 \$/kg
Methanol	0.286 \$/kg
Sodium methylate	0.980 \$/kg
Hydrochloric acid	0.132 \$/kg
Water	0.353 \$/MT
Natural gas	4.80 \$/ft^3
Electricity	0.91 \$/kWh
Process water	0.353 \$/MT

List of Figures

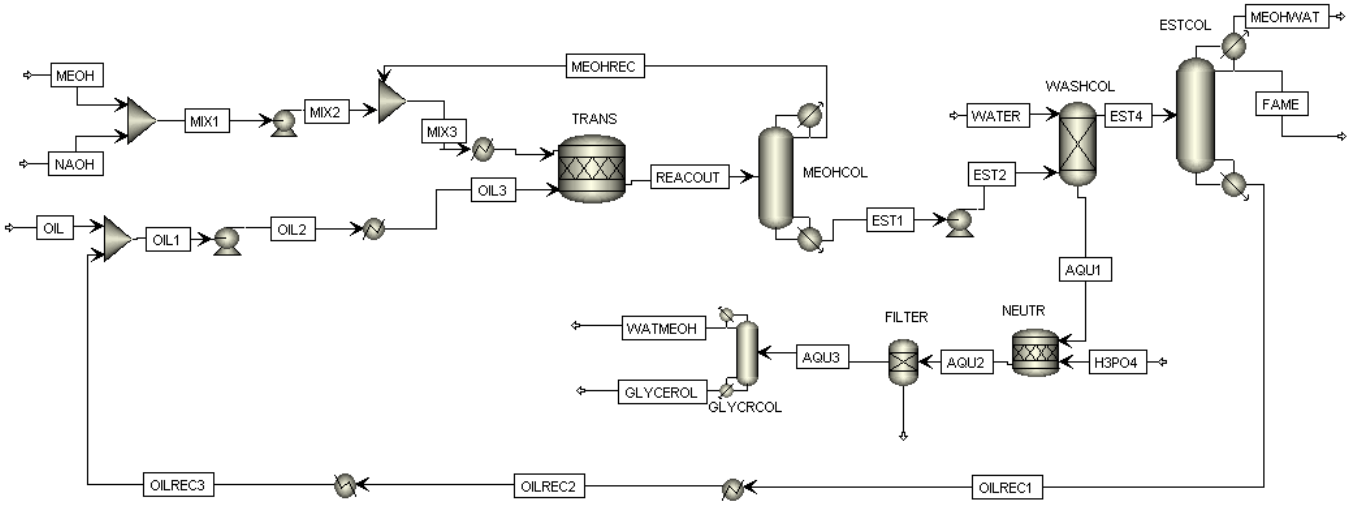

Figure 1: Flowsheet for the production of biodiesel from vegetable oil

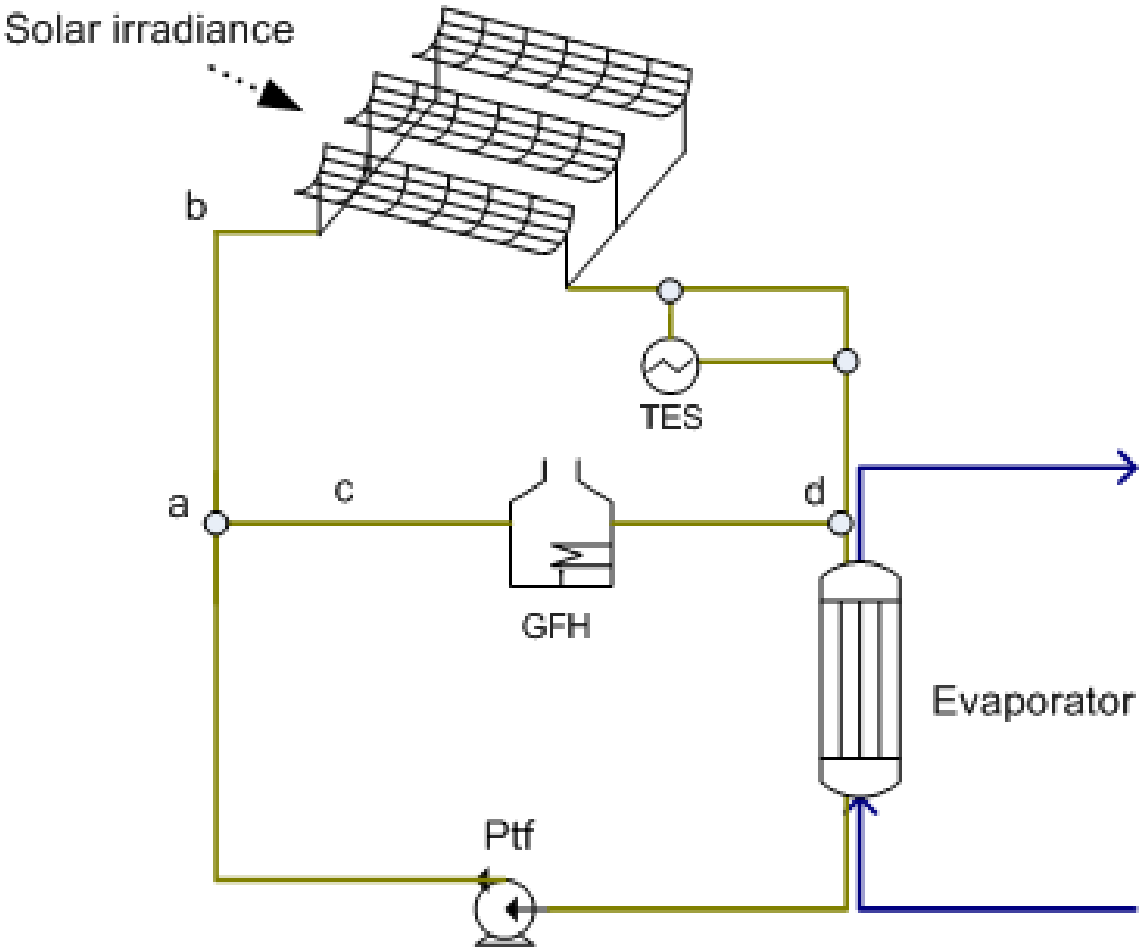

Figure 2: Solar assisted steam generation system with heat storage

Figure 3: Energy balance applied to the storage system

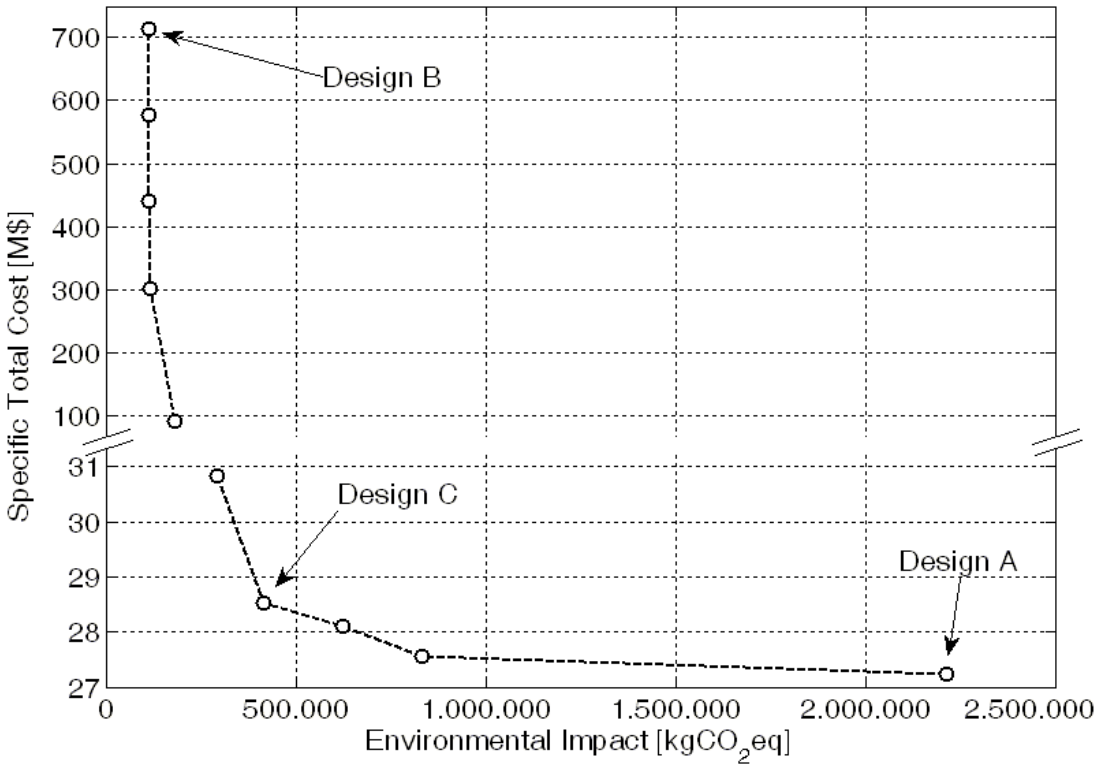

Figure 4: Pareto set of optimal solutions in the solar assisted steam generation system

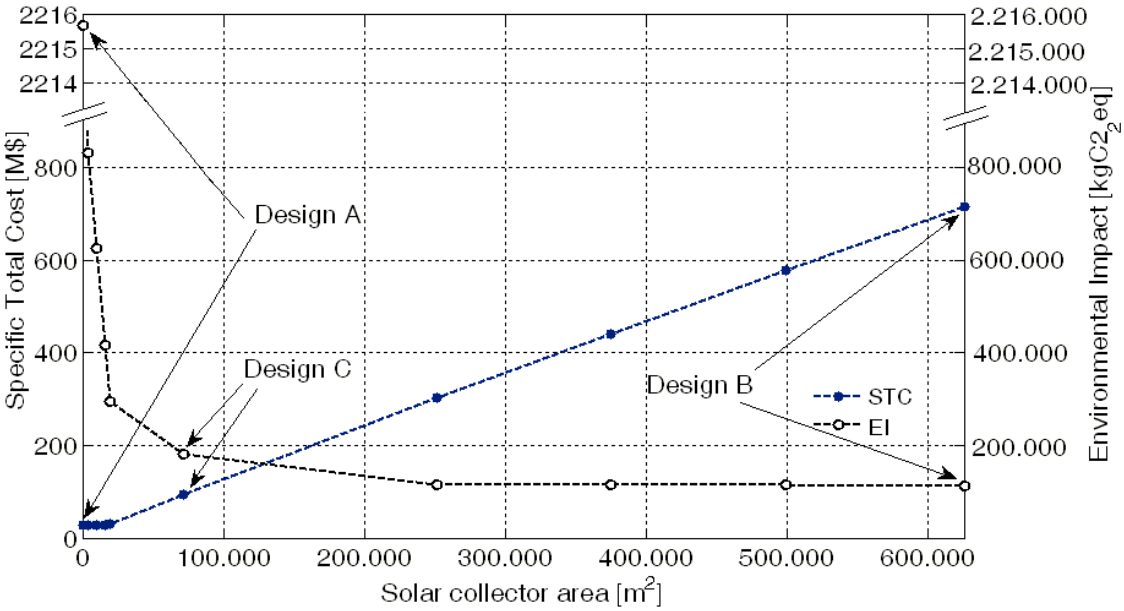

Figure 5: Specific total cost and environmental impact versus solar collector area

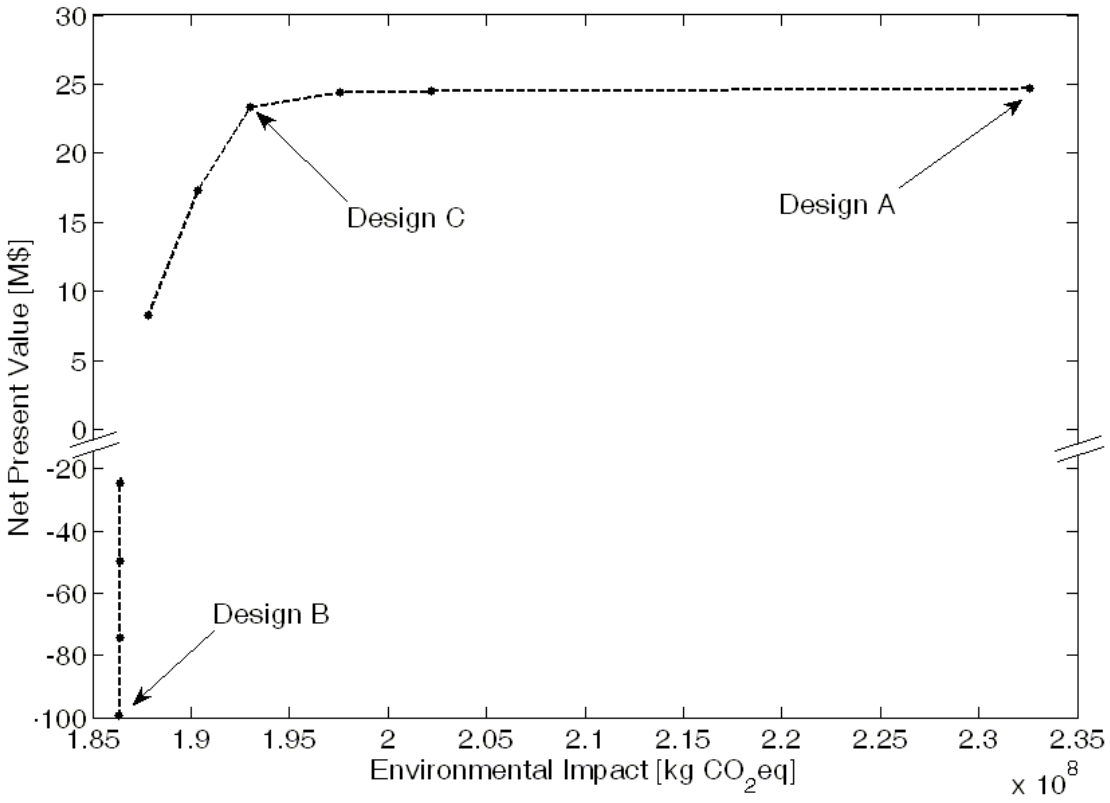

Figure 6: Pareto set of optimal solutions in the biodiesel production plant

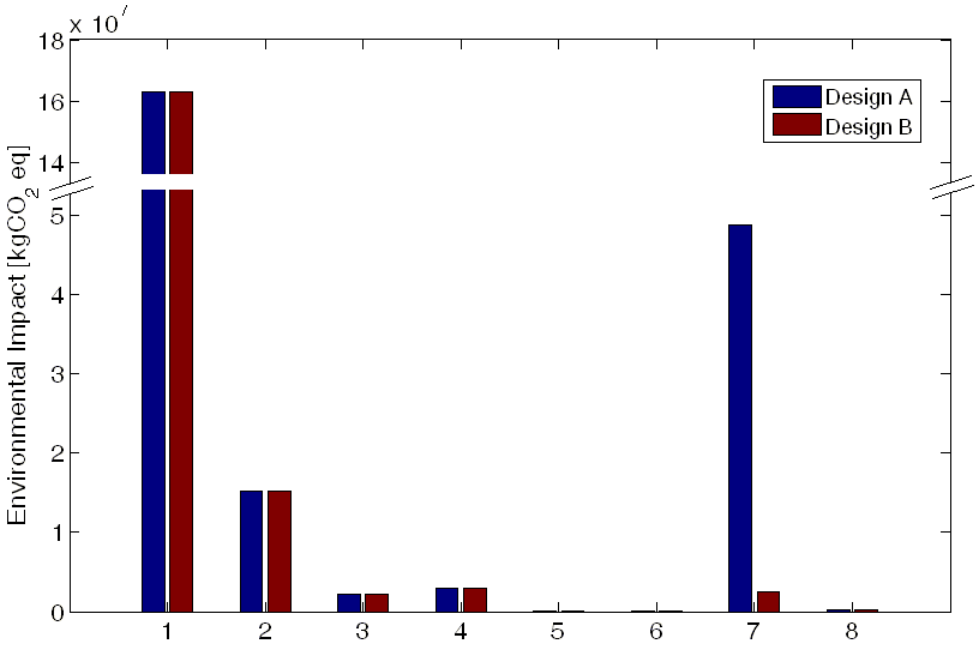

Figure 7: Breakdown of main sources of impact contributing to different environmental impact categories: (1)vegetable oil, (2)methanol, (3)NaOH, (4)H_3PO_4, (5)water, (6)electricity, (7)steam, (8)natural gas and (9)steel

Article 6

Authors: **R. Brunet**, E. Antipova, G. Guillén-Gosálbez, L. Jiménez.
Title: Minimization of the energy consumption in bioethanol production processes using a solar assisted steam generation system with heat storage
Journal: *AIChE Journal*
Volume: **Pages:** **Year:** 2012
ISI category: Chemical Engineering **AIF:** 0.707
Impact Index: 2.030
Position in the category: 32/135 (Q1)
Cites: -
Observations: Under review

Minimization of the energy consumption in bioethanol production processes using a solar assisted steam generation system with heat storage

Robert Brunet, Gonzalo Guillén-Gosálbez*and Laureano Jiménez
Departament d'Enginyeria Quimica, Escola Tecnica Superior d'Enginyeria Quimica, Universitat Rovira i Virgili, Campus Sescelades, Avinguda Paisos Catalans 26, 43007, Tarragona, Spain

September 8, 2012

*Corresponding author. E-mail: gonzalo.guillen@urv.cat, telephone: +34 977558618

Abstract

In this work, we address the multi-objective optimization (MOO) of a corn-based bioethanol plant coupled with a solar assisted steam generation system with heat storage. Our approach relies on the combined use of process simulation, rigorous optimization tools and, economic and energetic plant analysis. The design task is posed as a bi-criteria nonlinear programming (biNLP) problem that considers the simultaneous optimization of the plant profitability and the energy consumption. The capabilities of the proposed methodology are illustrated through a fixed production of 120 kton/year corn-based bioethanol considering weather data of Tarragona (Spain).

Keywords: *Bioethanol; Corn dry-grind; Solar panels; cost analysis; energy consumption.*

1 INTRODUCTION

The continued use of fossil fuels to meet the majority of the world's energy demand is threatened by increasing concentrations of CO_2 in the atmosphere and concerns over global warming. The combustion of fossil fuels is responsible for 73% of the CO_2 production [1]. To reduce the net contribution of GHGs to the atmosphere, bioethanol has been recognized as a potential alternative to petroleum-derived transportation fuels [2].

Bioethanol is the most important biofuel today with a worldwide output of about 32 million tones in 2006 [3]. Bioethanol is a liquid biofuel which can be produced from a large variety of natural renewable materials and conversion technologies. The corn dry-grind process is the most widely used method in the U.S. for generating fuel ethanol by fermentation of grain [4]. However, corn grain as other first generation bioethanol processes has raised questions regarding its feasibility as an alternative fuel in terms of low Net Energy Balance (NEB) because of the high energy input required to produce corn and to convert it into ethanol [5, 6].

In order to analyze the potential economic, environmental and/or energetic benefits of bioethanol production processes, several works have used process simulation techniques. Kwiatkowski et al. [7] presented a process in SuperPro Designer of the fermentation of corn dry-grind for the production of ethanol. Quintero et al. [8] presented an economical and environmental comparative study between fuel ethanol production from sugarcane and corn using Aspen Plus. Dias et al. [9] simulate different scenarios of the bioethanol production from sugarcane using SuperPro Designer. More recently, Tasic and Veljkovic [10] developed a simulation model for fuel ethanol production from potato tubers using Aspen Plus.

Apart from these works based on simulation, there are other contributions that address the optimal design of bioethanol production processes using "short-cut" models of the process units, that is, simplified equations employed to predict their performance processes. Karuppiah et al. [12], was the first to propose a superstructure optimization approach for the optimal design of corn-based ethanol plants. Grossmann and Martin [13], presented a

general approach based on mathematical programming techniques for the energy and water optimization in biofuel plants. Martin and Grossmann [14, 15], presented also an optimization approach for energy reduction in bioethanol production processes via gasification and hydrolosis of switchgrass.

As it can be seen, many approaches have focused on minimizing energy consumption in biofuels facilities. Pimentel [5] was the first to address this issue in bioethanol production plants, calculating an energy consumption of 75,118 Btu/gal of bioethanol from corn. Shapouri et al. [6] estimates a lower energy consumption of 51,779 Btu/gal in the corn-based bioethanol production. Wang et al. [16] presented a process with a significant energy reduction compared to the previous ones, 38,323 Btu/gal. Finally, Martin and Grossmann [14], used mathematical programming techniques for the minimization of the energy consumption, which was reduced to 19,996 Btu/gal.

The aforementioned works focused on improving the bioethanol production process by changing the operating conditions and structural configuration of the plant. An alternative approach to improve the performance of bioethanol plants consists of coupling them with renewable energy sources. In a recent work, Lewis and Nocera [17] highlighted the benefits of integrating solar energy with other technologies. Shinnar and Citro [18] claimed that solar thermal (ST) energy can be an environmentally friendly and economically competitive electric source. More recently, Gebresslassie et al. [19] addressed the minimization of the life cycle impact in cooling systems using solar collectors, while Salcedo et al. [20] developed a model for the optimization of reverse osmosis desalination plants coupled with solar Rankine cycles.

With all of these observations in mind, the aim of this paper is to present a systematic method for the optimal design of corn-based bioethanol facilities considering economic, environmental and energetic performance concerns in the decision-making process. Our approach relies on the combined use of process simulation, optimization tools and economic and energetic analysis within a unified framework. The optimization problem is formulated as a bi-criteria

nonlinear program (biNLP), involving economic and energetic objective functions. The solution approach presented combines process simulators (SuperPro Designer) and optimization software (Matlab and GAMS) in an integrated framework. The optimization algorithm provides as output a bi-objective optimization set of Pareto solutions representing the optimal compromise between plant profitability and energetic consumption. The methodology presented has been tested in a corn-based bioethanol production, considering weather data of Tarragona (Spain), for the solar collectors.

2 PROCESS DESCRIPTION

As already mentioned, our approach includes both a simulation model and an optimization model. The first is used to estimate the performance of the biofuel plant, while the second allows to determine the energy savings by coupling the production facility with solar collectors and energy storage. The simulation model has been implemented in SuperPro, and it is based on the one proposed by Kwiatkowski et al. [7]. In contrast, the optimization model has been developed in GAMS. We describe in detail next each of this models and then describe how they have been combined.

2.1. Bioethanol production from dry grind

We consider a facility for bioethanol production from corn to ethanol. There are two general manners of processing corn to produce ethanol: wet milling and dry grind. The corn dry-grind process is the most widely used method in the U.S. for generating fuel ethanol by fermentation of grain, because dry-grind processes are less capital and energy intensive than their wet mill counterparts. The corn-based bioethanol production process comprises six-stages: milling, liquidification, saccharification, fermentation, distillation and dehydration. A simplified flow diagram of the process is shown in Figure 1.

(Figure 1 could be placed here)

In the milling stage (Stage 1) of the dry-grind process, corn grain is cleaned in a hammer (104M) mill and sent through weighing tanks to the liquefaction step (Stage 2). To begin this section, the measured ground corn is sent to a slurry tank (307V) and is slurried with alpha-amylase, ammonia and lime. The mixture is then gelatinized using a "jet-cooker" and hydrolyzed with thermostable alpha-amylase into oligosaccharides, in the liquefaction equipment (310V).

In the saccharification (Stage 3) the conversion of the oligosaccharides by glucoamylase to glucose takes place. This is done in the saccharification reactor (321V) where we add g-amylase and sulfuric acid. The reaction is performed at 61°C with a ph of 4.5 and takes 5 hours. Following the saccharification reaction, the slurry is transferred to the fermentation vessel (405V). In the fermentation stage (Stage 4) the glucose iis converted into ethanol. The residence time is 68 hours, with a working volume of 83% in the fermentors.

The beer from the fermentation is then sent through a degasser drum (408E) to flash off the vapor (412V). The vapor stream (S-128) is primarily ethanol and water with some residual carbon dioxide. The stream is then condensed and recombined with a liquid stream prior to being sent to the distillation (Stage 5).

The first step in the distillation stage is the ethanol recovery in the beer column (501T). This unit recovers nearly all of the ethanol produced during the fermentation. The recovery of the ethanol from the beer column (501T) is accomplished through the combined action of the rectifier (503T), stripper (507T) and molecular sieve (504X). The distillate of the rectifier, containing primarily ethanol, feeds the molecular sieves, which captures the last bit of water, creating 99.6% pure ethanol. Molecular sieves are composed of a microporous substance, designed to separate small molecules from larger ones via a sieving action. Finally, the main product, fuel ethanol, is produced after mixing the refined ethanol with approximately 5% denaturant (gasoline) and is held in the product tank (513V) prior to transport out for sale

as a motor fuel additive. Concerning the by-products, the mixture of the non-fermentable material from the bottom of the beer column (501T) is fed to the whole stillage tank (601V). Then goes to the centrifuge (603) where 83% of the water content is removed. The liquid product from the centrifuge is split and used as backset. The concentrate from the evaporator (607Ev), is mixed with the wet distiller's grains coming from the distiller conveyor (604MH). The mixture goes to the drum dryer which reduces the moisture content of the mixture of wet grains and evaporator concentrate from 63.7% to 9.9%, and this becomes the coproduct known as distiller's dried grains with solubles (DDGS).

2.2. Integrated solar assisted steam generation system

One of the main sources of environmental impact in the process described above is the energy consumption in the reboilers of the distillation columns. According to our simulation, this consumption is 12.239 BTU/gal.

To decrease the energy requirements to generate steam, we propose to couple the facility with a solar assisted steam generation system with heat storage. Figure 2 shows a sketch of the steam generation system proposed, which is integrated with the bioethanol plant, thereby reducing the energy needs and associated impact.

(Figure 2 could be placed here)

The solar thermal unit provides heat to the evaporator in order to satisfy the energy demand of the bioethanol plant. Parabolic trough collectors are employed to transfer solar energy to the heat mineral oil. A gas fire heater (GFH) is coupled with the solar collectors as a back up system in order to cope with the intermittent radiation and maintain the oil temperature constant. This oil is used in the boiler to generate steam.

A thermal energy storage (TES) is integrated in the system to use the solar energy more efficiently. Particulary, molten-salt thermocline is considered. Particulary, molten salt is

used as the heat transfer fluid (HTF) that transports thermal energy between the storage unit and the remaining parts of the power system (e.g., collector field, GFH and boiler).

3 PROPOSED APPROACH

The design of the integrated facility could be accomplished following a superstructure optimization approach. This methodology relies on formulating a mixed-integer non-linear programming (MINLP) model, where continuous variables represent process conditions (i.e., temperature, pressures, concentrations, etc.), while binary variables denote the existence of a process unit in the flowsheet. This approach makes use of short-cut models to describe the performance of the process units. Hence, the ability to handle a large number of potential designs comes at the cost of using approximated models. An alternative approach to circumvent this limitation consists of combining simulation and optimization tools (see [21–23]). This approach optimizes a rigorous process model, which is implemented in a process simulator, using an external optimization tool. While this strategy has proved efficient for handling processes with complex unit operations, it still shows some limitations. Particularly, one mayor issue concerns the convergence problems that may arise in the process simulator during the optimization task.

In this work, the optimization of the integrated system is performed in two sequential steps. A rigorous simulation model is first constructed in SuperPro Designer. The optimization of the steam generation system is then implemented in GAMS. The outcome of the optimization is combined with the simulation results, which provides the performance of the overall integrated system. Note that the emphasis here is on assessing the economic and energetic performance of the integrated facility rather than on developing an efficient solution method for the optimization of such a system.

We therefore assume that the bioethanol plant is already under operation, and focus on optimizing the solar system that will power the reboilers of the facility. We should clarify

that while the optimization of the integrated system could be in principle addressed using either a simultaneous (i.e., MINLP) or sequential approach (i.e., simulation-optimization), it would lead to a highly complex model. The optimization of the combined biofuel facility with solar collectors is therefore out of the scope of this contribution, but will be the focus of future work. Finally, let us note that this general approach can be applied to other chemical processes, and it is therefore not restricted only to biofuels plants.

Note that, the following sections describes the modeling tools applied to each part of the process.

3.1. Process model of the bioethanol plant

As already mentioned, our approach includes both a simulation model and an optimization model. The first is used to estimate the performance of the biofuel plant, while the second allows to determine the energy savings by coupling the production facility with solar collectors and energy storage. The simulation model has been implemented in SuperPro, and it is based on the one proposed by Kwiatkowski et al. [7]. In contrast, the optimization model has been developed in GAMS.

The process simulator (SuperPro Designer) quantifies the energy requirements, and yield of each major piece of equipment for the specified operating scenario. Volumes, compositions, and other physical characteristics of input and output streams are also determined. This information becomes the basis for the calculation of utility consumptions and purchased equipment costs for each equipment item.

Non-starch polysaccharides are made up of corn fiber (pericarp and endosperm fiber) and other potentially valuable or fermentable components. Other solids include: cleaning compounds, minerals, and other residual matter in the process. Although corn was used as the basis for this process, other agricultural products high in starch may also be input to the model, though the process may require the user to adjust the given unit operations or incorporate new operations to accommodate the new feed.

3.2. Mathematical formulation of the solar energy system

The model of the energy system is based on mass and energy balances. These equations, which ensure mass and energy conservation, are applied to each unit of the system. The mass balance is defined by equation 1:

$$\sum_{i \in IN_k} m_{i,t} \cdot x_{i,p,t} - \sum_{i \in OUT_k} m_{i,t} \cdot x_{i,p,t} = 0 \qquad \forall k, p, t \tag{1}$$

where IN_k and OUT_k are the sets of streams entering and leaving unit k respectively, $m_{i,t}$ is the mass flow rate of stream i in period t, and $x_{i,p,t}$ is the mass fraction of component p in stream i in period t. The total summation of the mass fractions of components p in every stream i must equal 1 (see equation 2):

$$\sum_{p} x_{i,p,t} = 1 \qquad \forall i, t \tag{2}$$

The mass balance is defined by equation 3:

$$\sum_{i \in IN_k} m_{i,t} \cdot h_{i,t} - \sum_{i \in OUT_k} m_{i,t} \cdot h_{i,t} + Q_{k,t} - W_{k,t} = 0 \qquad \forall k, t \tag{3}$$

where $h_{i,t}$ is the enthalpy of stream i in period t, $Q_{k,t}$ is the thermal power supplied to unit k in period t, and $W_{k,t}$ is the mechanical power output of unit k in period t.

In the model of the solar assisted steam generation system with heat storage, we define the following energy balance (see Figure 3):

196

$$Q_{k,t} + Q_{k',t} + Q_{k'',t-1} = Q_{k'',t} + Q_{k''',t} \qquad k = COL, k' = GFH, k'' = TES, k''' = E, \qquad \forall t \tag{4}$$

197 where $Q_{COL,t}$ is the thermal energy captured by the collectors, $Q_{GFH,t}$ is the energy provided
198 by the fossil fuel combusted in the GFH, $Q_{E,t}$ is the thermal energy accumulated in the
199 storage at the end of period t and $Q_{B,t}$ is the energy required by the evaporator.
200 The maximum amount of thermal energy that can be accumulated is given by the maximum
201 storage capacity CAP:

$$Q_{TES,t} \leq CAP \qquad \forall t \tag{5}$$

202 The heat produced in the solar collectors is calculated from equation 6:

$$Q_{k,t} = G_t \cdot A_k \cdot \eta_{k,t} \qquad k = COL, \qquad \forall t \tag{6}$$

203 where G_t represents the solar radiation, which depends on the time period of the day and
204 month. The daily solar radiation expressed in MJ/m^2 day is available for different locations
205 in Catalonia [24]. The efficiency of the medium-high temperature parabolic trough collectors
206 η_{col} is calculated according to the work by Bruno et al. [25] (equation 7):

$$\eta_{k,t} = \eta_t^0 - a_1(T_t^{av} - T_t^{amb}) - a_2(\tfrac{T_t^{av} - T_t^{amb}}{G_t}) - a_3(\tfrac{T_t^{av} - T_t^{amb}}{G_t}) \qquad k = COL, \qquad \forall t \tag{7}$$

where η_t^0 is the collector optical efficiency, a_1, a_2, a_3 are coefficients, T_t^{amb} is the ambient temperature in time period t, and T_t^{av} is the average temperature of the solar collector, which is determined by equation 8:

$$T_t^{av} = \frac{T_{OUT_k} - T_{IN_k}}{2} \qquad k = COL, \qquad \forall t \tag{8}$$

The heat produced by the combustion of natural gas in the heater is given by equation 9:

$$Q_{k,t} = m_k \cdot LHV \cdot \eta_k \qquad k = GFH, \qquad \forall t \tag{9}$$

In this equation, m_{NG} is the mass flow rate of natural gas, LHV is the lower heating value of natural gas, and η_{GFH} is the thermal efficiency of the natural gas heater.

3.3. Economic and energetic analysis

The economic objective function is the Net Present Value (NPV), which quantifies the plant profitability and it is equal to the sum of the net profit in year j plus the depreciation:

$$\sum_{j=1}^{J} \frac{N_j + d_j}{(1+ir)^j} \tag{10}$$

Where N_j is the annual gross profit minus the income tax, d_j is the depreciation of that year, parameter ir is the interest rate and j is the number of year that the plant is working, in this case 25. This economic assessment is based on the costs analysis of Henderson et al. [26], Tiffany et al. [27], Bryan and Bryan [28].

With regard to the energy costs, the total amount of energy input into the process compared to the energy released by burning the resulting ethanol fuel is known as the ethanol fuel

energy balance (sometimes called "Net energy gain") and studied as part of the wider field of energy economics.

3.4. Bi-criteria nonlinear programming (biNLP) model

The design of the integrated system with economic and environmental concerns can be expressed in mathematical terms as a biNLP. We solve this model using the ε constraint method [29, 32]. This technique is based on calculating a set of single-objective models in which one objective is kept in the objective function while the others are transferred to auxiliary constraints and forced to be lower than a set of epsilon parameters:

$$
\begin{aligned}
\min_{x_D} \quad & z = f_1(x,y) \\
s.t. \quad & f_2(x,y) \leq \ \varepsilon \\
& \underline{\varepsilon} \leq \ \varepsilon \leq \ \overline{\varepsilon} \\
& f_1(x,y) = f_1^P(x^P,y^P) + f_1^S(x^S) \\
& f_1(x,y) = f_2^P(x^P,y^P) + f_2^S(x^S) \\
& h^P(x^P,y^P) = 0 \\
& h^S(x^S) = 0 \\
& g_P(x^P,y^P) \leq \ 0 \\
& g_S(x^S) \leq \ 0
\end{aligned}
\tag{11}
$$

The economic objective function, represented by f_1, is quantified using the NPV while f_2 quantifies the impact according to the energy consumption. ε is an auxiliary parameter that bounds the values of the objectives transferred to the auxiliary inequality constraints. While x and y represent continuous and discrete variables defined for the plant and solar assisted system (x^P, y^P and x^S, respectively). For simplicity, in this formulation, we fully decouple the optimization of the plant and the steam generating system. Furthermore, we consider that the plant will not be modified, so variables x^P and y^P are fixed, while variables x^S are

optimized using a gradient-based method. This reflects the situation in which we aim to retrofit an existing facility by adding the energy system but without changing neither the operating conditions nor the topology of the plant.

4 NUMERICAL RESULTS

We study the design of a solar assisted dry-grind bioethanol production plant considering weather data of Tarragona (Spain). We first present the economic and energetic analysis of the base case, a bioethanol plant in which the heat capacity is generated by the GFH. We will then analyze the alternative system proposed here in which the solar assisted steam generation with heat storage is used to cover the steam required by the plant. We finally discuss the Pareto curve of optimal results of the bioethanol plant integrated with the solar assisted generation system.

4.1. Dry-grind bioethanol production

Economic analysis

The presented ethanol cost information, is based on equipment and operating costs. It is used general accepted methods for conduction conceptual technical and economic methods in the process industry [31, 33, 34]. The purchased costs for the major equipment items were based on budgetary quotations from equipment suppliers and erectors. Other sources of equipment pricing that were used included Richardson's Process Plant Construction Estimating Standards 2001, SuperPro Designer and Chemcost. Additional literature on the construction of ethanol plants is available as well in [26–28]. However, for the sake of brevity, the details on the economic balances calculations are given in Appendix A.

The capital costs calculated are summarized in Table 1. The estimated total capital cost of the 119,171,463 kg/year dry-grind bioethanol production was 60.52 MM$. The cost of the process equipments is 19.03 MM$, the most expensive equipments are the transesterification

reactor (2.81 MM$) and the molecular sieve (1.72 MM$). The utility equipment used in the process are summarized separately, these equipments are the cooling tower, the steam generation system, the instrument air system and the electrical system. The total cost of the utility equipment is 4.24 MM$. Additionally other costs are taken into account such as the installation cost and miscellaneous cost.

(Table 1 could be placed here)

The plant operating costs are based on material and utility costs. Costs agree with actual production cost information collected in surveys conducted by USDA [6]. Ethanol dry-grind plant operates 24 h/day, with time set aside for maintenance and repairs. A basis of 330 days per year (7920 h) operating time was used for this model, and the nominal capacity of the plant is approximately 35,837 kg/h of corn.

The projected annual operating costs for the modeled biodiesel production facility are shown in Table 2. The cost of raw materials is the most significant, specially the cost of the corn (50.57 MM$/year) which represents the 92.96% of the raw materials total cost (54,40 MM$/year) and 57.83% of the total operational costs (80.27 MM$/year). The other raw materials are: lime, ammonia, alpha-amylase, glucoamylase, sulfuric acid, caustic, yeast, water and octane. The cost of utilities is 15.11 MM$/year, which accounts for the following utilities: steam, cold water, electricity, wastewater treatment and natural gas. Finally other costs such as: miscellaneous, maintenance, operating labor, lab costs, supervision, capital charges and insurance are taken into account.

(Table 2 could be placed here)

Table 3 shows the NPV of the plant along with the most significant items related with the economic analysis.

(Table 3 could be placed here)

Energetic analysis

We studied the operating energy analysis to produce one gallon of bioethanol. In the energetic analysis we considered all the raw materials present in the system and the energy of the unit procedure in the system. The energy required to obtain one gallon of bioethanol is 24.681 Btu. The raw materials represents, the 16.32% of the total energy required for the bioethanol production. Most of the energy 39.38% is wasted in the reboiler of the beer column, rectifier and stripping.

(Table 4 could be placed here)

4.2. Optimal design of the solar assisted dry-grind bioethanol production

In this section we present the optimal results of the dry-grind bioethanol production plant coupled with solar assisted steam generation with heat storage. We first describe the biNLP optimization of the solar assisted steam generation system and the detailed study of the variables that most influenced in the bi-criterion optimization. Then, we present the Pareto set of solutions of the completed system with heat storage.

The process model was implemented in SuperPro Designer, whereas the biNLP model of the solar system was coded in GAMS and solved with CONOPT3. The algorithm took around 23.5 sec to generate 10 Pareto solutions on a computer AMD PhenomTM 86000B, with Triple-Core Processor 2.29GHz and 3.23 GB of RAM.

Figure 4 shows the Pareto curve of the NPV of the plant, including the steam generation

system and the energy consumed per gallon of bioethanol produced (NRG). The NRG consumed is reduced by 29.79% (27.309 Btu/gal vs. 19.173 Btu/gal) along the Pareto curve. This is accomplished by reducing the consumption of the natural gas. However, the NPV is dramatically decreases from design A to B (92,752,281 $vs - 328,817,003$), this is because the solar collector area in the minimum NRG is very large and the total capital investment to produce all the steam for the plant just using solar collectors is very expensive. However, design C, has similar plant profitability as design A (92,752,281 $vs 75,610,887$), but the main factor is that the environmental impact in C is 25.87% lower than the environmental impact in A (27.309 Btu/gal vs 20.244 Btu/gal), this is because in design C, we use 71,053m^2 of solar collectors and we save the 45.20% of natural gas used in design A.

(Figure 3 could be placed here)

Finally, Table 8 summarizes the main characteristics of designs A, B and C. As observed, in the design A, the NPV is the highest. Mainly, because the total capital investment is lower. In design B the NPV is dramatically decreased, to the point that the profitability of the plant is negative. This is because to generate almost all of the steam with just solar collectors, you need a very high area, up to 5,000,000m^2 and the cost of this technology is therefore very high. In the design C the NPV is very similar to that associated with the design A because on the one hand the total capital investment is increased but on the other the operating costs are decreased. Concerning the NRG, in design A the natural gas consumed is very high compared to that associated with the other 2 designs. Design C consumes consumes more natural gas, but the difference has not a big impact in the final NRG. In light of these results, solution C seems to be more appealing.

(Table 5 could be placed here)

5 Conclusions

In this work we have proposed a systematic method based on the combined used of process simulation and mathematical programming techniques, for the optimal design of dry-grind bioethanol production processes with economic, environmental and energetic concerns. The design task was formulated as biNLP that minimizes simultaneously the net present value (NPV) and energetic consumption (NRG).

The capabilities of the approach presented were tested in the design of a 120 kton/year dry-grind corn-to-ethanol production plant considering weather data of Tarragona (Spain). The Pareto solutions set were generated using the epsilon constraint methodology. The results obtained show that is possible to achieve reductions in the energetic consumption with respect to the maximum profitability design. This is acomplished at the expense of reducing the drastically the NPV.

As it can be seen, our method provides a comprehensive framework for the design of bioethanol plants integrated with solar energy that systematically identifies the best process alternatives in terms of economic, environmental and energetic performance. This information is valuable for decision-makers, as it allows them to adopt more sustainable technological alternatives for bioethanol processes.

Acknowledgements

The authors wish to acknowledge support from the Spanish Ministry of Education and Science (projects DPI2008-04099 and CTQ2009-14420-C02) and the Spanish Ministry of External Affairs (projects PHB 2008-0090-PC).

References

[1] Lokhorst A, Wildenborg T. Introduction on CO2 geological storage. Classification of storage options. *Oil and Gas Science and Technology.* 2005;60:513-515.

[2] Govindaswamy S, Vane LM. Kinetics of growth and ethanol production on different carbon substrates using genetically engineered xylose-fermenting yeast. *Bioresource Technology.* 2007;98:677-685.

[3] International Energy Agency. World Energy Outlook. 2006.

[4] Dimian A, Bildea CS. Chemical Process Design. 2007. WILEY-VCH Verlag GmbH & Co. KGaA, Weinheim

[5] Pimentel D. Ethanol fuels: Energy balance, economics, and environmental impacts are negative. *Natural Resources Research.* 2003;12:127-134.

[6] Shapouri H, Duffield JA,Wang M. The Energy Balance of Corn Ethanol Revisited. *Transactions of the American Society of Agricultural Engineers.* 2003;46:959-968.

[7] Kwiatkowski JR, McAloon AJ, Taylor F, Johnston DB. Modeling the process and costs of fuel ethanol production by the corn dry-grind process. *Industrial Crops and Products.* 2006;23:288-296.

[8] Quintero, J.A., Montoya, M.I.,Sánchez, O.J., Giraldo, O.H.,Cardona, C.A. Fuel ethanol production from sugarcane and corn: Comparative analysis for a Colombian case. *Energy.* 2008;33:385-399.

[9] Dias, M.O.S., Cunha, M.P.,Jesus, C.D.F., Scandiffio, M.I.G., Rossell, C.E.V., Filho, R.M., Bonomi, A. Simulation of ethanol production from sugarcane in Brazil: Economic study of an autonomous distillery. *Computer Aided Chemical Engineering .* 2010;28:733-738.

[10] Tasic MB, Veljkovic VB. Simulation of fuel ethanol production from potato tubers. *Computers and Chemical Engineering.* 2011;35:2284-2293.

[11] Morais, S.T.; Mata, A.; Martins, G.; Pinto, G.A.; Costa, C. Simulation and LCA of Process Design Alternatives for Biodiesel Production from Waste Vegetable Oils. *Journal of Cleaner Production.* **2010**,18,1251-259.

[12] Karuppiah R, Peschel A, Grossmann IE, Martin M, Martinson W, Zullo L. Energy optimization for the design of corn-based ethanol plants. *AIChE Journal.* 2008;54:1499-1525.

[13] Grossmann, I.E.; Martin, M. Energy and water optimization in biofuel plants. *Chinese Journal of Chemical Engineering.* **2010**,18,914-922.

[14] Martin M, Grossmann IE. Energy optimization of bioethanol production via gasification of switchgrass. *AIChE Journal.* 2011;57:3408-3428.

[15] Martin M, Grossmann IE. Process optimization of FT-diesel production from lignocellulosic switchgrass. *Industrial and Engineering Chemistry Research.* 2011;50:13485-13499.

[16] Wang, M., Wu, M., Huo, H. Life-cycle energy and greenhouse gas emission impacts of different corn ethanol plant types. *Environmental Research Letters.* 2007;2:024001.

[17] Lewis, N.S.; Nocera, D.G. Powering the planet: Chemical challenges in solar energy utilization. *Proceedings of the National Academy of Sciences.* **2006**,103,15729-15735.

[18] Shinnar, R.; Citro, F. Solar thermal energy: The forgotten energy source. *Technology in Society.* **2007**,29,261-270.

[19] Gebresslassie, B.; Guillen-Gosalbez, G.; Jimenez, L.; Boer, D. A systematic tool for the minimization of life cycle impact of solar assisted absorption cooling systems. *Energy.* **2010**,35,3849-3862.

[20] Salcedo, R.; Antipova, E.; Boer, D.; Jiménez, L.; Guillén-Gosálbez, G. Multi-objective optimization of solar Rankine cycles cupled with reverse osmosis desalination considering economic and life cycle environmental concerns. *International Journal of Desalination.* **2011**,20,358-371.

[21] Caballero, J.A.; Milan-Yañez, D.; Grossmann, I.E. Rigorous design of distillation columns. *Industrial & Engineering Chemistry Research.* **2005**,44,6760-6775.

[22] Brunet, R.; Guillen-Gosalbez, G.; Jimenez, L. Cleaner Design of Single-Product Biotechnological Facilities through the Integration of Process Simulation, Multiobjective Optimization, Life Cycle Assessment, and Principal Component Analysis. *Industrial & Engineering Chemistry Research.* **2012a**,51,410-424.

[23] Brunet, R.; Cortes, D.; Guillen-Gosalbez, G.; Jimenez, L.; Boer, D. Minimization of the LCA impact of thermodynamic cycles using a combined simulation-optimization approach. *Applied Thermal Engineering.* **2012b**,48,367-377.

[24] Generalitat de Catalunya Departament d'Indústria, Comerç i Turisme, 2000. Atlas 543 de radiacio solar a Catalunya.

[25] Bruno, JC.; Lopez-Villada, J.; Letelier, E.; Romera, S.; Coronas, A. Modelling and optimisation of solar organic rankine cycle engines for reverse osmosis desalination. *Applied Termal Engineering.* **2008**,28,2212-2226.

[26] Henderson M, Kosstrin H, Crump B. Renewable Energy Bulletin. R.W. Beck Inc., http://www.rwebeck.com/oil-and-gas. 2005.

[27] Tiffany DG, Eidman Vr. Factors Associated with Success of Fuel Ethanol Producers. Department of Applied Economics Staff Paper P03-7. Department of Applied Economics, University of Minnesota. 2003.

[28] Bryan and Bryan International, 2003. Ethanol Plant Development Handbook, fourth ed., Cotopaxi, BBI International

[29] Haimes Y, Lasdon L, Wismer D. On a bicriterion formulaiton of the problems of integrated system identification and system optimization.*IEEE Transaction on systems.* 1971;1:296-297.

[32] Mavrotas G. Effective implementation of the ε-constraint method in multi-objective mathematical programming problems. *Applied mathematics and computation.* 2009;212:455-465.

[31] Jelen, FC. Cost and Optimization Engineering. McGraw-Hill, NY. 1970.

[32] Mavrotas, G. Effective implementation of the ε-constraint method in multi-objective mathematical programming problems. *Applied mathematics and computation.* **2009**,212,455-465.

[33] Association for the Advancement of Cost Engineering International, 1990. Conducting Technical and Economic Evaluations in the Process and Utility Industry. In: ACCE Recommended Practices and Standards. AACE International, Morgantown, WV, 84pp.

[34] Dysert LR, 2003. Sharpen your cost estimating skills, CCC, Cost Engineering, Vol. 45. No. 06, AACE International, Morgantown, WV.

447 # Nomenclature

Sets/Indices

i	streams
j	year
k	units
P	plant variables
p	components
rm	raw materials
S	solar system variables
t	time period
ut	utilities

Abbreviatures

biNLP	bi-criteria nonlinear programming
COL	solar collectors
DDGS	Distiller dried grains with solubes
E	evaporator
GFH	gas fire heater
GHG	green house gases
HTF	heat transfer fluid
MINLP	mixed-integer nonlinear programming
NEB	Net Energy Balance
NLP	non-linear programming
NPV	net present value
ST	Solar Thermal
TES	Thermal energy storage

Variables

A	solar collector area

d	depreciation
df	damage factors of component b
G	solar radiation
m	mass flow
N	annual net profit
NPV	Net present value
Q	thermal power
r	annual revenues
T^{amb}	ambient temperature
T^{av}	average temperature
V	volume of the equipment
Vq	volumetric flowrates
W	mechanical power
x	continuous variables
y	integer variables
η	collector optical efficiency
ε	auxiliary parameter
x	mass fraction

Parameters

a_1	solar collector coefficient
a_2	solar collector coefficient
a_3	solar collector coefficient
CAP	maximum storage capacity
LHV	lower heating value of natural gas
ir	interest rate
top	operation time

List of Tables

Table 1: Capital costs summary of the bioethanol production process

Item	**Costs[$]**
Process equipment	
Grain Handling (101MH)	121,000
Corn Storage (102V)	979,000
Cleaning (103MH)	61,000
Hammer Mill (104M)	98,000
Batch Weighing (106W)	51,000
Slurry Mixer (307V)	69,000
Liquefaction (310V)	161,000
Saccharification (321V)	103,000
Fermenter (405V)	2,812,000
Degasser (412V)	62,000
Beer Column (501T)	597,000
Rectifier (503T)	254,000
Molecular Sieve (504X)	1,718,000
Scrubber (409V)	91,000
Stripping (507T)	168,000
Centrifuge (603X)	825,000
Evaporator (607Ev)	3,418,000
DDGS Dryer (610D)	2,278,000
Thermal Oxidizer (611X)	925,000
DDGS Handling (612MH)	123,000
Total Tanks	1,340,000
Total Heat exchangers	2,380,000
Total Pumps	311,000
	19,028,000
Utility equipment	
Cooling tower	1,003,880
Steam generation	2,522,388
Instrument air system	144,417
Electrical system	577,682
	4,248,376
Other cost	
Installation	34,914,564
Miscellaneous	2,327,637
	37,242,201
Total Capital Investment	**60,518,577**

Table 2: Operating costs summary of the bioethanol production process

Item	**Costs[$/yr]**
Raw materials	
Corn	39,437
Lime	161,334
Ammonia	578,562
Alpha-amylase	835,669
Sulfuric Acid	80,667
Caustic	223,296
Yeast	179,426
Water	7,037
Octane	1,722,266
	54,395,407
Utilities	
Steam	5,510,241
Cold water	4,348,379
Electricity	1,461,453
Natural gas	4,140,705
	15,110,779
Other costs	
Miscellaneous	5,439,541
Maintenance	5,439,541
Operating Labor	1,760,000
Lab Costs	352,000
Supervision	352,000
Overheads	880,000
Capital Charges	8,159,311
Insurance	2,175,816
	24,558,209
Operating Costs	**94,064,209**

Table 3: Executive economic summary of the bioethanol production process

Item	**Bioethanol process**
Net Present Value [$]	116,379,916
Total Capital Investment [$]	60,518,577
Operating Cost [$/yr]	94,064,209
Production Rate [kg/ yr]	119,171,463
Unit Production Cost [$/kg]	0.67
Unit Selling Price [$/kg]	0.69
Total revenues[$]	81,826,000

Table 4: Energy balance of the bioethanol production process

Item	**Energy consumed [BTU/gal]**
Raw materials	
Corn	1,924.46
Alpha-amylase	23.83
Ammonia	5.19
Lime	3.10
G-amylase	4.64
Sulfuric Acid	3,11
Caustic	877.67
Yeast	1.44
Water	1,215.06
Octane	18.89
	4,057.38
Process equipment	
Grain Handling (101MH)	65.74
Cleaning (103MH)	18.84
Hammer Mill (104M)	212.15
Slurry Mixer (307V)	7.79
Liquefaction (310V)	51.71
Saccharification (321V)	1.15
Fermenter (405V)	164.57
Degasser (412V)	36.60
Beer Column/Condenser (501T)	3,568.40
Beer Column/Reboiler (501T)	7,978.75
RECTIFIER/Condenser (501T)	1,595.30
Rectifier /Reboiler (501T)	2,130.59
Molecular Sieve (504X)	9.76
Scrubber (409V)	73.88
Stripping/Condenser (507T)	1,595.30
Stripping/Reboiler (507T)	2,130.59
Centrifuge (603X)	87.43
Evaporator (607Ev)	2,940.46
DDGS Dryer (610D)	640.50
Thermal Oxidizer (611X)	157.92
DDGS Handling (612MH)	25.08
Total Heat exchangers	158.60
Total Pumps	50.16
	23,251.27
Energy Balance	**27,309.00**

Table 5: Economic and energetic summary of the bioethanol process

Item	Design A	Design B	Design C
Net Present Value [$]	92,752,281	-328,817,003	75,610,887
Energy consumed [Btu/gal]	27,309	19,179	20,244
Total Capital Investment [$]	37,159,397	316,441,020	44,862,192
Operating Cost [$/yr]	63,021,995	79,893,062	62,606,124
Production Rate [kg/ yr]	119,171,463	119,171,463	119,171,463
Unit Production Cost [$/kg]	0.67	1.12	0.68
Unit Selling Price [$/kg]	0.69	0.69	0.69
Total revenues[$]	81,826,000	81,826,000	81,826,000
Area solar panels [m^2]	0	5,430,794	71,053
Natural gas consumed [kg/yr]	22,066,980	10,570,180	12,102,040

List of Figures

UNIVERSITAT ROVIRA I VIRGILI
OPTIMAL DESIGN OF SUSTAINABLE CHEMICAL PROCESSES VIA A COMBINED SIMULATION OPTIMIZATION APPROACH
Robert Brunet Solé
Dipòsit Legal: T. 458-2013

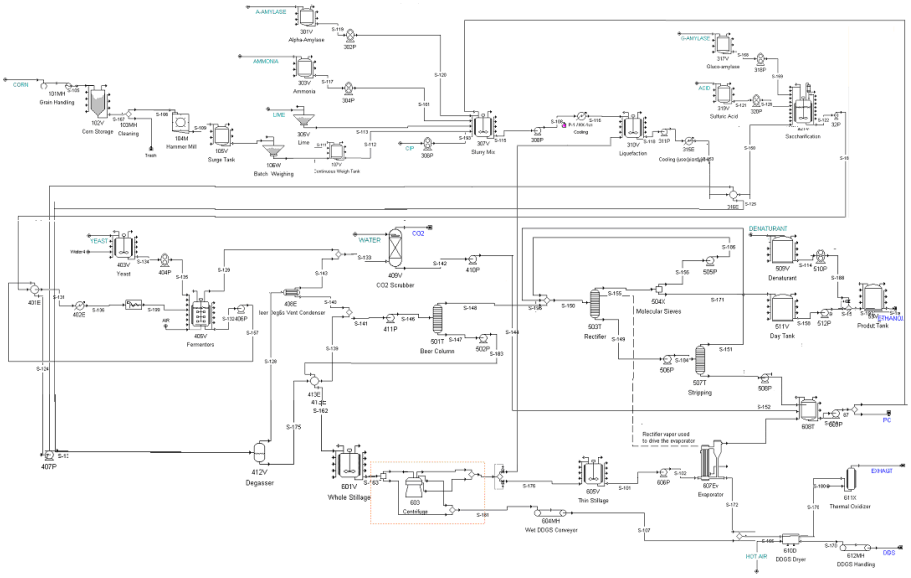

Figure 1: Flowsheet for the corn-based bioethanol production model

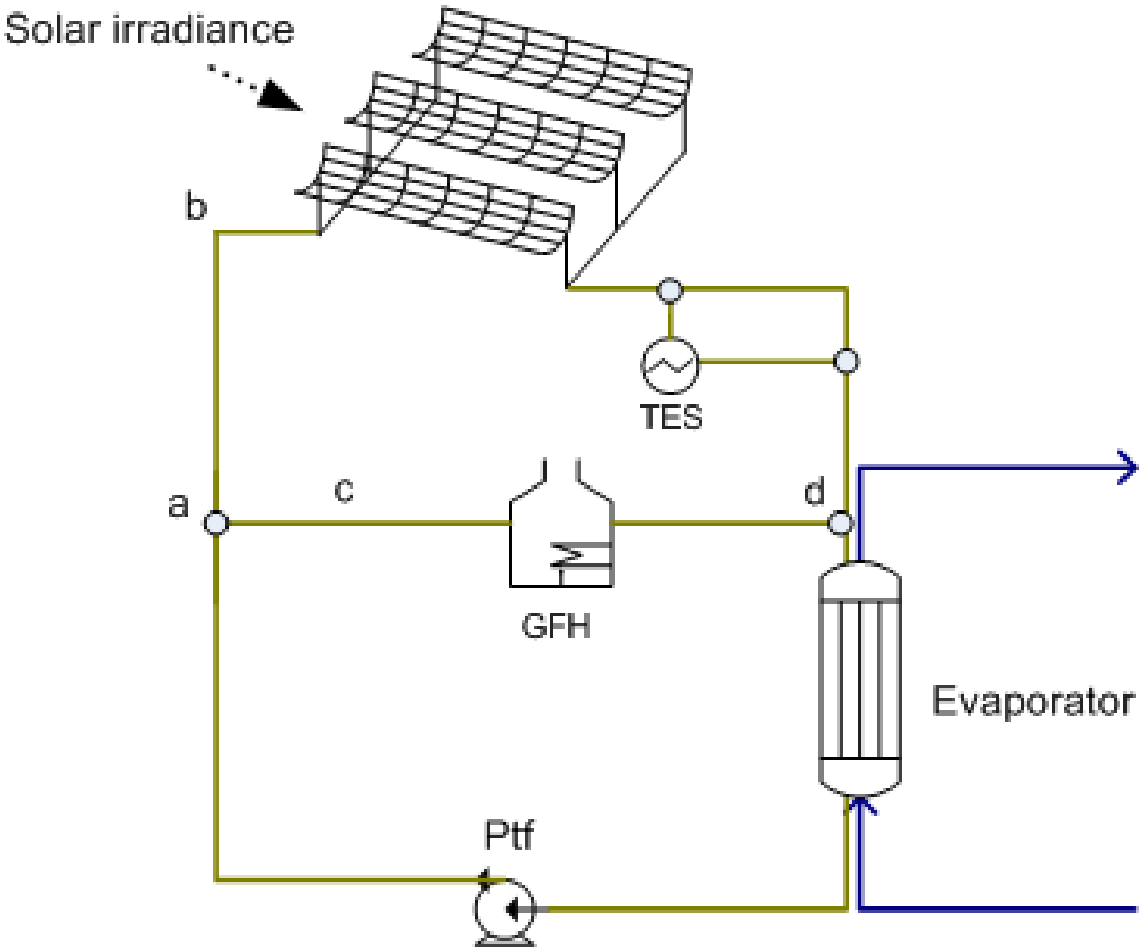

Figure 2: Solar assisted steam generation system with heat storage

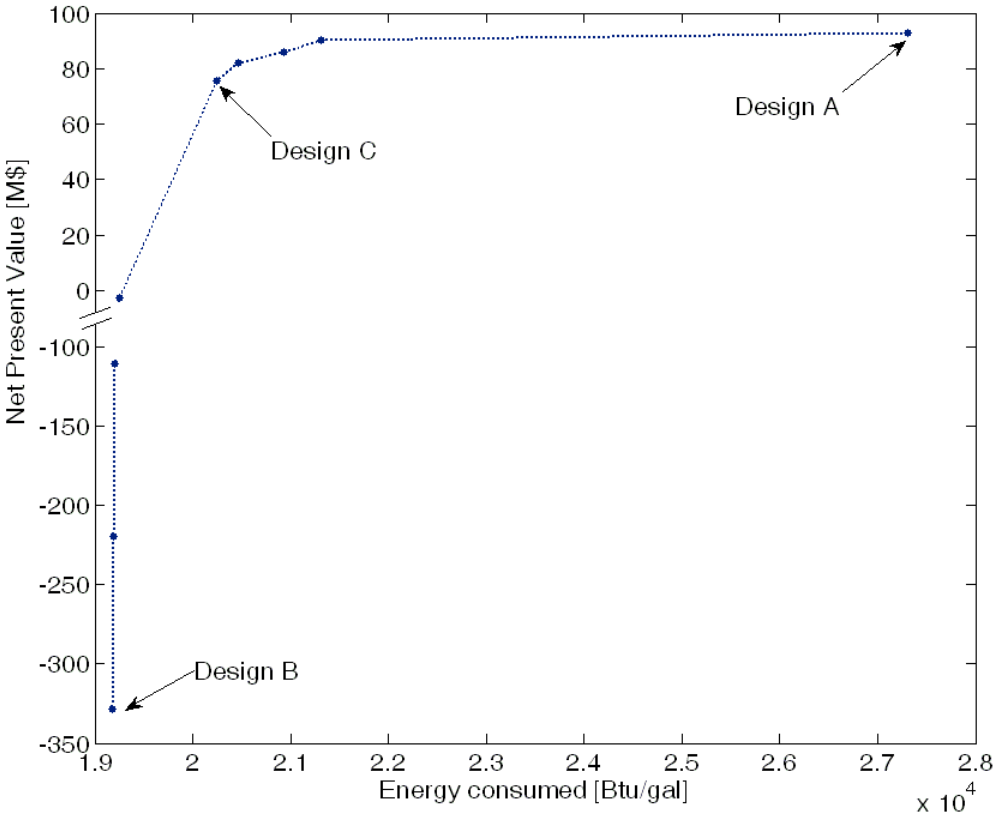

Figure 3: Pareto set of optimal solutions in the bioethanol production plant

3. Conclusions and future work

This thesis introduces a novel framework for the optimal design of sustainable chemical processes. The methodology presented combines process simulation, multi-objective optimization tools (MOO), economic analysis, life cycle assessment (LCA) and decision support systems (DSS). Numerical results show that it is possible to achieve environmental and cost saving using this rigorous approach in different types of chemical processes. We consider that the method presented will very useful for decision-makers in order to evaluate new technologies to improve their chemical process and operation designs.

Additionally, the developed strategy is used to solve very complex problems. For that it was necessary to develop new algorithms and decomposition strategies to divide the original problem in more manageable sub-problems, to obtain the optimum design of the process. Therefore, in this PhD dissertation is also presented new strategies to solve complex mathematical problems.

The PhD dissertation is divided in three parts: introduction, articles and conclusions. In the introduction is presented the background of the thesis and in articles is presented the main core. Six articles have been published in different international peer reviewed journals.

The 1st article, titled (*Hybrid simulation-optimization based approach for the optimal design of single-product biotechnological processes*), introduces a systematic strategy to assist in the development of biotechnological processes, the nobility of this strategy is that combines the process simulator SuperPro Designer with optimization toolsimplemented in Matlab and Gams. In this case the problem has only one objective function the NPV, which is increased by 13.77% compared to the base case (195,688 M$ vs. 172,003 M$).

In the 2nd article (*Cleaner design of single-product biotechnological facilities through the integration of process simulation, multiobjective optimization, life cycle assessment, and principal component analysis*) we introduces a novel framework that integrates process simulation, multi-objective optimization, economical analysis, LCA and principal

component analysis. This new method is tested in the same bioprocess model as before, the NPV is still increased by 13.77% compared to the base case and the environmental impact categories are decreased by 10.10% (damage to ecosystem quality), 8.17% (depletion resources) and 3.59% (damage to human health) compared to the maximum NPV solution.

In the 3rd article (*Combined simulation-optimization methodology for the design of environmental conscious absorption systems*) we address the optimal design of ammonia-water absorption cycles for cooling and refrigeration applications with economic and environmental concerns. This is the first work that this strategy is applied in this type of systems. At cooling conditions the total annualized cost (TAC) is reduced by 9.35% (23,445 €/year vs. 21,916 €/year) along the Pareto curve and the environmental impact (EI) is reduced by 7.28% (16,927 points vs. 15,435 points). At refrigeration conditions the TAC is reduced by 10.90% (32,293 €/year vs. 28,771 €/year) and the EI is reduced by 11.27% (23,451 points vs. 20,807 points).

In the 4th article (*Minimization of the LCA impact of thermodynamic cycles using a combined simulation-optimization approach*) we present a computational approach for the simultaneous minimization of the total cost and environmental impact of thermodynamic cycles. The method is similar to the one presented in the 3rd article but in this case we tested with a 10 MW Rankine cycle modeled in Aspen Hysys, and a 90 kW ammonia-water absorption cooling cycle implemented in Aspen Plus.

In the 5th article (*Reducing the environmental impact of biodiesel production from vegetable oil using a solar assisted steam generation system with heat storage*), we address the problem of reducing the environmental impact of biodiesel production plants. Here we present a new approach were we combine a process model of the plant with a model of a solar assisted steam generation system in Gams, we optimize the second in order to obtain environmental saving in the integrated system. The results obtained show that is possible to achieve reductions in CO2 emissions of up to 19.88%.

In the 6th article (*Minimization of the energy consumption in bioethanol production using a solar assisted steam generation system with heat storage*) it is used a similar strategy as in the article 5th, but in this case we analyze the energy reduction in corn-based

bioethanol plant, we demonstrate that is possible to reduce 25.87% the energy consumption by integrating with a solar assisted steam generation system with heat storage.

We can conclude that this thesis brings new methods for the design of economic and environmental conscious chemical processes and it has been tested with different types of chemical processes.

As any PhD dissertation, the work does not finish here. There are many works and project to continue in this line:

- The presented methodology can be tested for the optimal design of other chemical processes such as: basic chemicals, fuel processing, plastic processing, consumer goods, waste water treatment, mineral processing, air pollution, pulp and paper, pharmaceutical among others.
- Use this methodology to improve the process operation conditions in a real case of study and see the improvements in the economic and environmental way.